THE UNIVERSITY
of EDINBURGH

The Role of the NS Segment of Influenza A Virus in Setting Host Range and Pathogenicity

Matthew Luke Turnbull

THE UNIVERSITY *of* EDINBURGH

Submitted for the degree of Doctor of Philosophy

The University of Edinburgh

August 2016

Acknowledgements

It has been an honour and a pleasure to have worked under the supervision of Prof. Paul Digard. Without his guidance and support this work would not have been possible, and for that I am extremely grateful. I also thank Prof. Bernadette Dutia, my secondary supervisor, for her encouragement and scientific discussion.

I thank members of the Digard and Dutia laboratories, as well as many others at the Roslin Institute, who have provided essential help, advice, and friendship during my PhD. In particular, I thank Drs. Helen Wise, Nikki Smith, and Saira Hussain, who have all taught me essential techniques both inside and outside the lab needed to complete this work. I am also grateful to Drs. Lita Murphy, Liliane Chung, Elly Gaunt, and Seema Jasim for useful advice and discussion along the way. It has been a pleasure to work alongside fellow students Alice, Becca, Anabel, Rute and Carina. Good luck with your PhDs – I'll be checking you have all been attending seminars when I have gone!

I also need to say how much I have appreciated the support and friendship I have been blessed with over my time in Edinburgh. Laura, Tom R, Tom E, Eddie, Murray and all my teammates on the football field, all really helped me through my PhD. And of course Mum, Martin, Alex and Dom - the family. It was the good times I shared with you all I relied on when the going got tough!

Finally, I'd like to thank my late Grandfather, Terry White. He strived to provide me with the best education I could have received, and for that I am eternally thankful.

Preface

Declaration

I declare that this thesis was composed by myself, that the work contained herein is my own except where explicitly stated otherwise in the text, and that this work has not been submitted for any other degree or processional qualification.

Signed……..... Date……

Matthew Turnbull

Published material

The work described in this thesis has been published in the Journal of Virology:

Role of the B Allele of Influenza A Virus Segment 8 in Setting Mammalian Host Range and Pathogenicity (Turnbull ML, Wise HM, Nicol MQ, Smith N, Dunfee RL, Beard PM, Jagger BW, Ligertwood Y, Hardisty GR, Xiao H, Benton DJ, Coburn AM, Paulo JA, Gygi SP, McCauley JW, Taubenberger JK, Lycett SJ, Weekes MP, Dutia BM, Digard P). 2016. Journal of Virology. 90, 9263-84. DOI: 10.1128/JVI.01205-16.

The manuscript was accepted for publication at the latter stages of thesis writing, therefore it has not been referenced or discussed in this thesis. The publication includes work from all results chapters of this thesis.

The publication is Open Access and can be accessed at http://jvi.asm.org/content/90/20/9263.long. A PDF is also included on CD with this thesis.

Table of contents

List of figures and tables

Chapter 1 Introduction

Chapter 2 Replicative fitness of segment 8 reassortant viruses *in vitro*

Chapter 3 Host cell responses to infection with segment 8 reassortant viruses

Chapter 4 *In vivo* studies with segment 8 reassortant viruses

Chapter 5 Phylogenetic analyses of segment 8 genes of IAV – *Aves* to *Mammalia* transmission rates

Chapter 7 Materials and Methods

Lay summary

Influenza A virus (IAV) is a major pathogen affecting many host species. The natural host is aquatic birds, in which the virus only causes mild or asymptomatic infections. The virus is able to adapt to domestic birds and mammals in which it can evolve to cause serious disease and high mortality rates, causing major losses in food production and putting severe strain on economies. IAV occasionally causes pandemics in humans, in which millions of people can die worldwide from a single outbreak. There is currently a lack of a universal vaccine and the antiviral drug options are far from ideal. Therefore, it is important to fully understand how avian IAV can cross the species barrier into domestic mammals and cause disease. This study set out to improve this understanding by investigating a group of avian IAV genes that are considered to be non-functional in mammalian hosts, thus understanding the mechanisms behind this could reveal precious information regarding the mechanisms behind host adaptation.

The IAV genome is composed of eight segments of RNA. The segment 8 (NS) has evolved into two distinct lineages – the 'A-' and 'B-alleles'. The B-allele NS genes are only rarely found in mammals and have been declared avian-restricted. However, when A- and B-allele NS genes were introduced into human H1N1 and H3N2 viruses, there was surprisingly little difference in virus replication in multiple mammalian cell types. Furthermore, the viruses replicated well and caused disease in mice, and the representative B-allele virus actually caused more severe disease than the A-allele counterpart. When computational analysis of available IAV sequences was performed, it was revealed that B-allele NS genes enter the mammalian population at a similar rate to A-allele genes. Thus, the data described in this study suggest that B-allele NS

segments are in fact able to complement virus replication in mammalian hosts and also contribute to severe disease. Thus, the dogma of the B-allele genes being avian restricted is misleading, and they should be considered when risk assessing the potential of avian IAV to cause outbreaks in domestic mammals and human pandemics.

Abstract

Influenza A virus (IAV) circulates in waterfowl, causing mostly asymptomatic infections. IAV can undergo host adaptation and evolve to cause significant disease and mortality in domestic poultry and mammals, applying an enormous socio-economic burden on society. Sporadically, IAV causes global pandemics in man due to its zoonotic nature, and this can result in millions of deaths worldwide during a single outbreak. Host adaptation of IAV is an incompletely understood phenomenon, but is known to involve both host and viral determinants. It is essential to improve the understanding of the factors governing host range and pathogenicity of avian IAV, especially given the absence of a universal influenza vaccine and a limited weaponry of effective antiviral compounds. This study set out to improve the understanding of host adaptation of avian IAV, focussing on segment 8 (NS segment) of the virus genome.

The NS segment of non-chiropteran IAV circulates as two phylogenetically distinct clades – the 'A-' and 'B-alleles'. The A-allele is found in avian and mammalian viruses, but the B-allele is considered to be almost exclusively avian. This might result from one or both of the major NS gene products (NS1 and NEP) being non-functional in mammalian host cells, or from an inability of segment 8 RNA to package into mammalian-adapted strains. To investigate this, the NS segments from a panel of avian A- and B-allele strains were introduced into human H1N1 and H3N2 viruses by reverse genetics. A- and B-allele reassortant viruses replicated equally well in a variety of mammalian cell types *in vitro*. Surprisingly, the consensus B-allele segment 8 out-competed an A-allele counterpart when reassortant H1N1 viruses were co-infected, with the parental WT segment 8 being most fit in this system. A- and B-

allele NS1 proteins were equally efficient at blocking the mammalian IFN response both in the context of viral infection and in transfection-based reporter assays. Consensus A- and B-allele H1N1 viruses also caused disease in mice and replicated to high virus titre in the lung. Interestingly, the B-allele virus induced more weight-loss than the A-allele, although the parental WT virus was most pathogenic *in vivo*.

To re-address the hypothesis that B-allele NS genes really are avian-restricted, the relative rates of independent *Aves* to *Mammalia* incursion events of A- and B-allele lineage IAV strains was estimated and compared using phylogenetic analyses of all publically available segment 8 sequences. 32 A-allele introduction events were estimated compared to 6 B-allele incursions, however the total number of avian A-allele sequences outnumbered B-allele sequences by over 3.5 to 1, and the relative rates of introduction were not significantly different across the two lineages suggesting no bias against avian B-allele NS segments entering mammalian hosts in nature. Therefore, this study provides evidence that avian B-allele NS genes are not attenuating in mammalian hosts and are able to cause severe disease. Thus, this lineage of IAV genes, previously assumed to be avian-restricted, should be considered when assessing zoonotic potential and pandemic risk of circulating avian IAVs.

Abbreviations

cDNA	Complementary deoxyribonucleic acid.
cRNA	Complementary ribonucleic acid.
DAPI	4',6-diamidino-2-phenylindole.
DNA	Deoxyribonucleic acid.
dsRNA	Double-stranded ribonucleic acid.
HA	Hemagglutinin.
HPAI	Highly pathogenic avian influenza.
IAV	Influenza A virus.
LPAI	Low pathogenic avian influenza.
M1	Matrix protein 1.
M2	M2 proton channel.
mRNA	Messenger ribonucleic acid.
MOI	Multiplicity of infection.
NA	Neuraminidase.
NEP	Nuclear export protein.
NP	Nucleoprotein.
NS1	Nonstructural protein 1.
PA	Polymerase acidic protein.
PB1	Polymerase basic protein 1.
PB2	Polymerase basic protein 2.
p.i.	Post-infection.
PCR	Polymerase chain reaction.
PFU	Plaque forming units.
RNA	Ribonucleic acid.
RNP	Ribonucleoprotein.
RT-PCR	Reverse transcription polymerase chain reaction.
SDS-PAGE	Sodium dodecyl sulfate polyacrylamide gel electrophoresis.
ssRNA	Single-stranded ribonucleic acid.
vRNA	Viral ribonucleic acid.
WT	Wild-type.

Chapter 1: Introduction to influenza A virus

1.1 General introduction to influenza A virus

Influenza A virus (IAV) belongs to the family *Orthomyxoviridae* and has a genome composed of eight molecules of negative sense, single-stranded RNA (McGeogh et al., 1976) (Fig 1.1). The natural host of IAV are wild aquatic birds of the orders Anseriformes and Charadriiformes which are reservoirs for all subtypes of IAV, although the virus can undergo host adaptation to infect a variety of avian and mammalian species (reviewed by (Webster et al., 1992)). The virus is subtyped by the antigenicity of its surface glycoproteins hemagglutinin (HA) and neuraminidase (NA). To date, there have been 16 HA subtypes and 9 NA subtypes described in avian viruses. Each strain of IAV contains one subtype each of HA and NA. All subtypes of both HA and NA have been isolated from wild aquatic birds, in the majority of possible combinations. Two chiropteran-specific subtypes of HA (H17 and H18) and NA (N10 and N11) have been described in bat isolates (Tong et al., 2012, Tong et al., 2013), which have not been seen in any other species.

Two forms of avian influenza viruses are described historically according to the severity of disease caused in the galliform host. IAV circulates in wild Anseriformes and Charadriiformes as an asymptomatic or low virulence form commonly referred to as ‘low pathogenic avian influenza’ (LPAI). LPAI replicates in cells lining the gut epithelium of waterfowl, is spread by the faecal-oral route, and remains infectious for a matter of weeks in cool lake water therefore promoting efficient spread within the natural host (Webster et al., 1978). LPAI can infect domestic poultry causing only mild or asymptomatic infections. The other form

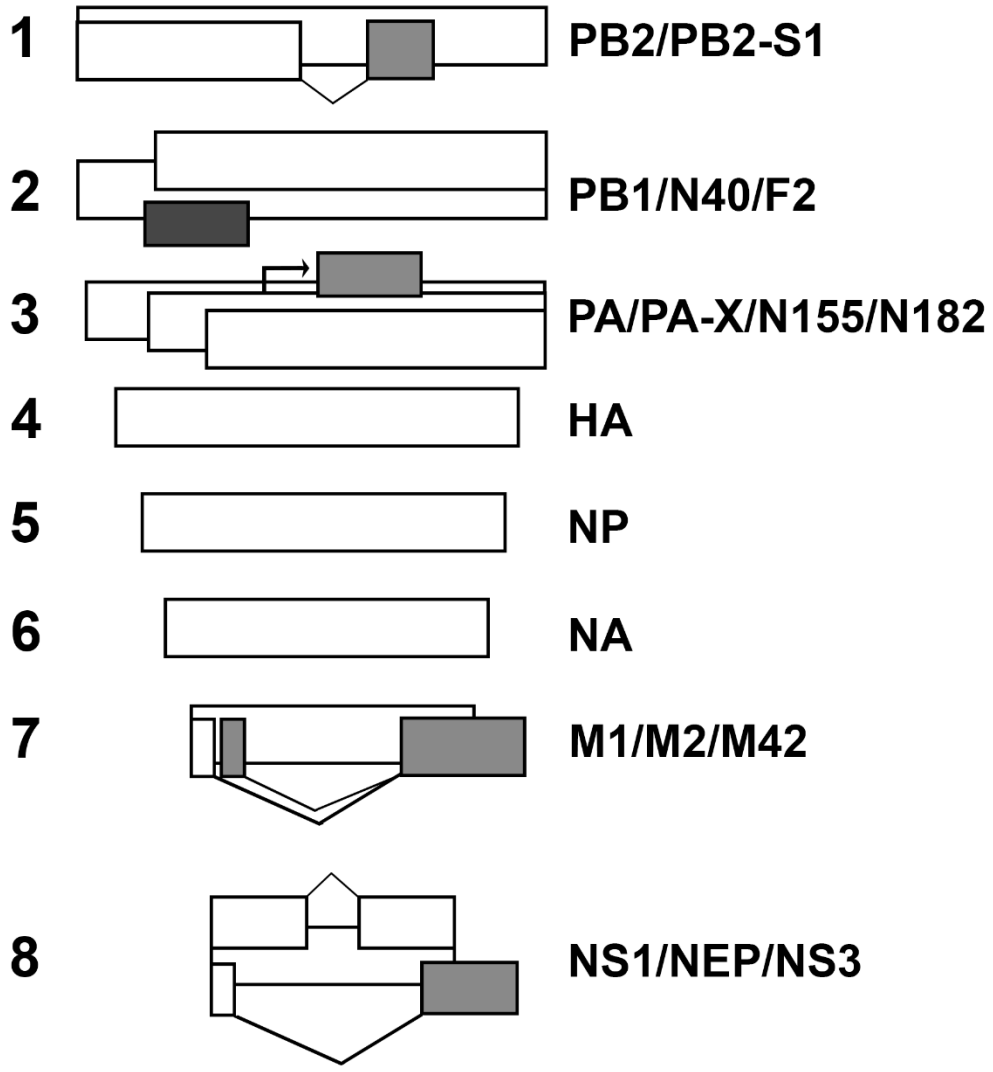

Fig 1.1. Influenza A virus genome. Shown is a schematic of the eight segments of the RNA genome and current known gene products. Coding regions are represented as rectangles with shading employed to denote alternative frames. The virus employs various protein coding strategies to express more than one protein per segment in certain cases. Splicing of mRNA is denoted by lines connecting two coding regions and ribosomal frame-shifting is shown by the right-angled arrow. Diagram represents an updated schematic presented by Jackson et al (Jackson et al., 2011).

consists of highly virulent strains that cause mortality rates of up to 100% within flocks within 2-3 days. This form is referred to as 'highly pathogenic avian influenza' (HPAI). HPAI infections in nature have, so far, only been reported with H5 and H7 subtypes, although not all H5 and H7 subtypes cause HPAI. Serious disease caused by HPAI is associated with systemic spread in the host and an exaggerated pro-inflammatory response, leading to severe pathology and often mortality (To et al., 2001, Cheung et al., 2002, de Jong et al., 2006, Cornelissen et al., 2013, Kuchipudi et al., 2014). HPAI has become endemic in poultry in certain regions, particularly in South East Asia, with devastating impact on the agriculture and food security sectors (Chen et al., 2006b).

Avian IAV can cross the host species barrier and evolve to cause severe disease and significant mortality in domestic mammals, including man. Human influenza virus predominantly targets the epithelial cells of the respiratory tract, and is transmitted directly or indirectly in airborne droplets with or without fomite contact (reviewed in (Killingley and Nguyen-Van-Tam, 2013)). IAV currently circulates in man as 'seasonal influenza' with subtypes of H1N1 and H3N2 (and previously H2N2, as discussed below). The term seasonal influenza is used as the antigenicity of the HA and NA changes over time, a process called antigenic drift, which allows the virus to escape established population immunity and cause annual epidemics, typically over the winter months. The World Health Organisation (WHO) estimate that 3-5 million people suffer severe illness and 250 000 - 500 000 people die every year from these seasonal epidemics (World Health Organisation, 2014).

Only H1, H2 and H3 subtype viruses have been confirmed to persist in humans to date. Infections with H5, H6, H7, H9 and H10 subtypes have all been noted but

these viruses tend to be isolated bird-to-human transmission events following direct contact with domestic birds (Schrauwen and Fouchier, 2014). It is through contact with domestic birds that HPAI can infect man and cause serious disease with high mortality rates. The first cases of HPAI H5N1 infections of humans occurred in 1997 in Hong Kong, from which 6 of 18 people infected died (reviewed in (Chan, 2002)). H5N1 HPAI re-emerged in China in 2003 and spread across the Middle-East to North-East Africa, and has caused over 400 deaths in humans since (World Health Organisation, 2016b). Beginning in March 2013, severe LPAI H7N9 infections of humans have been reported from contact with poultry in China (Gao et al., 2013). 133 human infections and 43 deaths were reported during the spring of 2013 (World Health Organisation, 2013) and the virus is still continuing to cause disease and fatalities in China (World Health Organisation, 2016a). Therefore, avian IAV continues to pose a significant threat to human health. Fortunately, avian viruses generally transmit poorly between humans, although there is evidence of limited human-to-human transmission (Wang et al., 2008a). There is a global fear that a highly pathogenic virus will infect humans, evolve to be able to spread rapidly, and cause another pandemic.

1.1.1 Influenza A virus pandemics

There have been five confirmed IAV pandemics in man since the 20th century, each of which are described below. All prevalence and mortality statistics reported below were taken from the World Health Organisation (WHO) pandemic influenza website (World Health Organisation, 2016c).

1.1.1.1 1918 H1N1 pandemic

The first IAV pandemic of the 20th Century was caused by an H1N1 virus that spread globally in 1918 (pdm1918 H1N1), commonly referred to as ‘Spanish Flu’. The

pdm1918 H1N1 is estimated to have caused approximately 50 million deaths worldwide and therefore represents one of the most deadly human pathogens in history. The virus caused particularly high mortality (estimated ~2.5%) in young adults (20-40 years old), the majority of whom probably perished from secondary bacterial pneumonia (Taubenberger and Morens, 2006, Morens et al., 2008). The origins of the pdm1918 H1N1 virus are still the subject of debate in the field. It has been proposed that a fully avian virus, or an avian virus with a human H1 subtype, adapted to humans (Taubenberger et al., 2005, Worobey et al., 2014c). Others have suggested that it arose from the genetic reassortment of viruses circulating in humans and swine (Smith et al., 2009). The impact of this pandemic was not only huge because of the number of associated fatalities, but also because all subsequent human pandemic strains are derived from pdm1918 H1N1, and descendants still continue to be endemic in humans and swine (Taubenberger and Morens, 2006).

1.1.1.2 1957 H2N2 pandemic

The 1957 H2N2 pandemic virus (pdm1957 H2N2), often referred to as 'Asian flu', incurred a much lower mortality rate than the pdm1918 H1N1 pandemic and caused approximately 1-4 million deaths worldwide. The pdm1957 H2N2 emerged following genetic reassortment of an avian H2N2 virus with a circulating human H1N1 virus – with the former donating HA, NA and polymerase basic protein 1 (PB1) segments (Scholtissek et al., 1978). H2N2 continued to circulate in humans for just over a decade, until the emergence of the 1968 H3N2 pandemic.

1.1.1.3 1968 H3N2 pandemic

The 1968 H3N2 pandemic (pdm1968 H3N2) virus, also known as 'Hong Kong flu', arose following reassortment of an avian H3 subtype virus with the circulating

H2N2 strain, resulting in an H3N2 virus harbouring avian-derived PB1 and HA segments (Scholtissek et al., 1978). The virus caused approximately 1-4 million deaths worldwide and has persisted in the human host as H3N2 seasonal influenza to date, having replaced the H2N2 subtype.

1.1.1.4 1977 H1N1 pandemic

The 1977 H1N1 strain (pdm1977 H1N1), also called 'Russian Flu', marked the re-introduction of an H1N1 virus circulating in man. The Russian Flu viruses were reported to be genetically very similar to H1N1 viruses circulating in the 1950s prior to the H2N2 Asian Flu outbreak, apparently missing years of evolution that would be expected from persistence in the human host (Nakajima et al., 1978). This has led to the suggestion of an accidental or deliberate release of the virus from a laboratory or live vaccine trial (Rozo and Gronvall, 2015). Given the close relation to H1N1 circulating in the 1950s, the pdm1977 H1N1 virus primarily caused mortality in young adults under the age of 25, as they had not been exposed to pre-circulating H1N1 and had not acquired immunological memory.

1.1.1.5 2009 H1N1 pandemic

In 2009 a swine-derived H1N1 virus (pdm2009 H1N1) emerged in humans and spread worldwide, originating in Mexico. Pdm2009 H1N1 spread efficiently between humans but mostly only caused mild infections, accounting for approximately 100 000 to 400 000 deaths within the first year of the outbreak. The virus was the result of reassortment between three lineages of swine influenza (Garten et al., 2009). The HA, nucleoprotein (NP) and nonstructural (NS) segments were derived from the 'classical swine' lineage, an H1N1 descendant of the pdm1918 H1N1 strain circulating in pigs in North America (Taubenberger and Morens, 2006). The NA and M segments were

derived from ‘Eurasian swine flu’, an avian virus that adapted to and has subsequently circulated in pigs in Europe and Asia since the late 1970s (Scholtissek et al., 1983). Finally, the polymerase segments PB2 (polymerase basic protein 2), PB1 and PA (polymerase acidic protein) were derived from ‘triple reassortant swine flu’, a lineage of swine flu that itself is a reassortment of avian, human and swine origin viruses (Zhou et al., 1999, Garten et al., 2009). Pdm2009 H1N1 is still circulating currently in man, having replaced the 1977 Russian Flu origin H1N1 strain.

1.2 IAV genome

The IAV genome is approximately 13.5 kb in size. Each segment encodes for at least one protein that is essential for virus replication. Table 1.1 summarises the main roles of all characterised IAV gene products. IAV utilises various protein coding strategies to expand the coding capacity of its small genome, which are outlined below in *1.2.2 Virus gene products and protein coding strategies* and represented diagrammatically in Fig 1.1.

1.2.1 Genomic viral RNA and ribonucleoproteins

Genomic viral RNA (vRNA) is normally encapsidated by multiple copies of the nucleoprotein (NP). One copy of each subunit of the trimeric viral polymerase (PB2, PB1 and PA) is also bound to the promoter region of vRNA forming the viral ribonucleoprotein (vRNP), the minimal unit of transcription and replication (Huang et al., 1990). NP binds to the phosphate backbone of vRNA with high affinity in a sequence-independent manner (Baudin et al., 1994). NP homo-oligomerises and binds RNA via an RNA-binding groove between two protein domains, with one NP covering

Table 1.1: Gene products of influenza A virus. Segment and protein sizes are based on A/Puerto Rico/8/1934 (H1N1).

Segment number	Segment name	Segment size (bases)	Gene product	Expression mechanism	Protein size (AA)	Main Role(s)
1	**PB2**	2341	PB2	Faithful transcription	759	Part of heterotrimeric polymerase. Binds host mRNA 5' cap for 'cap snatching' to prime viral mRNA transcription (Blaas et al., 1982)
			PB2-S1	Spliced mRNA	508	Inhibitor of RIG-I signalling (Yamayoshi et al., 2016).
2	**PB1**	2341	PB1	Faithful transcription	757	Part of heterotrimeric polymerase. Catalyses elongation of nascent RNA (Braam et al., 1983).
			PB1-N40	Alternative AUG site	718	Currently unknown
			PB1-F2	Alternative AUG site	87	Inhibits cellular MAVS to reduce IFN induction (Varga et al., 2012)
3	**PA**	2233	PA	Faithful transcription	716	Part of heterotrimeric polymerase. Endonuclease activity for 'cap snatching' of host mRNA 5' cap to prime transcription of IAV transcripts (Dias et al., 2009).
			PA-X	Ribosomal frame-shift	152	Endonuclease activity contributes to host cell shut-off (Jagger et al., 2012).
			PA-N155	Alternative AUG site	562	Currently unknown
			PA-N182	Alternative AUG site	535	Currently unknown
4	**HA**	1775	HA	Faithful transcription	565	Receptor binding, virus entry and virion budding.
5	**NP**	1565	NP	Faithful transcription	498	Encapsidation of vRNA and required for polymerase activity.
6	**NA**	1413	NA	Faithful transcription	454	Cleaves sialic acid receptors on surface of host cell to allow release of progeny virus and cleaves sialylated glycans in mucus to facilitate virus attachment to host cells.
7	**M**	1027	M1	Faithful transcription	252	Major structural protein of virion and involved in virus assembly and budding.
			M2	Spliced mRNA	97	Proton channel involved in acidification of virion during virus entry and required for membrane scission during virion budding.
			M42	Spliced mRNA	99	Modified version of M2 (Wise et al., 2012)
			M3	?	?	Protein expression not detected to date.
8	**NS**	890	NS1	Faithful transcription	230	IFN antagonism (Hale et al., 2008b)
			NEP	Spliced mRNA	121	Required for nuclear export of vRNPs (O'Neill et al., 1998).
			NS3	Spliced mRNA	187	Currently unknown.
			NSP	?	?	Protein expression not detected to date.
			tNS1	Alternative AUG site	150 or 152	Contributes to IRF inhibition (Kuo et al., 2016)

approximately 24 nucleotides to encapsidate the RNA (Ortega et al., 2000, Ye et al., 2006). Encapsidation reduces opportunity for the host cell to recognise non-self RNA and trigger an antiviral immune response which would be detrimental for virus replication. Each genomic segment contains conserved sequences at their termini (13 nucleotides at the 5' end, and 12 nucleotides at the 3' end) that have partial complementarity (Robertson, 1979). The polymerase sits on the panhandle structure in the RNA formed by this complementarity, holding the ends together (Hsu et al., 1987, Baudin et al., 1994, Klumpp et al., 1997). It is thought that PB1 forms the 'core' of the polymerase hetero-trimer and the overall structure is globular with multiple interactions between all subunits (reviewed in (Stubbs and te Velthuis, 2014)). vRNPs take the form of a helical filament, with the panhandle structure at one end opposite a helical loop structure at the other (Compans et al., 1972, Moeller et al., 2012, Arranz et al., 2012).

1.2.2 Virus gene products and protein coding strategies

Each segment of vRNA contains one major open reading frame (ORF) from which a protein product is translated following faithful transcription of mRNA. To date, it has been reported that IAV employs mRNA splicing, ribosomal frame-shifting, and alternative translation initiation mechanisms to expand its coding capacity.

1.2.2.1 Faithful mRNA transcription from vRNA

PB2, PB1 and PA are translated following transcription of unspliced mRNA from segments 1, 2 and 3 respectively. Segments 4 and 6 encode for the spike glycoproteins HA and NA respectively. Segment 5 encodes for NP, while unspliced mRNA transcribed from segments 7 and 8 are translated into matrix protein 1 (M1) and nonstructural protein 1 (NS1) respectively.

1.2.2.2 Splicing of viral mRNA

Unspliced PB2 mRNA is translated into the 759 amino acid PB2 protein. The PB2 mRNA can be spliced to express the recently described 508 amino acid PB2-S1 product, a gene product conserved in pre-2009 human strains of IAV (Yamayoshi et al., 2016). PB2-S1 shares the N-terminal 495 amino acids with PB2, but the C-terminal 13 amino acids are from the +1 reading frame. It has been suggested that PB2-S1 may inhibit RIG-I to dampen the IFN response during infection (Yamayoshi et al., 2016).

There are three spliced mRNA species from segment 7 described to date (mRNAs 2-4) which all share the same splice acceptor site, but utilise different 5' donor sites (Lamb and Choppin, 1981, Alonso-Caplen et al., 1992, Shih et al., 1998). mRNA 2 is translated into the M2 proton channel (M2) which shares its 9 N-terminal amino acids with M1 but the C-terminal 88 amino acids are translated from the +1 frame (Lamb and Choppin, 1981). mRNA 4 leads to M42 expression, a variant form of the M2 proton channel which shares its C-terminus with M2 but a distinct N-terminus translated from the second AUG in the mRNA and from the +1 frame (Wise et al., 2012). mRNA 4 is also predicted to lead to translation of an internally deleted version of M1 called M4, but this protein has not been detected to date (Shih et al., 1998, Wise et al., 2012). mRNA 3, which harbours an ORF with the potential to express a 9 amino acid product, has also been described. While protein expression has not been detected from this mRNA, there is evidence to suggest it regulates segment 7 gene expression (Shih et al., 1995).

Similarly, segment 8 mRNA is known to be spliced. The nuclear export protein (NEP), a 121 amino acid polypeptide essential for vRNP export from the nucleus during replication (O'Neill et al., 1998), is translated from spliced segment 8 mRNA

in all strains of IAV (Lamb and Lai, 1980). NEP shares its N-terminal 10 amino acids with NS1, but the C-terminal 111 amino acids are translated from the +1 reading frame. Another spliced mRNA of segment 8 leads to translation of nonstructural protein 3 (NS3) in a minority of strains that have acquired a mutation to introduce a splice acceptor site into the NS1 mRNA (Selman et al., 2012). NS3 represents an internally deleted version of NS1 that lacks residues 126-168, with a currently uncharacterised role in IAV replication (Selman et al., 2012).

1.2.2.3 Ribosomal frame-shifting

PA-X is a protein that shares the 191 amino acid endonuclease N-terminus of PA but has a strain-specific C-terminus of 41 or 61 amino acids translated from the +1 reading frame of PA mRNA (Jagger et al., 2012). PA-X is expressed following a ribosomal frameshift event during translation of segment 3 mRNA (Firth et al., 2012). The PA-X protein contributes to host cell shut-off by destroying cellular RNA polymerase II (pol II) transcripts (Jagger et al., 2012, Khaperskyy et al., 2016). It is the only IAV protein currently described that is translated following a ribosomal frame-shifting event.

1.2.2.4 Alternative translation initiation events

PB1 mRNA has several start codons downstream of the conventional AUG for PB1 expression, which can be utilised in an alternative translation initiation process (Wise et al., 2011). PB1-F2 is expressed from the fourth start codon in PB1 mRNA in the +1 reading frame with respect to PB1. PB1-F2 has been reported to induce cell death and also inhibit interferon (IFN) production in the host cell (Chen et al., 2001, Varga et al., 2011). PB1-N40 is an N-terminally truncated version of PB1 translated from the fifth start codon in PB1 mRNA, lacking the N-terminal 39 amino acids, with

a currently unknown function (Wise et al., 2009). PA-N155 and PA-N182 are expressed from the highly conserved in-frame AUG codons in segment 3 mRNA at codon positions 155 and 182, respectively, and therefore are N-terminally truncated (154 amino acids and 181 amino acids respectively) forms of PA that lack the endonuclease domain with currently unknown functions (Muramoto et al., 2013). Recently, alternative in-frame start codons in NS1 mRNA have been shown to be used which leads to translation of N-terminally truncated versions of NS1 (tNS1) (Kuo et al., 2016). The second and third in-frame codon of NS1 mRNA lie at codons 79 and 81 which can both be used to yield a truncated version of NS1, of approximately 17 kDa, that contributes to IFN antagonism (Kuo et al., 2016). It has also been suggested that segment 8 vRNA contains an ORF in the opposite sense to mRNA that may be utilised, but no protein product has been detected to date (Zhirnov et al., 2007, Clifford et al., 2009).

1.3 Influenza virions

Influenza virions are pleomorphic and can adopt either a spherical or filamentous morphology (Mosley and Wyckoff, 1946). Lab-adapted strains tend to be predominantly spherical with a typical diameter of 100 nm, while clinical isolates tend to be filamentous and can be up to 20 μm in length with a 100 nm diameter (Mosley and Wyckoff, 1946, Harris et al., 2006). A schematic of a spherical influenza virion is shown in Fig 1.2. The structural support of the virion is provided by oligomerised M1 that forms a 'shell' underlying the host-derived phospholipid bilayer envelope. Embedded in the lipid envelope are the rod-shaped 'spike' glycoproteins HA and NA that protrude outwards (Laver and Valentine, 1969), as well as the homotetrameric integral membrane M2 proton channel (Zebedee and Lamb, 1988). HA exists as a

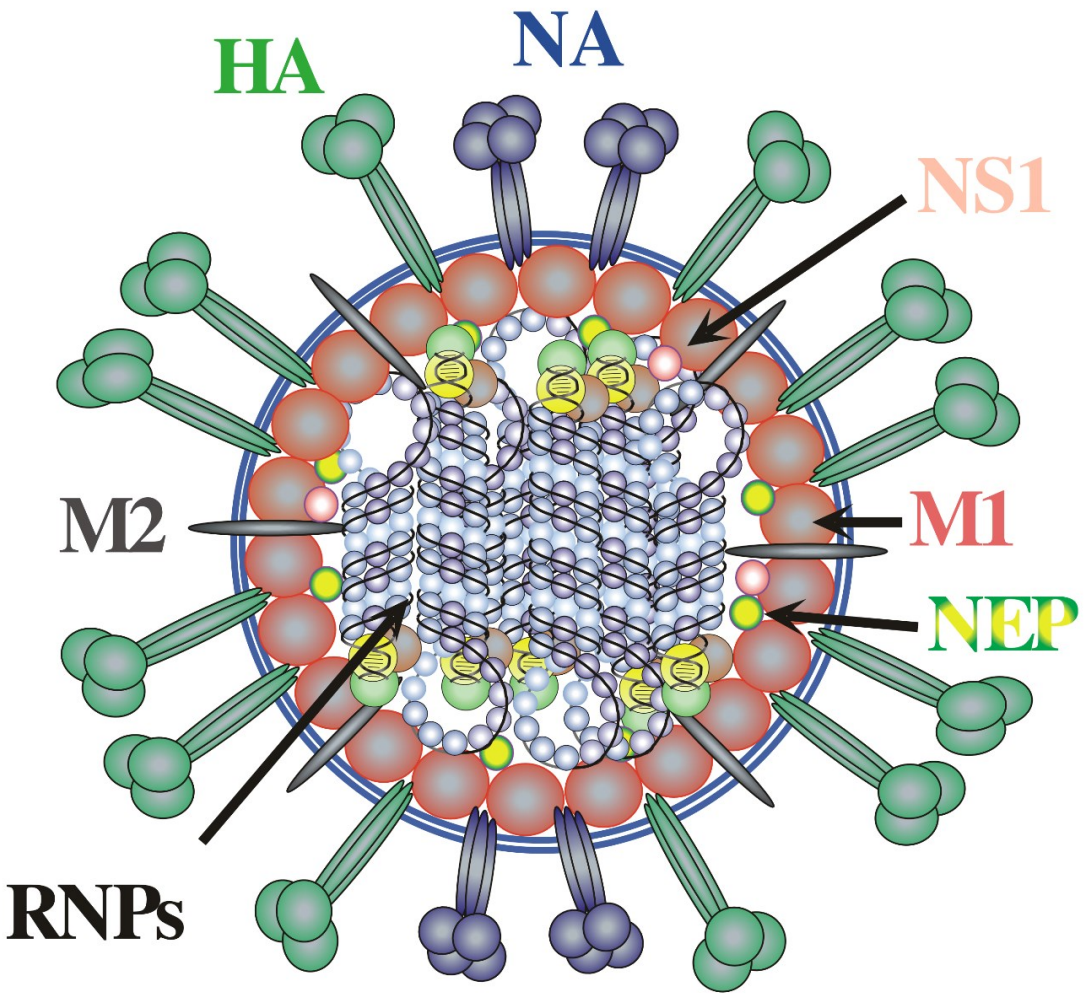

Fig 1.2. Spherical influenza A virion. Shown is a cartoon of a spherical influenza A virion. Oligomers of the M1 protein provide a structural 'shell' to the virion, which lie beneath the host-derived lipid bilayer envelope. Surface glycoproteins HA and NA protrude outwards, embedded in the envelope by a transmembrane region located in the stem. The M2 proton channel is also embedded in the envelope. The ssRNA genome is encapsidated by multiple copies of NP. The heterotrimeric polymerase sits on the panhandle structure formed by complementation of the conserved sequences found at the termini of vRNA, forming the vRNP. One vRNP unit per segment of the genome is packaged per virion. Cartoon drawn by, and included with permission from, Prof. Paul Digard (The Roslin Institute, The University of Edinburgh, UK).

trimer, and NA a tetramer, in the lipid envelope. The number of HA molecules on the virus surface is thought to be present approximately four times more than NA; thus it is the dominant surface antigen of IAV (Webster et al., 1968). The vRNPs are packaged into the space within the M1 support layer, along with a few copies of NS1 and NEP and other cellular factors that are incorporated during virus assembly and budding (Richardson and Akkina, 1991, Hutchinson et al., 2014). M1 forms interactions with both the lipid envelope and the vRNPs, the latter through interaction with NP (Ruigrok et al., 2000, Noton et al., 2007, Noton et al., 2009). Scanning transmission electron microscopy has allowed the 3D reconstruction of the structure of vRNPs in virions, and a '7+1' arrangement has been proposed in which 7 segments encircle a central segment within the virion (Noda et al., 2012).

1.3.1 Hemagglutinin structure and cellular processing

As HA is involved in multiple aspects of IAV biology that are referred to throughout this chapter, a short introduction on its structure and cellular processing is outlined here. HA is co-translationally inserted into the host cell endoplasmic reticulum (ER) as a homotrimer of precursor polypeptides termed HA_0. The trimer is transported to the cell surface via the trans-Golgi network where it is incorporated into the plasma membrane prior to virus budding (reviewed in (Skehel and Wiley, 2000)). HA_0 contains a C-terminal transmembrane domain, a protease cleavage site, and a fusion peptide that mediates virus entry (Skehel and Wiley, 2000). HA undergoes proteolytic cleavage by cellular trypsin-like or furin-like proteases into its activated conformation: a prerequisite for virus entry into newly infected cells (Klenk et al., 1975). The sequence of the protease cleavage site determines its susceptibility to cleavage by proteases and therefore whether cleavage occurs intracellularly before

reaching the plasma membrane or extracellularly (Klenk and Garten, 1994). Post-cleavage, the two resulting peptides (HA_1 and HA_2) are held together by a disulfide bridge. HA_1 comprises the N-terminal region and HA_2 the C-terminal region containing the transmembrane domain, which is inserted into the lipid envelope of the virion, and also the fusion peptide (Skehel and Wiley, 2000). The ectodomain is composed of a 'stem', a triple stranded coiled-coil of α-helices formed by both the HA_1 and HA_2 peptides, and a globular 'head' of anti-parallel β-sheets which contains the receptor-binding site and the major epitopes for antibody binding formed by the HA_1 peptide (Skehel and Wiley, 2000). Each monomer of the HA trimer has a receptor binding site located in a depression on the top of the HA trimer, distal to the transmembrane C-terminal stem (Weis et al., 1988).

HA is N-glycosylated in both the stem and head regions, which is important for function. The glycosylation of the head region is variable between HA subtypes and contributes to immune evasion by blocking antibody access to epitopes (Skehel et al., 1984), but in the stem region oligosaccharides are more conserved and are important for HA stability and membrane fusion (Ohuchi et al., 1997).

1.4 Virus life cycle

A defining aspect of IAV biology is that all RNA synthesis occurs in the nucleus, which is uncommon for RNA viruses. One immediate advantage of this is the utilisation of the host splicing machinery to expand the coding capacity of the virus. Additionally, this may help reduce the likelihood of activating cytoplasmic sensors of viral RNA and triggering an immune response. Nuclear replication also grants easier access to host messenger RNA (mRNA) transcription and processing machinery,

which is important for replication as described in this section. A schematic of the influenza replication cycle is shown in Fig 1.3.

1.4.1 Virus entry

IAV infection begins with the attachment of virion(s) to the surface of a host cell. The HA protein binds to N-acetylneuraminic (sialic) acids commonly found at the termini of various glycol-conjugates on the surface of host cells (Johnson et al., 1964). Spherical virions bound on the surface of cells are internalised by clathrin-mediated endocytosis, triggered by activation of cellular receptor tyrosine kinases (Eierhoff et al., 2010), while filamentous virions enter via micropinocytosis (Rossman et al., 2012). To enter the cell cytoplasm, the virus must fuse its own membrane with that of the endosome. Membrane fusion is carried out by cleaved HA. In the N-terminus of the HA_2 peptide, adjacent to the protease cleavage site, lies a hydrophobic stretch of 20-25 amino acids known as the fusion peptide. Following acidification of late endosomes, cleaved HA undergoes a pH-dependent conformational change allowing the insertion of the fusion peptide into the endosome membrane, thus HA is inserted into both viral and endosomal membrane at this point (Jardetzky and Lamb, 2004). Multiple HA trimers undergo this conformational change. This is then followed by further substantial protein re-folding, bringing the fusion peptide (in the endosomal membrane) close to the C-terminal transmembrane domain of HA (in the viral envelope), thus bringing the two membranes into close proximity. The energy released following this conformational change provides the energy for the two membranes to fuse (Jardetzky and Lamb, 2004). H^+ ions also pass through the M2 proton channel to acidify the virion interior, and this disrupts protein-protein interactions between M1

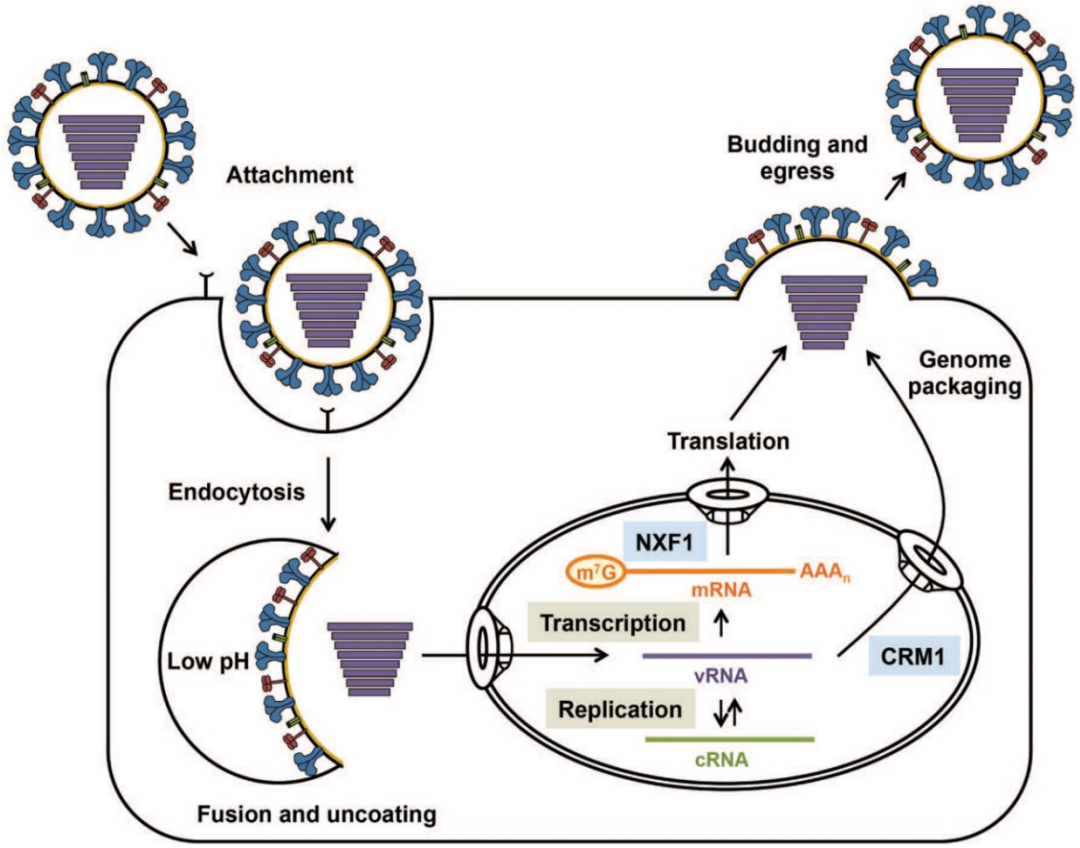

Fig. 1.3. Schematic of virus life cycle. Shown is a diagram of the IAV replication cycle. The virus enters the host cell following attachment of HA to sialic acids on the cell surface and subsequent endocytosis. Acidification of endosomes triggers membrane fusion driven by HA and entry of vRNPs. vRNPs enter the nucleus where transcription and replication takes place. Newly synthesised copies of the virus genome assemble with translated viral proteins to form progeny vRNPs, which undergo nuclear export and trafficking to the cell surface. Virus assembly and budding occurs and infectious virus particles are released to infect new cells. Figure is taken from (York and Fodor, 2013).

and vRNPs (Bui et al., 1996). Free vRNPs are then able to enter the cytoplasm of the cell, completing virus entry.

1.4.2 Nuclear import of vRNPs and transcription and replication machinery

The nucleus is surrounded by a double membrane known as the nuclear envelope. Supramolecular protein assemblies termed nuclear pore complexes (NPCs), mediate molecular exchange between the nucleus and the cytoplasm through the nuclear envelope. Ions and molecules with a radius of 2.6 nm or below can passively diffuse through the NPC, but anything larger must be actively transported using signal-dependent mechanisms and specific receptors (Eibauer et al., 2015). Soluble transport proteins, such as importins which belong to the karyopherin family of proteins, can bind directly to cargo and mediate shuttling into the nucleus, (Stewart, 2007). Importins bind cargo containing a nuclear localisation signal (NLS) in the cytoplasm, transport it through the NPC by interacting with nucleoporins, and dissociate from their cargo in the nucleus. The import pathway can be referred to as classical or non-classical. In classical nuclear import, the NLS contains basic amino acids arranged in either a single cluster or a bipartite motif separated by a short linker. The NLS interacts with an importin α isoform, of which six have been described in man (α1, α3, α4, α5, α6, α7) which in turn interacts with importin β1 before entering the nucleus. Alternatively, a non-classical pathway can be employed using a different NLS and transport protein. There have been several non-classical pathways described, for example a direct interaction of the NLS with an importin-β isoform (Cingolani et al., 2002).

vRNPs are too large to diffuse through the NPC, so active transport is required for nuclear import. The pH-induced dissociation of M1 from vRNPs exposes NLSs on NP which drive vRNP nuclear import (O'Neill et al., 1995). There have been three NLSs described in NP, but an N-terminal 'unconventional' NLS, NLS1 (1-MASQGTKRSYxxM-13), is thought to be the major driver of vRNP nuclear import (Bullido et al., 2000, Cros et al., 2005, Hutchinson and Fodor, 2012) . The subtype of importin-α utilised by IAV vRNPs has been shown to be strain-specific (Gabriel et al., 2011). Once in the nucleus, the viral polymerase can carry out a primary round of transcription and the viral mRNAs are subsequently exported to the cytoplasm for translation.

Viral polymerase components that are translated in the cytoplasm require nuclear import to aid further transcription and replication of the genome. As these translated polymerase components do not exist as RNPs, different nuclear import mechanisms are employed. Two regions of PB2 are required for nuclear import. Residues 449–495 and a C-terminal bipartite NLS (738-KRx_{12}KRIR-755) are required for classical nuclear import using importin α5 (Tarendeau et al., 2007). PB1 and PA must interact and form heterodimers in the cytoplasm prior to nuclear import, which is via a non-classical pathway utilising ran binding protein 5 (Fodor and Smith, 2004, Deng et al., 2006b). It is thought that a bipartite NLS (187-RKRRx_{16}KRKQR-211) in PB1 mediates the interaction with ran binding protein 5 (Hutchinson et al., 2009, Hutchinson and Fodor, 2012). As mentioned above, NP utilises the classical import pathway to enter the nucleus. Now, all components required for transcription and replication of the virus genome are localised to the nucleus to carry out further RNA synthesis.

1.4.3 Transcription and replication of the IAV genome

All transcription and replication of the viral genome is conducted by the trimeric polymerase. The panhandle structure formed by complementarity of the 5' and 3' ends of the encapsidated vRNA serves as the promoter for this (Luytjes et al., 1989). Each of the eight vRNPs of the IAV genome serve as a separate transcription unit. Transcription is primed by a 'cap-snatching' mechanism, which involves the binding to and cleavage of RNA fragments (10-13 nucleotides in length) containing a 5' 7-methylguanosine cap (m^7GpppX^m) from host precursor mRNAs (pre-mRNAs) to provide a primer for viral transcription (Plotch et al., 1981). The IAV polymerase interacts with actively transcribing RNA polymerase II, and this may allow easier access to a pool of host capped pre-mRNAs (Engelhardt et al., 2005). The binding of the polymerase to host pre-mRNA 5' caps is mediated by the PB2 subunit (Blaas et al., 1982). The PA subunit of the polymerase harbours endonuclease activity in its N-terminal 209 residues, and this conducts the cleavage of the cap (Hara et al., 2006, Yuan et al., 2009, Dias et al., 2009). PB1 harbours the polymerase function, catalysing RNA elongation reading the vRNA as a template in the 3' to 5' direction (Braam et al., 1983). Transcription is terminated at a 5-7 nucleotide long poly(uridine) (poly(U)) stretch located 15-17 nucleotides from the 5' end of the vRNA template (Robertson et al., 1981). It is thought that the 5' end of vRNA is associated with the polymerase throughout transcription while the template is 'threaded' through the PB1 active site in the 3' to 5' direction, and when the polymerase reaches the poly(U) stretch it cannot move any further due to steric hindrance causing the active site to pause over the poly(U) tract (Moeller et al., 2012). The poly(U) stretch serves as a template for polyadenylation of the 3' end of nascent mRNA by reiterative stuttering of the viral

polymerase (Poon et al., 1999). Therefore, the nascent viral mRNA resembles a mature host mRNA with a 5' 7-methylguanosine cap and a 3' poly(A) tail. The viral mRNA can then assemble into messenger ribonucleoproteins (mRNPs) and utilise the host cell nuclear export and translation machinery for protein expression, with or without splicing depending on the segment.

In contrast to transcription, genome replication utilises a full, positive-sense, copy of vRNA as an intermediate template termed complementary RNA (cRNA). Therefore, there are two stages of genome replication: i) synthesis of cRNA using vRNA as a template and ii) synthesis of vRNA using cRNA as a template. Both cRNA and vRNA contain a 5' triphosphate moiety, suggesting genome replication is primer-independent (Hay et al., 1982). The precise mechanism of initiation of cRNA and vRNA synthesis is the subject of debate, but involves different strategies for both (Deng et al., 2006a, Zhang et al., 2010). Nascent RNA synthesised during replication is encapsidated by free NP and polymerase subunits in the nucleus to form progeny vRNPs, and these will subsequently undergo nuclear export prior to virus assembly and egress. One copy of cRNA can provide a template for multiple rounds of vRNA synthesis, and cell-fractionation studies have shown that cRNA remains in the nucleus throughout infection (Shapiro et al., 1987, Tchatalbachev et al., 2001).

It is currently not fully understood how the viral polymerase distinguishes between transcription and replication functions, since the same promoter is used in both instances. Some studies have implied a role of accumulating viral proteins following translation, such as NEP, while others have suggested a role for small RNAs (22-27 nucleotides in length) corresponding to the 5' end of vRNA which appear important for vRNA synthesis (Robb et al., 2009, Perez et al., 2010). Another model

proposes that newly synthesised *trans*-acting polymerases associate with free 5' ends of vRNA and synthesise cRNA, whilst the 3' end is still associated with the original polymerase of the vRNP (Moeller et al., 2012, Fodor, 2013). However, there is conflicting data in the literature regarding this mechanism which needs further study (Fodor, 2013).

1.4.4 Viral mRNA processing

After transcription of viral mRNAs is complete, they are thought to resemble host mature mRNAs during the processes of splicing, nuclear export and translation and are therefore processed in a similar fashion (Amorim et al., 2007, Read and Digard, 2010, Bier et al., 2011, York and Fodor, 2013). All splicing of viral mRNAs that contain an intron is performed by the host splicing machinery, although viral proteins, such as NS1, may regulate this process (Robb and Fodor, 2012).

Mature cellular mRNAs interact with a host of proteins during nuclear export, including the cap binding complex (CBC), poly(A) binding proteins, and the transcription/export complex (TREX). The major nuclear export factor for cellular mRNA through the NPC is the nuclear export factor 1 (NXF1) pathway. It is thought that the 5' end of nascent viral mRNA is released from the transcribing polymerase, allowing the binding of the CBC which initiates mRNP assembly (Bier et al., 2011). The observation that the viral polymerase interacts with actively transcribing cellular RNA pol II suggests that newly synthesised viral mRNAs will be in close proximity to host proteins involved in mRNA assembly into mRNPs (Engelhardt et al., 2005). Indeed, inhibition of cellular RNA pol II leads to retention of viral transcripts in the nucleus, suggesting that nuclear export is reliant on host transcription (Amorim et al., 2007). Viral mRNA has been shown to interact with the CBC, the RNA and export

factor which is part of the TREX, and also NXF1, suggesting they utilise similar pathways to host mRNA nuclear export (Wang et al., 2008b, Hao et al., 2008, Read and Digard, 2010, Bier et al., 2011). However, there is also evidence that specific viral mRNAs may utilise alternative nuclear export pathways other than NFX1 (Read and Digard, 2010, Larsen et al., 2014). Eukaryotic initiation factor 4E (eIF4E) was also found to bind to viral mRNAs, providing evidence that viral mRNAs are recruited to ribosomes and translated as cellular mRNAs would be (Bier et al., 2011).

1.4.5 Nuclear export and trafficking of vRNPs

At later stages of infection, progeny vRNPs must undergo nuclear export and trafficking to the plasma membrane for virion assembly and virus budding in order to infect new host cells. IAV vRNPs utilise the nuclear transport factor chromosome region maintenance (CRM1), also called exportin 1, to actively transport vRNPs across the NPC into the cytoplasm- as demonstrated by nuclear retention of vRNPs following addition of a specific CRM1 inhibitor leptomycin B (Elton et al., 2001, Watanabe et al., 2001). CRM1 binds to leucine-rich nuclear export signals (NES) on cargo, and also to Ran-GTP (guanosine triphosphate-binding nuclear protein Ran), and traverses the NPC by interacting with nucleoporins. Once in the cytoplasm, Ran-GAP (Ran-GTPase activating protein) catalyses the conversion of Ran-GTP to Ran-GDP (Ran-guanosine diphosphate), and results in dissociation of CRM1 from its cargo.

After progeny vRNPs are made in the nucleus, they are trafficked to the nuclear periphery where they tether to chromatin, which may improve access to the CRM1-mediated nuclear export pathway (Chase et al., 2011). Both M1 and NEP have been shown to be essential for vRNP export (Martin and Helenius, 1991, O'Neill et al., 1998). The NEP of IAV has two NESs (NES 1: 12-ILMRMSKMQL-21 and NES 2:

31-MITQFESLKL-40) and it is thought that NES 2 forms the predominant interaction with CRM1, while NES1 interacts with cellular chromodomain-helicase-DNA-binding protein 3 (CHD3) to aid recruitment to chromatin to increase exposure to CRM1 (O'Neill et al., 1998, Neumann et al., 2000, Huang et al., 2013, Hu et al., 2015b). NEP has not been associated with binding to vRNPs alone, but M1 and NEP are known to interact via the NLS on M1 and a site including tryptophan-78 of NEP (Yasuda et al., 1993, Akarsu et al., 2003). Therefore, a proposed model implicates the M1 protein in forming a 'bridge' to connect vRNPs to the NEP, and CRM1-mediated nuclear export is facilitated by NEP-CRM1 interactions.

Once in the cytoplasm, vRNPs need to reach the plasma membrane prior to virus assembly and budding. vRNPs associate at the microtubule organisation centre (MTOC) at the outside of the nucleus following nuclear export, which requires an interaction with cellular Y-box-binding protein 1 (YB-1) (Amorim et al., 2011, Kawaguchi et al., 2012). It is thought that vRNPs 'piggy-back' on Rab11 GTPase-positive recycling vesicles that are trafficked to the apical membrane on tubulin networks (Momose et al., 2011, Amorim et al., 2011, Eisfeld et al., 2011). Rab11 interacts with vRNPs via the PB2 subunit of the polymerase (Amorim et al., 2011), and there is thought to be a form of dissociation mechanism at the apical membrane, as Rab11 has not been detected in virions to date (Hutchinson et al., 2014, Eisfeld et al., 2015).

1.4.6 Virus assembly and budding

All eight genomic RNA segments must package into a budding particle for it to be infectious. Available data has revealed that a segment-specific packaging mechanism is utilised, rather than a random packaging mechanism (reviewed in

(Hutchinson et al., 2010)). Electron tomography and scanning transmission electron microscopy data revealed that the majority of virions contain eight segments (Noda et al., 2006, Noda et al., 2012). Additionally, fluorescent in situ hybridisation studies on RNA inside captured IAV virions also suggested that each of the eight segments are present in one copy per virion in the majority of particles (Chou et al., 2012).

Each segment of the IAV genome contains conserved RNA 'packaging signals' in the terminal coding and non-coding regions (Duhaut and McCauley, 1996, Fujii et al., 2003, Gog et al., 2007). IAV displays a lack of synonymous variation within these regions, and synonymous mutations of these conserved codons can reduce packaging efficiency (Fujii et al., 2003, Gog et al., 2007, Hutchinson et al., 2008). These terminal sequences are also sufficient to allow packaging of non-IAV RNA into budding virions in place of a genuine IAV segment (Liang et al., 2005). Therefore it is thought that these RNA signals mediate segment-specific packaging to ensure one copy of each segment is incorporated into a budding virion. The precise mechanism of how the virus utilises these signals (RNA-RNA or RNA-protein interactions) to mediate selective packaging is still debated, although there is accumulating evidence to suggest RNA-RNA interactions are important (reviewed in (Gerber et al., 2014).

The assembly and packaging of the vRNPs into the virion is thought to be driven by interactions between the integral membrane proteins HA, NA and M2, with M1, which in turn interacts with vRNPs. IAV utilises lipid rafts for sites of budding – regions of the plasma membrane that are rich in cholesterol and sphingolipids (Scheiffele et al., 1999). HA and NA molecules naturally congregate at lipid rafts and insert into the membrane (Leser and Lamb, 2005), while M2 accumulates in areas of the membrane directly adjacent to lipid rafts (Rossman et al., 2010). Deletion or

mutation of the cytoplasmic tails of HA or NA reduce lipid raft association, cause abnormal virion morphology, and inhibit virus assembly (Zhang et al., 2000, Takeda et al., 2003), and mutation to the M2 cytoplasmic tail interferes with the M1-M2 interaction and inhibits efficient virus assembly (Chen et al., 2008). Therefore it is thought that the cytoplasmic tails of HA, NA and M2 all interact with M1 (which will in turn be interacting with NP of vRNPs) and this interaction is important for virus assembly at points of budding.

Insertion of HA and NA into the plasma membrane initiates membrane curvature and budding. Additionally, it has been shown that cellular F-type proton-translocating ATPase (F_1F_o-ATPase) is required for efficient budding and is recruited by NEP (Gorai et al., 2012), suggesting that host factors are also likely to be important in the process. M1 is recruited to sites of budding by interactions with the cytoplasmic tails of HA, NA and M2. M1 monomers will polymerise following these interactions, possibly through an induced conformational change, and begin to form the structural 'shell' of the virion underneath the host-derived lipid bilayer, with which it forms electrostatic interactions (Ruigrok et al., 2001). vRNPs arrange in the '7+1' arrangement perpendicular to the budding tip (Noda et al., 2006), and are packaged into the budding virion through interactions with the M1 oligomers. Once the membrane has curved sufficiently, M2 performs membrane scission by insertion of an amphipathic helix in its cytoplasmic tail into the membrane, inducing positive membrane curvature at the neck of the budding virion (Rossman et al., 2010). The fact that M2 localises to the membrane adjacent to lipid rafts will concentrate M2 molecules at the neck of the budding virion to aid scission (Rossman et al., 2010). Finally, the NA on the surface of the virion enzymatically cleaves sialic acid receptors

to prevent re-attachment of progeny virions to the cell that has already been infected, allowing release of virions to infect new cells (Palese et al., 1974).

1.5 Influenza A virus evolution

1.5.1 Antigenic drift

Antigenic drift describes the gradual mutation of the epitope regions of viral surface proteins with time, resulting in structurally distinct antigenic regions that can 'escape' existing host acquired adaptive immune responses (neutralising antibodies). Drift arises from a high error rate of the viral RNA polymerase that lacks a proof-reading mechanism. It is estimated that the virus polymerase makes one error every time the full genome is replicated (Drake, 1993). Indeed, it is thought that for every round of virus replication in an infected cell, a 'quasi-species' of virus is released, the majority with a mutation(s) in the genome with respect to the original infecting virus (Lauring and Andino, 2010). Most mutations will be deleterious to the virus, compromising replicative ability, and these mutant viruses will not propagate well. Some mutations will be advantageous for replicative fitness and these mutations can become dominant in the virus population over multiple rounds of replication.

Antigenic drift explains the seasonal nature of H1N1 and H3N2 outbreaks in man. Population humoral immunity to circulating viruses will become ineffective as antigenic drift causes divergence in the epitopes of the virus – most notably the receptor binding 'head' of HA. This phenomenon provides a serious challenge in developing efficient universal vaccines.

1.5.2 Antigenic shift

Antigenic shift describes the swapping of genetic material between two or more viruses by reassortment leading to the emergence of a new subtype of virus in a population. Reassortment is the 'swapping' of genome segments between two or more genetically distinct viruses that co-infect the same host cell at the same time. If the resulting combination of segments produces a viable virus that can successfully replicate, a 'reassortant' virus emerges. This provides an opportunity for the virus to mutate extremely rapidly and to a dramatic extent. This also provides an opportunity for genetic material to cross the host species-barrier by reassorting into a virus background that is adapted to a different host species. In addition, Anseriform and Charadriiform birds can carry IAV by seasonal migration over a range of distances that can span across continents, allowing long range transmission and also genetic reassortment between strains that would be otherwise geographically separated (Olsen et al., 2006).

Sequence and surveillance data suggest genetic reassortment occurs between viruses that are adapted to different host species, allowing the emergence of new subtypes within a particular host (reviewed in (Steel and Lowen, 2014)). Reassortment events between avian and mammalian IAV strains were pivotal in the induction of four of the five reported human influenza pandemics during the last century (see *1.1.1 Influenza A virus pandemics*). Similarly, reassortment within wild and domestic birds was important for the evolution of HPAI H5N1 viruses that are endemic in South East Asia in wild and domestic birds (Steel and Lowen, 2014, Schrauwen and Fouchier, 2014). Reassortment poses a serious challenge in the control of IAV.

1.6 Control of influenza A virus

The rapid evolution of the virus presents a major challenge in developing efficient vaccines and antivirals due to the selection of resistant strains. Currently, there is a lack of an effective universal vaccine, and only a limited supply of fully effective antiviral compounds.

1.6.1 Vaccination

The aim of vaccination is to elicit an adaptive immune response in the host, by the administration of antigen, that will be activated upon subsequent infection of the pathogen and prevent severe infection. The main antigen of IAV for activation of the adaptive immune response lies in the membrane-distal receptor-binding 'head' of the HA surface glycoprotein, although NA also contains significant epitopes. The epitopes in the HA globular head are too distinct between (and even within) different subtypes for a vaccine to be designed targeting all strains of the virus (Wiley and Skehel, 1987). Instead, either a trivalent inactivated vaccine (TIV) is used which includes antigens for relevant circulating human H1 and H3 strains, and also a relevant circulating influenza B virus strain, or a trivalent live attenuated virus vaccine (TLAV) is used (reviewed in (Pica and Palese, 2013)). More recently, TIVs are becoming phased out and replaced by a quadrivalent inactivated vaccine (QIV) which includes an additional influenza B lineage strain (Beran et al., 2013). Inactivation of viruses in TIVs is achieved by treatment of purified virus with non-ionic detergents, while live-attenuated viruses are cold-adapted and can only replicate well in the cooler temperatures of the nasal epithelium (Pica and Palese, 2013). TIVs or QIVs are usually administered intramuscularly while TLAVs are administered intranasally. Vaccines are usually

offered to children, elderly, immunocompromised or individuals with current respiratory complications such as asthma.

Antigenic drift of IAV requires new vaccines to be made each year. The World Health Organisation are responsible for selecting which virus strains are included in annual vaccines and this process involves consulting surveillance data to choose appropriate candidates. Reassortment is the current method of choice for generating vaccines by co-infecting eggs with a high-growth virus (e.g. the lab-adapted A/Puerto Rico/8/1934 (H1N1); PR8) and a strain containing the surface glycoproteins of interest, and selecting the highest growing reassortant virus containing the HA and NA of interest (Fulvini et al., 2011). The high-growth background of PR8 permits high HA titre in egg-grown stocks, the equivalent of which would not be achievable with wild-type clinical strains. This process of vaccine production can take months, which highlights the importance of developing and stockpiling effective antiviral compounds in the case of a new outbreak.

Vaccines directed against broadly conserved regions (universal vaccines), which in theory would be much more difficult for viruses to escape from by antigenic drift, are the focus of much research. Examples include targeting the ectodomain of the M2 proton channel, the conserved stem region and protease cleavage site of HA, conserved sites near the enzymatic active site or cytoplasmic tail of NA, and also inducing a T-cell response to conserved viral epitopes in NP and M1 (reviewed in (Pica and Palese, 2013)). This area of research presents a very promising avenue of potential in the bid to control IAV.

1.6.2 Antivirals

In the absence of effective universal vaccines, antiviral drugs provide much needed prophylaxis of IAV during major outbreaks. Currently, there are two classes of FDA-approved antiviral drugs for IAV treatment: i) Neuraminidase inhibitors oseltamivir (Tamiflu™), zanamivir (Relenza™) and the more recently approved peramivir (Rapivab™) and laninamavir (Inavir™) and ii) adamantanes (adamantine and rimantadine) that inhibit the M2 proton channel. Adamantanes were traditionally the drug of choice, but preference has switched to NA inhibitors as adamantane-resistant IAV strains have become widespread.

Adamantanes were the first antiviral drugs to be approved for the treatment of IAV infection. The adamantanes used as antivirals against IAV are amantadine (1-aminoadamantane hydrochloride) and rimantadine (α-methyl-1-adamantane methylamine hydrochloride). Amantadine and rimantadine inhibit the M2 proton channel of IAV, probably by occluding the pore and therefore preventing virus uncoating (Cady et al., 2010). Resistance to adamantanes has been reported to occur very rapidly in subjects treated for IAV infection, and mutations in the hydrophobic transmembrane domain of M2 (residues 26 – 38), appear to confer this resistance (Hay et al., 1986, Belshe et al., 1988). Although adamantane resistance is not ubiquitous across all IAV subtypes, it is thought that global incidence of resistance is increasing in human IAV, as well as HPAI H5N1 strains in Asia (Dong et al., 2015). In 2009, the Centers for Disease Control and Prevention (CDC) reported that all circulating human H3N2 and pdm2009 H1N1 viruses sampled in the United States of America were resistant to amantadine (Centers for Disease Control and Prevention, 2009). Amantadine is therefore no longer recommended for the prophylaxis of IAV.

Tamiflu™ and Relenza™ are currently the only NA inhibitors approved in the majority of countries worldwide. Rapivab™ is approved in Japan, Korea, China and USA, while Inavir™ is only approved in Japan. NA inhibitors were designed using structure-based drug discovery, utilising crystal structures of the NA enzyme with sialic acid analogues bound to the active site (von Itzstein et al., 1993). These neuraminidase inhibitors block the active site of all subtypes of NA with high affinity, an inhibition which prevents the release of virions from infected cells (Palese et al., 1974). Tamiflu™ is the most heavily used NA inhibitor worldwide, but resistance has developed, predominantly in human H1N1 seasonal strains but also in a minority of cases of pdm2009 H1N1 and HPAI strains (Hurt et al., 2009b). H1N1 seasonal IAV has evolved resistance to Tamiflu™ via a H275Y amino acid substitution in NA, which still permits replication and transmission of the virus as efficiently as wild-type but the IC_{50} value of Tamiflu™ is heavily increased (Kawai et al., 2009). The efficacy of Rapivab™ to the H275Y Tamiflu™-resistant NA is also reduced, but Relenza™ efficacy is not affected (Hurt et al., 2009a). NA inhibitors are stockpiled in case of future serious IAV outbreaks to provide a level of control until an effective vaccine is developed.

There is currently ongoing research to develop novel antiviral compounds that target conserved viral or host factors that could safely inhibit virus replication in the host (reviewed in (Yen, 2016)). One promising drug is Favipiravir (T-705; 6-fluoro-3-hydroxy-2-pyrazinecarboxamide) which is currently under clinical evaluation for use as an anti-IAV compound. T-705 is a prodrug that has been shown to inhibit the RNA polymerase of a broad spectrum of IAV strains, and other RNA viruses, with high potency without inhibiting host DNA or RNA polymerases (Furuta et al., 2013). T-

705 is phosphoribosylated by cellular enzymes and is incorporated into nascent RNA molecules made by the viral polymerase, preventing efficient elongation (Furuta et al., 2013).

1.7 Host adaptation

Host adaptation is an important facet of IAV biology. Generally speaking, it is quite rare for a virus to successfully adapt to a new species. Usually, specific genetic traits of a virus are required to facilitate efficient replication in a new host and to cause disease. These traits can be acquired through reassortment and/or adaptive mutations. Host factors are also key in setting host range of IAV strains. The contribution of both host and viral factors in setting host range and pathogenicity of IAVs is incompletely understood and is an area of intense research. Host adaptation can result in a virus becoming introduced into a population that may not have existing adaptive immunity. If the virus is able to cause disease and transmit well between individuals in the new host species, then serious outbreaks can result (the pdm1918 H1N1 strain being an example). Of particular concern is the ability of HPAI to cross the species barrier into man and adapt to transmit well. Therefore, it is imperative that the determinants of host range and pathogenicity are fully elucidated to improve risk assessment of IAV strains that may have potential to cause serious outbreaks in domestic mammals or man.

Given the aims of the study described in this thesis, the adaptation of avian influenza viruses to mammalian hosts will be the main focus of discussion in this section unless otherwise stated. Below, some of the best characterised viral determinants of avian to mammalian adaptation are outlined.

1.7.1 Viral determinants of host switching and virulence

Several IAV genes have been implicated in setting mammalian host range and pathogenicity (reviewed in (Cauldwell et al., 2014, Schrauwen and Fouchier, 2014)). The most important viral determinant is widely accepted as being the HA gene, as receptor-binding and virus entry is strongly dependent on both the HA subtype and host species, while the protease cleavage site of the precursor HA_0 polypeptide is a determinant of virulence and tissue tropism (Webster and Rott, 1987).

1.7.1.1 Hemagglutinin

The receptor of IAV, sialic acid, is commonly found at the terminus of glycans and glycosphingolipids on the surface of host cells (reviewed in (Varki et al., 2009)). The second carbon atom of sialic acid forms a glycosidic bond (alpha linkage) with the underlying sugar. The most common alpha linkage is with either the third or the sixth carbon atom of galactose to form α-2-3- or α-2-6- linkages, respectively. These two variations have different conformations that are often specifically recognised by different HA subtypes. Avian IAV HAs predominantly bind preferentially to the α-2-3- linkage, whereas human IAV HAs preferentially bind to α-2-6- linkages (Connor et al., 1994). The location and abundance of the α-2-3- and α-2-6- linkages on the surface of host cells differ from species to species, influencing the species- and tissue-tropism of IAVs (Matrosovich et al., 2004). α2,6-linked sialic acids are predominantly found on ciliated epithelium cells of the upper respiratory tract in humans, while α2,3-linked receptors that are broadly present on the epithelial cells of the avian gut but are only found predominantly in the lower respiratory tract of man (Matrosovich et al., 2004). This species-specific distribution of receptor subtypes poses a barrier for avian viruses that must access the lower respiratory tract of humans, unless adaptive mutations are

acquired allowing a switch of specificity to α2,6-linked receptors. Indeed, mutations to the receptor binding domain of HA have been linked to a switch in receptor specificity following the adaptation of avian viruses to humans (Matrosovich et al., 2000). A single point mutation, Q226L, conferred increased binding of avian H2 and H3 subtypes for α2,6-linked receptors, and E190D and D225G mutations were linked to the H1 switch to α2,6-linked receptors (Matrosovich et al., 2000). Interestingly, dual specificity in pdm2009 H1N1 viruses has been reported and is associated with a D222G adaptive mutation (Chutinimitkul et al., 2010).

The cleavage sequence of HA_0 determines which cellular proteases are able to cleave HA into its active form. Most HAs contain a single arginine residue in the cleavage sequence (monobasic cleavage site) and are cleaved by trypsin-like proteases, which are predominantly secreted into the respiratory epithelia of birds and mammals, and gut epithelium of avian species (Klenk and Garten, 1994). HPAI H5 and H7 viruses possess a multi-basic cleavage site (MBCS) that can be cleaved by furin-like proteases that are expressed ubiquitously and can act intracellularly, and this is correlated with systemic infection and high virulence in birds and mammals (Webster and Rott, 1987, Stieneke-Größer et al., 1992, Hatta et al., 2001). Removal of the MBCS from an H5N1 HPAI virus restricted infection to the respiratory tract of ferrets and reduced virulence, but insertion of an MBCS into an H3N2 human virus did not permit systemic infection and high virulence (Schrauwen et al., 2011, Schrauwen et al., 2012). Thus, the MBCS is likely required for high virulence in gallinaceous poultry, but not sufficient, and there is likely an interplay of multiple host and viral factors.

The pH stability of cleaved HA is also a determinant of host range. Premature changes in HA conformation into its fusogenic state induced by acidification

inactivates the virus, as HA can no longer perform membrane fusion (Stegmann et al., 1987). It was reported that IAV of different HA subtypes differed in their sensitivity to acidic pH - HPAI of H5 and H7 subtypes seemed most sensitive to acidic pH in comparison to human and LPAI HA subtypes (Scholtissek, 1985). The human nasal cavity can display acidic pH as low as 5.2 (Washington et al., 2000), thus HPAI subtypes are likely required to acquire adaptive mutations to improve pH stability in order to avoid premature fusogenic activation of HA in the nasal cavity.

1.7.1.2 Neuraminidase

Adaptive mutations in both the enzymatic region of NA and the 'stalk' have been described following a change in host tropism (Wagner et al., 2002). A compatible combination of HA and NA genes is required for a virus to replicate efficiently – as both effectively perform the opposite role to each other during the virus life cycle. The compatibility is dependent on the trade-off of receptor-binding affinity of HA versus the NA enzymatic activity and stalk length (Wagner et al., 2002). The evolution of a 'short stalk' by a 19 amino acid deletion has been reported following host adaptation of avian influenza from waterfowl into domestic poultry, which is linked to increased virulence in poultry and mammals despite a reduction in receptor cleavage of host cells (Matrosovich et al., 2000, Matsuoka et al., 2009). Conversely, there is evidence to suggest that a short stalk inhibits efficient mammal-to-mammal transmission of HPAI (Blumenkrantz et al., 2013). This is correlated with inefficient virus release from infected cells and also an inability of the virus to penetrate host mucus layers in the epithelia which are rich in sialylated glycans which bind and inhibit receptor binding by HA (Blumenkrantz et al., 2013). Taken together, the evidence shows that the NA gene is important for host adaptation.

1.7.1.3 PB2

Avian IAV polymerases usually require adaptive mutations for efficient transcription and replication activity in mammalian host cells, and to cause high pathogenicity (Taft et al., 2015). The best characterised signature of host range lies at position 627 of the PB2 subunit of the polymerase. Most avian viruses contain glutamate at position 627 (E627), while many mammalian-adapted viruses have acquired a lysine (K627) (Subbarao et al., 1993, Chen et al., 2006a). E627 in PB2 usually confers poor polymerase activity in mammalian cells in RNP reconstitution assays, but introducing the E627K adaptive mutation can improve polymerase activity (Naffakh et al., 2000, Massin et al., 2001, Moncorge et al., 2010, Foeglein et al., 2011). It is thought that cRNA synthesis is compromised for E627 polymerases in mammalian cells, and therefore genome replication is inhibited (Mänz et al., 2012). Furthermore, mutating the PB2 of an H3N2 and an H5N1 virus isolated from man to lose the mammalian-adaptation signature (K627E) reduced transmission between guinea pigs (Steel et al., 2009). High virulence of HPAI H5N1 and H7N9 in man has also been correlated with the E627K signature (Hatta et al., 2001, Zhang et al., 2014a). Recently, it was determined that the E627K adaptive mutation is required for complementarity of the polymerase with human acidic nuclear phosphoprotein 32 family member A (ANP32A) (Long et al., 2016). ANP32A is a host factor involved in transcriptional regulation and mRNA export that is diverse between avian and human species, and appears to be essential to support avian IAV polymerase function in human cells (Long et al., 2016). E627K is not essential for all infections of mammalian hosts, however. This is exemplified by the pdm2009 H1N1 virus which harbours the avian E627 signature in PB2. It is thought that other adaptive mutations in PB2, such as G590S

and Q591R (Mehle and Doudna, 2009, Yamada et al., 2010), and D701N, (Li et al., 2005, Steel et al., 2009), can compensate.

1.7.1.4 NS segment and host range

The products of the NS segment are important for setting host range and pathogenicity, which forms the foundation of this project. Adaptive mutations have been noted in the major products of segment 8, NS1 and NEP (Forbes et al., 2012, Mänz et al., 2012). The roles of the NS genes during infection, and their influence on host adaptation and pathogenicity, are discussed more extensively below in *1.9 The NS segment of IAV*.

1.8 The innate immune response and influenza virus infection

In this section, the innate immune response to IAV is discussed, with a particular focus on the mammalian type I IFN response.

1.8.1 The interferons

Interferons (IFN) are cytokines that have potent antiviral activities, and contribute to the innate immune response to viral infection. Following detection of a viral pathogen, cells secrete interferons which act through a cognate receptor to upregulate a host of interferon sensitive genes (ISGs) that include antiviral restriction factors. It is thought that a fully functional IFN response is sufficient to limit virus replication and prevent disease in the host; although most viruses have evolved mechanisms to circumvent the IFN response (reviewed in (Randall and Goodbourn, 2008)). The IFNs exist as three families, each with distinct structural homologies and a family-specific receptor through which antiviral mechanisms are mediated: type I, type II and type III IFN (reviewed in (Platanias, 2005) and (Wack et al., 2015)). Type

I and type III IFNs are used in direct response to viral infection and involve similar sensing and signalling pathways, leading to the upregulation of a similar array of ISGs (Kotenko et al., 2003, Sheppard et al., 2003, Crotta et al., 2013, Wack et al., 2015). Type II IFN (IFN-γ) is secreted by activated T cells and natural killer cells, and has an immunomodulatory role (Platanias, 2005). Type III IFN includes IFN-λ1, IFN-λ2, IFN-λ3 (also known as interleukin-29, interleukin-28A, interleukin-28B, ; IL-29, IL-28A and IL-28B, respectively), and IFN-λ4, and is predominantly produced by infected airway epithelial cells (Kotenko et al., 2003, Sheppard et al., 2003, Crotta et al., 2013, Wack et al., 2015). There are many type I IFNs, and in humans these include IFN-α (IFN-α itself has at least 14 different subtypes), IFN-β, IFN-ε, IFN-κ, and IFN-ω. The best characterised type I IFNs are IFN-α and IFN-β, while the roles of IFN-ε, -κ, and –ω are less well understood. From here onwards the term 'type I IFN' will refer to IFN-α and IFN-β only. IFN-β is secreted by most cell types, while IFN-α is predominantly secreted from leukocytes (Platanias, 2005).

1.8.2 Sensing of IAV infection and IFN response

The primary cells that produce IFN in response to IAV infection are infected airway epithelial cells, plasmacytoid dendritic cells and macrophages (reviewed in (Killip et al., 2015)). Infected cells can sense pathogen associated molecular patterns (PAMPs) using either the RIG-I-like receptor (RLR) cascade, Toll-like receptor (TLR) pathway, or the Nod-like receptor cascade. Influenza A virus infection is detected in most cell types by the RLR pathway, which contains the cytoplasmic DExD/H box RNA helicases retinoic acid-inducible gene 1 (RIG-I), melanoma differentiation-associated protein 5 (MDA5) and laboratory of genetics and physiology 2 and a homolog of mouse D11lgp2 (LGP2) (Killip et al., 2015). IAV infection is thought to

be predominantly sensed by cytoplasmic RIG-I, although MDA5 has also been reported to be important for efficient ISG upregulation in response to IAV (Benitez et al., 2015). Conversely, LGP2 overexpression has been reported to reduce IFN production caused by H3N2 infection (Malur et al., 2012). The RLR pathway senses IAV infection in most cell types, barring plasmacytoid dendritic cells, which use TLR family proteins TLR3 and TLR7 to detect IAV (Killip et al., 2015). Fig 1.4 shows a schematic for the pathways involved in IFN induction and signalling in response to IAV infection.

RIG-I possesses two N-terminal caspase activation and recruitment domains (CARD), an RNA helicase domain, and a C-terminal regulatory domain (CTD) that normally inhibits the exposure of the N-terminal CARD domains by holding the protein in a 'closed' conformation (Loo and Gale, 2011). It is thought that blunt-ended RNA duplexes with a 5' triphosphate moiety are primarily responsible for RIG-I activation during influenza infection (Schlee et al., 2009), and the panhandle structure present in each segment of vRNA is sufficient to activate RIG-I (Liu et al., 2015a). The 5' triphosphate RNA binds to the CTD and RNA helicase domains of RIG-I, inducing a conformational change to expose the N-terminal CARDs (Loo and Gale, 2011). The CARDs require ubiquitination for full activity, which is mediated by cellular tripartite motif-containing protein 25 (TRIM25) (Gack et al., 2007), RING finger protein leading to RIG-I activation (RIPLET) (Oshiumi et al., 2009), or Mex-3 RNA Binding Family Member C MEXC (Kuniyoshi et al., 2014). RIG-I signalling is also potentiated by the binding of cellular PACT (protein kinase, interferon-

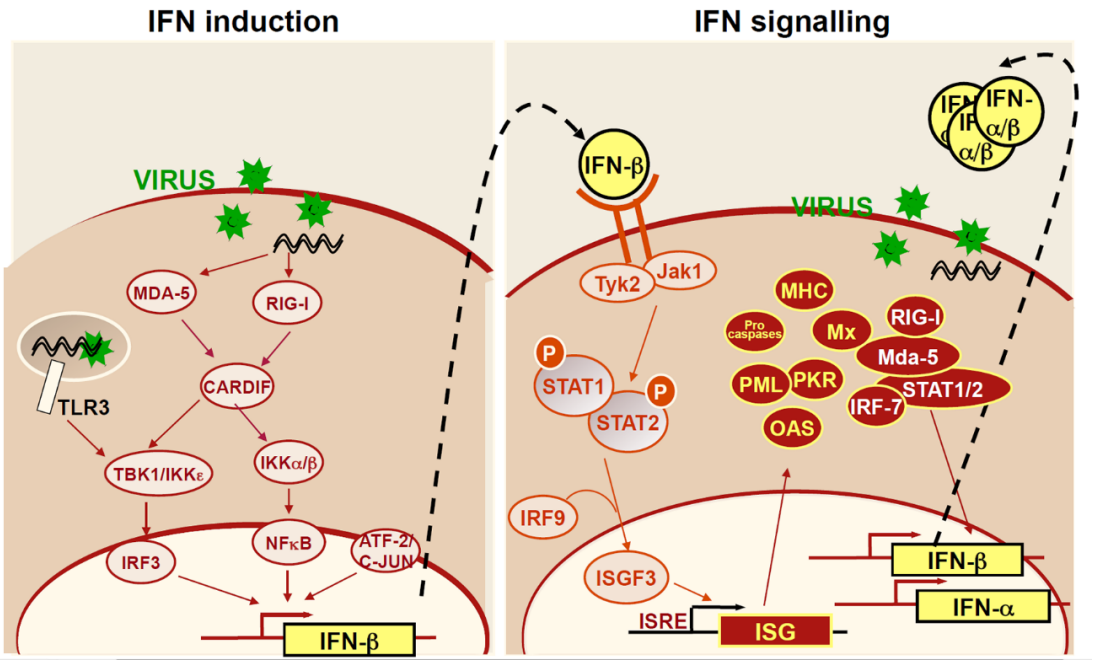

Fig. 1.4. The interferon system. Shown are schematics of the pathways involved in type I interferon (IFN) induction following IAV infection (left hand side) and signalling (right hand side). Cytoplasmic RIG-I and MDA-5, and endosomal TLR3, all sense dsRNA associated with viral infection. Signalling cascades are induced (arrows show activation) and ultimately activate the transcription factors IRF-3 and NF-κB which upregulate the IFN-β promoter. Secreted IFN-β works in an autocrine and paracrine fashion to induce an antiviral state in host cells through activation of the type I IFN receptor and kinases Jak1 and Tyk2. Jak/STAT signalling results in the activation of the transcription factor complex ISGF3 which acts to upregulate the promoter of a plethora of ISGs. The induced ISGs act to restrict virus replication through a variety of mechanisms. Jak/STAT signalling also up-regulates type I IFN expression to amplify the response to infection. Figure was made by Prof. Rick Randall (The University of St. Andrews, UK) and included with permission.

-inducible double stranded RNA dependent activator) to the C-terminal regulatory domain, which is required for a full IFN response to viral infection (Kok et al., 2011). The exposed and polyubiquitinated CARDs of RIG-I then interact with mitochondrial antiviral signalling protein (MAVS), which polymerises and activates I kappa B kinase (IKK) and TANK-binding kinase 1 (TBK1) (Loo and Gale, 2011). TBK1 and IKK phosphorylate the transcription factor interferon regulatory factor-3 (IRF-3) which subsequently localises to the nucleus. IKK phosphorylates inhibitor of κB (IκBα) which induces its degradation. IκB degradation frees the transcription factor nuclear factor kappa B (NF-κB) to also localise to the nucleus. These transcription factors subsequently upregulate the activity of the IFN-β promoter in conjunction with other transcription factors (such as the AP-1 heterodimer of ATF-2 and c-Jun) as part of the 'enhanceosome' (Fig 1.4) (Loo and Gale, 2011).

IFN-β is translated and secreted, and mediates responses in an autocrine and paracrine fashion via the IFN-α/β receptor (IFNAR) – leading to the upregulation of hundreds of interferon sensitive genes (ISGs) (Fig 1.4) (Randall and Goodbourn, 2008). Neighbouring uninfected cells are therefore primed for virus infection, inhibiting virus spread. IFN-β binding to IFNAR activates janus kinase 1 (JAK1) and tyrosine kinase 2 (TYK2), and these phosphorylate signal transducer and activator of transcription 1 and 2 (STAT1 and STAT2) which form a heterodimer (Randall and Goodbourn, 2008). The phosphorylated STAT1/STAT2 heterodimer complexes with interferon regulatory factor 9 (IRF9), forming a complex called interferon stimulated gene factor 3 (ISGF3) in the cytoplasm. ISGF3 then undergoes nuclear import, where the complex acts to activate the promoters of many ISGs, by binding to IFN-stimulated response elements (ISREs) (Randall and Goodbourn, 2008). ISRE elements are found

in the promoters of type I IFNs to engage in a positive feedback loop to amplify the response to viral infection. The mechanism of action of select ISGs, known to be involved in the control of IAV, are overviewed below in *1.8.3 Interferon sensitive genes*.

The RIG-I pathway for sensing IAV infection has been well characterised for a number of years. Recently, there has also been evidence published proposing a role of a stimulator of interferon genes (STING)-mediated activation of IFN production following membrane fusion during IAV infection (Holm et al., 2016). STING-mediated induction has been best described for DNA viruses. Cytoplasmic DNA is sensed by cyclic GMP-AMP (cGAMP) synthase (cGAS), which leads to 2' 3' cGAMP production. 2' 3' cGAMP binds to STING inducing a conformational change, which is then able to activate TBK1 (Ishikawa et al., 2009). As in the RIG-I pathway, TBK1 activates IRF3 leading to IFN-β production. In the context of IAV infection, STING was shown to sense membrane fusion during IAV entry, independently of cGAS. Furthermore, a recombinant fusion peptide derived from HA was shown to interact with and inhibit STING to prevent IFN induction (Holm et al., 2016).

It has been proposed that IFN production in response to IAV infection is stimulated by defective interfering particles (DIPs) containing defective viral genomes (DVGs). DVGs do not contain a fully functioning complement of vRNA segments, usually with an internal deletion or truncation in a larger genomic segment (PB2, PB1, PA) (Nayak, 1980). Although the mechanism of increased IFN induction has yet to be fully elucidated, studies have correlated an increased proportion of DVGs with increased IFN production both *in vitro* and *in vivo* (Tapia et al., 2013, Frensing et al.,

2014). Therefore, IFN induction during IAV infection may be mediated by DI particles, rather than fully functional particles.

1.8.3 Interferon sensitive genes

Select ISGs are discussed below that have been well characterised in IAV infection and/or are relevant to experiments described in the results chapters of this thesis.

1.8.3.1 Mx1

Interferon-induced GTP-binding protein Mx1 (Mx1) is a mammalian guanosine triphosphatase (GTPase) that is induced by type I and type III IFN and confers protection against a variety of viruses including IAV (Staeheli et al., 1986). Protection against IAV is thought to be mediated by disrupting the interactions of the NP and PB2 proteins, resulting in an inhibition of polymerase activity (Verhelst et al., 2012). The origin of NP appears to determine sensitivity to Mx1, with avian viruses appearing more sensitive to its antiviral mechanisms, and therefore Mx1 is considered an important barrier to avian influenza infection of mammals (Dittmann et al., 2008, Zimmermann et al., 2011, Verhelst et al., 2012).

1.8.3.2 PKR

The double-stranded RNA-dependent protein kinase PKR is an important mediator of antiviral response to infection (Gale and Katze, 1998). PKR is expressed ubiquitously, but is also upregulated by IFN signalling. PKR binds dsRNA and phosphorylates itself upon activation. PKR targets include the alpha subunit of eukaryotic initiation factor 2 (eIF2α) and I kappa B (IκB), the regulatory subunit of NF-κB. eIF2α is involved in recruiting methionine-$tRNA_i$ at the initial step of

eukaryotic translation and requires bound GTP. Inactive eIF2α-GDP is released from the ribosome, and is normally 'recycled' by the eIF2β subunit, a guanine nucleotide exchange factor, to active eIF2α-GTP. Phosphorylation of eIF2α by PKR increases eIF2α affinity to eIF2β, rendering it unavailable for recycling and subsequent initiation events (de Haro et al., 1996). Thus, translation is inhibited and this reduces virus protein synthesis and therefore production of infectious virus (Gale and Katze, 1998). Phosphorylation of IκB activates NF-κB, which becomes free to enter the nucleus and upregulate type I IFN and ISG promoter activity (Kumar et al., 1994). The IAV interferon antagonist NS1 has evolved to bind and inhibit PKR (Min et al., 2007), and PKR knockout mice permit efficient replication of an IAV lacking NS1 that fails to replicate in WT mice (Bergmann et al., 2000). Therefore PKR is an important inhibitor of IAV.

1.8.3.3 2' 5'-oligoadenylate synthetase family

The 2' 5'-oligoandenylate (2-5A) synthetase (OAS) family consists of OAS1, OAS2, OAS3 and the 2' 5' oligoadenylate synthetase-like protein (OASL). OAS1, OAS2 and OAS3 all synthesise 2-5As from ATP, while OASL lacks this enzymatic activity. OAS proteins, like PKR, are activated by dsRNA during viral infection. The synthesis of 2-5As in response to viral infection activates ribonuclease L (RNase L). Activated RNase L destroys RNA species in the host cell, including viral mRNAs and cellular ribosomal RNAs, contributing to a reduction in viral protein synthesis and therefore replication (Drappier and Michiels, 2015). A recent study has implicated OAS3 as the major activator of the RNase L pathway in response to viral infection (Li et al., 2016).

OASL does not activate the RNase L pathway as it lacks the enzymatic activity to produce 2-5As. It has been proposed that OASL acts to increase the sensitivity of RIG-I to viral RNA species by mimicking polyubiquitin to facilitate RIG-I activation, and also by binding and recruiting dsRNA to RIG-I (Zhu et al., 2014).

1.8.3.4 IFITM family

The interferon induced transmembrane protein (IFITM) family are a family of proteins with two transmembrane domains linked by a highly conserved loop. In humans there are five IFITM genes (IFITM 1, 2, 3, 5 and 10), of which IFITM1, 2 and 3 have been reported to possess antiviral activity against a wide range of viruses including IAV (reviewed in (Perreira et al., 2013). The IFITM proteins are thought to inhibit IAV at the entry step of virus infection (Brass et al., 2009, Feeley et al., 2011, Amini-Bavil-Olyaee et al., 2013). IFITM1 localises at the cell surface and early endosomes, while IFITM2 and 3 localise to late endosomes and lysosomes (Feeley et al., 2011, Mudhasani et al., 2013, Amini-Bavil-Olyaee et al., 2013). IFITM3 has been shown to be important in restricting morbidity and mortality *in vivo* against IAV (Everitt et al., 2012). Notably, IFITM1, 2 and 3 were highly induced in ducks infected with an H5N1 HPAI strain which did not cause significant pathogenicity, but were not up-regulated chickens which were highly susceptible to disease (Smith et al., 2015). It has therefore been suggested that the increased susceptibility of chickens to HPAI, relative to ducks, may be due to a poor upregulation of ISGs, including IFITM 1, 2 and 3, which may be correlated with the galliform host lacking RIG-I (Magor et al., 2013, Smith et al., 2015). Thus, the IFITM family of proteins represent host factors that are important for restriction of IAV and appear significant in defining the susceptibility of the host to IAV pathogenicity in a species-specific manner.

1.8.3.5 IFIT family

The interferon-induced protein with tetratricopeptide repeats (IFIT) family members include IFIT1, IFIT2, IFIT3, and IFIT5. The IFIT family proteins are usually expressed at low levels under normal conditions, but are among the highest upregulated ISGs in response to IFN and viral infection (reviewed in (Fensterl and Sen, 2015)). IFIT1, 2 and 3 work in tandem to form a large multiprotein complex following stimulation with IFN, which sequesters 5' triphosphate RNA via IFIT1-RNA interactions; and this has antiviral effects against IAV (Pichlmair et al., 2011). Overexpression of either IFIT1, IFIT2 or IFIT3 alone did not exhibit antiviral activity, demonstrating the importance of the multiprotein complex assembly in the antiviral activity (Pichlmair et al., 2011). Additionally, it has been suggested that some IFIT family members may directly inhibit translation by interfering with the assembly of the translation initiation complex, reducing viral protein synthesis (Fensterl and Sen, 2015).

1.8.4 Viral IFN antagonists

IAV has evolved mechanisms to counter and circumvent the IFN response, which would otherwise clear the virus (reviewed in (Randall and Goodbourn, 2008)). The NS1 protein is the major viral IFN antagonist and has evolved multiple mechanisms to inhibit the RLR pathway, reduce the expression of IFNs and ISGs, and block the action of multiple antiviral effectors. The roles and mechanisms of this protein are discussed in depth below. In addition to the NS1 protein, other viral proteins have been linked to inhibiting the IFN response, and are briefly outlined in this section.

1.8.4.1 The IAV polymerase and IFN antagonism

As described earlier, the polymerase of IAV synthesises mRNA in a mechanism involving the 'cap-snatching' of 5' 7-methylated caps from host pre-mRNAs, destroying them. This is expected to contribute to host shut-off, and therefore would reduce the expression of proteins involved in RLR signalling, IFN induction and ISG expression. Furthermore, PB2, PB1 and PA of the influenza polymerase have all been shown to inhibit RIG-I signalling by binding to and inhibiting MAVS (Iwai et al., 2010, Graef et al., 2010).

1.8.4.2 PB1-F2

PB1-F2, expressed from an alternative start codon in the +1 ORF to PB1 from PB1 mRNA, also binds and inhibits MAVS to reduce IFN expression (Conenello et al., 2011, Varga et al., 2011, Varga et al., 2012). Following interaction with MAVS, PB1-F2 is thought to decrease mitochondrial membrane potential (Varga et al., 2012), which has been reported to be important for full MAVS-mediated IFN induction (Koshiba et al., 2011).

1.8.4.3 PA-X

PA-X selectively destroys host pol II derived mRNA transcripts in a process that requires host RNA endonuclease Xrn1 (Khaperskyy et al., 2016). It is thought that PA-X discriminates between host and viral mRNAs by mRNAs that use host 3' processing machinery (Khaperskyy et al., 2016). This process results in a reduced immune response to infection in H1N1 and H5N1 viruses (Jagger et al., 2012, Gao et al., 2015b, Hayashi et al., 2015, Hu et al., 2015a) but conversely an increased response for H9N2 viruses (Gao et al., 2015a).

1.8.4.4 Hemagglutinin

IAV hemagglutinin has been proposed to target the IFN-α/β receptor IFNAR for degradation by inducing its ubiquitination, and this has been shown to reduce the activation of the IFN-β promoter (Xia et al., 2015). As described earlier, HA also binds to STING to reduce STING-mediated induction of the IFN response (Holm et al., 2016).

1.8.5 Macrophages and IAV infection

Macrophages are sentinel cells with key roles in mounting innate and adaptive immune responses to pathogens. Alveolar macrophages (AM) are among the first immune cells that will come into contact with IAV during infection, residing in the lumen of the airways and alveoli. AMs contribute to viral clearance by phagocytosis of virions and infected cells, and are the main producers of type I IFN and pro-inflammatory cytokines during IAV infection, and studies have shown the importance of macrophages in controlling influenza replication and disease (Tumpey et al., 2005, Kumagai et al., 2007, Kim et al., 2008, Tate et al., 2010). The release of pro-inflammatory mediators, such as TNF-α and interleukin-1β, act to trigger inflammation in the area of infection leading to the recruitment of various innate immune cell populations that act to clear the virus and virus-infected cells. The pro-inflammatory response, however, contributes to inflammation-induced lung damage. Pro-inflammatory mediators, particularly TNF-α, have been proposed to be responsible for the increased severity of lung pathology noted in human infection with HPAI H5N1 and the 2013 H7N9 viruses (Cheung et al., 2002, Lee et al., 2009b, To et al., 2016). Macrophages are also important in the induction of immunological memory to IAV (Macdonald et al., 2014). Therefore, macrophages are important immune cells

in the control of IAV, but can also contribute to severe pathology during infection with HPAI and other strains.

While airway epithelial cells are the primary target for IAV, macrophages can still be infected and undergo productive replication, although this appears to be in a strain- and macrophage-subtype specific fashion (reviewed in (Nicol and Dutia, 2014)). The role of productive infection of macrophages in pathogenicity is not clear and remains to be elucidated (Nicol and Dutia, 2014).

1.9 The NS segment of IAV

The NS segment (segment 8) and its role in setting host range and pathogenicity of IAV in mammalian hosts forms the focus of this study. This section provides an introduction to the segment 8 genes of IAV. In particular, the phylogeny of the NS segment is discussed.

1.9.1 NS segment gene products

1.9.1.1 Nuclear export protein

As described previously, NEP is translated from spliced segment 8 mRNA (Lamb and Lai, 1980). While the structure of the N-terminus of NEP (residues 1-53) has not been reported, a crystal structure of the C-terminus has revealed it forms a dimer of two helical hairpins composed of two antiparallel helices, forming an antiparallel four-helix bundle (Akarsu et al., 2003). The N-terminus harbours two hydrophobic nuclear export signals which mediate nuclear export of vRNPs as described earlier in *1.4.5 Nuclear export and trafficking of vRNPs*. NEP is therefore essential for virus replication (Neumann et al., 2000).

NEP accumulation is typically 'late' in infection due to low abundance of NEP mRNA (only ~ 10% of all segment 8 mRNA), resulting from a 'suboptimal' 5' splice donor site (Robb et al., 2010, Chua et al., 2013). It has been suggested that NEP regulates genome replication by triggering the switch of the viral polymerase complex from transcription to replication, following observations that NEP expression increases the levels of cRNA and vRNA in RNP reconstitution assays (Robb et al., 2009). It has been proposed that the use of a suboptimal 5' splice donor site is important as an early accumulation of NEP might cause a premature switch from transcription to replication and be detrimental to virus replication (Chua et al., 2013)

NEP has been show to incur adaptive mutations when a virus crosses the species barrier (Mänz et al., 2012, Forbes et al., 2012). In particular, the M16I adaptive mutation is thought to compensate for the lack of activity of H5N1 avian polymerases with the PB2 E627 signature in human cells by allowing efficient cRNA synthesis (Mänz et al., 2012). This function is thought to be mediated by the C-terminal end of NEP, and it has been proposed that the M16I adaptive mutation allows a more efficient structural conformation to expose the C-terminus (Reuther et al., 2014b).

NEP is known to undergo post-translational modification by phosphorylation and conjugation with a small ubiquitin-like modifier (SUMO; SUMOylation), but the role of this in infection is not yet clear (Pal et al., 2011). S23, S24 and S25 of NEP can be phosphorylated (Hutchinson et al., 2012), but site-directed mutations of these serine residues to alanine (thus preventing phosphorylation) did not have any effect on virus replication *in vitro* or *in vivo* (Reuther et al., 2014a). Thus, it remains unclear whether post-translational modification of NEP influences IAV replication and if so, by what mechanism.

1.9.1.2 Nonstructural protein 1

i) General introduction

NS1 is a multifunctional dimeric protein with a strain-specific size typically between 217-237 amino acids, but is commonly 230 amino acids in length (Suarez and Perdue, 1998). NS1 was traditionally thought to be a nonstructural protein, but recent mass-spectrometry analysis of purified virions has provided evidence that a small number of NS1 molecules are incorporated into virus particles (Hutchinson et al., 2014). NS1 interacts with RNA and a variety of host-cell proteins in a host-and strain-specific manner to primarily antagonise the innate immune response of the host, but also to optimise the host cell environment for virus replication (reviewed in (Hale et al., 2008b)). NS1 is a virulence factor essential for efficient viral replication and its main role is thought to be the antagonism of the host IFN response. An NS1-deletion mutant is heavily attenuated in tissue culture, but replication is significantly rescued in IFN-deficient VERO cells (García-Sastre et al., 1998), demonstrating the importance of IFN-antagonism by the NS1 protein.

Efficient IFN antagonism by NS1 is likely an important facet of host adaptation of IAV. The consequences of an avian virus' NS1 protein being unable to block the mammalian innate immune response could lead to rapid virus clearance and an inability to persist and adapt to the new host. Indeed, an analysis of NS1 protein sequences clearly showed host-dependent clustering, indicating a relationship between NS1 genotype and host range (Sevilla-Reyes et al., 2013). The NS1 protein of the 2013 H7N9 subtype was shown to be competent in antagonising the IFN response in human cells without prior adaptation to the human host, unlike NS1 from other LPAI H7 subtype strains (Knepper et al., 2013). Conversely, Hayman and others tested a range

of avian NS1 proteins and found them all to be competent at blocking the IFN response in human cells, despite some WT avian viruses displaying attenuation in replication (Hayman et al., 2007). Also, pdm2009 H1N1 and seasonal H3N2 NS1 proteins have been shown to be poor at blocking the IFN response in human cells (Kuo et al., 2010, Hale et al., 2010b). However, efficient IFN antagonism may not be essential for host adaptation, but probably 'helps' a virus to persist long enough to acquire adaptive mutations in other regions of the genome (Hayman et al., 2007).

ii) NS1 protein domain organisation

Fig 1.5 shows schematic representations of the NS1 protein structure and domain organisation. Functional residues of NS1 are discussed and shown in Chapter 2. The N-terminal 73 amino acids form an RNA-binding domain (RBD), a symmetrical homodimer composed of two monomers of three alpha-helices (Liu et al., 1997) (Fig 1.5B). The RBD dimer binds single- and double-stranded RNA with low affinity (Hatada et al., 1992, Hatada and Fukuda, 1992) via electrostatic interaction with basic amino acids in helix 2 (R38 and K41) that are absolutely conserved across all IAVs (Wang et al., 1999). dsRNA-binding prevents the activation of the antiviral ISG OAS (Min and Krug, 2006). The RBD also binds polyadenylated mRNAs (Qiu and Krug, 1994), viral genomic RNA (Hatada et al., 1997), vRNPs via interaction with NP (Robb et al., 2011), and binds specifically to a conserved motif in the 5' end of all positive-sense viral RNA as well as a motif in the 3' untranslated region (UTR) of NS1 mRNA (Marc et al., 2013). The RBD contains nuclear localisation signals to allow nuclear import to perform its functions in the host cell (Greenspan et al., 1988), and NS1 has also been shown to be targeted to the nucleolus in a strain- and host-dependent manner (Melen et al., 2007, Volmer et al., 2010, Han et al., 2010).

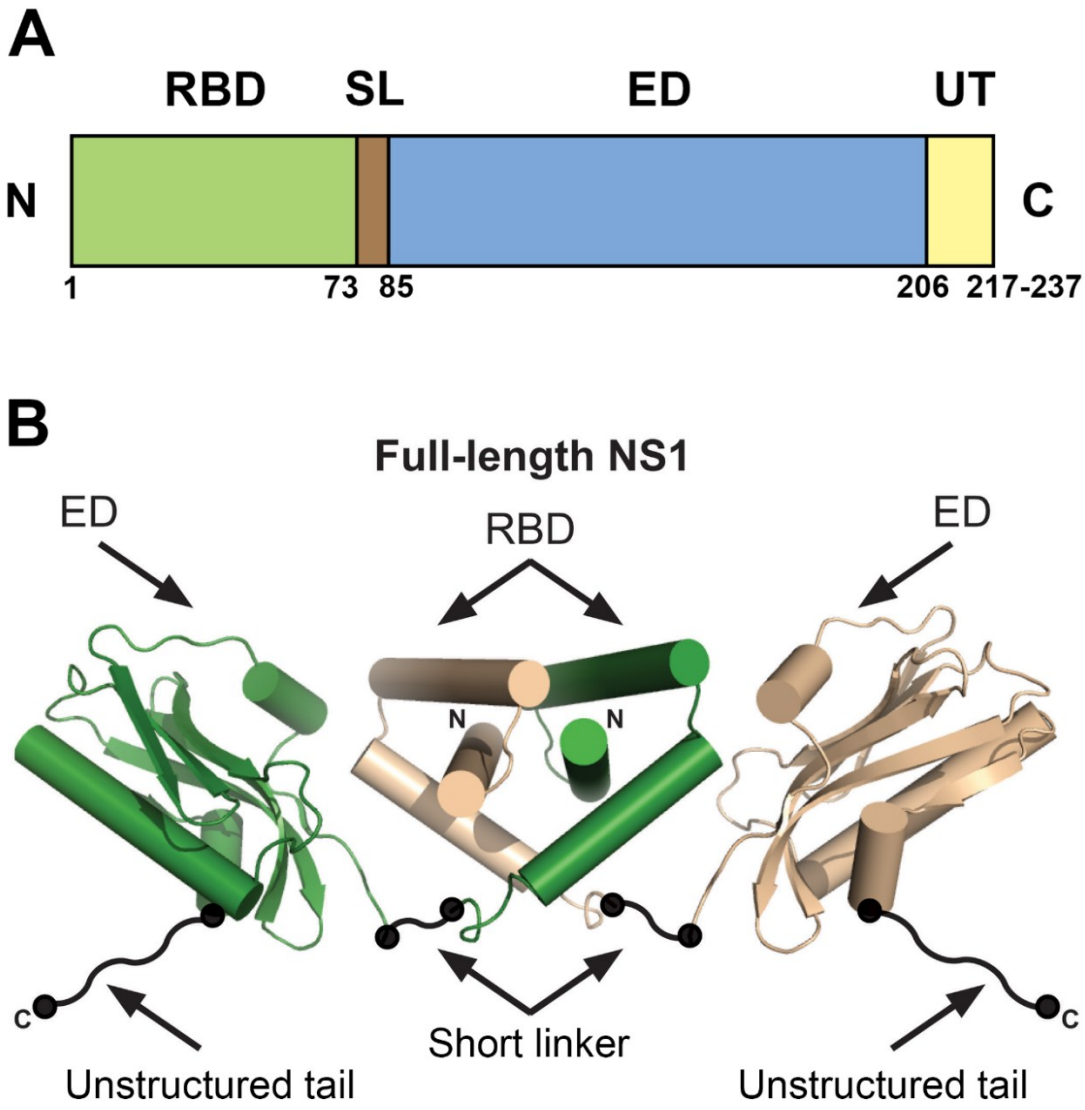

Fig 1.5. NS1 structure and domain organisation. (A) A schematic of the domain organisation is shown for an NS1 monomer with the residue positions annotated. The RNA-binding domain (RBD, 1-73) and effector domain (ED, 85-206) are connected by a short linker (SL). Residues 206 to end (typically 217-237) form an unstructured tail (UT). 'N' and 'C' represent the N- and C-termini of the protein, respectively. (B) Shown is a dimer of two full-length NS1 proteins (green and wheat). The crystal structures of the RBD and ED have been characterised and are shown. The short linker and unstructured tail have not been observed in crystal structures and have been represented schematically in this diagram by the authors. EDs are shown in the proposed 'helix open' conformation. Cylinders represent α-helices and arrows represent β-sheets. Diagram is from (Kerry et al., 2011a) with annotations adapted.

The RBD is connected to a C-terminal effector domain (ED) by a short, flexible, linker (residues 74-85). Like the RBD, the ED (residues 85 to 206) of both human and avian NS1s forms a homodimer, each of which consists of seven β-sheets and three α-helices (Bornholdt and Prasad, 2006, Hale et al., 2008a) (Fig 1.5B). W187 is highly conserved and is important for ED dimerisation, which has been shown to be required for efficient RNA-binding by the RBD (Hale et al., 2008a). It has also been suggested that the NS1 ED displays structural polymorphism to allow interaction with multiple different cellular binding partners dependent on conformation (Kerry et al., 2011a, Carrillo et al., 2014). The ED interacts with a plethora of host cell and viral proteins (these are detailed below) to influence the cellular environment to be optimal for viral replication. The ED also contains a nuclear export signal (residues 138-147) (Li et al., 1998), and together with the NLSs in the RBD allow nucleocytoplasmic shuttling of the protein during infection to interact with multiple binding-partners in different sub-cellular locations in the infected host cell.

The C-terminus is formed of an unstructured tail (206 to end). The unstructured tail of NS1 sometimes contains a PDZ-binding motif (PBM) of the X-S/T-X-V type at residues 227-230 that differs between strains in a host-dependent manner. RSKV or RSEV sequences are found in the majority of human isolates, and an ESEV or an EPEV sequence is a signature for avian NS1s (Obenauer et al., 2006). Introducing the avian ESEV PBM into a lab-adapted H1N1 NS1 or an H5N1 NS1 increased virulence in mice and improved transmission efficiency (Jackson et al., 2008, Kim et al., 2014). Conversely, reverse genetics to re-instate the unstructured tail and to introduce a PBM into pdm2009 H1N1 NS1 (only 219 amino acids in length) did not improve virus fitness in mammalian cells *in vitro* or in mouse or ferret models *in vivo* (Hale et al.,

2010c). Thus, the role of the PBM in NS1 in setting host range and pathogenicity is not fully understood. The unstructured tail is also thought to be involved in the inhibition of poly(A)-binding protein II (PABPII) (Chen et al., 1999), as described below.

iii) IFN antagonism

NS1 has evolved multiple mechanisms to block IFN induction and to inhibit intracellular antiviral effectors. The activation of the transcription factors IRF-3, NF-κB, and AP-1 are inhibited by NS1 in a strain-dependent manner, reducing the activity of the IFN-β promoter (Talon et al., 2000, Wang et al., 2000, Ludwig et al., 2002). However, the precise mechanism of how NS1 inhibits these transcription factors is currently not fully understood (Krug, 2015). A direct interaction of NS1 with RIG-I, which inhibits downstream signalling and therefore IRF-3 and NF-κB activation, has been reported (Mibayashi et al., 2007). NS1 also binds the cellular E3 ligases TRIM25 (Gack et al., 2009) and Riplet (Rajsbaum et al., 2012) in a species-specific manner to inhibit the ubiquitination and activation of RIG-I. Additionally, NS1 inhibits cellular PACT, also important in RIG-I activation (Tawaratsumida et al., 2014). However, NS1 proteins from human seasonal H2N2 and H3N2, and some seasonal H1N1 strains, have been reported to be poor at blocking IRF-3 phosphorylation and IFN-β production despite an interaction with TRIM25 (Kuo et al., 2010). Thus, the mechanisms of IRF-3 and NF-κB inhibition by NS1 are yet to be fully elucidated.

NS1 also dampens host responses by inhibiting nucleocytoplasmic transport of mRNAs (Fortes et al., 1994, Qiu and Krug, 1994). The NS1 protein of certain strains interacts with and inhibits 30-kDa cleavage and polyadenylation specificity factor

(CPSF30) (Nemeroff et al., 1998) and PABPII (Chen et al., 1999) of the cellular 3'-end pre-mRNA processing machinery. This leads to a reduction in cellular mRNA processing and nuclear export, and a subsequent decrease in IFN and ISG expression (Li et al., 2001, Noah et al., 2003). Viral mRNAs are thought to be unaffected by this since the 3' poly(A) tails are obtained by re-iterative copying of the viral polymerase on poly-U tracts of the template (Poon et al., 1999), rather than by the cellular 3' processing machinery. NS1 has also been reported to form inhibitory interactions with components of the mRNA nuclear export machinery (Satterly et al., 2007).

As mentioned previously, NS1 is known to bind and inhibit PKR (Min et al., 2007) and OAS (Min and Krug, 2006) to block these intracellular antiviral effectors.

iv) NS1 and regulation of virus replication

The NS1 protein binds to the AGCAAAAG motif in the 5' UTR of viral mRNAs and enhances their translation (de la Luna et al., 1995, Marc et al., 2013). This is thought to be mediated by interactions with eukaryotic initiation factor 4G (EIF4G) (Aragón et al., 2000) and poly(A)-binding protein I (PAB1) (Burgui et al., 2003), to form viral mRNA 'translation initiation complexes'. NS1 also regulates viral polymerase activity, as a reduction in the production of viral vRNA, cRNA and mRNA has been observed in RNP reconstitution assays when NS1 is also expressed (Wang et al., 2010). It is currently unknown how NS1 regulates the polymerase.

NS1 binds to and inhibits U6 spliceosomal RNA (sRNA) of the host spliceosome and this inhibits interactions with U2 and U4 sRNAs to regulate host cell splicing of pre-mRNA (Lu et al., 1994, Qiu et al., 1995). The effect on viral mRNA splicing is the subject of debate, however. There is evidence in the literature to suggest

that NS1 inhibits the splicing of its own mRNA (Fortes et al., 1994, Garaigorta and Ortin, 2007), while others have reported NS1 does not influence segment 8 mRNA splicing (Lu et al., 1994, Robb et al., 2010). Likewise, while there is evidence to suggest segment 7 mRNA splicing is unaffected by NS1 (Salvatore et al., 2002), others have suggested that NS1 does regulate this (Lu et al., 1994, Robb and Fodor, 2012). Thus, it is not fully clear how NS1 regulates viral mRNA splicing. However, the inhibition of cellular pre-mRNA splicing is expected to contribute to host shut-off.

v) NS1 and cell signalling

The NS1 protein has been reported to regulate host-cell signalling via multiple mechanisms. It is known that NS1 binds to and prevents the regulatory p85β subunit of phosphoinositide 3-kinase (PI3K) preventing its auto-inhibitory function, which results in the activation of the catalytic p110 subunit of the kinase (Hale et al., 2006, Hale et al., 2010a). Mutating an essential amino acid required for the p85β interaction (Y89F) attenuated virus replication in tissue culture (Hale et al., 2006), and reduced virulence and pathogenicity in mice (Hrincius et al., 2012), suggesting the PI3K activation is important for virus replication. However, the mechanisms behind this pro-viral response of PI3K activation are not fully understood (Ayllon et al., 2012). Furthermore, NS1 proteins from avian IAVs, and the pdm1918 H1N1 strain, are known to interact with an N-terminal Src homology 3 (SH3) domain in Crk (CT10 (chicken tumour virus number 10) regulator of kinase) and CrkL (Crk-like) adapter proteins (Heikkinen et al., 2008), which regulate various cellular signalling pathways. The interaction of NS1 with Crk proteins inhibits the IAV-triggered activation of the Jun-N-terminal kinase (JNK) signalling pathway, and this is thought to be important for efficient virus replication by reducing premature death of infected cells (Hrincius

et al., 2010). NS1 has also been implicated in altering the cell cycle by inhibiting RhoA (Ras homolog family member A) expression and activity to cause G0/G1 cell cycle arrest (Jiang et al., 2013). The G0/G1 phase has been suggested to be the most efficient stage for virus replication, possibly because cellular RNA polymerase II is most active and capped mRNAs are most abundant (He et al., 2010).

vi) Post-translational modification of NS1

NS1 is known to undergo strain-specific, post-translational modification. This includes phosphorylation and conjugation with SUMO and interferon-sensitive gene 15 ubiquitin-like modifier (ISG15). T125 was identified as a phosphorylation site in human IAV NS1, which is phosphorylated by host cyclin-dependent kinases (CDK) and extracellular signal-regulated kinases (ERK) (Hale et al., 2009). Whilst a T125A mutation reduced viral fitness of A/Udorn/1972 (H3N2) (Udorn72), it has been suggested that this mutation alters the structure of NS1, abrogating a different function (Hale et al., 2009, Hsiang et al., 2012). Serines 42 and 48, and T197 have also been observed to be phosphorylated, but the roles of phosphorylation of these residues are currently not clear (Hsiang et al., 2012, Hutchinson et al., 2012). Phosphorylation of NS1 at T49 has been proposed to inhibit the ability of NS1 to perform IFN-antagonistic functions (Kathum et al., 2016). Thus, phosphorylation of NS1 may be important for virus replication.

NS1 is also SUMOylated at three lysine residues (K70, K219 and K221), predominantly at K70 and K219 (Xu et al., 2011, Santos et al., 2013). Santos et al propose that an optimal level of SUMOylation is required for efficient IFN-antagonism, as too little or too many SUMO-conjugates on NS1 interfered with ability

to block IFN induction (Santos et al., 2013). Additionally, NS1 is targeted for conjugation by the IFN-inducible ISG15, an ubiquitin-like protein, which conjugates to NS1 at K41, mediated by HECT and RLD domain containing E3 ubiquitin protein ligase 5 (Herc5 E3 ligase) (Zhao et al., 2010). ISG15 conjugation prevents NS1 nuclear import and IFN-antagonism to attenuate virus replication, but does not inhibit RNA-binding by the NS1 protein despite conjugating to one of the RNA-binding residues (Zhao et al., 2010). It is not known whether NS1 sequesters cellular ISG15 from conjugation to other viral proteins, or whether the ISG15 conjugation prevents NS1 carrying out its functions as efficiently (Zhao et al., 2010). Therefore, there are several reports suggesting the post-translational modification of NS1 may be important for IAV replication, but the mechanisms remain to be fully elucidated.

1.9.1.3 Additional segment 8 gene products

The NS3 protein is expressed in IAV strains in which the NS1 protein has incurred a D125G mutation (A374G in nucleotide sequence representing GAT->GGT in NS mRNA sequence) to introduce a second splice acceptor site into the mRNA. NS3 is an internally deleted version of NS1 protein that lacks residues 126-168 (Selman et al., 2012). This mutation was initially noted following serial passage of a human H3N2 virus in mice and was found to increase virulence (Forbes et al., 2012). It has been speculated to be selected for following adaptation of avian viruses to mammalian hosts (Selman et al., 2012). However, the A-to-G substitution to form the NS3 splice acceptor site was only detected in 33 viruses out of over 18 000 isolates examined (Selman et al., 2012). Currently, the function of NS3 in virus replication is not known.

Negative sense protein (NSP; also referred to as NEG8) is a putative accessory gene product from an ORF in certain IAV strains, of strain-specific length, located on segment 8 vRNA (reading 5' to 3') and therefore in the opposite sense to mRNA (Zhirnov et al., 2007, Clifford et al., 2009). If actually utilised, this ORF would represent the first described ambisense property of the IAV genome. The putative gene product is predicted to be a transmembrane protein, although no protein product has been detected in a laboratory setting. Nevertheless, both sets of authors claim that the ORF has been positively selected for in human viruses (Zhirnov et al., 2007, Clifford et al., 2009). However, since an expression mechanism has yet to be validated (Clifford et al. suggest the possibility of translation initiation from segment 8 vRNA by an, as of yet undescribed, internal ribosome entry site and translation in a poly(A) tail-independent manner) and no functional studies have been performed, it is difficult to speculate the importance of this putative gene product in IAV biology.

Recently, it has been reported that alternative downstream AUG start codons can be utilised in NS1 mRNA to express an N-terminally truncated variant of the NS1 protein (tNS1) (Kuo et al., 2016). The second and third in-frame AUG codons of NS1 mRNA lie at position 79 and 81 respectively, with the latter being in a strong Kozak sequence and the former in a weak Kozak sequence. Both start codons were utilised by PR8 and Udorn72 to express a 17kDa product (Kuo et al., 2016). The tNS1 contributed to inhibition of IRF3 activation and a reduction in IFN-β transcription in stimulated human cells for PR8, but not for Udorn72 (Kuo et al., 2016). Preventing the expression of tNS1 in PR8 by site-directed mutagenesis reduced virus replication in human cells *in vitro* and also in the lungs of mice *in vivo* (Kuo et al., 2016).

1.10 The A- and B-alleles of the NS segment

Traditionally, the NS segment of non-chiropteran IAV has been divided into two phylogenetically distinct 'alleles' (the 'A- and B-alleles') with strikingly low sequence similarity. The amino acid sequence identity of the NS1 protein is typically at least 93% within an allele but can be as low as 62% across the two lineages (Treanor et al., 1989, Ludwig et al., 1991, Suarez and Perdue, 1998, Hale et al., 2008b). Despite this variation in amino acid sequence identity, a crystal structure of a B-allele NS1 ED showed that the overall conformation is highly similar to that of an A-allele (Hale et al., 2008a). The A-allele lineage contains both avian and mammalian IAV sequences, while the B-allele lineage is predominantly avian (Ludwig et al., 1991). The vast majority of functional studies of the NS1 and NEP proteins of IAV to date have been conducted on A-allele genes.

It has been widely accepted that B-allele NS segments are avian-restricted and attenuating in mammalian hosts. This hypothesis was formed over 25 years ago, and at the time of the study there were no reports of a B-allele virus being isolated from a mammalian host (Treanor et al., 1989). Treanor and colleagues generated segment 8 reassortant viruses in the backbone of Udorn72 and assessed virus replication in squirrel monkeys. The B-allele reassortant viruses did not replicate as well in the nasopharynx in comparison to an avian A-allele counterpart, and were cleared more rapidly. However, virus titre in the trachea was not significantly different and the reassortant viruses replicated well *in vitro*. Nevertheless, the authors concluded that B-allele NS segments are attenuating for IAV in mammalian hosts, a view that has been maintained in the field without challenge for over 25 years.

The first reported B-allele sequence isolated from a mammalian host was recorded following a major equine influenza outbreak in China in 1989. This equine virus outbreak, typified by A/equine/Jilin/1/1989 (H3N8), caused a high mortality rate (approximately 20%) and spread readily within horse populations (Guo et al., 1992). This provided the first piece of evidence that B-allele NS segments are not necessarily avian-restricted. Since then, additional B-allele viruses have been isolated from mammalian hosts. At the time of this study, there have been eight mammalian-derived B-allele sequences uploaded to GenBank, however there are tens of thousands of mammalian A-allele sequences available (discussed in detail in Chapter 5).

Following the report by Treanor and colleagues, the Berg laboratory published a series of studies investigating the ability of A- and B-allele NS1 proteins to inhibit the IFN response in mammalian cells. Zohari et al reported that the NS1 protein from an A-allele H10 mink virus was more efficient at suppressing IFN-β gene expression in mink and human lung cells than a closely related H10 chicken B-allele virus NS1 (Zohari et al., 2010b, Zohari et al., 2010a). Likewise, Munir and colleagues assessed A- and B- allele NS1 proteins of closely related H6N8 viruses isolated from mallards, and found that the A-allele NS1s were more competent than the B-alleles at preventing IFN-β, NF-κB and AP-1 promoter activation in stimulated human and mink lung cells (Munir et al., 2011b, Munir et al., 2011a, Munir et al., 2012). Thus, it was proposed that the mechanism underlying the apparent avian-restriction of B-allele viruses was an inability of avian B-allele NS1 proteins to counter the IFN response in the mammalian host. However, at no point were the differences seen in IFN reporter-based assays linked to an attenuation of virus replication *in vitro* or *in vivo* in mammalian cells.

Contrary to the above reports, there is evidence to suggest that B-allele NS segments are not necessarily attenuating in mammalian hosts. Hayman and colleagues assessed a panel of avian NS1 proteins, including a B-allele representative (A/duck/Albany/76), using transfection-based reporter assays and found all were able to successfully inhibit IFN-β expression in human cells (Hayman et al., 2007). Others have described that a B-allele segment 8 increased the virulence and pathogenicity of an A-allele IAV parent in a mammalian host (Ma et al., 2010). The authors introduced the segment 8 from an H5N1 HPAI strain into the backbone of an A-allele H7N1 HPAI virus and found this improved replication in mammalian cells and improved the inhibition of IFN-β production (Ma et al., 2010, Wang et al., 2010). Additionally, the reassortant H7N1 caused mortality in mice, unlike the parental virus (Ma et al., 2010). Furthermore, A- and B-allele NS segment reassortant viruses on the background of PR8 induced similar degrees of pathology in mice (Kim et al., 2015a). Therefore, it is not clear why the B-allele NS segments are apparently restricted to avian hosts.

1.11 Aims and approach

The overall aim of this project was to improve the understanding of the mammalian adaptation of avian influenza viruses. If the mechanisms that cause the apparent avian-restriction of the B-allele lineage of NS genes could be fully elucidated, the understanding of viral and host determinants behind host adaptation would potentially be significantly enhanced. It is crucial that the scientific community improves understanding of the viral and host determinants that allow avian IAV to adapt to a new host and cause disease, particularly given the current absence of a universally effective vaccine or prophylactic drug. The 1918 H1N1 pandemic serves

as a warning of the potential devastation that can result from a highly pathogenic virus adapting to the human host.

The basis of the project was the generation of segment 8 reassortant viruses harbouring segments 1-7 from a mammalian-adapted virus and the segment 8 from either the A- or the B-allele lineage. The viruses were generated by reverse genetics to be used as tools to assess replicative fitness in mammalian cells *in vitro* and *in vivo*, so that any differences could be attributed to the lineage of NS segment. Subsequently, functional analyses of segment 8 products and analysis of host cell responses to infection could reveal determinants of host adaptation linked to the genetic traits of IAV NS segments.

Chapter 2 describes the generation of segment 8 reassortant viruses by reverse genetics and the characterisation their replicative fitness in mammalian host cells *in vitro*. In Chapter 3, the influence of segment 8 lineage on host cell responses, in particular the type I IFN response, is assessed. Analyses on the replicative fitness of NS reassortant viruses and host immune responses *in vivo* are reported in Chapter 4. In Chapter 5, an extensive phylogenetic analysis of available IAV segment 8 sequences is presented. Concluding remarks are presented in Chapter 6, and the materials and methods used in this study are given in Chapter 7.

Chapter 2: Replicative fitness of segment 8 reassortant viruses *in vitro.*

2.1 Introduction

2.1.1 Aims

As discussed in more detail in Chapter 1, the overall aim of this study was to better elucidate mechanisms underpinning the proposed avian-restriction of IAV strains harbouring a B-allele NS segment. Understanding the mechanism of restriction would allow an improved understanding of the ability of avian IAVs to infect mammalian hosts, and in particular the contribution of the NS segment in *Aves* to *Mammalia* transmission.

The aim of this section of the study was to assess replicative fitness of mammalian viruses that had been forcibly reassorted to contain an avian IAV segment 8, from either the A- or B-allele lineage, in mammalian host systems *in vitro*. Differences in replicative fitness could therefore be attributed to the NS genes and this could provide a platform to understand the mechanisms behind the proposed avian-restriction of B-allele NS segments.

2.1.2 Hypothesis

In this study, it was hypothesised that incorporation of an NS segment belonging to the B-allele clade of avian influenza strains would attenuate the replicative fitness of a mammalian-adapted IAV in mammalian cells *in vitro*, since B-allele genes have been proposed to be unable to allow efficient IAV infection of mammalian hosts in previous reports (Treanor et al., 1989, Zohari et al., 2010a, Munir et al., 2011b) and the vast majority of mammalian IAV isolate NS genes belong to the

A-allele lineage. It was speculated that deficiencies of B-allele NS segments in mammalian host systems could arise from one or more of several mechanisms: i) an inadequate complementation with the viral polymerase could reduce replicative fitness, since NS1 and NEP have both been implicated in regulating viral polymerase activity in RNP reconstitution assays (Bullido et al., 2001, Robb et al., 2009, Wang et al., 2010). ii) Abnormal regulation of viral protein synthesis, since NS1 recruits eIF4G and PABPI to enhance viral mRNA translation (Burgui et al., 2003), inhibits the host cell spliceosome (Lu et al., 1994, Qiu et al., 1995) and may regulate segment 7 mRNA splicing (Robb and Fodor, 2012). iii) Inefficient control of the mammalian IFN response by B-allele NS1 proteins, as has been speculated in previous reports (Zohari et al., 2010a, Munir et al., 2011a, Munir et al., 2011b, Munir et al., 2012). iv) B-allele NS segments could be disadvantaged at the level of genetic reassortment into mammalian-adapted viruses compared to A-allele NS segments, due to differences in RNA packaging signals (Gog et al., 2007). v) An inability of B-allele NEP to perform nuclear export of vRNPs in mammalian cells would abolish virus propagation.

2.1.3 Approach

Initially, a panel of A- and B-allele segment 8 genes from North America (See Table 2.1 for NS genes) were incorporated into the mouse-adapted PR8 backbone, and used as tools to assess replicative fitness in mammalian cells *in vitro*. The NS segments were selected from a variety of LPAI strains isolated in North America between 1986 and 2005, from multiple H and N subtype backgrounds (Table 2.1) by Prof. Jeffery Taubenberger (The National Institute of Allergy and Infectious Diseases, Maryland, USA). These NS genes were cloned into pHH21 plasmids and kindly donated by Dr.

Table 2.1. Virus strains.

Virus Name	Strain from which NS segment isolated	Allele	Accession number (NS)
PR8	A/Puerto Rico/8/1934 (H1N1)	A	EF467817.1
Cal7	A/California/7/2009 (H1N1)	A	Unpublished
Udorn72	A/Udorn/72 (H3N2)	A	CY009640.1
O175A[a]	A/green-winged teal/Ohio/175/1986 (H2N1)	A	CY018881.1
O173A	A/mallard/Ohio/173/1990 (H11N9)	A	CY021665.1
O340A	A/green-winged teal/Ohio/340/1987 (H11N9)	A	CY021873.1
M1124A	A/mallard/Maryland/1124/2005 (H11N9)	A	CY021473.1
O265B[a]	A/Mallard/Ohio/265/1987 (H1N9)	B	CY017279.1
O430B	A/green-winged teal/Ohio/430/1987 (H1N1)	B	CY011044.1
O264B	A/mallard/Ohio/264/1986 (H3N8)	B	CY016399.1
O339B	A/pintail/Ohio/339/1987 (H3N8)	B	CY019201.1
O668B	A/mallard/Ohio/668/2002 (H4N6)	B	CY020793.1
O671B	A/mallard/Ohio/671/2002 (H4N6)	B	CY020801.1
O35B	A/northern shoveler/Ohio/35/1986 (H3N8)	B	CY020937.1
O246B	A/bufflehead/Ohio/246/1986 (H11N2)	B	CY017079.1
Alb88B[b]	A/mallard/Alberta/88/1976 (H6N8)	B	M25373.1
NY6750A[c]	A/mallard/New York/6750/1978 (H2N2)	A	M25376.1
Sw412A[d]	A/mallard/Sweden/S90412/2005 (H6N8)	A	EU518721.1
Sw418B[e]	A/mallard/Sweden/S90418/2005 (H6N8)	B	EU518722
NY107B[f]	A/New York/107/2003 (H7N8)	B	EU587374.2
J89B	A/equine/Jilin/1/1989 (H3N8)	B	M65020.1

[a] Used as representative "consensus" A and B genes for specific experiments.

[b] 1-15 & 855-890 from A/blue-winged teal/ALB/221/1978(H7N2) (CY005035.1). g242a to remove BsmBI site.

[c] 1-16 and 855-890 from A/mallard/New York/6750/1978(H2N2) (M80945.1).

[d] 1-26 and 888-890 from A/duck/Italy/194659/2006(H3N2) (FJ432766.1).

[e] 1-26 and 882-890 from A/tufted duck/Mongolia/1409/2010(H1N1) (KC871435.1). a696c to remove BsmBI site.

[f] 1-15 and 871-890 from A/guinea fowl/New York/20221-11/1995(H2N2) (CY014833.1).

Rebecca Dunfee from Prof. Jeffery Taubenberger's laboratory. The influence of the lineage of segment 8 on virus polymerase transcriptional activity, virus protein expression, and infectious virus production was studied in mammalian cells.

2.1.3.1 A-and B-allele NS genes

The amino acid sequences of the NS1 proteins from these LPAI viruses were at least 99% homologous within their respective clade, and typically shared only 71% sequence homology across the two groups (Fig 2.1), which is in keeping with previous publications (Ludwig et al., 1991, Suarez and Perdue, 1998). The NEP proteins were generally less divergent between the two clades, typically sharing 84% sequence identity (Fig 2.2). The literature was reviewed on NS1 and NEP proteins and residues which have been characterised as being important for protein function were noted. These were compared across the A- and B- allele NS1 and NEP proteins used in this report (Figs 2.1 and 2.2). Most key functional residues of NS1 and NEP were conserved in B-allele proteins. In NS1, R38 and K41 which are important for RNA binding and circumvention of the antiviral response (Wang et al., 1999, Min and Krug, 2006) as well as E96 and E97, which are involved in binding to and inhibiting TRIM25 and therefore activation of RIG-I (Gack et al., 2009), were conserved in B-allele NS1s. However, the F103 residue - which has been shown, along with M106, to be essential for the binding and inhibition of cellular 30-kDa cleavage and polyadenylation specificity factor 30 (CPSF30), a protein involved in the 3' processing of pre-mRNAs (Nemeroff et al., 1998, Li et al., 2001, Kochs et al., 2007, Das et al., 2008) - was highly conserved in A-allele NS1s but appeared to be invariably different (Y103) in B-allele NS1 proteins used in this study (Fig 2.1). This observation has been reported elsewhere (Zohari et al., 2010a). However, the M106 residue was conserved in all avian NS1s in

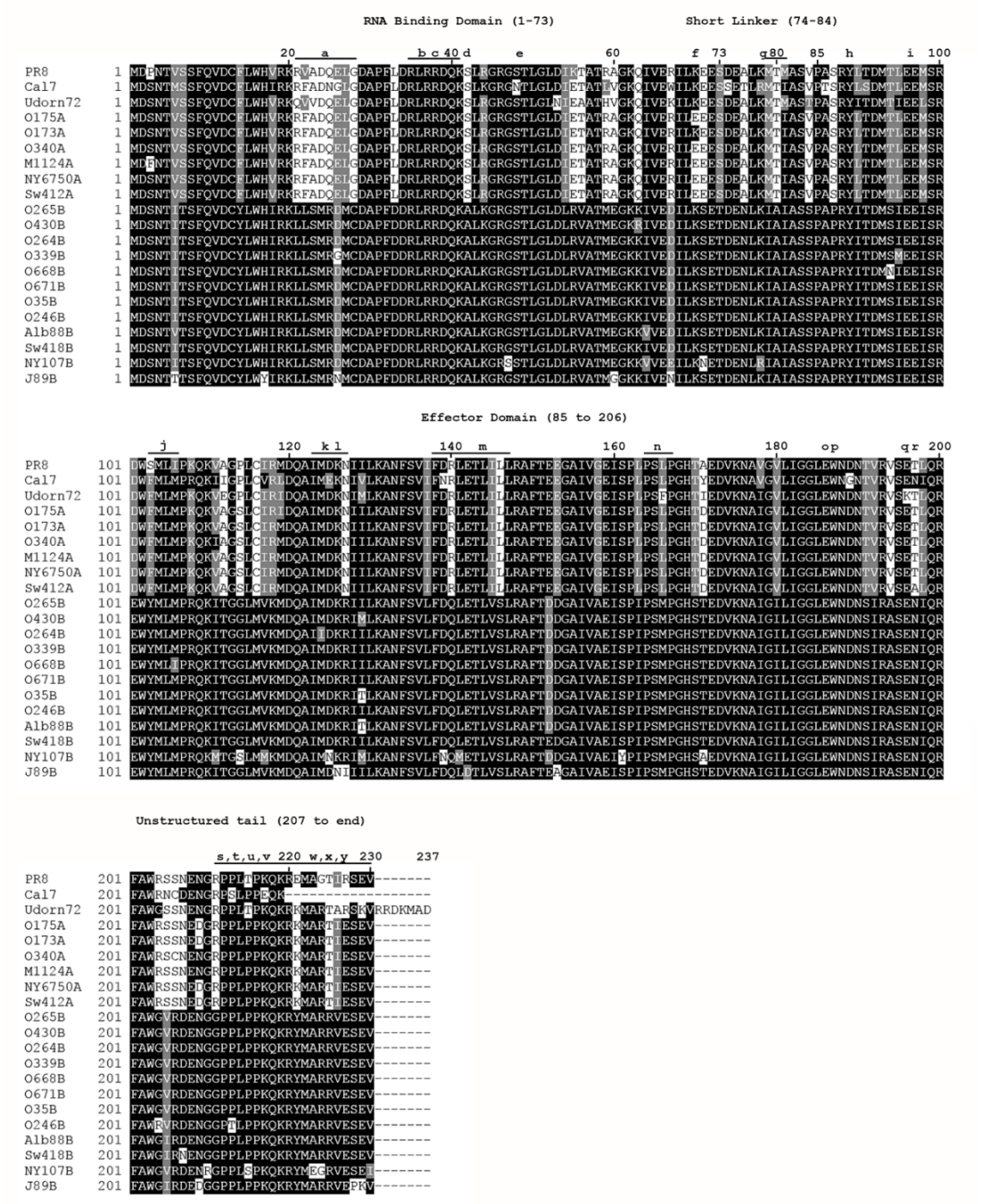

Fig 2.1 NS1 protein alignment. NS1 protein sequences from selected IAV strains were aligned using clustal omega (http://www.ebi.ac.uk/Tools/msa/clustalo/) using default parameters. Alignments were processed using Boxshade Server (http://www.ch.embnet.org/software/BOX_form.html). Features of functional interest are annotated in the alignment.

a – ^{21}RFADQELG^{28} and ^{21}LLSMRDMC^{28} mostly conserved within A- and B- alleles, respectively (Munir et al., 2011b).

b – 35-41 nuclear localisation signal (Greenspan et al., 1988, Melen et al., 2007, Han et al., 2010).

c – R38 essential for RNA binding. K41 plays important role. (Wang et al., 1999).

d – S42 is a phosphorylation site (Hsiang et al., 2012).

e – S48 and T49 are phosphorylation sites (Hutchinson et al., 2012). T49 phosphorylation inhibits IFN-antagonism (Kathum et al., 2016).
f – K70 SUMOylation site (Santos et al., 2013).
g- Codons 79 and 81 can be used as an alternative start site for tNS1 expression in PR8 and Udorn72 (Kuo et al., 2016).
h – Y89 required for PI3K binding (Hale et al., 2006, Hale et al., 2010a).
i – E96 and E97 dictate TRIM25 binding and inhibition (Gack et al., 2009).
j – F103 and M106 important for efficient CPSF30 binding and inhibition (Twu et al., 2007, Kochs et al., 2007, Das et al., 2008).
k – 123-127 involved in PKR binding and inhibition (Min et al., 2007).
l – D125G mutation (GAT > GTT) forms splice acceptor site leading to NS3 expression (Selman et al., 2012).
m – 138-147 nuclear export signal (Li et al., 1998).
n – P164 and P167 involved in PI3K binding (Shin et al., 2007, Hale et al., 2010a).
o – E186 involved in CPSF30 binding and inhibition (Nemeroff et al., 1998, Li et al., 2001, Noah et al., 2003).
p – W187 required for effector domain dimerisation (Kerry et al., 2011b).
q – E196K mutation fails to inhibit IRF3 activation (Kuo et al., 2010).
r - T197 phosphorylation site (Hutchinson et al., 2012).
s - ^{211}GPPLPPKQKRYMARRV^{226} A2 rabbit polyclonal antiserum epitope.
t – ^{212}PPLPPK CRKL^{217} motif binds CRKI/II and CRKL proteins to prevent strong activation of JNK-AFT2 pathway (Heikkinen et al., 2008, Hale et al., 2009).
u – T215 phosphorylation site (Hale et al., 2009)
v – 216-229 second nuclear localisation signal (Greenspan et al., 1988, Melen et al., 2007, Han et al., 2010).
w – K219 and K221 are SUMOylation sites (Xu et al., 2011, Santos et al., 2013).
x – 223-230 involved in PABPII binding and inhibition (Chen et al., 1999, Li et al., 2001).
y – ^{227}ESEV^{230} motif for PDZ-domain binding and virulence factor (Obenauer et al., 2006, Jackson et al., 2008).

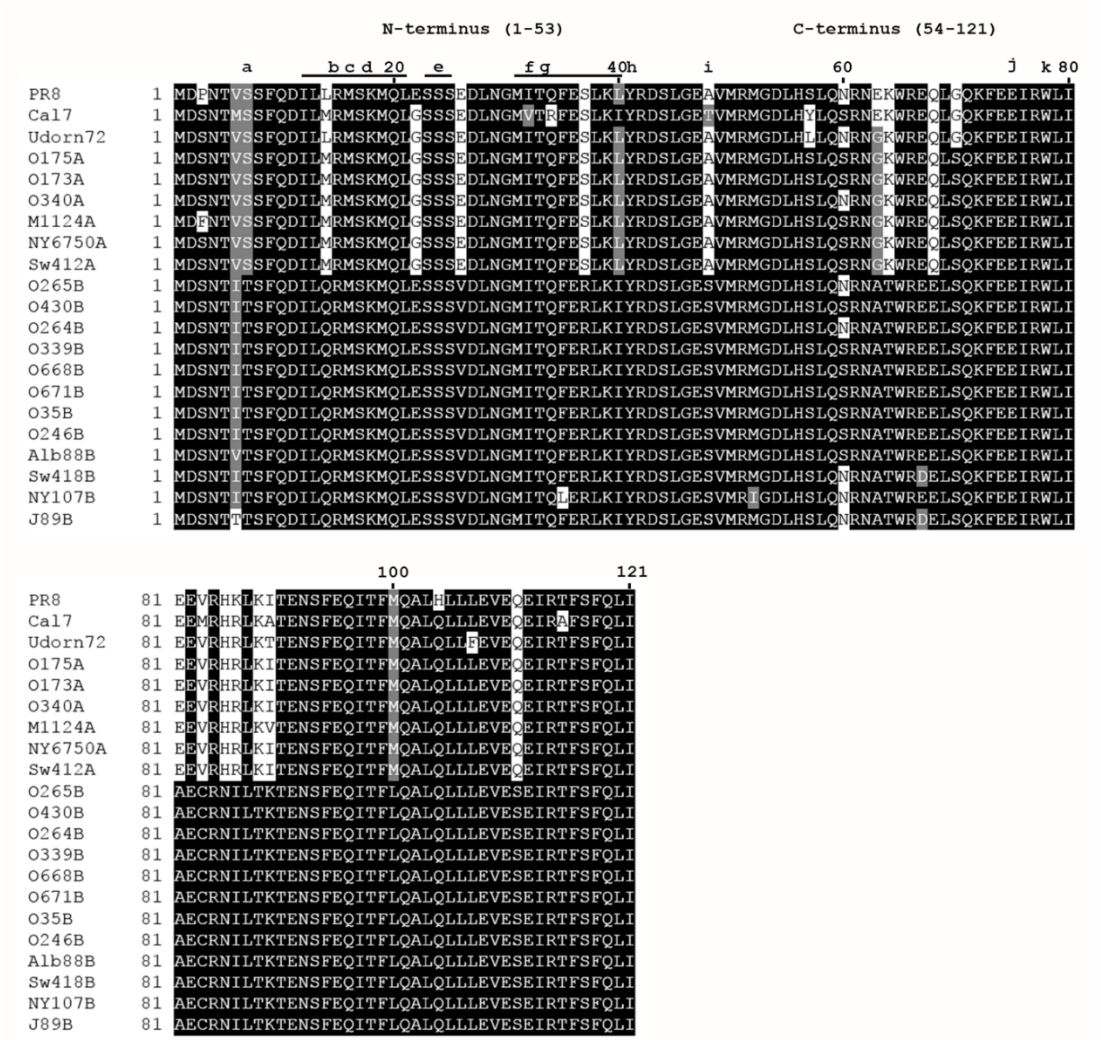

Fig 2.2. NEP protein alignment. NEP protein sequences from selected IAV strains were aligned using clustal omega (http://www.ebi.ac.uk/Tools/msa/clustalo/) using default parameters. Alignments were processed using Boxshade Server (http://www.ch.embnet.org/software/BOX_form.html). Features of functional interest are annotated on the alignment.
a – S7L mutation seen in H5N1 human isolates which enhances avian H5N1 polymerase activity (PB2 E627) in human cells (Mänz et al., 2012).

b – 12-21 hydrophobic NES-1 that is important for nuclear export of vRNPS via interactions with CRM1 (O'Neill et al., 1998, Iwatsuki-Horimoto et al., 2004).

c - M16I enhances avian H5N1 polymerase activity (PB2 E627) in human cells (Mänz et al., 2012).

d – M16, M19 and L21 replacement with alanine abolishes NP nucleocytoplasmic transport (Neumann et al., 2000).

e – S23, S24 and S25 highly conserved in NEP, and have been observed to be phosphorylated (Hutchinson et al., 2012).

f – I32T results in virion packaging defects (Odagiri et al., 1994)

g – 31-40 hydrophobic NES-2 which is important in nuclear export of vRNPs via interaction with CRM1 (Huang et al., 2013).

h - Y41C enhances avian H5N1 polymerase activity (PB2 E627) in human cells (Mänz et al., 2012).

i – A48T enhances avian H5N1 polymerase activity (PB2 E627) in human cells (Mänz et al., 2012).

j – E75G enhances avian H5N1 polymerase activity (PB2 E627) in human cells (Mänz et al., 2012).

k – W78 involved in interaction with M1 to mediate nuclear export of vRNPs (Akarsu et al., 2003).

this study except in O668B, which has an isoleucine at this position. E186, which has also been reported to be an important residue for binding and inhibiting CPSF30 (Nemeroff et al., 1998, Li et al., 2001, Noah et al., 2003) appeared conserved in both A- and B-allele NS1 proteins. Notably, there was an eight amino acid sequence, ^{21}RFADQELG^{28} and ^{21}LLSMRDMC^{28}, in the RNA-binding domain that was relatively well but divergently conserved in A- and B- allele NS1 proteins, respectively. This has also been reported elsewhere (Munir et al., 2011a, Munir et al., 2012). However these sequences do not appear to be entirely conserved in all IAV NS1 strains and have not been characterised or attributed to a particular function of NS1 to date.

W78 of NEP, which is thought to interact with viral M1 to facilitate nuclear export of vRNPs (Akarsu et al., 2003), was conserved in both avian A- and B-allele NEP proteins. Within the first nuclear export signal of NEP (residues 12-21), the B-allele NEP proteins used here had a glutamic acid in place of a methionine/leucine at position 12 which was found in the A-allele NEP sequences (Fig 2.2). The significance of this in terms of NEP function is not currently known.

The phylogeny of NS genes of influenza has been studied by other groups and has been reported in various publications. Figure 2.3 shows a phylogenetic tree of NS1-coding RNA sequences from a report by Sevilla-Reyes and colleagues (Sevilla-Reyes et al., 2013) with the sub-groups that contain strains used in this report highlighted. The avian B-allele strains are clearly divergent from the A-allele sequences and form their own group. PR8 NS1 sequence falls into group A4.1 (H1N1), Udorn72 into A4.2 (H3N2), Cal7 into A3 (Classical swine), Sw412A falls into the A5.4 (Eurasian avian) lineage, and the North American A-allele sequences belong to

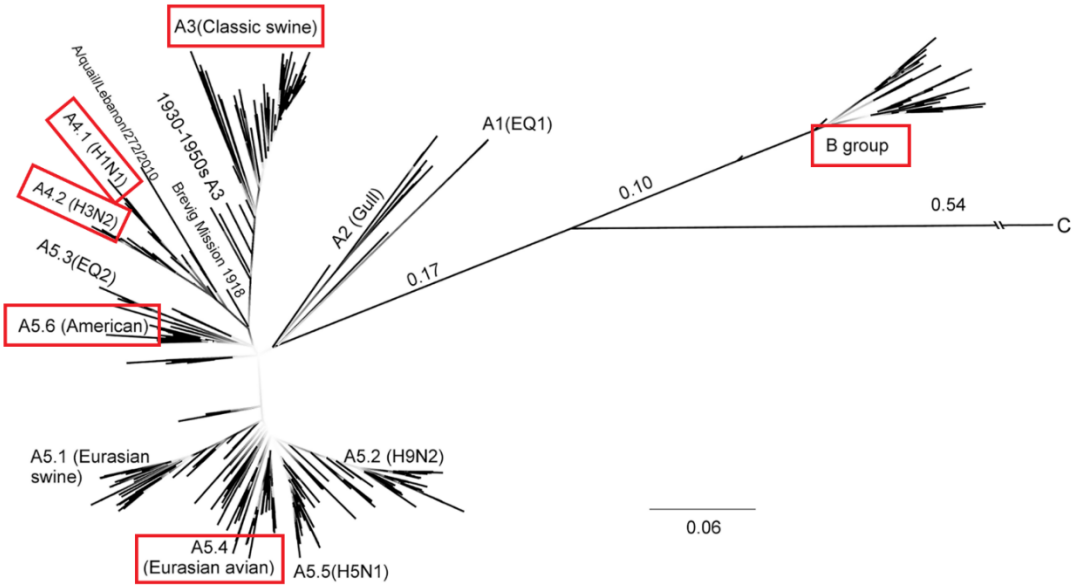

Fig 2.3. Phylogenetic tree of NS1-coding RNA sequences. Shown is a phylogenetic tree of IAV NS1-coding RNA sequences grouped into subtypes. Red boxes highlight the sub-groups in which the NS1 sequences from strains used in this study belong: All B-alleles sequences are in the B group, PR8 belongs to A4.1 (H1N1), Udorn72 in A4.2 (H3N2), Cal7 in A3 (Classical swine), Sw412A in A5.4 (Eurasian avian), and the North American A-allele sequences in A5.6 (American). Adapted from (Sevilla-Reyes et al., 2013).

the A5.6 (American) sub-group (Fig 2.3) (Sevilla-Reyes et al., 2013). Therefore a diverse range of NS segments were investigated in this study.

2.2 Results

2.2.1 Virus rescue of PR8-based segment 8 reassortants

The first assessment of the ability of A- and B-allele LPAI NS segments to complement a mammalian-adapted virus was to attempt virus rescues. 293T cells were transfected with the PR8 reverse genetics plasmids (pDUAL) for segments 1-7 (de Wit et al., 2004), with segment 8 replaced with pHH21 plasmids for each of the avian IAV segment 8s of interest (Fig 2.4). A negative control sample was included that lacked a PB2 pDUAL plasmid, which was unable to generate infectious virus, and a fully wild-type PR8 rescue was performed as a positive control. The supernatant was collected after 48 h, and this was termed the 'passage zero' (P_0) stock.

'Passage one' (P_1) virus stocks were generated by infecting T25 flasks of MDCK cells with diluted P_0 supernatants. 100 µl of P_0 virus was diluted in 1 ml of VGM and used to infect MDCK cells (MOI < 0.01). Throughout the course of infection, cells were monitored using microscopy and successful infection was judged based on cell morphology in comparison to the mock-infected negative control sample (no PB2). At 48 h post-infection the supernatant of infected cells was clarified (3000 rpm, 5 min) and stored. The P_1 viruses were titrated by plaque assay and used for subsequent experiments. All viruses rescued readily. Mock-infected MDCK cells produced undetectable levels of virus (limit of detection 2.5 PFU/ml) (Fig 2.5). All viruses replicated to titres of 10^8 PFU/ml, with no statistically significant differences in titres observed (unpaired t-test, n = 5). Furthermore, plaque phenotypes were

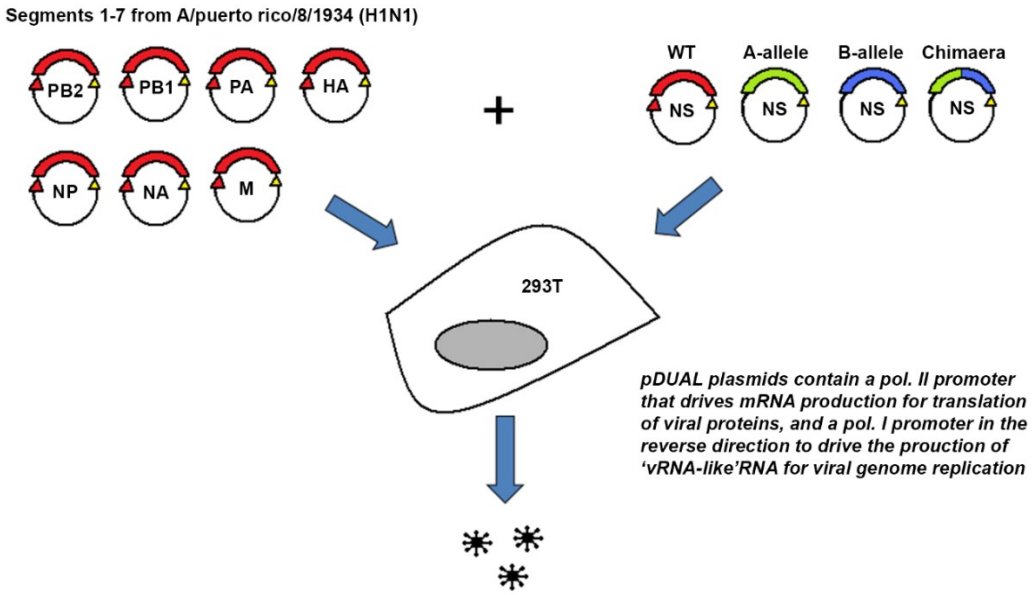

Fig 2.4. Schematic of reverse genetics system. 293T cells are co-transfected with 8 pDUAL plasmids, each driving the production of mRNA and 'vRNA-like' RNA from each segment of the influenza A virus genome, and this leads to infectious virus particle production.

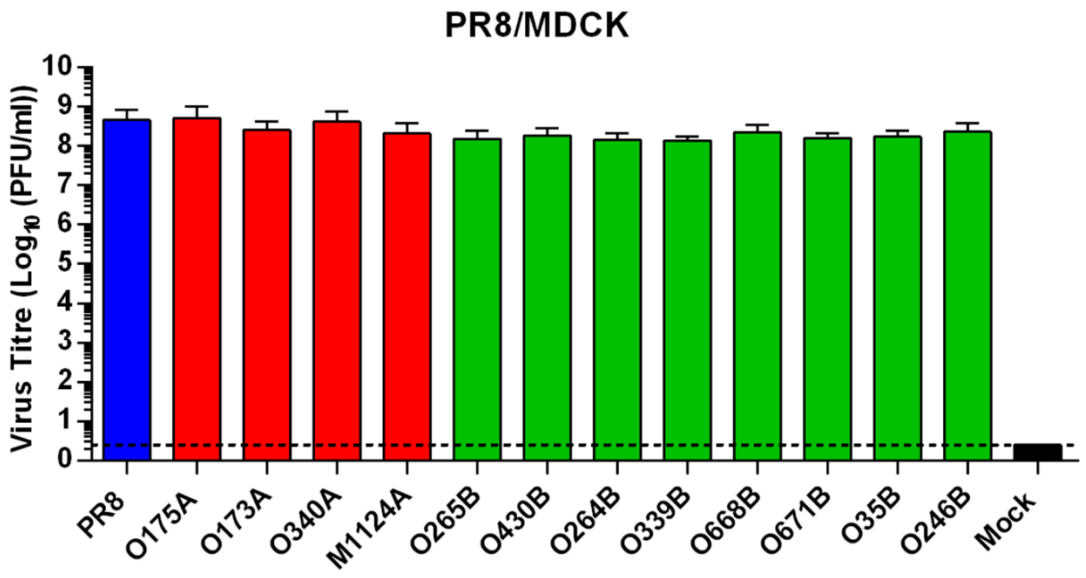

Fig 2.5. Multi-cycle growth of PR8 NS segment reassortant viruses in MDCK cells. MDCK cell monolayers were infected at an MOI of 0.001 and virus in the supernatant was titrated by plaque assay after 48h. Data are the mean +/- SD (n = 5). Dotted line indicates the limit of detection of the plaque assay.

indistinguishable between WT PR8 and all of the segment 8 reassortant viruses (data not shown). RNA was extracted from virus in the supernatant and segment 8 RT-PCR was performed. DNA sequencing was used to confirm NS genes were correct and no mutations had occurred during virus growth (data not shown). Therefore, both avian A- and B-allele NS segments appeared to be compatible in a mammalian-adapted virus background in mammalian cells *in vitro*. These results suggest that B-allele NS segment products (NEP, NS1) are able to carry out functions important for virus replication efficiently in mammalian cells to allow infectious virus production, and that the avian segment 8s of both lineages are able to package into an otherwise mammalian-adapted virus. A panel of NS reassortant viruses was now available to systematically assess replicative fitness of A- and B-allele viruses in mammalian systems *in vitro*.

2.2.2 Viral protein synthesis in infected MDCK cells

There is evidence that both NEP and NS1 influence viral protein synthesis. NEP has been shown to reduce the levels of mRNA made by the viral polymerase in reconstitution assays (Bullido et al., 2001, Robb et al., 2009). NS1 is thought to recruit viral mRNAs, eIF4G and PABPI to form viral mRNA translation initiation complexes to enhance the translation of viral proteins (Burgui et al., 2003). Additionally, NS1 has been reported inhibit the host cell splicing machinery (Lu et al., 1994, Qiu et al., 1995), and this may influence the splicing of segment 7 pre-mRNAs (Robb and Fodor, 2012). Thus, given a clear role of segment 8 products in viral gene expression, the abundances of several viral proteins were quantified by western blotting during infection to see if the A- and B- allele lineage NS segment products were capable of supporting efficient protein synthesis by a mammalian-adapted virus in mammalian cells *in vitro*. MDCK

cells were infected at high multiplicity and cell lysates were generated at 8 h post-infection. Efficient infection was confirmed in all samples by immunofluorescence (IF) analysis of intracellular NP in a parallel infection (data not shown). SDS-PAGE and western blotting for various virus proteins was performed. Mock-infected samples contained undetectable levels of all viral proteins immunoblotted (Fig 2.6A). The levels of NP, M1, and M2 were similar, barring minor fluctuations, for all reassortant viruses. The ratio of M1:M2 was also quantified by densitometry, to assess any differences in splicing efficiency of segment 7 mRNA across the different virus infections. The ratios of M1:M2 were similar across all samples, with all ratios falling within two-fold of the WT PR8 sample (Fig 2.6B). Whilst the relative quantities of NS1 across the reassortant viruses could not be accurately determined due to potential different affinities of our available anti-NS1 antibodies, NS1 was detected in all virus-infected samples. Anti-PR8-NS1 antiserum (V29) did not pick up B-allele NS1 proteins, but anti-O265B-NS1 (A2, see Chapter 7: Materials and Methods for validation of antiserum, and see Fig 2.1 for epitope sequence on NS1 alignment) detected all avian NS1 proteins but not PR8 NS1. Avian NEPs were not detected by western blotting with the available antisera, but NEP expression was demonstrated using immunoprecipitation of ^{35}S-labelled cell lysates with a rabbit polyclonal antiserum raised to PR8 NEP (Fig 2.6A). Again, a reliable comparison of NEP quantification was not viable due to potential epitope differences between different NEP proteins.

These data show that avian A- and B- allele NS segment products are capable of supporting efficient viral protein synthesis during infection. There were also no

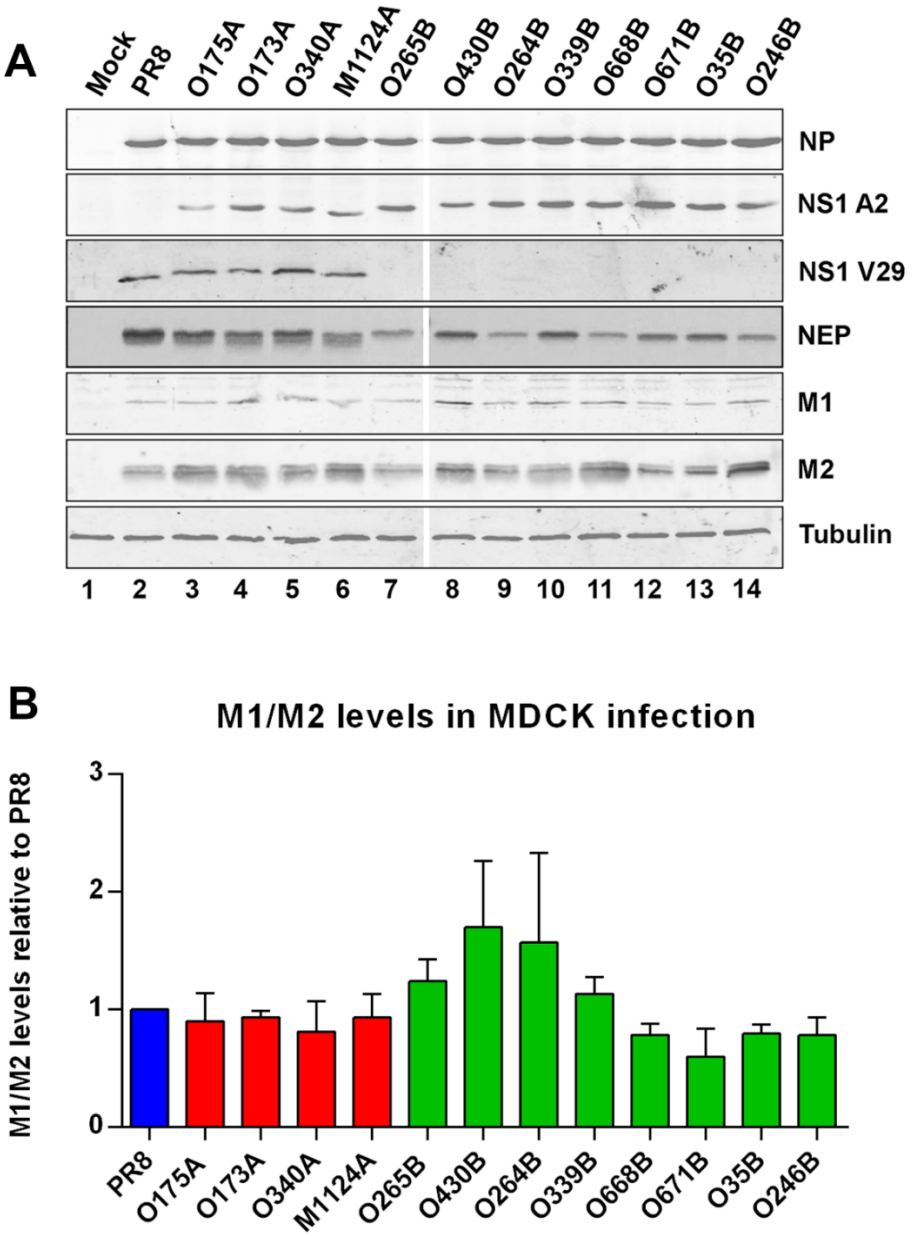

Fig 2.6 Protein synthesis by NS segment reassortant viruses in mammalian cell culture. (A) MDCK cells were infected at an MOI of 3 and cell lysates were prepared at 8 h p.i. To detect viral NP, NS1, M1 and M2 polypeptides as well as cellular tubulin, lysates were subjected to SDS-PAGE and immunoblotted with the appropriate antisera. To detect NEP protein, cells were infected at an MOI of 10 and metabolically labelled with ^{35}S protein labeling mix between 6 h and 8 h p.i. Lysates were then immunoprecipitated with anti-NEP antiserum and precipitates analysed by SDS-PAGE and autoradiography. Data are representative of more than one independent experiment. (B) The ratios of M1:M2 quantification determined by western blotting and densitometry following three independent MDCK cell infections as in (A). Data are mean +/- SEM (n = 3, except O35B which is n = 2).

substantial differences in M1:M2 ratio, suggesting that splicing efficiency of segment 7 mRNA is similar during infection with A- and B-allele reassortant viruses.

2.2.3 Sub-cellular localisation of NS1 proteins in human cells

It has been documented that the subcellular localisation of IAV NS1 is both host- and strain-specific (Melen et al., 2007, Volmer et al., 2010, Han et al., 2010). There is published evidence of differing sub-cellular localisations of A- and a B- allele NS1 proteins, derived from avian viruses, in transfection-based experiments using mammalian cells (Munir et al., 2011b). The authors suggested that the B-allele proteins displayed a delayed entry into the nucleus which may have detrimental consequences for virus replication. To ask whether there was a lineage-dependent difference in NS1 sub-cellular localisation in mammalian cells for the strains used in this study, sub-cellular localisation was assessed both in the context of virus infection by immunostaining and also using fluorescently-labelled NS1 proteins (NS1-GFP) in transfection-based studies (see Chapter 7: Materials and Methods for generation of NS1-GFP constructs). As discussed in Chapter 1, NS1 has been reported to interact with numerous cellular proteins both in the nucleus and in the cytoplasm to manipulate the cell for optimal conditions for virus replication. Therefore, differing sub-cellular localisation between A- and B-allele NS1 proteins may point to differences in function in mammalian cells between the two lineages, which could impact on virus replication.

To assess NS1 subcellular localisation during infection, A549 cells were infected with PR8, O175A or O265B at an MOI of 5 and fixed at 8, 16 and 24 h post-infection. The fixed cells were permeabilised and were stained for NS1 using rabbit polyclonal antisera (anti-RBD). Mock-infected samples were used to determine background staining. NS1 was detected predominantly in the cytoplasm of infected

cells at all time-points post-infection with all viruses, although nuclear staining was also observed to a lesser degree (Fig 2.7A, 16 h time-point not shown). The sub-cellular localisation was similar between WT PR8, O175A and O265B NS1 proteins at all time-points. In no case was NS1 detected within the nucleolus (see arrowheads in 'crop' column of Fig 2.7A). Attempts to study NS1 sub-cellular localisation at earlier time-points during infection were not successful due to poor signal:noise of available antisera (data not shown). Therefore, NS1-GFP expressing plasmids were employed and sub-cellular localisation was assessed at early time-points post-transfection.

293T cells were transfected with pEGFPN1 (Clontech) with the NS1 ORF of either PR8, O175A or O265B upstream of the eGFP ORF which expressed the NS1 protein C-terminally tagged with eGFP. An empty pEGFPN1 plasmid was transfected as a control which expressed eGFP only, and a mock transfection was performed in which no plasmid was included in the transfection mix. Cells were fixed at 4, 5, 6, and 8 h post-transfection, the DNA was stained with Hoechst dye, and GFP and Hoechst fluorescence was imaged using laser scanning confocal microscopy. The laser properties were kept the same across all samples at each time-point. Cells transfected with the empty pEGFPN1 vector displayed GFP fluorescence in both the nucleus and cytoplasm at all time-points (Figs 2.7B and 2.7C show the 4 h and 8 h samples respectively, 5 h and 6 h are not shown). Mock-transfections did not display detectable GFP fluorescence using the same laser properties. PR8 NS1-GFP displayed stronger fluorescence in the cytoplasm than the nucleus at all time-points, although nuclear fluorescence was also detected but to a lesser extent. At 4 h post-transfection, O175A and O265B NS1-GFP was observed in both the nucleus and cytoplasm at similar levels

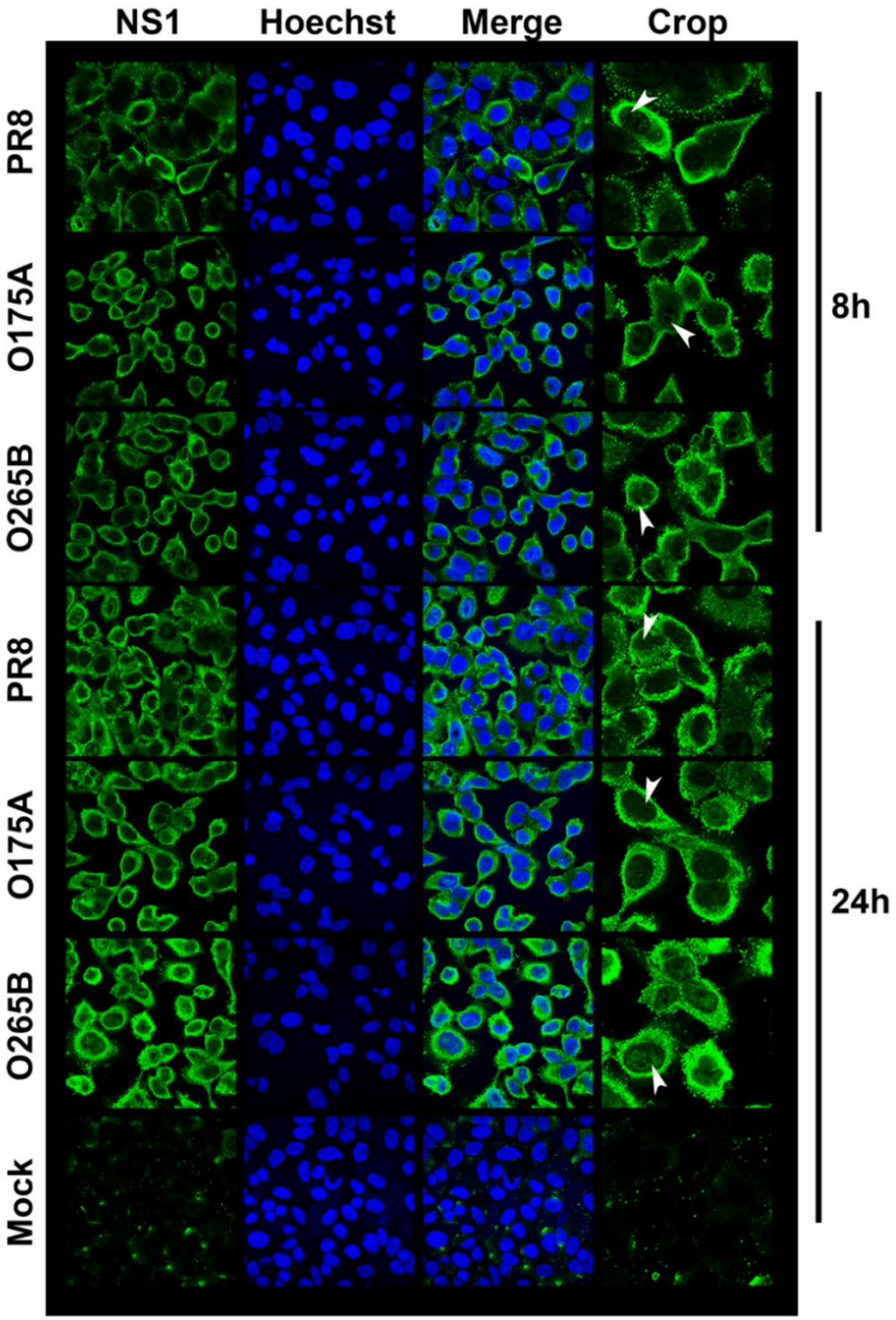

Fig 2.7A. Sub-cellular localisation of NS1 during infection. A549 cells were infected with segment 8 reassortant viruses at an MOI of 5 and fixed at 24 h post-infection. Cells were permeabilised and immunostained for viral NS1 (green, anti-NS1-RBD) and DNA (Blue, Hoechst). White arrowheads show nucleoli. Images were obtained using laser scanning confocal microscopy.

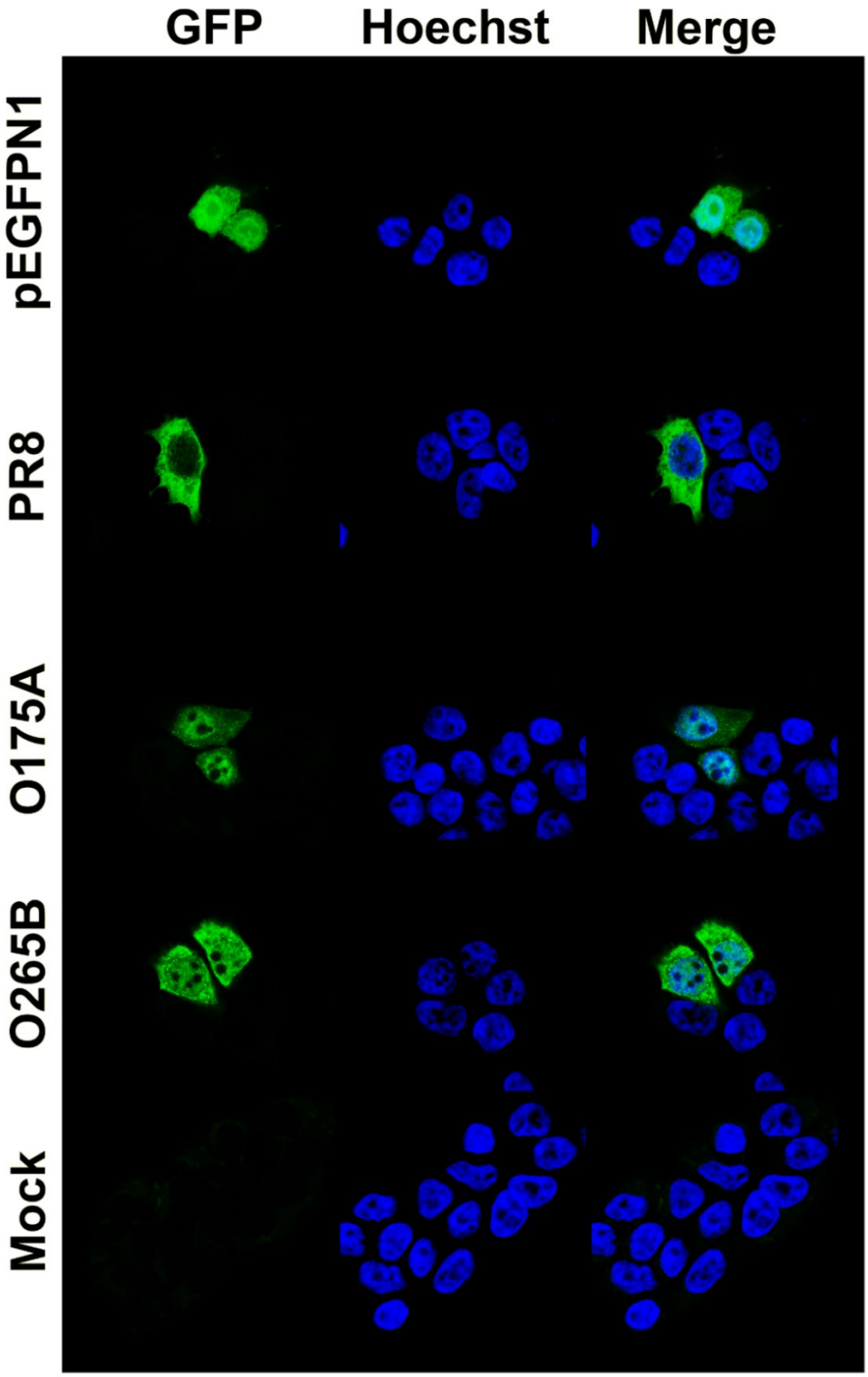

Fig 2.7B. NS1-GFP sub-cellular localisation at 4 h post-transfection. 293T cells were transfected with either empty pEFPN1 plasmid or with pEGFPN1 with NS1 ORF of PR8, O175A or O265B upstream of GFP (green), or mock-transfected. DNA was stained with Hoechst dye (blue). Images were obtained using laser scanning confocal microscopy.

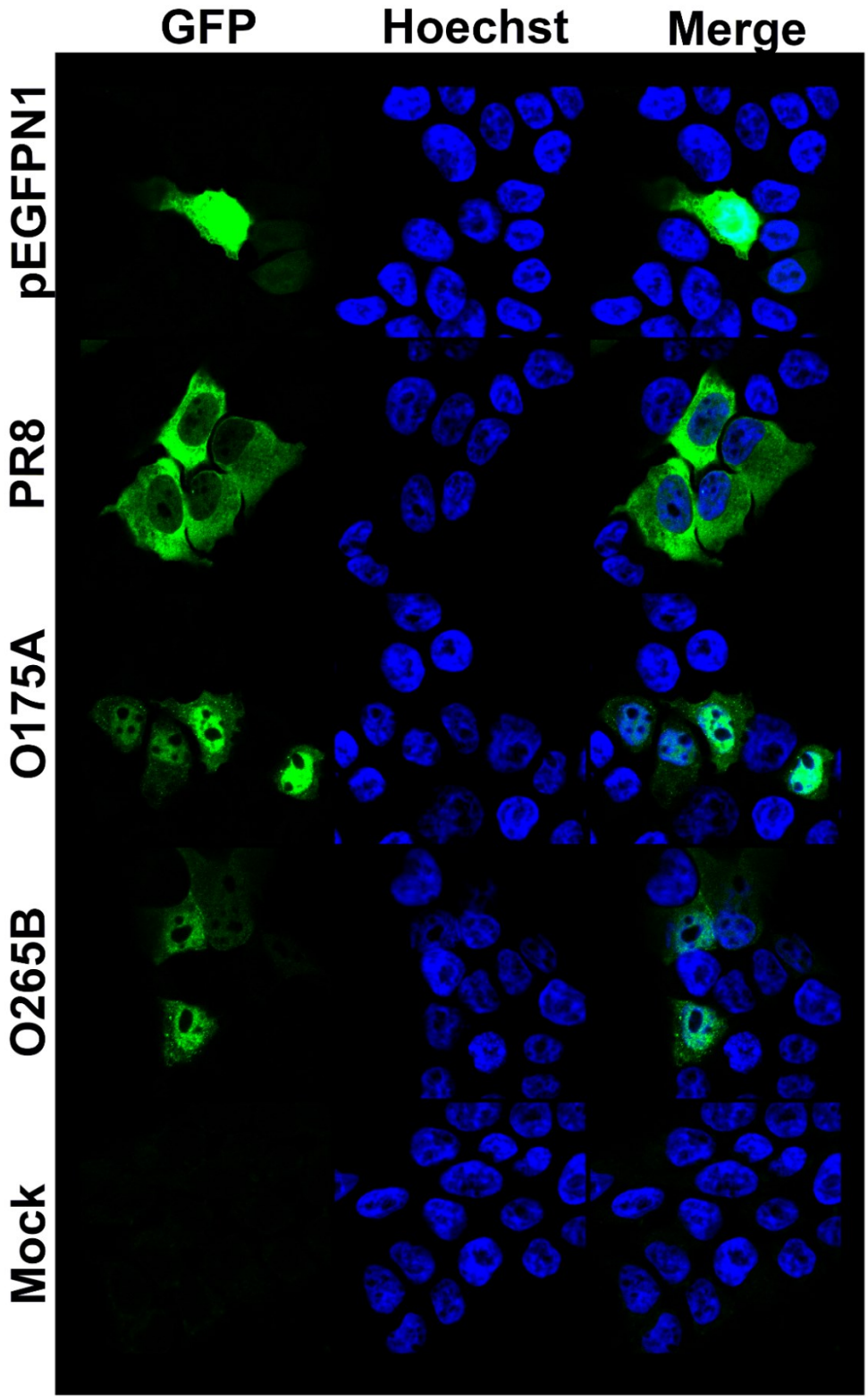

Fig 2.7C. NS1-GFP sub-cellular localisation at 8 h post-transfection. 293T cells were transfected with either empty pEFPN1 plasmid or with pEGFPN1 with NS1 ORF of PR8, O175A or O265B upstream of GFP (green), or mock-transfected. DNA was stained with Hoechst dye (blue). Images were obtained using laser scanning confocal microscopy.

(Fig 2.7B). With increasing lengths of time post-infection, both O175A and O265B NS1-GFP showed more dominant nuclear localisation and to similar extents between the two strains (Fig 2.7C). Indeed, in experiments described in Chapter 3 using the same NS1-GFP expression plasmids, O175A and O265B showed a strong tendency for nuclear localisation over cytoplasmic localisation at 24 and 48 h post-transfection, while PR8 NS1-GFP was mostly cytoplasmic (data not shown).

Overall these data suggest that the lineage of NS1 did not obviously alter NS1 sub-cellular localisation during infection of A549 cells or transfection of 293T cells, although there were differences between WT PR8 NS1 and the avian NS1s tested in transfection based studies, but not during infection. Additionally, the avian NS1 proteins tested showed a different localisation pattern across the two systems used, however this is not particularly surprising as the cellular environments are different across infection and transfection studies. Finally, there was little evidence to suggest that the B-allele NS1 protein displayed a delay in nuclear localisation relative to A-allele NS1, which has been suggested in a previous study using a transfection-based system (Munir et al., 2011b).

2.2.4 The influence of A- and B- allele segment 8s on PR8 polymerase activity

Both NS1 and NEP have been reported to influence influenza polymerase activity in IAV reconstitution assays, although there is conflicting evidence in the literature. Wang and colleagues reported that NS1 reduced the levels of all three viral RNA species (mRNA, cRNA and vRNA) (Wang et al., 2010), whilst little effect was noted in a separate study (Robb et al., 2009). Bullido and colleagues reported that NEP reduced RNA synthesis using an IAV chloramphenicol acetyltransferase (CAT)

reporter (Bullido et al., 2001), while Robb and others reported that NEP increased the levels of both cRNA and vRNA, but reduced mRNA levels, of various IAV segments (Robb et al., 2009).

Therefore the influence of PR8 segment 8 and the avian A- and B- allele segment 8s on polymerase activity in a reconstitution assay was assessed. The reconstitution assay indirectly measures mRNA production from vRNA-like templates by the virus polymerase. pDUAL vectors for the components of the polymerase (PB2, PB1, PA, and NP - '3PNP complex') are co-transfected, cellular RNA polymerase II will make mRNA for each component, and this will be translated to yield the polymerase complex. A reporter construct is co-transfected which contains a luciferase reporter gene in the reverse orientation, flanked by the UTRs of PR8 segment 8, under the control of an RNA polymerase I (pol I) promoter. Cellular pol I generates RNA that resembles vRNA to the polymerase complex, which will then be transcribed into mRNA by the polymerase and this is translated to produce luciferase (Lutz et al., 2005). The luciferase activity is therefore proportional to the activity of the viral polymerase.

293T cells were co-transfected with pDUAL plasmids for each component of the PR8 polymerase complex (3PNP) and the appropriate segment 8 plasmids (pDUAL PR8 segment 8, pHH21 plasmids for O175A and O265B segment 8 genes), along with the polI luciferase reporter plasmid. A no segment 8 control was included to assay the transcriptional activity of the PR8 polymerase in the absence of segment 8 products. After 48 h, cells were lysed and luciferase activity assayed. Additionally, cell lysates were generated from parallel transfections for SDS-PAGE and western blotting analysis of PB2, NP and NS1 was performed. A 'no PB2' negative control

sample was also included, in which the viral polymerase cannot form and therefore any luciferase activity measured is not a result of viral transcription. This control gave relative luminescence units several orders of magnitude lower than samples with expected polymerase assay (data not shown).

Polymerase activity was highest without the presence of segment 8 genes from any virus across two independent experiments (Fig 2.8A). The PR8 polymerase with WT segment 8 led to a mean luciferase activity of 69.5% compared to the 3PNP-only sample. Introduction of O175A or O265B segment 8 in place of WT PR8 NS led to average activities of 13.0% and 19.4%, respectively, in comparison to 3PNP-only, although there was no significant difference between O175A and O265B. NS1 expression was confirmed by western blotting in the PR8 and O175A samples using the V29 antiserum, and O265B NS1 expression was detected with A2 antiserum, while NS1 was undetected in the 3PNP-only sample with either antisera (Fig 2.8B). PB2 expression was not detected in the no PB2 control, and was consistently detected at lower levels in O175A and O265B samples relative to PR8 and 3PNP-only across the two experiments (Fig 2.8B). NP was detected in all samples, although levels appeared reduced in O175A and O265B samples relative to the PR8 and 3PNP-only controls (Fig 2.8B). These data could perhaps suggest that an avian segment 8, from either the A- or B-allele, is not as efficient at complementing the PR8 polymerase. However, since there was less PB2 and NP expression in the O175A and O265B samples (Fig 2.8B), the apparent reduction in virus transcription might result from lower levels of viral polymerase in the cell rather than an incompatibility of NS genes with the polymerase. NS1 is known to induce host shut-off, and this raises the question of

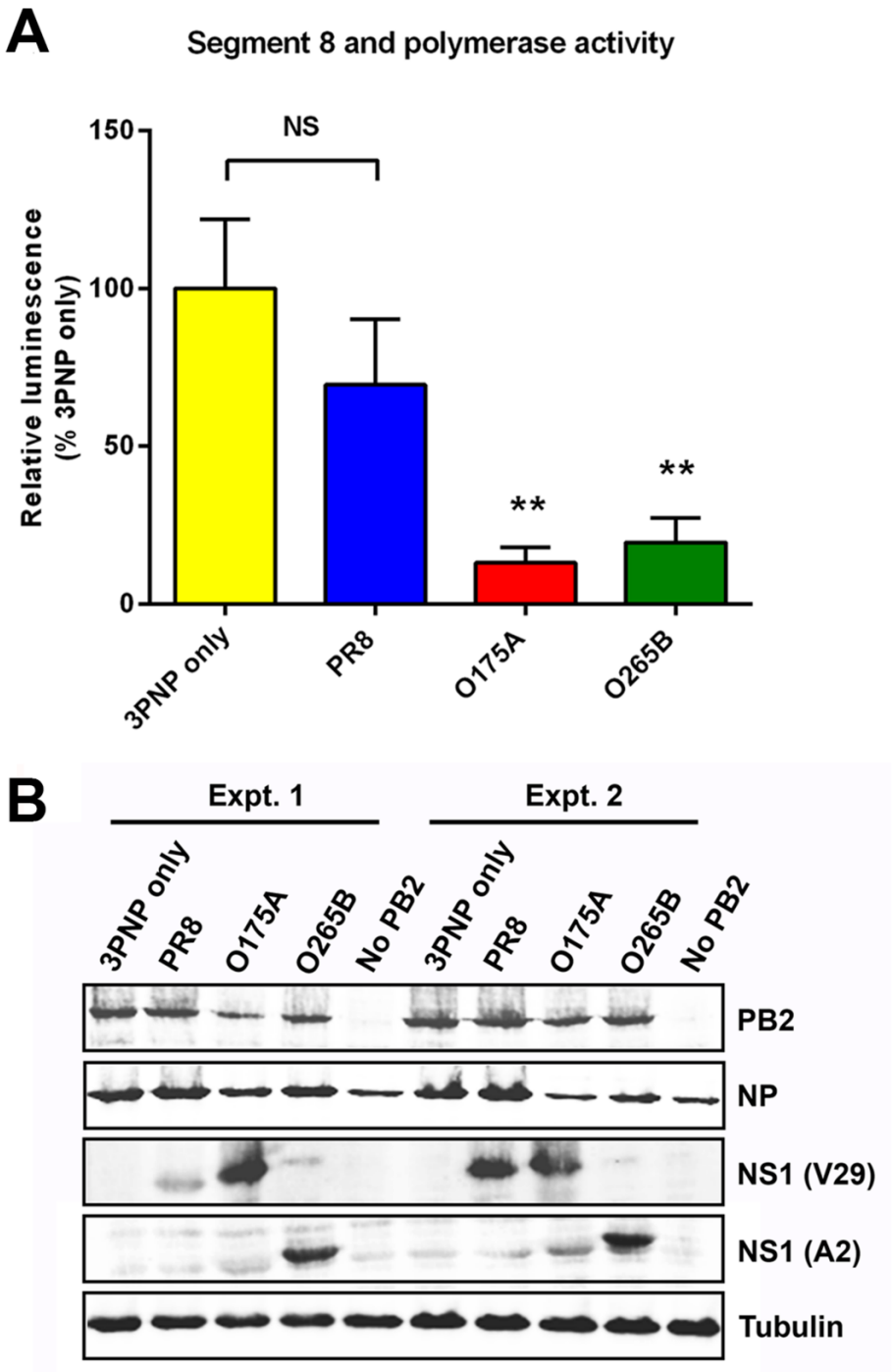

Fig 2.8. Influenza polymerase activity with segment 8 products. (A) 293T cells were co-transfected with pDUAL plasmids for the polymerase and NP genes of PR8 and a segment 8 plasmid (pDUAL for PR8, pHH21 for O175A and O265B) alongside a polI firefly luciferase reporter for 48 h. Luciferase activity was measured at 48 h post-transfection as a readout for viral polymerase activity. Data are the mean +/- SEM (n =5). (B) Western blot of transfected cell lysates for viral PB2, NP and NS1. Cellular alpha-tubulin was blotted as a loading control. Shown are immunoblots from two independent experiments ('Expt.1' and 'Expt. 2'). NS – non-significant, * $p \leq 0.05$, ** $p \leq 0.01$ in unpaired t-tests (n = 5).

whether the reduction in luciferase activity in O175A and O265B samples was caused by reduced expression of polymerase and NP proteins in the reconstitution assay or perhaps a dampening of the expression of luciferase mRNA due to NS1-driven shut-off. The shut-off properties of various NS1 proteins are investigated in Chapter 3.

2.2.5 Growth of PR8-based reassortant viruses in human cells

Virus replication in other types of mammalian cells was also assessed to ensure that any potential fitness penalty of incorporating an avian B-allele segment 8 into a mammalian-adapted virus was not being 'missed' by looking solely in MDCK cells. Human lung A549 cells, human colorectal Caco-2 cells, and primary human $CD14^+$ monocyte-derived macrophages were infected and peak virus titres were assessed. A549 cells were infected at an MOI of 0.001 and infectious virus was titrated at 48 h post-infection by plaque assay. All viruses replicated to titres above 10^6 PFU/ml in A549 cells (Fig 2.9A). There was no obvious attenuation for any of the segment 8 reassortant viruses. Caco-2 cells were also infected at an MOI of 0.001 and virus titre was determined at 48 h post-infection. All viruses replicated to titres exceeding 10^8 PFU/ml, and again there was no evidence of fitness penalty for A- or B-allele reassortant viruses (Fig 2.9B). $CD14^+$ monocyte-derived macrophages were infected at an MOI of 3 for 24 h. As in other human cells, there was no evidence of attenuation for any virus assessed, with all viruses replicating to titres above 10^6 PFU/ml (Fig 2.9C).Virus replication was verified by titrating a 'post-wash' sample at t = 0, in which cell supernatant was taken immediately after washing the cells three times with serum-free media and therefore titrating residual input virus. The post-wash sample contained 10^3 PFU/ml, approximately 3 $\log_{10}$ lower than end-point titre, indicating that virus replication had taken place in infected macrophages. In all infections described, mock-

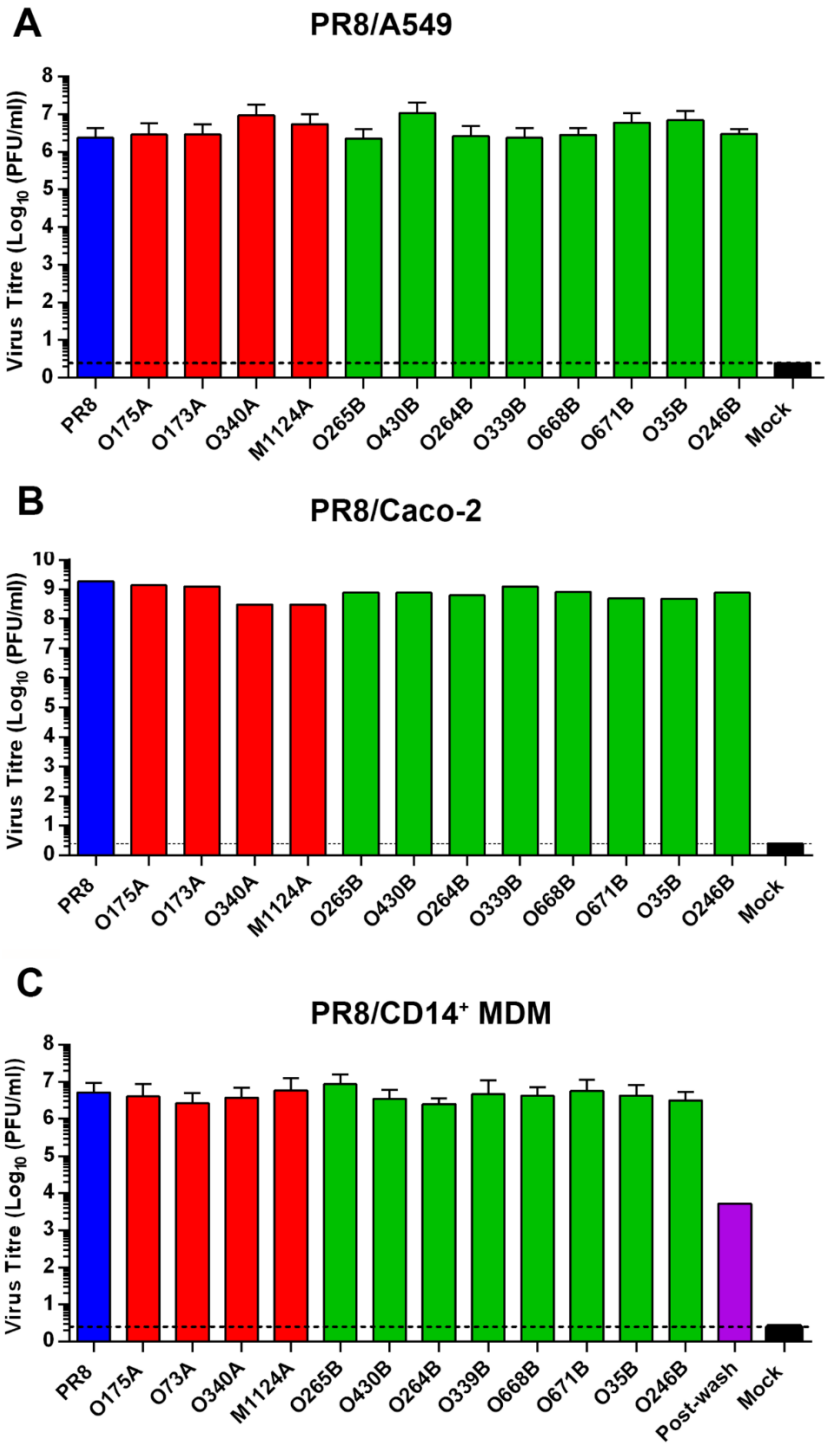

Fig 2.9. A- and B-allele segment 8 reassortant viruses replicate efficiently in human cells. (A) Human lung A549 cells were infected at an MOI of 0.001 and virus in the supernatant titrated at 48 h p.i. by plaque assay. Data are the mean +/- SD of 3 independent infections. (B) As in (A) but human Caco-2 cells were infected at an MOI of 0.001. The output of a single experiment is shown. (C) Primary human $CD14^+$ monocyte-derived macrophages were infected at an MOI of 3 and virus in the supernatant was titrated at 24 h p.i. by plaque assay. Data are the mean +/- range of 2 independent infections.

-infected samples contained undetectable levels of virus (limit of detection 2.5 PFU/ml) and plaque phenotypes were indistinguishable between all viruses (data not shown).

Therefore, all PR8-based segment 8 reassortant viruses tested replicated efficiently in a variety of both continuous and primary mammalian cells. These data provide further evidence that incorporation of an avian B-allele NS segment causes no obvious fitness penalty for an otherwise mammalian-adapted virus in mammalian cells *in vitro*.

2.2.6 *In vitro* fitness of additional A- and B- allele segment 8 reassortant viruses.

Since no significant attenuation of PR8-based segment 8 reassortant viruses bearing North American LPAI segment 8s from either the A- or the B- allele lineage was observed in a variety of mammalian cells, additional NS genes that have been discussed in previous reports were also assessed. NS genes from A/mallard/new york/6750/1978 (H2N2) (NY6750A) and A/mallard/Alberta/88/1976 (H6N8) (Alb88B) were selected, as these were the A- and B-allele representatives which were used in Treanor's squirrel monkey infection report (Treanor et al., 1989). A/mallard/Sweden/S90412/2005 (H6N8) (Sw412A) and A/mallard/Sweden/S90418/2005 (H6N8) (Sw418B) were also chosen as these NS1 proteins were assessed in studies by the Berg lab from which the authors proposed that B-allele NS1 proteins are deficient in preventing the induction of the mammalian innate immune response (Zohari et al., 2010a, Munir et al., 2011a, Munir et al., 2011b, Munir et al., 2012). A/New York/107/2003(H7N2) (NY107B) was included as this is the only B-allele IAV isolated from a human, and finally the NS segment of

A/equine/Jilin/1/1989 (H3N8) (J89B), an equine H3N8 B-allele virus which caused a major outbreak in horses in China that had a high mortality rate of up to 20% in some herds (Guo et al., 1992), was also selected.

Corresponding DNA sequences for Alb88B, NY6750A, Sw412A, Sw418B and NY107B NS genes were synthesised and cloned into plasmids by BioMatik. In each case, the segment 8 termini sequences were not available on GenBank and so the sequence from the closest relative, determined by nucleotide BLAST analysis, was used (Table 2.1). Alb88B and Sw418B sequences were silently mutated to remove BsmbI sites, without altering NS1 or NEP protein sequences or disrupting conserved codons (Table 2.1). The NS genes were cloned into the pDUAL vector using BsmBI sites and were validated by sequencing (see Chapter 7: Materials and Methods for a description of the cloning procedure). The NS segment of J89B was cloned into pDUAL and kindly provided by Alice Coburn (Dr. Pablo Murcia's laboratory, The Centre for Virus Research, The University of Glasgow).

Viruses were rescued as described above in *2.2.1 Virus rescue of PR8-based segment* 8 reassortants with the exception of Sw412A which did not rescue with multiple attempts. Replicative fitness of the reassortant viruses was assessed in MDCK cells by infecting at an MOI of 0.001 and titrating virus in the supernatant at 48 h post-infection. Mock-infected samples contained no detectable virus (Fig 2.10). All other viruses replicated to high virus titres of 10^8 PFU/ml. Therefore the NS segments selected, barring Sw412A, also facilitated efficient virus replication of a mammalian H1N1 virus in mammalian cells *in vitro*.

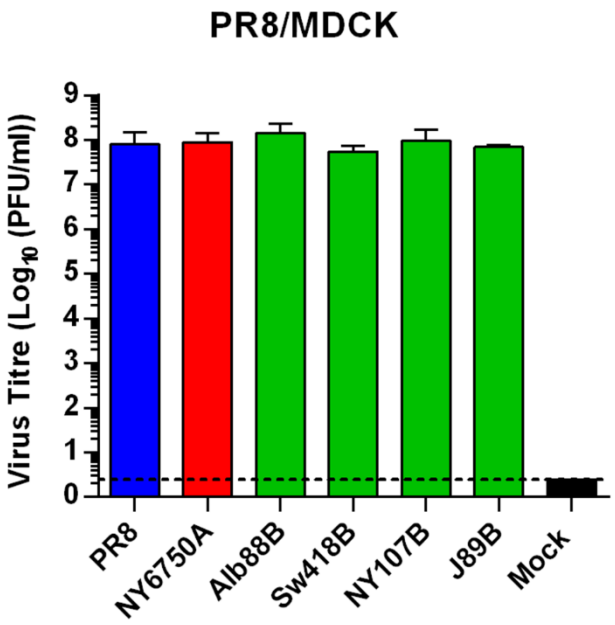

Fig 2.10. Multicycle growth of additional PR8-based segment 8 reassortant viruses. MDCK cells were infected at MOI 0.001 and virus in the supernatant at 48 h post-infection was determined by plaque assay. Data are the mean +/- range (n = 2).

2.2.7 Virus growth kinetics of PR8-based reassortants

Virus growth kinetics of consensus PR8-based viruses was assessed in MDCK cells and A549 cells, to determine if there was an attenuation at earlier time-points during infection for the B-allele segment 8 reassortant viruses that may have been missed by looking at end-point titres. In both cases, cells were infected at low multiplicity (MOI = 0.001) and cell supernatant was collected at increasing time-points post-infection. In both experiments, mock-infected samples contained no detectable virus. In MDCK cells, the growth curves of PR8, O175A and O265B were very similar, with virus titres peaking at 10^8 PFU/ml at 24 h post-infection (Fig 2.11A). In A549 cell infection, WT PR8 and O265B replicated with very similar kinetics, peaking at 48 h post-infection with a titre of 10^7 PFU/ml (Fig 2.11B). O175A replicated with delayed growth kinetics in comparison, showing a reduction in virus titre of approximately one order of magnitude at 36 h and 48 h post-infection. These results show that a B-allele NS segment is capable of allowing efficient virus replication of a mammalian-adapted virus at early time-points in mammalian cells *in vitro*, and provide evidence of improved fitness in comparison to a counterpart A-allele NS segment.

2.2.8 Growth of PR8-based reassortant viruses in embryonated chicken eggs

To assess virus fitness in an avian host system, the allantoic cavities of 10-day old embryonated chicken eggs were inoculated with 1000 PFU of PR8, O175A or O265B. After 48 h, allantoic fluid was harvested, clarified and virus was titrated by

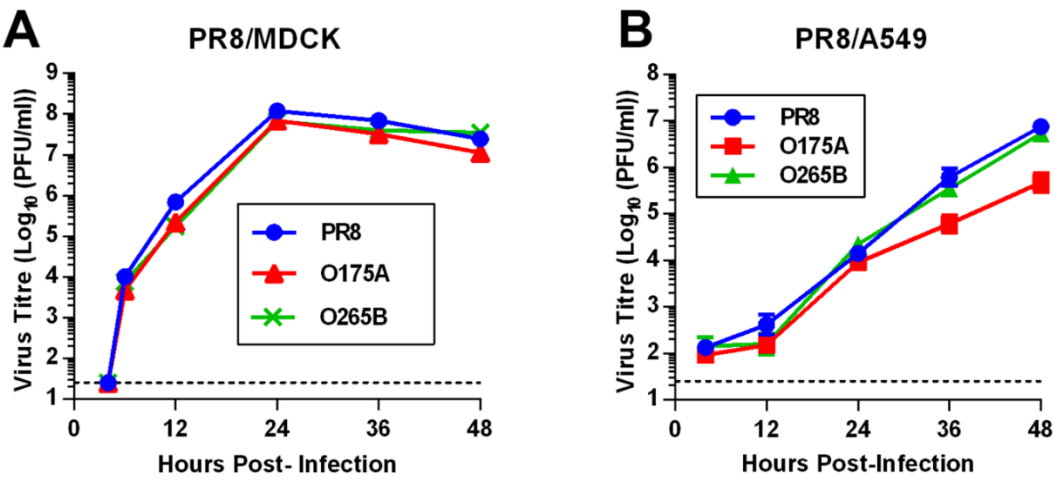

Fig 2.11. Virus growth kinetics. (A) MDCK cells and (B) A549 cells were infected at an MOI of 0.001 and virus in the supernatant was titrated by plaque assay at stated time-point. (A) Data are from a single experiment. (B) Data represents mean +/- SD of 3 independent infections. Dotted line indicates limit of detection of the plaque assay.

plaque assay. Mock-infected eggs contained no detectable virus (Fig 2.12). All three viruses replicated to mean titres of 10^8 PFU/ml, and there was no statistically significant difference between the virus titres (unpaired t-test, n = 5) (Fig 2.12). These data suggest that the PR8-based segment 8 reassortant viruses are competent in an avian host system as well as a mammalian host system *in vitro*.

2.2.9 Competition assays

Since no obvious fitness penalties were observed for PR8-based segment 8 reassortant viruses in terms of virus growth *in vitro*, the possibility of there being a more subtle 'selection advantage' for A-allele segment 8s into a mammalian-adapted viruses in mammalian cells was explored. A 'competition assay' was developed in order to estimate the proportion of virus progeny resulting from the co-infection of cells at low multiplicity with two different NS reassortant viruses which could reveal subtle changes in replication kinetics as the two viruses compete for uninfected cells (Fig 2.13A). A method of distinguishing between different segment 8 reassortant viruses was initially required. Therefore, an RT-PCR assay using primers specific for O175A and O265B segment 8 cDNA was developed. Specificity of these primer pairs on pHH21 plasmids for O175A and O265B cDNA was demonstrated by PCR, and strong signal:noise was only observed in homologous primer-template reactions (see Chapter 7: Materials and Methods for primer validation). Next, the RT-PCR specificity was tested following plaque-purification. MDCK cells were infected at MOI 0.001 for 48 h with controls of either O175A- or O265B-only, or were co-infected with both (MOI 0.001 each), and virus in the supernatant was subjected to agarose plaque assay. Virus from isolated plaques was amplified in MDCK cells by plaque purification and viral RNA was extracted. Segment 8 RT-PCR was performed from isolated vRNA.

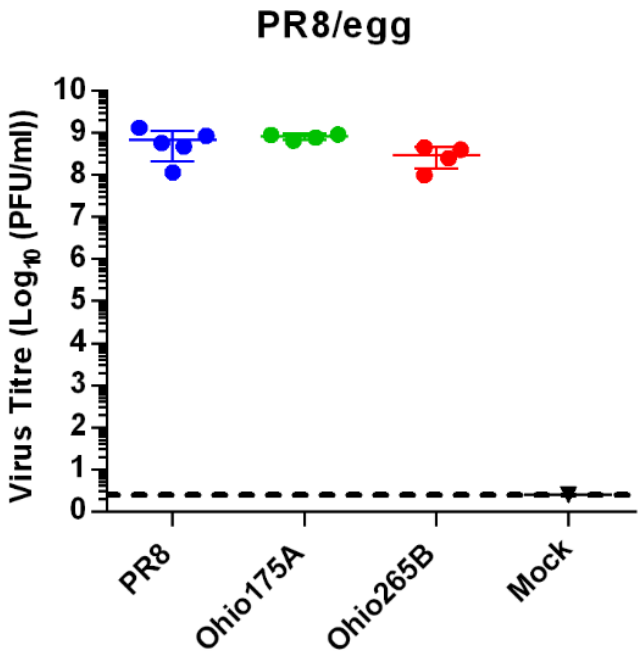

Fig 2.12. Growth of PR8-based viruses in embryonated chicken eggs. The allantoic cavities of 10-day-old embryonated chicken eggs were inoculated with 1000 PFU of virus. Virus in the allantoic fluid at 48 h post-infection was titrated by plaque assay on MDCK cells. Data are mean +/- SD (n = 5).

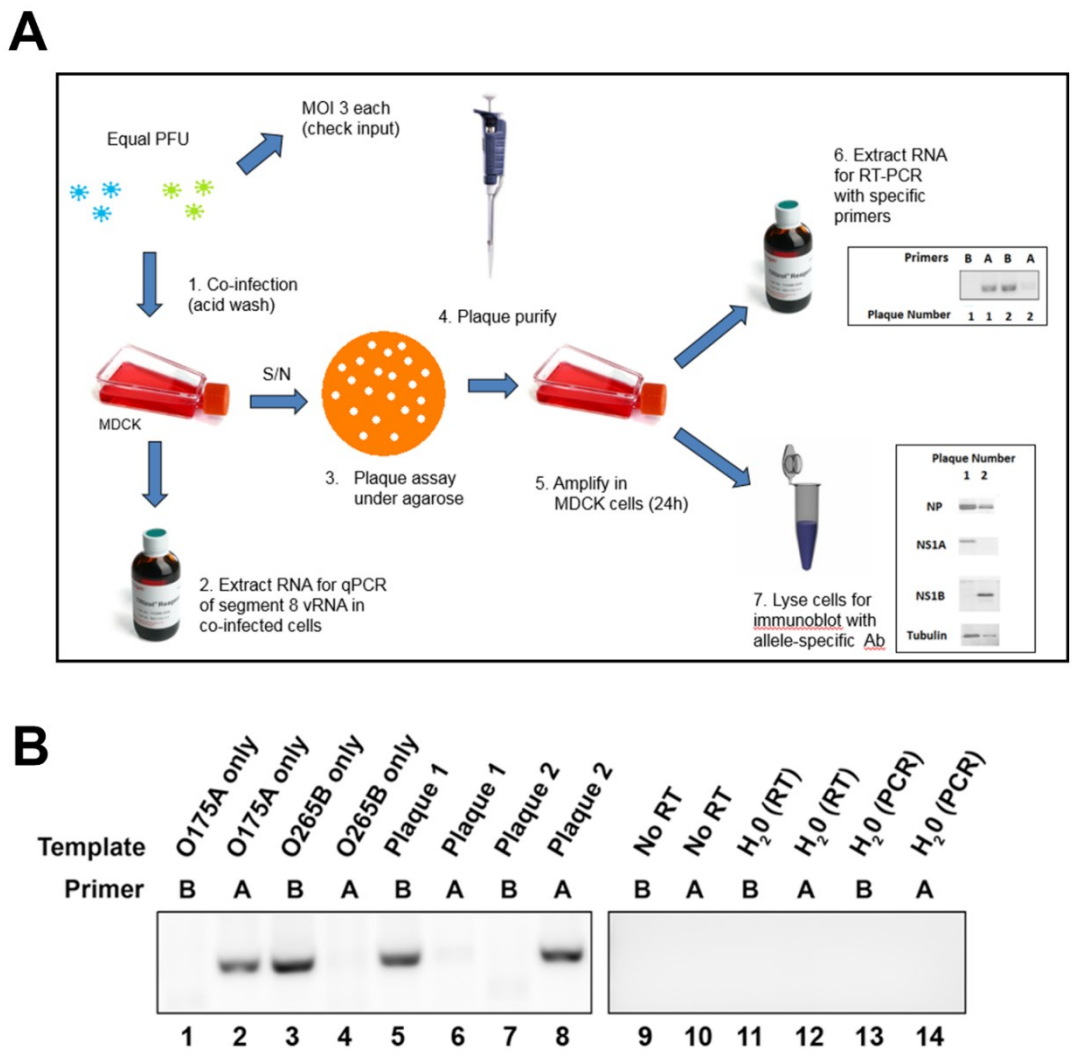

Fig 2.13. Competition assay validation. (A) Schematic diagram of completion assay experimental set-up. Cells are co-infected with an equal PFU of each reassortant virus and the output progeny subjected to plaque assay under a semi-solid overlay. Once visible, isolated plaques are purified by taking up cellular debris and overlay in a pipet and ejecting material onto MDCK cells in culture. Virus is allowed to amplify before extracting RNA and lysing cells in an SDS buffer. Viruses forming isolated plaques are identified using RT-PCR for segment 8 vRNA and/or western blotting for specific NS1 proteins. (B) Establishment of a strain-specific RT-PCR assay for A- and B-allele viruses. Viral RNA was extracted following plaque purification of either O175A, O265B or (as examples) 2 unidentified viruses obtained from co-infection with both and analysed by RT-PCR with primers specific for the NS segment of either O175A and O265B was performed.

'No RT' samples, in which the reverse transcriptase enzyme was removed from the RT-PCR, and no-template reactions ('H_2O') gave no detectable PCR product (Fig 2.13B). Strong signal was only detected in homologous primer-template reactions, as shown in the assay of the O175A- and O265B- only control infections and subsequent plaque purification (Fig 2.13B). The primer pairs were also tested on plaques that were purified following co-infection of MDCK cells with O175A and O265B – plaque 1 only gave strong segment 8 RT-PCR product using O265B-specific primers, and plaque 2 with O175A-specific primers, thus the plaques were unambiguously scored as O265B and O175A respectively (Fig 2.13B). Therefore, this RT-PCR assay could be used reliably following plaque-purification of virus in the supernatant of co-infected cells to distinguish between O175A and O265B viruses, allowing an estimate of the proportion of each virus in the supernatant. To assay co-infections including WT PR8 with either O175A or O265B, western blotting was employed using strain-specific anti-NS1 antiserum on cell lysates of MDCK cells following individual plaque purification. The V29 anti-NS1 antiserum only detected PR8 and O175A NS1 proteins, while anti-O265B-NS1 antiserum (A2) only detected O265B and O175A NS1 proteins (see Fig 2.6A). Therefore, using a combination of RT-PCR and western-blotting based assays, PR8, O175A and O265B viruses could be reliably distinguished following plaque purification.

The initial question asked whether the consensus A-allele segment 8 had a selection advantage over the consensus B-allele segment 8 during a multi-cycle co-infection in this system. This would 'mimic' a natural co-infection of a mammalian host where genetic reassortment could potentially take place in nature. MDCK cells were infected with both O175A and O265B at a low MOI (0.001 each) and the

proportion of infectious virus produced in the system was estimated by RT-PCR assay of 25 plaques following a 48 h infection. The output was then passaged at low MOI (0.001) twice further and 25 plaque purifications were assayed after each passage. In MDCK cells co-infected with both O175A and O265B, O265B appeared to consistently out-compete O175A, reaching a 72% proportion of all progeny virus after 3 passages (Fig 2.14A). When WT PR8 was co-infected with either O175A or O265B, and 25 plaques assayed after 3 passages, PR8 comfortably out-competed both segment 8 reassortant viruses, accounting for 96% of plaques in the O175A competition infection and 88% in the O265BB infection (Fig 2.14A). These data suggest that the WT PR8 segment 8 has a selection advantage over the avian segment 8s over multiple rounds of replication, but that the B-allele segment 8 was certainly no less fit in the PR8 backbone than the A-allele counterpart in this system, and possibly slightly fitter.

In a previous report from the Digard lab, it was suggested that differences in the terminal RNA packaging signals in segment 8 might restrict the reassortment of B-alleles into a mammalian-adapted viruses (Gog et al., 2007). The competition assay was employed to test this hypothesis. High-multiplicity co-infections of MDCK cells were performed, such that the majority of infected cells would contain both A- and B-allele segment 8 vRNA. The proportion of A- and B-allele segment 8 vRNA in the progeny virions following a co-infection would therefore reflect the ability of each to be packaged into the PR8 backbone. MDCK cells were co-infected at an MOI of 3 for each virus for 16 h, and 25 plaques were purified from the infected cell supernatant and assayed using RT-PCR as described above. O265B out-competed O175A with a mean ratio of approximately 3:1 following three individual co-infections (Fig 2.14B).

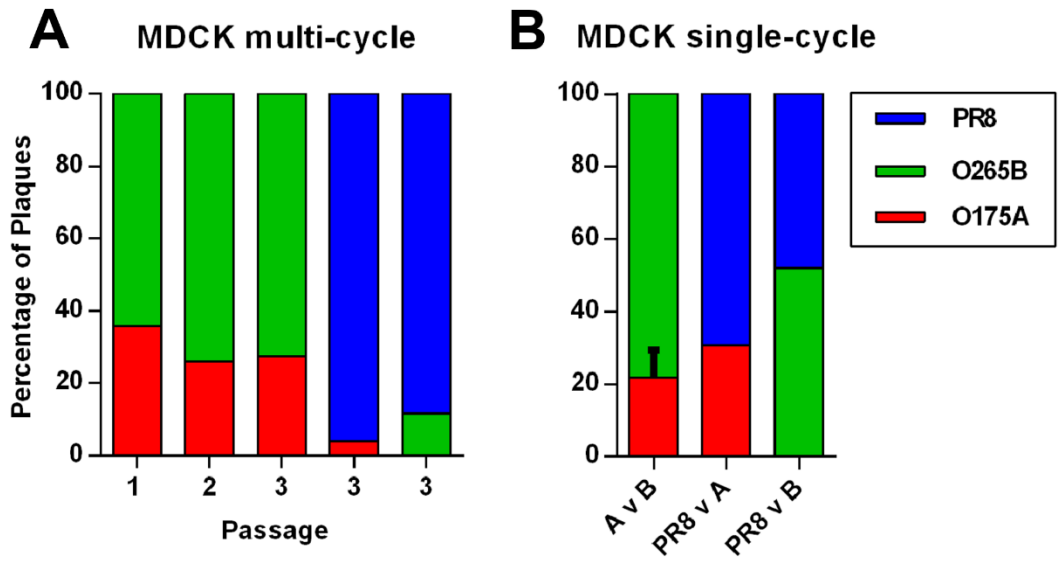

Fig 2.14. Segment 8 reassortant competition assays. (A) MDCK cells were co-infected at an MOI of 0.001 (each) with the indicated mixtures of viruses and at 48 h p.i. the supernatant was analysed by plaque assay. 25 plaques were scored for the proportion of progeny and a further portion of the original supernatant passaged further at an MOI of 0.001. Data are from a single experiment. (B) MDCK cells were infected at an MOI of 3 per virus and the proportion of each virus in the supernatant was assessed after 16 h. Data are the mean +/- SEM for A v B (n = 3), and single experiments for other samples.

To ensure that there was not a 'bias' of O265B vRNA in the infected MDCK cells, which could possibly compensate for any potential restriction of packaging into the PR8 background, the comparative levels of O175A vRNA and O265B vRNA in the co-infected cells was assessed using RT-qPCR. Following co-infection, total RNA was extracted from infected MDCK cells and cDNA of all vRNA was synthesised in an RT reaction using the Uni12' primer. The comparative levels of O175A vRNA and O265B vRNA were then assessed using RT-qPCR with primers specific for both respective cDNA sequences (primer validation is described in Chapter 7: Materials and Methods). RT-qPCR data showed that O265B segment 8 vRNA was present in infected cells at levels approximately 2.5-fold greater than O175A (data not shown). This is a similar ratio to the infectious virus in the supernatant, and suggests that the packaging efficiency of O265B vRNA into PR8 is comparable to O175A vRNA. When WT PR8 was competed against O175A or O265B in an identical co-infection setup, the proportion of PR8- and O265B-containing plaques was similar (52% to 48% respectively), while PR8 modestly out-competed O175A (69% to 31% respectively) (Fig 2.14B). Therefore, these data suggest that there is no obvious bias against an avian B-allele NS vRNP to be packaged into a mammalian-adapted virus background relative to an A-allele when both are present within a co-infected host cell.

Overall, assessing the consensus viruses in this particular system revealed that WT PR8 segment 8 contained a selection advantage over the two consensus A- and B-allele avian segment 8s in mammalian cells *in vitro*. However, the data also indicated that the consensus B-allele vRNA, O265B, had a modest selection advantage over an A-allele counterpart in this system.

2.2.10 Fitness of avian segment 8s in Udorn72 and Cal7 backgrounds

PR8 is a useful and well-studied model for mammalian adapted viruses, although it has been heavily mouse-adapted following many passages (Taylor, 1941), during which it has diverged from clinically relevant strains. Therefore, the possibility of any potential fitness penalty of B-allele segment 8 viruses in mammalian hosts being 'masked' by using a mouse-adapted strain was explored by generating reassortant viruses on additional virus backgrounds. Udorn72, a human H3N2 virus isolated in Russia in 1972 that has been well studied in influenza literature, was employed. Cal7, a prototypic 2009 H1N1 pandemic strain (reviewed in (Girard et al., 2010), and therefore a clinically relevant virus, was also used.

The consensus North American LPAI A- and B-allele segment 8s (O175A and O265B, respectively) were chosen, as well as PR8 segment 8, to rescue on the background of these human viruses. The reverse genetics system for Udorn72, consisting of four pcDNA3.1 plasmids for the expression of the viral polymerase components (PB2, PB1, PA, NP) and eight pol I pHH21 plasmids for each of the eight segments of the genome (see Chapter 7: Materials and Methods for plasmid information) was kindly provided by Prof. Robert Lamb (Department of Molecular Biosciences, Northwestern University, Illinois, USA). The Cal7 reverse genetics system, an eight-plasmid system using bidirectional pHW2000 plasmids, was made by and kindly provided by Prof. John McCauley's laboratory (The Francis Crick Institute, Mill Hill Laboratory, Mill Hill, London, UK). The Udorn72 viruses were rescued essentially as described in *2.2.1 Virus rescue of PR8-based segment* 8 reassortants. The Cal7 viruses did not amplify well in tissue culture after rescue, and so viruses were grown in embryonated chicken eggs.

To assess Udorn72-based viruses *in vitro*, multicycle infections of MDCK cells were performed. For an initial assessment, MDCK cells were infected at an MOI of 0.001 and endpoint titres were assessed by titrating infectious virus in the supernatant at 48 h post-infection. Mock-infected cells produced no detectable virus (Fig 2.15A). All viruses replicated well in MDCK cells, achieving titres of 10^7 PFU/ml. Next, virus growth kinetics were assessed, and MDCK cells were infected at an MOI of 0.001. The supernatant of infected MDCK cells was collected at 4, 12, 24, 36, and 48 h post-infection and virus was titrated by plaque assay. All viruses grew to titres of 10^7 PFU/ml by 48 h post-infection with similar kinetics (Fig 2.15B). Whilst there were minor differences in virus titre noted at 24 h post-infection, peak titres were very similar, suggesting that the avian segment 8s were able to complement a mammalian-adapted H3N2 virus *in vitro*.

Egg-grown titres of Cal7-based viruses were similar – each virus replicated to mean titres of 10^5 PFU/ml (Fig 2.15C). No virus was detected in the mock-infected control (limit of detection 2.5 PFU/ml). To assess virus growth *in vitro,* MDCK-SIAT cells, a transfected cell line which stably express more human 2,6-sialyltransferase and therefore have higher levels of alpha -2,6- linked sialic acid-galactose moieties, were chosen (Matrosovich et al., 2003). This enhances Cal7 growth. MDCK-SIAT cells were infected at an MOI of 0.01, supernatant was collected at various time-points and infectious virus titrated by plaque assay on MDCK-SIAT cells. WT Cal7 and a Cal7/PR8 NS reassortant virus grew with similar growth kinetics during the multicycle infection (Fig 2.15D). In contrast, the Cal7/O175A and Cal7/O265B viruses grew with

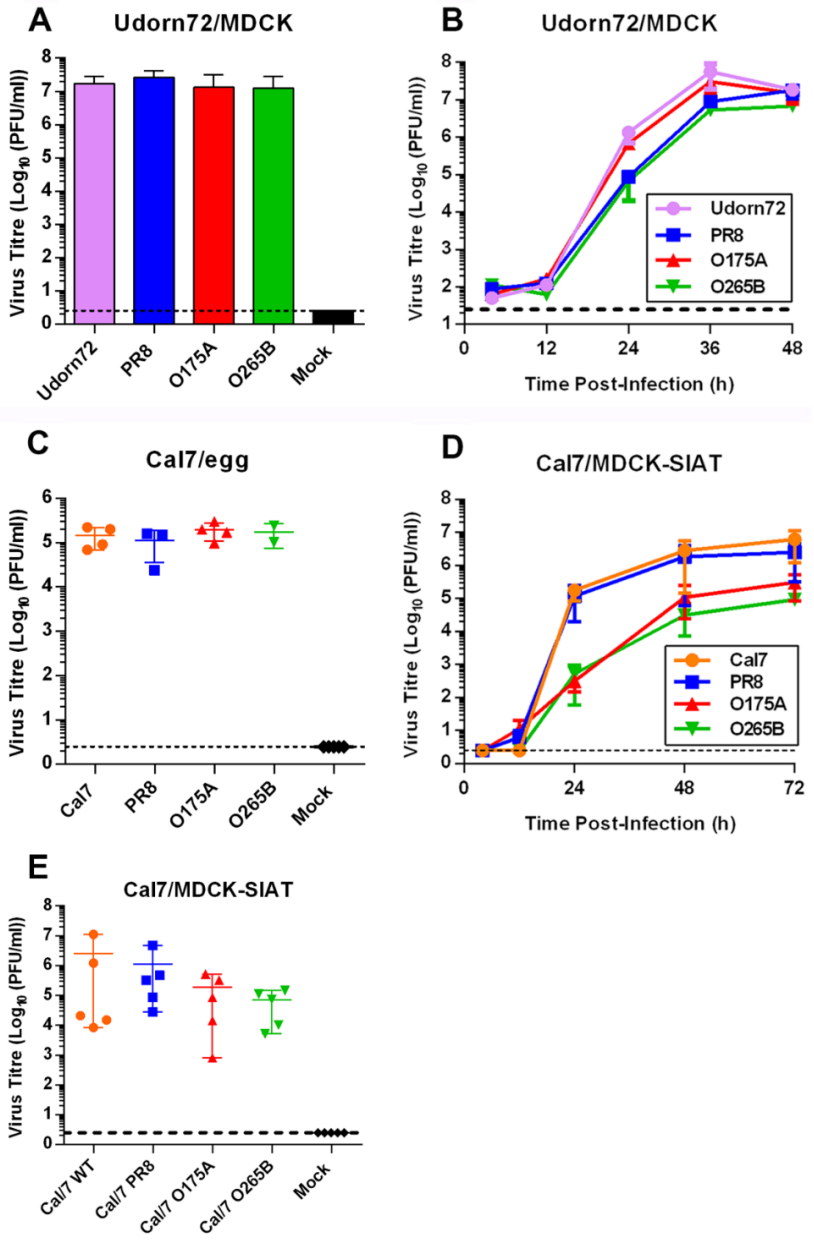

Fig 2.15. Multicycle replication of Udorn72- and Cal7-based segment 8 reassortant viruses. (A) MDCK cells were infected with Udorn72-based viruses at an MOI of 0.001 and virus in the supernatant was titrated at 48 h post-infection. Data are the mean +/- SD (n = 3). (B) MDCK cells were infected as in (A) and virus in the supernatant was titrated at indicated time-points. Data are the mean +/- range (n = 2). (C) The allantoic fluid of 10-day-old embryonated chicken eggs were inoculated with 100 µl of Cal7-based P_0 stocks. At 72 h post-infection, allantoic fluid was harvested and virus was titrate by plaque assay on MDCK-SIAT cells. Data are the mean +/- SD. (D) MDCK-SIAT cells were infected at an MOI of 0.01 with Cal7-based viruses and the supernatant titrated at indicated time-points. Data are the mean +/- range (n = 2). (E) As in (D) but 72 h post-infection only. Data are mean +/- range of five independent infections. There were no significant differences between the samples in an unpaired t-test (n = 5). Dotted lines indicate the limit of detection of the plaque assay.

delayed growth kinetics, particularly at 24 h post-infection where virus titres were nearly 3 orders of magnitude lower than WT Cal7 and Cal7/PR8. However, a more thorough investigation into end-point (72 h) titres yielded no statistically significant difference in peak-titres across all viruses assessed across five independent infections (Fig 2.15E), suggesting that peak virus titres can be achieved with an avian A- or B-allele virus in the background of a pandemic 2009 H1N1 virus, albeit with delayed kinetics.

Overall, there was little evidence to suggest that a B-allele avian segment 8 is any more attenuated in a mammalian-adapted virus than an A-allele counterpart, *in vitro* in a mammalian host setting in H1N1 and H3N2 backgrounds. However, these data show that avian NS genes can attenuate growth kinetics of a recent human H1N1 virus *in vitro*, but to indistinguishable degrees between A- and B-alleles.

2.3 Discussion

In this chapter, mammalian-adapted H1N1 and H3N2 segment 8 reassortant viruses were characterised in mammalian cells *in vitro*. These viruses harboured NS genes from a variety of A- and B-allele IAV strains isolated from a variety of hosts, with a diverse range of H and N subtypes, various locations and dates of isolation observed (Table 2.1). The initial hypothesis was that reassortants with a B-allele NS segment would be attenuated in a mammalian-adapted virus in a mammalian host setting, based on several reports that the B-allele genes are avian-restricted (Treanor et al., 1989, Zohari et al., 2010a, Munir et al., 2011a, Munir et al., 2011b, Munir et al., 2012). However, this hypothesis was not supported by the data described in this chapter which provided strong evidence that a B-allele NS segment can complement a mammalian-adapted IAV strain in the mammalian host *in vitro* efficiently.

All viruses tested were able to produce expected levels of viral proteins during infection of MDCK cells, suggesting the B-allele NS1 and NEP proteins were not deficient in regulating viral protein synthesis (Figs 2.6A and 2.6B). NS1 sub-cellular localisation studies performed following infection or transfection of human cells revealed that consensus avian A- and B-allele NS1 proteins displayed similar localisation patterns at the time-points tested, although both showed a more nuclear localisation during transfection in comparison to WT PR8 NS1 (Figs 2.7A, 2.7B and 2.7C). Although Munir and colleagues previously reported a delay in nuclear localisation of B-allele NS1 proteins using transfection-based experiments, and speculated that this may negatively impact virus replication (Munir et al., 2011b), NS1 sub-cellular localisation is known to be strain- and host- specific (Melen et al., 2007, Volmer et al., 2010, Han et al., 2010). The data here agree with the latter, and it cannot

be concluded that there is a B-allele lineage-specific difference in NS1 sub-cellular localisation. Furthermore, the study by Munir and colleagues failed to demonstrate that the B-allele viruses were attenuated at the level of virus replication.

The PR8-based reassortant viruses all replicated to high end-point titres during multicycle infections of MDCK cells (Fig 2.5), A549 cells (Fig 2.9A), Caco-2 cells (Fig 2.9B) and primary human $CD14^+$ macrophages (Fig 2.9C). Similar replication kinetics during multicycle infections of MDCK and A549 cells (Figs 2.11A and 2.11B) were observed, although O175A failed to reach the peak titres achieved by WT PR8 and O265B (Fig 2.11B). These data suggest that B-allele NS genes are in fact able to complement a mammalian-adapted virus in a variety of mammalian cells. It has been well established that both NS1 and NEP are required for efficient virus replication. Deletion of NS1 from PR8 leads to a serious attenuation of virus replication *in vitro* in MDCK cells (García-Sastre et al., 1998), and mutation of NEP to disrupt nuclear export function obliterates virus production (Neumann et al., 2000). Therefore, these data are a strong indicator that the NS1 and NEP proteins are performing essential functions adequately in mammalian cells. In Chapter 3, studies exploring the ability of NS1 to antagonise the IFN response and to perform host cell shut-off are described.

When A- and B-allele viruses were co-infected in MDCK cells, the consensus B-allele virus out-competed the A-allele counterpart in both multi-cycle and single-cycle competition assays (Figs 2.14A and 2.14B). RT-qPCR of O175A and O265B vRNA in the infected cells suggested that there was no preferential vRNP packaging into the PR8 backbone for O175A over the vRNPs of O265B, which is an interesting result as it has been previously proposed that differences in RNA packaging signals of A- and B-allele NS genes might exert a preference for A-allele vRNPs to be packaged

into mammalian-adapted viruses over B-allele vRNPs (Gog et al., 2007). However, it has been shown in a separate study that the terminal regions of segment 8 appear can undergo substantial sequence mutation without attenuating packaging (Fujii et al., 2009), implying that there is a degree of plasticity in the segment 8 RNA packaging signals.

The consensus avian B-allele NS segment also complemented a human H3N2 virus efficiently *in vitro* (Figs 2.15A and 2.15B), further strengthening the argument that B-allele NS segments are not globally attenuating for mammalian viruses in the mammalian host. Whilst there was an observed attenuation of growth kinetics of a human p2009 H1N1 virus, this was no worse than the A-allele counterpart that was also assessed (Fig 2.15D), and peak viral titres were actually comparable to WT (Fig 2.15E). Therefore, there is no evidence that an avian A-allele NS gene is more suited to a mammalian virus backbone than an avian B-allele counterpart.

Treanor et al were amongst the first to suggest that avian B-allele genes attenuate IAV in the mammalian host (Treanor et al., 1989). They concluded that an H3N2 B-allele reassortant was attenuated in the squirrel monkey host, noting significantly reduced virus titres from nasopharyngeal swabs, and a reduced duration of shedding of infectious virus (Treanor et al., 1989). Furthermore, at the time of publication, there were no reports of B-allele IAV strains isolated from mammals, with an abundance of A-allele mammalian isolates, strengthening their conclusions. However, infectious virus titres in tracheal swabs were not significantly different, and *in vitro* the viruses replicated equally well (Treanor et al., 1989). This suggested that B-allele NS segments could permit replication in mammalian cells, but this was overlooked.

Since the Treanor et al publication (Treanor et al., 1989), there have been conflicting publications regarding the apparent avian-restriction of B-allele NS genes. For example, Ma et al reported that introducing a B-allele NS segment from (A/Goose/Guangdong/1/96 (H5N1)) into an H7N1 HPAI virus (A/FPV/Rostock/34 (H7N1)) improved growth kinetics in MDCK cells and also increased pathogenicity in mice relative to WT (Ma et al., 2010). These data raise doubt that all B-allele NS segments attenuate IAV in mammalian hosts. Additionally, since surveillance and sequencing efforts for IAV has improved vastly over time, there have been an increasing number of mammalian IAV isolates harbouring a B-allele NS segment appearing on public databases (a detailed assessment is described in Chapter 5), with the A/equine/Jilin/1/1989 (H3N8) prototype isolate being a particularly relevant example; a highly pathogenic virus that spread rapidly in horses and caused a high level of mortality (Guo et al., 1992). The latter example clearly shows that a B-allele virus is not only able to permit infection of a mammalian host, but can also cause serious disease.

The data described in this section add further doubt to the dogma of B-allele NS genes being avian-restricted. Furthermore, there is even evidence that a B-allele NS segment may be more advantageous for the replicative fitness of a mammalian virus in the mammalian host *in vitro*. In the next chapter, the ability of B-allele NS1 proteins to control the mammalian IFN response is examined. Additionally, host-cell responses to reassortant virus infection are explored.

Chapter 3: Host cell responses to infection with segment 8 reassortant viruses

3.1 Introduction

3.1.1 Aims

In the previous chapter, a variety of H1N1 and H3N2 segment 8 reassortant viruses were characterised *in vitro* and it was concluded that B-allele NS genes were able to facilitate efficient virus replication in mammalian host cells. These experiments were mostly concerned with assessing virus replication and propagation. In this section, the aim was to investigate host cell responses to infection with A- and B-allele NS reassortant viruses, asking whether; i) B-allele reassortant viruses could replicate in mammalian cells in which the antiviral state was active, and ii) if B-allele viruses/NS1 proteins could efficiently block the induction of the mammalian innate immune response.

3.1.2 Hypothesis

There have been reports published suggesting that B-allele NS1 proteins are deficient in controlling the mammalian innate immune response (Zohari et al., 2010a, Munir et al., 2011a, Munir et al., 2011b, Munir et al., 2012). These studies focused on NS1 proteins from virus strains that harboured an A- or a B-allele NS segment but were otherwise closely related. Reporter assays in human and mink lung cells suggested that the B-allele NS1 proteins were unable to efficiently block activation of IFN-β, NF-κB and AP-1 promoters. The authors speculated that this could contribute to an apparent avian-restriction of B-allele viruses, as mammalian hosts would induce a strong IFN response to infection and prevent virus replication. However, these

studies failed to link their findings to an attenuation of virus replication *in vitro* or *in vivo*.

Given that the data described in Chapter 2 strongly suggested that B-allele NS reassortant viruses were not attenuated *in vitro*, it was hypothesised that B-allele NS1 proteins were able to antagonise the mammalian immune response efficiently. It has been shown that a PR8 mutant virus that does not express NS1 is heavily attenuated in MDCK cells, but can replicate to titres comparable to WT in IFN-deficient VERO cells (García-Sastre et al., 1998). This shows that effective IFN-antagonism from the NS1 protein is required for efficient virus replication *in vitro*, and since the B-allele reassortant viruses assessed in Chapter 2 all replicated well *in vitro*, it seemed possible that the IFN-response is well controlled during infection.

3.1.3 Approach

To assess the ability of NS reassortant viruses to circumvent the mammalian innate immune response, replication of PR8-based reassortant viruses in cells pre-treated with IFN-β was compared across A- and B-allele viruses. Transfection-based reporter assays for IFN-β and ISRE promoter activity, as well as quantification of the levels of type I IFN secreted during infection of human lung epithelium cells, were also employed to measure the induction of the IFN-response and JAK/STAT-signalling. Additionally, cytokine and chemokine profiling of infected human primary macrophages was investigated, as macrophages are important mediators of the host immune response and are important for clearance of IAV during infection. In collaboration, an intricate 10-plex mass-spectrometry technique was employed to perform quantitative temporal proteomics of infected human lung cells to compare host cell responses across consensus reassortant viruses. Finally, the ability of A- and

B-allele NS1 proteins to induce host-cell shut-off was also assessed by metabolic labelling of infected cells and RNA polymerase II promoter reporter assays, as the consensus CPSF30-binding site differs in B-allele NS1 proteins (See Fig 2.1) and a deficiency in shut-off may lead to increased IFN- or ISG-expression.

3.2 Results

3.2.1 Ability of segment 8 reassortant viruses to replicate in established antiviral conditions.

The first assessment of B-allele reassortant viruses to cope with the mammalian IFN response was to assess virus replication in human lung cells that had been stimulated with IFN-β. Cells were pre-treated for 24 h with differing concentrations of recombinant human IFN-β prior to a 48 h low multiplicity infection (MOI 0.01) with WT PR8 or the consensus PR8-based avian NS reassortant viruses (O175A and O265B). Virus titres were determined by plaque assay of infected cell supernatant, and titres were plotted normalised to 'no-IFN' control. Dose-inhibition curves demonstrated a clear dose-dependent antiviral effect of IFN-β pre-treatment (Fig 3.1A) High concentrations of IFN-β pre-treatment (300 U/ml and above) inhibited virus replication by several orders of magnitude relative to no-IFN samples for all viruses. All viruses were largely unaffected by concentrations of 6 U/ml and below. In terms of dose-inhibition, similar IC_{90} values were obtained for PR8, O175A and O265B (28.5 U/ml, 29.6 U/ml and 33.5 U/ml respectively). Cell lysates were generated at the end of the infection to assess the levels of an IFN-inducible protein (Mx1) to ensure that the IFN-β had initiated the antiviral state during treatment. Western blotting of

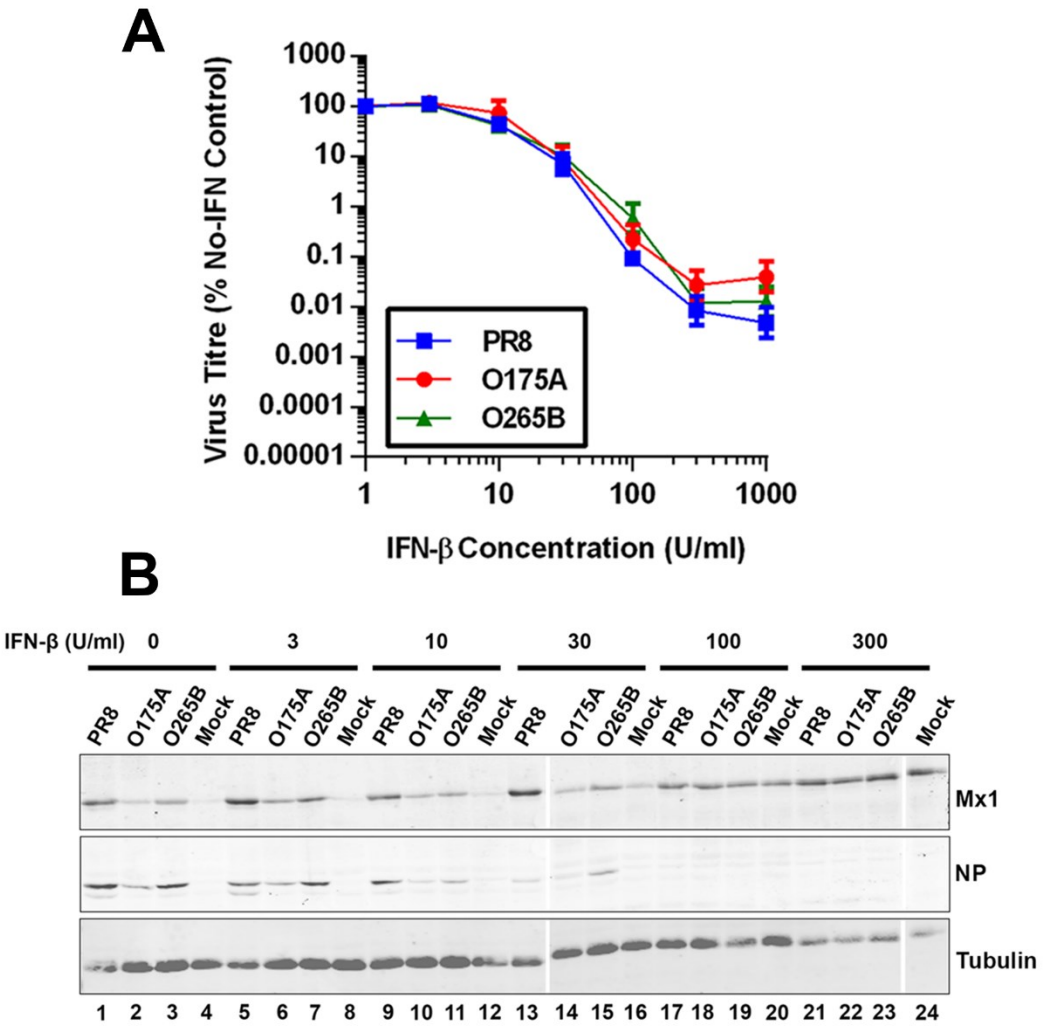

Fig 3.1. Ability of viruses to replicate in the presence of an established antiviral conditions. A549 cells were pre-treated with varying concentrations of human recombinant IFN-β for 24 h prior to infection with the indicated PR8-based reassortant viruses at an MOI of 0.01. (A) Virus in the supernatant was titrated by plaque assay at 48 h p.i.. Data are plotted as percentage of the no-IFN control for each virus. Data are mean +/- SD (n = 3). (B) Cell lysates were prepared at 48 h p.i., subjected to SDS-PAGE, and immunoblotted for cellular IFN-inducible Mx1, viral NP, and tubulin.

these lysates confirmed that Mx1 was up-regulated with IFN-β treatment in a dose-dependent manner (Fig 3.1B). Additionally, viral NP levels were reduced in samples pre-treated with higher concentrations of IFN-β (Fig 3.1B).

Since the dose-inhibition curves were similar across the viruses tested, there was no evidence for a specific defect for a B-allele NS reassortant viruses in this system. The NS1 protein is implicated in inhibiting antiviral proteins that are induced by type I IFN such as PKR and OAS (which were discussed in more detail in Chapter 1), therefore if a B-allele NS1 protein lacked the ability to inhibit certain mammalian antiviral effectors that an A-allele NS1 could, one would expect to see an increased sensitivity to IFN treatment for O265B and therefore a shift (to the left) in the dose-inhibition curve presented in Fig 3.1A. Thus, the data from this experiment do not support the hypothesis that there is a specific deficiency of B-allele NS1 proteins in inhibiting the actions of IFN-inducible antiviral effectors in mammalian cells *in vitro*.

3.2.2 Quantifying type I IFN production during infection

Next, the levels of active type I IFN secreted during infection of human lung cells were quantified to ask if B-allele viruses are able to control the activation of the type I IFN response in the context of viral infection. To address this question, a reporter cell line (HEK-Blue™ IFN-α/β cells) was employed that expresses human secreted embryonic alkaline phosphatase (SEAP) under the control of the ISG54 promoter (Ahmed et al., 2013). This promoter is activated by an ISRE-dependent mechanism following JAK/STAT signalling which is induced by exogenous type I IFN.

Initially, A549 cells were infected with varying multiplicities with WT PR8 or consensus NS reassortant viruses (O175A and O265B) for 24 h. MOIs of 3, 0.3 and

0.03 were tested and a PR8 NS1 RNA-binding mutant virus (residues R38 and K41 mutated to alanine, 'R38K41A', made by Dr. Helen Wise previously in the Digard laboratory) which is known to be deficient in IFN-antagonism (Talon et al., 2000, Newby et al., 2007) was included as a positive control to test which multiplicity of infection was most appropriate to use for IFN quantification assays following infection. At the end of the 24 h infection, cells were fixed, permeabilised and immunostained for intracellular NP in all samples to assess the successful infection rate. Fig 3.2A shows the mock-infected sample, containing no detectable NP at the imaging parameters used, alongside WT PR8 at the three multiplicities tested which are included as representatives for all virus infections. At an MOI of 3, the majority of cells were infected. The infection rate accordingly dropped by approximately ten-fold for the MOI of 0.3 infection, and ten-fold further for the MOI of 0.03 infection. In order to inactivate virus in the supernatant prior to incubation with HEK-Blue cells, supernatants of all samples were treated with UV-irradiation. Fig 3.2B shows PR8 virus titre in the supernatant pre- and post-UV treatment at the three multiplicities tested as determined by plaque assay. Prior to irradiation, there was 10^6 - 10^7 PFU/ml in the supernatant of the MOI 3 and 0.3 infections, and 10^4 PFU/ml in the supernatant of the MOI 0.03 infection, which was reduced to levels below the limit of detection (25 PFU/ml) by plaque assay following UV treatment. There was no detectable infectious virus in the mock-infected cells. To quantify the levels of type I IFN in the infected cell supernatants, the UV-treated supernatants were incubated with HEK-Blue cells for 24 h and the levels of SEAP secreted into the supernatant were quantified by

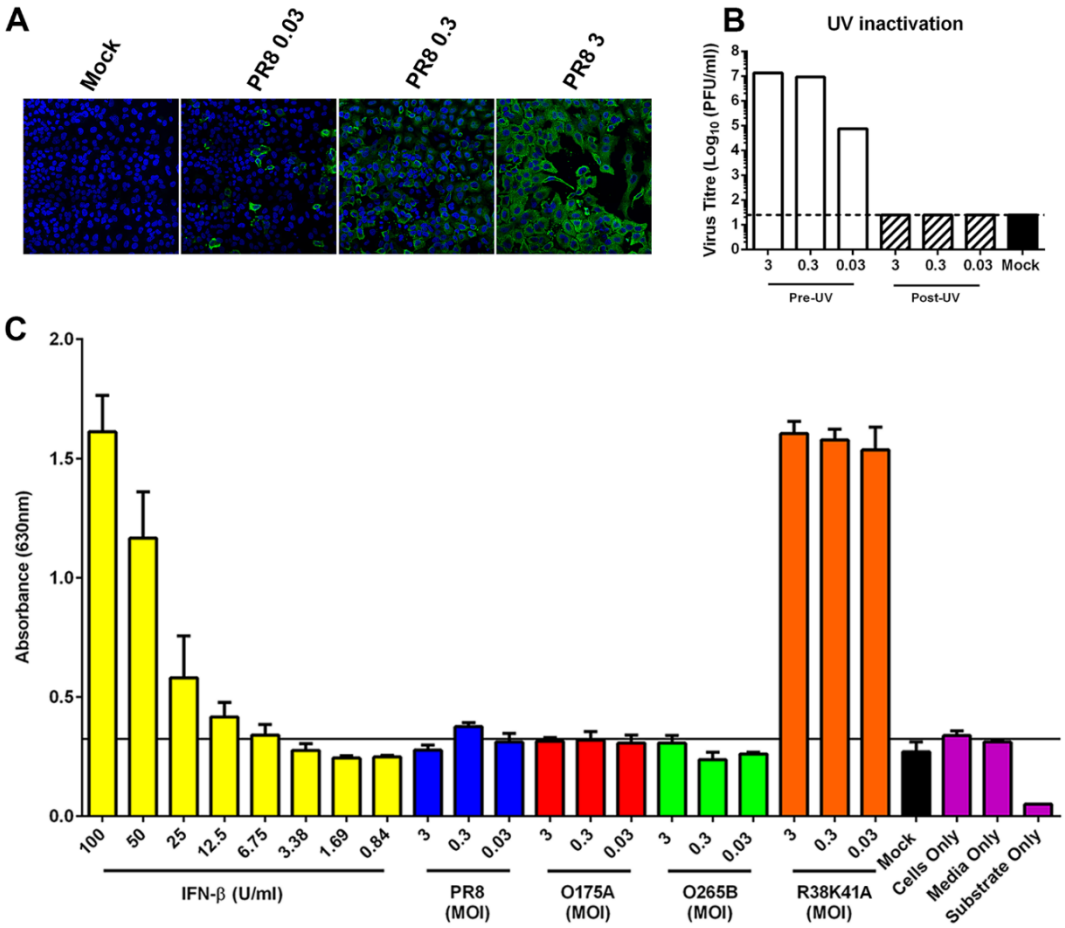

Fig 3.2. Establishment of the HEK-Blue cell reporter assay to quantify type I IFN. A549 cells were infected at varying multiplicity for 24 h. (A) Immunostaining for intracellular NP was performed to verify successful infection rates. MOI used is indicated. PR8 infections are shown as a representative of all samples. (B) The supernatant was UV-treated to inactivate infectious virus particles in all samples. Shown are the virus titres pre- and post-UV treatment for PR8 infections at the three multiplicities tested. (C) Type I IFN in the supernatant was quantified using the HEK-Blue cell reporter assay. Experiment was performed in triplicate for each sample and reproduced over two independent experiments. Shown are the data from a representative experiment. Solid line indicates 'cells only' background and represents the limit of detection which is approximately 6 U/ml according to the IFN-β standard. Data are mean +/- SD (n = 3).

colourimetry following addition of substrate. Human recombinant IFN-β, also treated with UV under the same conditions of the infected cell supernatants, was also incubated on the HEK-Blue cells in varying concentrations to form a standard curve. A 'cells only', 'media only' and 'substrate only' were all included as negative controls, to determine the background level of the assay. The SEAP activity levels in the supernatant of HEK-Blue cells increased with increasing concentrations of exogenous IFN-β, indicating that the HEK-Blue cells were responding to exogenous type I IFN as expected (Fig 3.2C). The limit of detection of the assay, determined by the SEAP activity of the 'cells only' control and shown on the graph as a solid line, was equivalent to approximately 6 U/ml as determined by the IFN-β standard curve. As demonstrated above, 6 U/ml of IFN-β did not inhibit multicycle replication of PR8 and consensus NS reassortant viruses in A549 cells pre-treated with exogenous IFN-β (Fig 3.1A). Mock-infected samples did not induce SEAP section above the levels of cell-only or media-only controls. A549 cells infected with the PR8 NS1 mutant virus R38K41A resulted in large levels of IFN secretion at all multiplicities tested, inducing SEAP secretion equivalent to incubating the HEK-Blue cells with 100 U/mL of recombinant IFN-β – levels which inhibited virus replication by approximately 100-fold in the dose-inhibition experiment described above (Fig 3.1A). Therefore, all three multiplicities tested were sufficient to induce a substantial IFN response in A549 cells. Infection of A549 cells with PR8, O175A or O265B did not induce type I IFN levels significantly above the limit of detection of the assay (unpaired t-test, $n = 3$). Therefore, PR8, O175A and O265B did not induce inhibitory levels of IFN, as determined by dose-inhibition curves described above (Fig 3.1A) during infection of A549 cells over a range of multiplicities tested.

The number of viruses analysed was expanded to include the full panel of PR8-based reassortants and the Udorn72-based reassortant viruses (see Table 2.1). In these experiments, an MOI of 3 was used in all infections. The results were similar to initial experiments, in that the only virus to induce notable type I IFN-secretion during infection of A549 cells was the PR8 R38K41A NS1 mutant virus (Figs 3.3A and 3.3B).

Therefore, none of the A- or B- allele reassortant virus tested lacked the ability to suppress type I IFN secretion during infection of A549 cells. Conversely, an NS1 mutant virus induced large responses, demonstrating the importance of the NS1 protein in suppressing type I IFN production in this system. These data suggest that B-allele NS1 proteins are in fact able to efficiently control the mammalian IFN immune response during infection, contrary to previous reports (Zohari et al., 2010a, Munir et al., 2011a, Munir et al., 2011b, Munir et al., 2012).

3.2.3 NS1 suppression of IFN-β and ISRE promoters in poly(I:C)-stimulated cells.

Next, the ability of various A- and B-allele NS1 proteins to inhibit the IFN-β and ISRE promoters in transfection-based reporter assays was assessed. A previous study has suggested that B-allele NS1 proteins are unable to efficiently block IFN-β production in mammalian cells, and also ISRE activation in transfection-based reporter assays (Munir et al., 2011b). Therefore, the representative NS1 proteins that were used in this study (Sw412A and Sw418B – see Table 2.1) were employed in transfection-based reporter assays to study their suppression of IFN-β and ISRE promoter activity, alongside consensus LPAI North American NS1s (O175A and O265B) and other NS1 proteins of interest (Alb88B, NY6750A, NY107B and J89B).

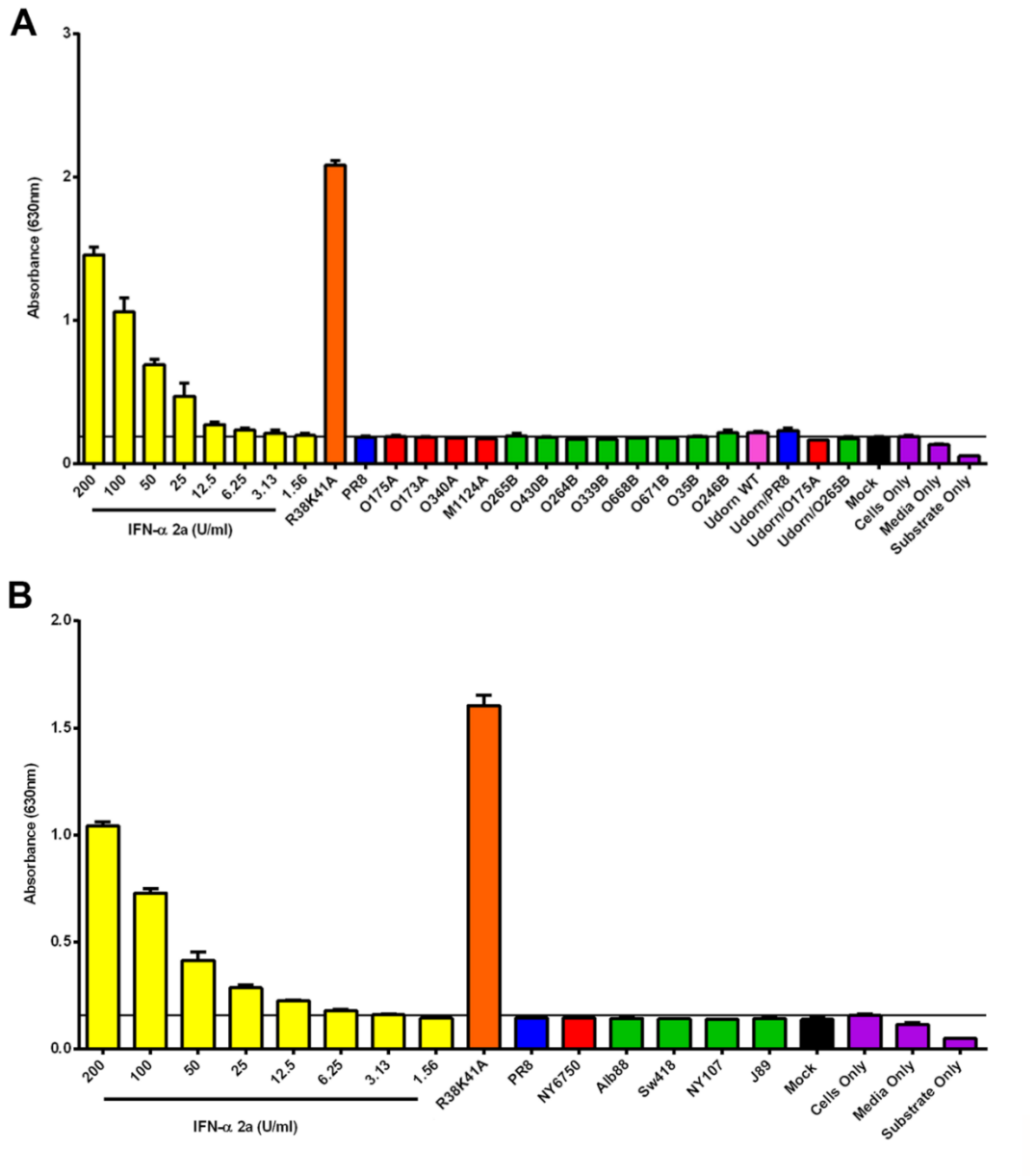

Fig 3.3. Type I IFN during infection of A549 cells with PR8- and Udorn72-based reassortant viruses. Experimental design is described in Fig 3.2, except MOI of 3 was used in all infections. Solid line indicates 'cells only' background and represents the limit of detection which is approximately 6 U/ml according to the IFN-α 2a standard. Data are mean +/- SD (n = 3).

The experimental design included transfecting 293T cells with reporter plasmids containing either the human IFN-β promoter or four tandem repeats of the IFN responsive (ISRE) core upstream of the *Photinus pyralis* (firefly) luciferase ORF ('IFNβ::Luc' and 'ISRE::Luc' respectively; kind gift of Prof. Richard Randall, The University of St Andrews (King and Goodbourn, 1994, King and Goodbourn, 1998, Didcock et al., 1999, Hagmaier et al., 2006)). These reporter plasmids were co-transfected with NS1-GFP constructs (pEGFPN1) for 24 h. Subsequently, cells were transfected with polyinosinic:polycytidylic acid (poly(I:C)), a synthetic mimic of dsRNA produced during viral infection which therefore stimulates intracellular dsRNA sensors such as RIG-I (Yoneyama et al., 2004) (described in more detail in Chapter 1), and luciferase activity measured to assess the ability of the various NS1 proteins to inhibit the induction of the cellular promoters *in vitro*. The luciferase activity following stimulation with poly(I:C) was therefore expected to be proportional to the induction of the promoter assessed. While the most appropriate measure of ISRE stimulation is to treat cells with type I IFN (King and Goodbourn, 1998), poly(I:C) treatment was employed here to use an experimental design similar to the ISRE reporter assays used in the study by Munir and colleagues along with their representative NS1 proteins (Munir et al., 2011b), for a direct comparison.

293T cells were seeded in 24-well plates, and were co-transfected with 50 ng/well of reporter plasmid and 400 ng/well of effector for 24 h. All cells were transfected at similar levels as assessed by epi-fluorescent microscopy for GFP fluorescence (data not shown). 24 h post-transfection, cells were stimulated by transfection of 5 µg/well of poly(I:C) or mock-stimulated by transfecting a mixture lacking reporter plasmid. 24 h post-stimulation, cells were lysed and luciferase activity

was quantified. PR8-NP-GFP was employed as a negative control, as influenza NP is not known to influence induction of IFN-β or ISRE promoters. Background levels of the assay were determined by measuring luciferase activity in cells transfected with PR8-NS1-GFP only and by measuring the relative luminescence values when lysis buffer only was added to substrate. Both of these controls exhibited values several orders of magnitude lower than samples containing reporter plasmid (data not shown). Each effector tested had a stimulated and mock-stimulated sample, and fold-stimulation values were calculated by dividing relative luminescence values obtained from stimulated cells over mock-stimulated cells. This would account for any potential influence on basal expression of luciferase between effectors used.

When the IFN-β promoter reporter plasmid was co-transfected with NP-GFP and cells were stimulated with poly(I:C), there was a mean up-regulation of 9.7-fold luciferase activity in comparison to mock-stimulated cells, indicating strong activation of the promoter (Fig 3.4A). When the NS1-GFP proteins from PR8 or selected A- and B-allele viruses were co-transfected, the mean up-regulation lay between 1.5- and 2.5-fold relative to unstimulated samples for all proteins tested, demonstrating an ability for all NS1s tested to inhibit the activity of the IFN-β promoter following stimulation, and to a similar extents (Fig 3.4A).

The ISRE::Luc promoter reporter was tested in the same experimental setup. Co-transfection of NP-GFP resulted a mean up-regulation of luciferase activity by 3.8-fold following stimulation with poly(I:C) with respect to mock-stimulated, indicating activation of the ISRE promoter element (Fig 3.4B). WT PR8-NS1 up-regulated luciferase activity by 7.3-fold relative to the unstimulated sample. The majority of the other NS1 proteins tested were able to efficiently down-regulate luciferase activity to

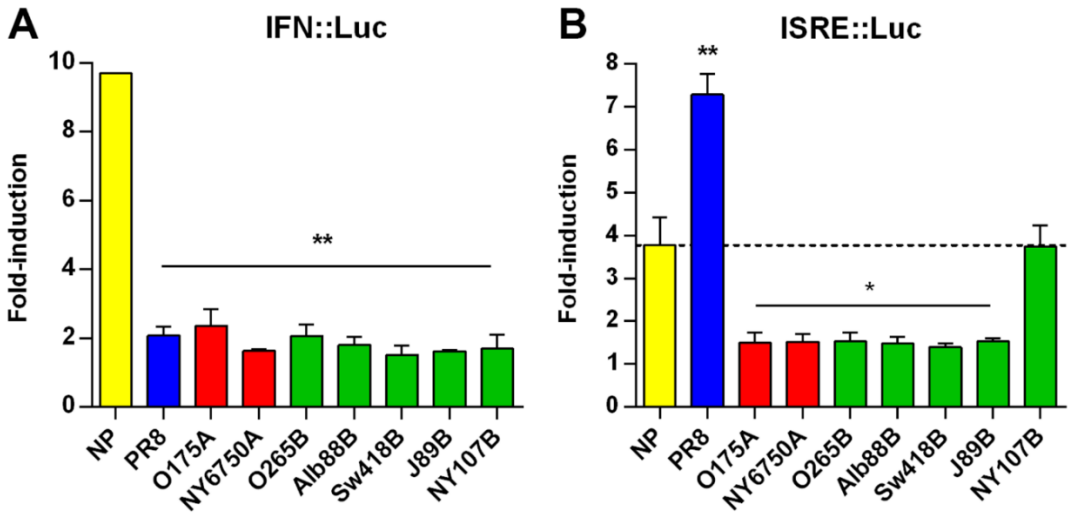

Fig 3.4. IFN and ISRE promoter activity in presence of NS1. 293T cells were co-transfected with a luciferase reporter plasmid, containing (A) the IFN-β promoter or (B) tandem repeats of the ISRE core upstream of firefly luciferase, alongside various NS1-GFP expression plasmids. After 24 h, the cells were stimulated with poly(I:C). Luciferase activity was measured 24 h post-stimulation. NP-GFP was employed as a negative control effector. Data are plotted as mean fold-change relative to unstimulated sample. Data represents (A) the mean +/- range (n = 2) and (B) mean +/- SEM (n = 4) and is plotted as fold-change of induction compared to unstimulated cells. Dashed line in (B) represents the mean fold-induction of the negative control sample (NP-GFP). Statistically significant differences from respective NP-GFP negative control effector in unpaired t-tests are marked with asterisk(s): * $p \leq 0.05$ and ** $p \leq 0.01$.

between 1.4- and 1.8-fold of the unstimulated values (Fig 3.4B). NY107B was an exception, as fold-stimulation values were effectively identical to the NP sample (mean up-regulation of 3.7-fold) indicating a failure to block activation of the ISRE promoter following poly(I:C) treatment (Fig 3.4B).

These data suggest that B-allele NS1 proteins are able to directly inhibit the activation of the IFN-β promoter in stimulated cells, contrary to the conclusions of a previous report (Munir et al., 2011b). Furthermore, the majority of B-allele NS1 proteins tested were able to supress ISRE promoter activation in stimulated cells, with the exception of NY107B. WT PR8 NS1 apparently increased ISRE promoter activation, and this finding is consistent with previous studies in which PR8 infection or transfection of a plasmid vector expressing PR8 NS1 protein either failed to block or increased the activity of an ISRE promoter in human cells following stimulation with type I IFN or poly(I:C) (Hayman et al., 2006, Hayman et al., 2007, Munir et al., 2011b). These findings suggest that the ability of the NS1 protein to inhibit ISRE promoter activation is not dependent on the A- or B-allele lineage origin, but there is likely to be a strain-specificity in this ability. Indeed, avian B-allele NS1 proteins have been found to supress IFN-β promoter activity in human cells as efficiently as counterpart A-allele NS1 proteins in previous studies (Hayman et al., 2007, Ma et al., 2010).

3.2.4 Cytokine and chemokine secretion following infection of primary human macrophages with segment 8 reassortant viruses

Macrophages are among the first immune cells to encounter IAV virions in the lung of the infected host, and studies have shown the importance of macrophages in controlling influenza replication and disease (Tumpey et al., 2005, Kim et al., 2008,

Tate et al., 2010). Macrophages are thought to be the main producers of pro-inflammatory cytokines and type I IFN during IAV infection, and this is important for control of virus propagation (Kumagai et al., 2007). Therefore, the cytokine and chemokine secretion profiles of infected human macrophages were examined, to ask whether a B-allele virus might elicit an overly-strong response in macrophages that could contribute to an increased rate of clearance from an infected host.

The production of cytokines and chemokines was assessed following the infection of primary Cluster of Differentiation 14-positive ($CD14^+$) human macrophages with PR8, O175A or O265B. $CD14^+$ monocytes were isolated from fresh blood donations and differentiated into macrophages by Dr. Alasdair Jubb, Dr. Malcolm Fisher (both of Prof. David Hume's laboratory, The Roslin Institute, The University of Edinburgh) and Dr. Sara Clohisey (of Dr. Kenny Bailey's laboratory, The Roslin Institute, The University of Edinburgh). Macrophages were infected at an MOI of 1, and after 24 h the supernatant was harvested and cells were fixed. Immunostaining of viral NP protein was performed on fixed and permeabilised cells. NP immunostaining was not observed in mock-infected cells, while successful infection of macrophages was seen in virus-infected samples, with the majority of cells infected in all samples (Fig 3.5A). The supernatant, containing secreted cytokines and

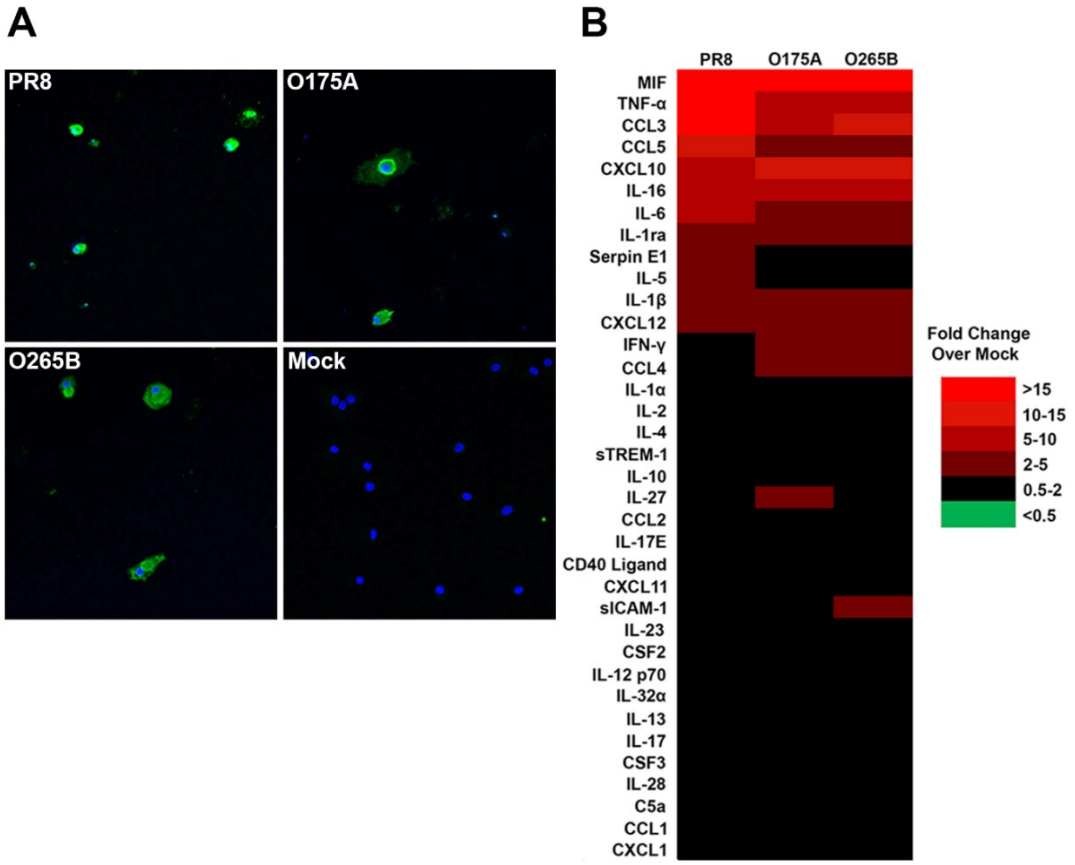

Fig 3.5. Cytokine and chemokine profiling of infected human macrophages. Human CD14^{+} MDMs were infected at an MOI of 1 for 24 h. (A) Immunofluorescent staining of viral NP (green) in fixed cells was performed at 24 h post-infection to confirm successful infection. DAPI staining (blue) shows nuclei of cells. (B) The levels of various cytokines and chemokines in the supernatant was quantified using an immuno spot-blot array. The mean fold-change with respect to a mock-infected sample is represented as a heat map (n = 2). Cytokines and chemokines are ranked in descending order according to the mean fold-induction values from the PR8 sample.

chemokines, was used in an immunoblot array proteome profiler (see Table 3.1 for list of cytokines and chemokines assayed). The levels of cytokines and chemokines in the supernatant was taken to be proportional to the spot intensity following the near infrared detection protocol using the LiCor Odyssey platform. Samples quantified in duplicate using densitometry, calculated as mean fold-change with respect to the mock-infected sample, and plotted as a heat-map (Fig 3.5B). Table 3.1 summarises the roles of the cytokines quantified in this array, and provides the mean fold-change values from the mock-infected sample. It also defines the abbreviations used for each cytokine and chemokine described below.

The cytokines and chemokines were ranked in descending order according to the fold-change values obtained in the PR8-infected sample. Visual inspection of the heat map revealed that, generally, the profiles of most cytokines and chemokines were similar across all samples. Certain proteins, such as MIF, TNF-α, CCL3 (a.k.a. MIP-1α), and CCL5 (also called RANTES), all pro-inflammatory mediators, were highly up-regulated in all infected samples. Some were down-regulated in all samples, such as CXCL1 (a.k.a. GROα) and CCL1, but only by a maximum of 2-fold. The most striking difference between the profiles of PR8, O175A and O265B samples was the much larger expression of the pro-inflammatory mediators TNF-α, CCL3 and CCL5 in PR8-infected macrophages in comparison to the NS reassortant viruses. There was 49.5-fold more TNF-α detected in PR8-infected samples in comparison to mock-infected macrophages, while the mean up-regulation was only 6.5-fold in O175A-infected macrophages, and 8.0-fold in the O265B-infected sample. CCL3 was up-regulated 36.5-fold in the PR8 sample, and only 7.5-fold for O175A and 11.5-fold for

Table 3.1 – Human CD14$^+$ MDM cytokine/chemokine profiling. Secreted cytokines and chemokines were quantified following infection of human macrophages. The fold-change values represent the abundance of protein relative to the mock-infected sample. A brief description of the main role(s) of each cytokine and chemokine is provided.

Cytokine/ chemokine	Alternative name	Function	Fold-change PR8	Fold-change O175A	Fold-change O265B	Reference
MIF (macrophage migration inhibitory factor)	-	Regulates innate immunity and stimulates pro-inflammatory response.	55.0	57.3	78.3	(Calandra and Roger, 2003)
TNF-α (Tumour Necrosis Factor α)	-	Pro-inflammatory roles. Mediator of fever and acute phase response. Antiviral properties by activating NF-κB pathway and inducing apoptosis. Correlated with lung tissue damage in HPAI infections.	47.5	6.5	8.0	(To et al., 2016, Lee et al., 2009b, Cheung et al., 2002)
CCL3 (chemokine (C-C) motif ligand 3)	MIP-1α (macrophage inflammatory protein)	Pro-inflammatory roles. Chemotactic for and activator of macrophages and CD8$^+$ T-cells.	36.5	7.5	11.5	(Trifilo et al., 2003)
CCL5 (chemokine (C-C) motif ligand 5)	RANTES (Regulated on Activation Normal T Cell Expressed and Secreted)	Chemotactic for several immune cell populations at inflammatory sites. Activator of NK cells. Important for anti-apoptotic signalling of alveolar macrophages during clearance of influenza-infected apoptotic cells.	11.4	4.0	3.4	(Tyner et al., 2005)
CXCL10 (C-X-C motif ligand 10)	IFN-γ-induced protein 10,IP-10)	Chemotactic for monocytes, macrophages, NK cells, T-cells, and dendritic cells. Secretion is stimulated by IFN-γ and also pro-inflammatory cytokines. Important for RSV clearance in mice.	9.9	14.6	11.4	(Lindell et al., 2008)

Cytokine/ chemokine	Alternative name	Function	Fold-change PR8	Fold-change O175A	Fold-change O265B	Reference
IL-16 (interleukin-16)	-	Pro-inflammatory cytokine. Chemoattractant for $CD4^+$ T-cells, monocytes, eosinophils and dendritic cells. Regulates $CD4^+$ T-cell development.	6.3	7.8	8.0	(Amiel et al., 1999)
IL-6 (interleukin-6)	-	Pro-inflammatory cytokine secreted by T-cells and macrophages. Important mediator of fever and acute phase response. Essential for effective clearance of H1N1 IAV in mice.	5.6	2.8	3.4	(Dienz et al., 2012)
IL-1ra (interleukin-1 receptor antagonist)	-	Anti-inflammatory cytokine. Antagonistic functions with the IL-1 receptor. Therefore inhibits of IL-1α and of IL-1β. Loss of IL-1ra leads to uncontrolled systemic inflammation and polyarthropathy.	3.8	3.9	3.2	(Horai et al., 2000)
Serpin E1 (serpin family E member 1)	PAI-1 (plasminogen activator inhibitor protein-1).	Serine protease inhibitor. Inhibits tissue plasminogen activator and urokinase. Inhibits plasminogen and therefore the breakdown of blood clots. Propose to be antiviral against IAV by inhibiting extracellular proteases required for HA cleavage.	2.6	1.1	1.1	(Dittmann et al., 2015)
IL-5 (interleukin-5)	-	Essential for eosinophil maturation and recruitment to infected airway during IAV infection and recovery phase.	2.4	1.0	0.9	(Gorski et al., 2013)
IL-1β (interleukin-1β)	Catabolin	Pro-inflammatory interleukin produced following activation of the nucleotide-binding oligomerization domain (NOD)-like receptor family pyrin domain-containing 3 (NLRP3) inflammasome, which is activated by IAV M2 protein. Contributes to lung tissue damage during IAV infection.	2.1	3.2	2.9	(Ichinohe et al., 2010, Kim et al., 2015b)
CXCL12 (C-X-C motif ligand 12)	SDF-1 (stromal cell-derived factor 1)	Chemotactic for leukocytes and up-regulated in inflammatory response. Required for $CD8^+$ T-cell recruitment during IAV infection.	2.0	4.9	2.6	(Lim et al., 2015)

Cytokine/ chemokine	Alternative name	Function	Fold-change PR8	Fold-change O175A	Fold-change O265B	Reference
IFN-γ (interferon-γ)	-	Type II IFN. Major macrophage activation roles. Chemoattractant of leukocytes, enhances NK cell activity, regulates B-cell functions.	1.9	2.2	2.1	(Schroder et al., 2004)
CCL4 (chemokine (C-C) motif ligand 4)	MIP-1β (macrophage inflammatory protein 1β)	Chemotactic for a variety of immune cells. Pro-inflammatory.	1.7	4.9	4.9	(Menten et al., 2002)
IL-1α (interleukin-1α)	-	Pro-inflammatory interleukin. Acts as an 'alarmin' to initiate the release of various pro-inflammatory cytokines and chemokines in acute inflammation.	1.4	1.4	1.3	(Garlanda et al., 2013)
IL-2 (interleukin-2)	-	Important for growth, proliferation and differentiation of T-cells and required for T-cell immunological memory. Also promotes proliferation of B cells and NK cells.	1.4	1.2	1.0	(Gaffen and Liu, 2004)
IL-4 (interleukin-4)	-	Induces differentiation of naïve helper T-cells into type 2 helper T cells. Multifunctional roles in regulating macrophages and lymphocytes.	1.3	1.1	0.8	(Luzina et al., 2012)
sTREM-1 (soluble triggering receptor expressed on myeloid cells)	-	Soluble form of the TREM-1 receptor. Released by monocytes and modulates pro-inflammatory response. Thought to help prevent hyper-responsiveness and therefore reduce inflammation-induced tissue damage.	1.3	1.2	1.7	(Gibot et al., 2004)
IL-10 (interleukin-10)	Human cytokine synthesis inhibitory factor.	Anti-inflammatory cytokine. Helps protect epithelial cell layers. Regulates production of pro-inflammatory cytokines such as TNF-α.	1.2	1.3	1.2	(Ouyang et al., 2011)
IL-27 (interleukin-27)	-	Anti-inflammatory cytokine. Suppressor of helper T cell responses and limits inflammation.	1.2	2.0	1.7	(Kastelein et al., 2007)

Cytokine/ chemokine	Alternative name	Function	Fold-change PR8	Fold-change O175A	Fold-change O265B	Reference
CCL2 (chemokine (C-C) motif ligand 2)	MCP-1 (Monocyte chemoattractant protein 1)	Chemotactic for monocytes, memory T-cells NK cells to sites of inflammation.	1.1	0.7	0.6	(Deshmane et al., 2009)
IL-17E (interleukin-17E)	IL-25 (interleukin-25)	Pro-inflammatory cytokine that induces type 2 helper T-cell response.	1.1	1.3	1.3	(Fort et al., 2001)
CD40 Ligand (cluster of differentiation 40 ligand)	CD154 (cluster of differentiation 154)	Expressed on surface of activated T-cells, B-cells, NK cells, and macrophages. Co-stimulatory protein required for activation of various immune cells via stimulation of CD40. Stimulates B cells to produce antibody. Induces release of pro-inflammatory cytokines from endothelial cells and fibroblasts to attract leukocytes to site of inflammation.	1.1	1.4	1.3	(Korniluk et al., 2014)
CXCL11 (C-X-C motif ligand 11)	I-TAC (interferon-inducible T-cell alpha chemoattractant) or IP-9 (interferon-gamma-inducible protein 9)	Chemotactic for activated T-cells.	1.1	1.6	1.5	(Cole et al., 1998)
sICAM-1 (soluble intercellular adhesion molecule 1)	CD54 (cluster of differentiation 54)	Adhesion molecule and activator of T-cells.	1.1	1.5	2.1	(Kuhlman et al., 1991)

Cytokine/ chemokine	Alternative name	Function	Fold-change PR8	Fold-change O175A	Fold-change O265B	Reference
IL-23 (interleukin-23)	-	Pro-inflammatory cytokine. Stimulates type 17 helper T-cell response.	1.1	1.3	1.2	(Teng et al., 2015)
CSF2 (colony stimulating factor 2)	GM-CSF (Granulocyte-macrophage colony stimulating factor).	Stimulates bone marrow stem cells to differentiate into granulocytes and monocytes.	1.1	1.2	1.2	(Shi et al., 2006)
IL-12 (interleukin-12)	p70	Pro-inflammatory cytokine. Stimulates differentiation of T-cells into IFN-γ producing class 1 helper T-cells.	1.1	1.0	1.2	(Teng et al., 2015)
IL-32α (interleukin-32α)	-	Pro-inflammatory properties. Induces inflammatory cytokine secretion, e.g. TNF-α, IL-1β and IL-6 from macrophages.	1.0	1.1	1.1	(Shoda et al., 2006)
IL-13 (interleukin-13)	-	Anti-inflammatory cytokine. Inhibits pro-inflammatory cytokine production in airway disease and allergic inflammation.	1.0	1.5	1.5	(Wynn, 2003)
IL-17 (interleukin-17)	-	Pro-inflammatory cytokine produced by type 17 helper T-cells. Stimulates pro-inflammatory cytokine release and therefore recruits macrophages and neutrophils to sites of inflammation.	0.8	0.9	0.9	(Jin and Dong, 2013)
CSF3 (colony stimulating factor 3)	G-CSF (Granulocyte colony-stimulating factor).	Stimulates bone marrow stem cells to differentiate into granulocytes. Stimulates growth, proliferation and differentiation of neutrophils.	0.8	0.6	0.9	(Bendall and Bradstock, 2014)
IL-28 (interleukin-28)	IFN-λ (interferon-λ)	Type III IFN with antiviral properties. Similar mechanisms of action as type I IFNs but via different receptor. Up-regulation of ISGs in response to infection.	0.7	0.7	0.6	(Donnelly and Kotenko, 2010)

Cytokine/ chemokine	Alternative name	Function	Fold-change PR8	Fold-change O175A	Fold-change O265B	Reference
C5a (complement component 5a)	-	Part of the complement system with multiple roles. Inflammatory peptide upregulating NF-κB and IL-1 in alveolar macrophages in lung injury.	0.7	0.8	0.5	(Guo and Ward, 2005)
CCL1 (chemokine (C-C) motif ligand 1)	I-309	Pro-inflammatory chemokine. Chemotactic for monocytes and T-cells.	0.5	0.7	0.9	(Miller and Krangel, 1992)
CXCL1 (C-X-C motif ligand 1)	GROα	Pro-inflammatory chemokine. Neutrophil chemotactic activity.	0.5	0.8	0.8	(Geiser et al., 1993)

O265B. CCL5 was up-regulated 11.4-fold in PR8-infected macrophages, but only 4.0-fold and 3.4-fold in O175A- and O265B-infected macrophages, respectively.

Serpin E1, a plasminogen inhibitor, and IL-5, a chemotactic cytokine for eosinophils, were both detected at levels over 2-fold greater in the PR8-infected samples in comparison to both O175A and O265B. CCL4 (a.k.a. MIP-1β), a chemotactic for a variety of immune cells, was up-regulated 4.9-fold in O175A and O265B samples, but only 1.7-fold in PR8-infected macrophages. Otherwise, all other cytokines/chemokines were detected at levels within a 2-fold range across PR8-, O175A- and O265B-infected samples.

Overall, PR8-infected macrophages appeared to produce and secrete a higher level of pro-inflammatory cytokines than O175A and O265B. The profiles of O175A and O265B were, in general, relatively similar. There was no evidence of an excessive, pro-inflammatory response in macrophages infected with the consensus B-allele reassortant virus.

3.2.5 Quantitative temporal proteomics – host response of infected human lung cells

In this experiment, a collaboration with Dr. Michael Weekes (Cambridge Institute for Medical Research, University of Cambridge, Cambridge, UK), Dr. Joao Paolo and Prof. Steven Gygi (University of Harvard, Massachusetts, USA) was formed to investigate changes to the overall host-cell proteome during infection using a multiplexed tandem mass tag (TMT)-based mass spectrometry technique (Weekes et al., 2014). Human lung A549 cells were infected at high MOI with PR8, O175A or O265B and cell lysates generated at various times post-infection. Mass-spectrometry

analysis allowed the direct comparison of the relative abundance of thousands of peptides in infected cells across different time-points and different viruses.

Human lung A549 cells were infected in 100 mm dishes with either PR8, O175A or O265B at an MOI of 5 for 8, 16 and 24 h (only O175A and O265B infections were performed at 24 h time-point, due to a processing limit of 10 samples overall for the TMT-based mass spectrometry system). Each dish contained two 13 mm glass coverslips that were retrieved at the end of infection for separate western blotting and immunofluorescence analyses. Successful infection was demonstrated by western blotting for viral NP and specific NS1 proteins in cells lysed in SDS lysis buffer (Fig 3.6A). V29 detected PR8 and O175A NS1 expression, and A2 detected O175A and O265B expression, as expected (see Fig 2.6). Mock-infected cell lysates did not contain detectable NP or NS1. Immunostaining of intracellular viral NP in cells fixed at each time-point confirmed a mean infection rate of approximately 95% across all samples (Fig 3.6B shows the 8 h time-point as a representative). The remaining cells were lysed using a guanidine-HCl lysis buffer and lysates were processed for mass-spectrometry in the Gygi lab as described in a previous report (Weekes et al., 2014). Dr. Michael Weekes processed the mass-spectrometry data and provided values for all quantified peptides as fold-change with respect to the average of the mock-infected samples.

Overall, 6862 unique proteins were quantified from the infected A549 cell samples (see Table S3.1 included as an .xlsx file on CD). Among these, peptides from the major viral proteins were identified at high abundance in infected cells (data not shown). Fig 3.7A shows the fold-change values with respect to the average of the mock-infected samples for all peptides at 16 h post-infection, ranked in descending

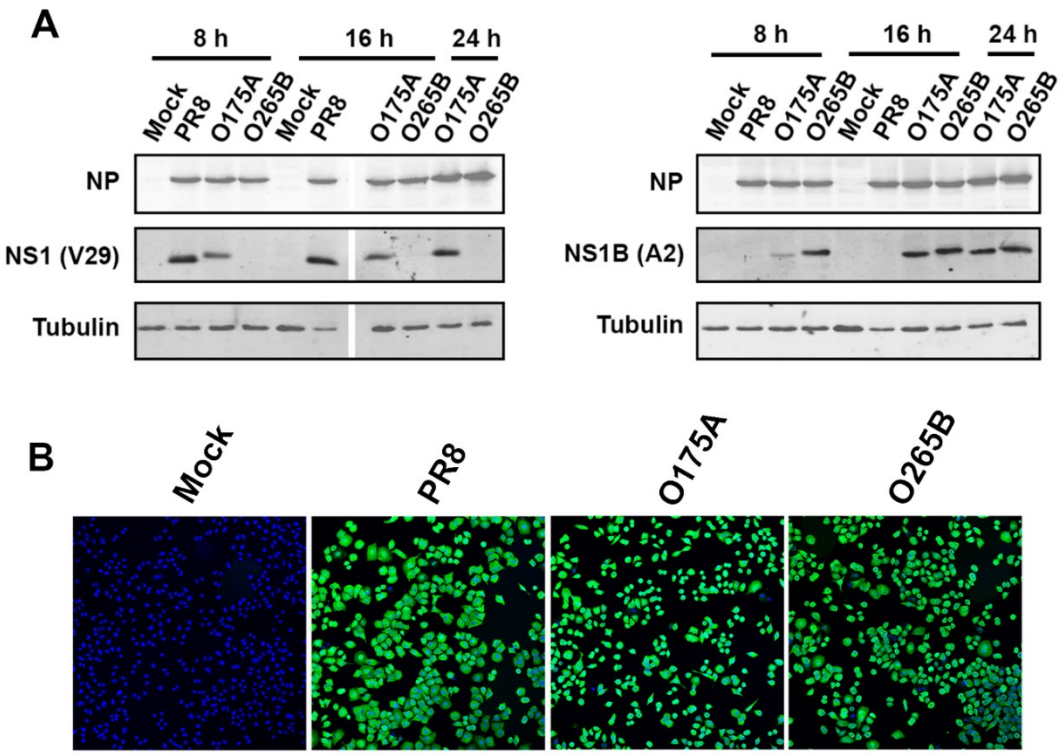

Fig 3.6. Validation of infection for quantitative temporal proteomics. (A) A549 cells were infected at an MOI of 5 and cell lysates were generated at the indicated time-points. Western blotting for viral NP and strain-specific NS1 was performed on cell lysates. Blotting for A-allele NS1s (V29) and avian NS1s (A2) was performed on separate gels. Alpha-tubulin was used as a loading control. (B) Immunofluorescent staining of intracellular NP (green) in fixed cells was used to estimate successful infection rates at each time-point. Shown are 8 h post-infection samples. DAPI staining (blue) shows cell nuclei.

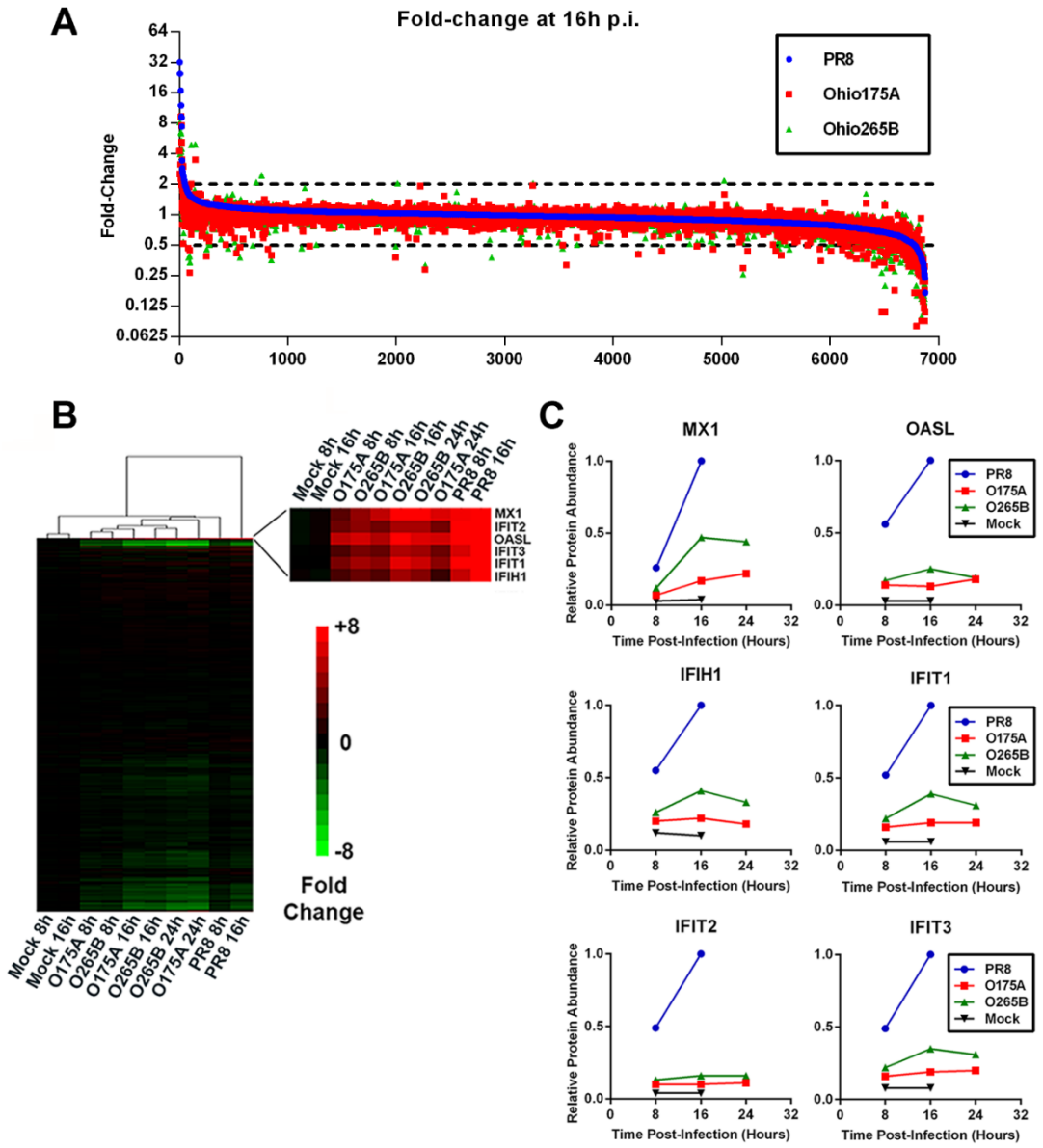

Fig 3.7. Quantitative temporal proteomics of infected A549 cells. A549 cells were infected at an MOI of 5, cell lysates generated at the indicated time-points and polypeptide composition determined by TMT-based quantitative mass spectrometry. (A) All host-cell peptides detected at 16 h p.i. represented as fold-change relative to mock-infected samples, and ranked in descending order of relative abundance in the PR8 sample. Dashed lines indicate the 2-fold relative abundance range relative to the mock-infected samples. (B) Values represented as a heat map of mean fold-change with respect to mock-infected samples. The zoomed portion shows a sub-cluster of heavily up-regulated antiviral proteins. (C) Quantitative temporal expression of specific antiviral restriction factors Mx1, OASL, IFIH1, IFIT1, IFIT2 and IFIT3 is plotted. Values are plotted normalised to maximum-detected fold-change per protein. Heat map in (B) was made by Dr. Michael Weekes (Cambridge Institute for Medical Research, University of Cambridge, Cambridge, UK).

order of relative abundance in the WT PR8-infected sample. The majority of peptides fell between the -2 and +2 fold-induction range in a similar expression profile for all viruses. Only a minority of host proteins changed abundance by 2-fold or more during infection, and the majority of these were down-regulated – see Tables 3.2 and 3.3 for the ten proteins that displayed the largest increase or decrease, respectively, at 16 h post-infection in the PR8-infected sample. All proteins identified that were up- or down-regulated by 2-fold or more, relative to mock-infected samples, were analysed to identify potentially interesting patterns.

All host-proteins were clustered (by Dr. Michael Weekes) according to fold-change relative to the average of the mock-infected samples, which was plotted as a heat-map (Fig 3.7B). Of the proteins that were highly up-regulated, a cluster of antiviral proteins was noted in all viral-infected samples. This group included the antiviral host proteins Mx1, OASL, IFIH1 (also known as Melanoma Differentiation-Associated protein 5 or MDA5), IFIT1, IFIT2, and IFIT3 (Figs 3.7B and 3.7C, and Table 3.2 which also defines abbreviations). Notably, these antiviral proteins were most highly up-regulated in PR8-infected samples at all time-points tested, with the quantity of these antiviral proteins invariably at least 2-fold greater than O175A and O265B at the 16 h time-point, while the abundance levels were more comparable between O175A and O265B infections. When Mx1 protein abundance in infected A549 cell lysates was quantified by western blot, it was noted that PR8 induced greater Mx1 expression than O175A and O265B relative to the mock-infected sample (see lanes 1-4 of Fig 3.1B), in agreement with these mass-spectrometry data.

Table 3.2. Up-regulated cellular proteins during infection of A549 cells quantified by mass-spectrometry. Shown are the top ten cellular proteins that were most strongly up-regulated in the 16 h infection with WT PR8, ranked in descending order. Values represent fold-change over mock-infected sample. Fold-change values are shown for all time-points tested for all samples.

Gene symbol	Protein name	PR8		O175A			O265B		
		8 h	16 h	8 h	16 h	24 h	8 h	16 h	24 h
OASL	2'-5'-oligoadenylate synthase-like protein	18.15	32.28	4.66	4.25	5.65	5.61	8.19	6.15
MX1	Interferon-induced GTP-binding protein Mx1	7.45	28.22	2.07	4.84	6.08	3.32	13.34	12.50
IFIT2	Interferon-induced protein with tetratricopeptide repeats 2	12.06	24.58	2.44	2.54	2.63	3.17	3.97	3.97
IFIT1	Interferon-induced protein with tetratricopeptide repeats 1	8.81	16.81	2.68	3.15	3.12	3.76	6.57	5.26
IFIT3	Interferon-induced protein with tetratricopeptide repeats 3	5.84	12.02	1.88	2.29	2.45	2.67	4.22	3.69
PLG	Plasminogen	4.59	9.31	4.64	9.35	8.38	3.52	6.38	8.10
ISG15	Ubiquitin-like protein ISG15	3.27	9.27	1.54	2.38	9.85	1.71	3.44	3.61
LRCH4	Leucine-rich repeat and calponin homology domain-containing protein 4	4.74	9.26	4.97	7.57	9.77	3.43	5.38	6.99
IFIH1	Interferon-induced helicase C domain-containing protein 1	5.04	9.12	1.80	1.98	1.60	2.37	3.77	2.97
CEP128	Centrosomal protein of 128 kDa	3.10	7.41	2.62	5.20	4.86	1.71	4.49	12.34

Table 3.3. Down-regulated cellular proteins during infection of A549 cells quantified by mass-spectrometry. Shown are the top ten cellular proteins that were most strongly down-regulated in the 16 h infection with WT PR8, ranked in descending order. Values represent fold-change over mock-infected sample. Fold-change values are shown for all time-points tested for all samples.

Gene symbol	Protein name	PR8		O175A			O265B		
		8 h	16 h	8 h	16 h	24 h	8 h	16 h	24 h
RFWD3	E3 ubiquitin-protein ligase RFWD3	0.49	0.17	0.26	0.11	0.14	0.32	0.12	0.14
AHR	Aryl hydrocarbon receptor	0.44	0.24	0.48	0.22	0.14	0.49	0.12	0.12
CRIM1	Cysteine-rich motor neuron 1 protein	0.34	0.24	0.40	0.22	0.16	0.52	0.23	0.20
ID1	DNA-binding protein inhibitor ID-1	0.62	0.24	0.12	0.11	0.07	0.20	0.09	0.05
FGFR4	Fibroblast growth factor receptor 4	0.53	0.24	0.14	0.18	0.00	0.24	0.15	0.14
FGFR1	Isoform 21 of Fibroblast growth factor receptor 1	0.45	0.24	0.48	0.25	0.17	0.44	0.24	0.19
TFAP4	Transcription factor AP-4	0.52	0.25	0.38	0.17	0.12	0.42	0.21	0.11
C14orf119	Uncharacterized protein C14orf119	0.54	0.26	0.30	0.09	0.06	0.53	0.14	0.10
MYO10	Unconventional myosin-X	0.55	0.27	0.70	0.31	0.26	0.68	0.34	0.25
AMD1	S-adenosylmethionine decarboxylase proenzyme	0.66	0.27	0.39	0.12	0.11	0.39	0.16	0.11

An analysis of down-regulated proteins was likewise performed. Table 3.3 shows the ten most down-regulated proteins at 16 h post-infection relative to the mock-infected samples in the WT PR8-infected sample, and also defines abbreviations. An initial inspection of these down-regulated proteins failed to highlight any striking patterns following a search in the literature in an attempt to link protein function to IAV replication. The majority of these hits, barring FGFR1 and AHR, have not been implicated in playing a role(s) in IAV infection. FGFR1 was down-regulated to 0.24-, 0.25- and 0.24-fold relative to the mock-infected samples in the PR8, O175A and O265B samples respectively at 16 h post-infection. While FGFR1 has previously been proposed to be a host factor required for efficient virus entry in an RNA-interference screen performed by Konig and colleagues (Konig et al., 2010), a more recent study has suggested that FGFR1 inhibits virus replication (Liu et al., 2015b). Thus, it is not currently clear how a downregulation in FGFR1 abundance may affect virus replication. AHR was also down-regulated in all samples and has been reported to increase lung inflammation and reduce survival rate in mice infected with IAV following its activation by pollutants (Teske et al., 2005). Likewise, it is difficult to speculate on the significance of this finding in terms of IAV replication in A549 cells *in vitro*.

Next, the components known to be involved in type I IFN induction and signalling were specifically analysed given the well characterised role of NS1 in antagonising IFN induction (reviewed in Chapter 1). Table 3.4 shows the proteins identified in the mass-spectrometry experiment that are known to play a role in either RIG-I-like signalling or JAK/STAT signalling as part of the type I IFN response. The majority of hits identified did not change substantially with infection relative to mock-

Table 3.4. Quantitative temporal proteomics of components involved in the type I IFN response during infection of A549 cells. Shown are selected proteins identified in the mass-spectrometry experiment that are known to be involved in the type I IFN response (reviewed in Chapter 1). Hits are ranked in descending order of relative abundance in the PR8-infected sample at 16 h post-infection. Values represent fold-change over mock-infected sample. Fold-change values are shown for all time-points tested for all samples.

Gene symbol	Protein name	PR8		O175A			O265B		
		8 h	16 h	8 h	16 h	24 h	8 h	16 h	24 h
IFIH1	Interferon-induced helicase C domain-containing protein 1 (also known as MDA5)	5.04	9.12	1.8	1.98	1.6	2.37	3.77	2.97
DDX58	Probable ATP-dependent RNA helicase DDX58 (also known as RIG-I)	2.18	3.44	1.22	1.31	1.32	1.31	1.79	1.6
IKBIP	Inhibitor of nuclear factor kappa-B kinase-interacting protein	1.08	1.16	0.98	1.11	1.02	1.21	1.1	1.17
STAT2	Signal transducer and activator of transcription 2	1.15	1.13	1.15	0.59	0.52	0.93	0.72	0.61
STAT1	Isoform Beta of Signal transducer and activator of transcription 1-alpha/beta	1.04	1.11	1.04	1.05	1.02	1.02	1.07	1.04
TANK	TRAF family member-associated NF-kappa-B activator	1.11	1.07	0.97	0.85	0.91	0.97	0.84	1
IRF3	Interferon regulatory factor 3	1.09	1.05	0.98	0.97	0.99	0.94	1.04	0.98
MAVS	Mitochondrial antiviral-signalling protein	0.95	1.01	0.95	1	0.98	1.21	0.99	1.01
NFKB1	Isoform 2 of Nuclear factor NF-kappa-B p105 subunit	0.94	0.98	0.92	0.94	0.86	0.94	0.94	0.93
NFKB2	Nuclear factor NF-kappa-B p100 subunit	1.11	0.97	1.17	0.96	0.86	1.11	0.89	1.12
TBK1	Serine/threonine-protein kinase TBK1	1	0.9	0.93	0.83	0.78	0.95	0.82	0.77
JAK1	Tyrosine-protein kinase JAK1	0.61	0.4	0.5	0.3	0.22	0.55	0.4	0.31

-infected samples. IFIH1 (or MDA5) was the protein most highly up-regulated in any sample, and this was in the PR8-infected sample at 16 h post-infection and was described above. RIG-I (DDX58) was also up-regulated in PR8-infection relative to O175A and O265B, which is consistent with the data described above that suggested that PR8 infection up-regulated interferon-inducible protein expression more so than the NS reassortant viruses. It was noted that PR8, O175A and O265B all reduced the expression of JAK1 (Janus kinase-1) to 0.40-, 0.34- and 0.38-fold respectively at 16 h post-infection. However, all other components of the type I IFN signalling pathway that were identified all fell within 2-fold of the mock-infected samples and therefore were not substantially altered during infection.

Overall, the ISG profiles of O175A and O265B were similar, while WT PR8 appeared to induce a stronger antiviral response in infected A549 cells. These data do not support a hypothesis that a B-allele virus induces an excessive antiviral response in mammalian cells that may lead to a disadvantage in terms of virus replication in a mammalian host in comparison to an A-allele counterpart virus.

3.2.6 Host cell shut-off during infection with NS reassortant viruses

Next, to investigate whether the differences in ISG profiles noted in the quantitative temporal proteomics study described above could be attributed to differences host protein synthesis rates during infection, metabolic labelling was employed as means of assessing host cell shut-off during infection with the panel of PR8-based NS reassortant viruses.

MDCK cells were infected at high multiplicity (MOI = 10) and were pulsed with a ^{35}S-labelled protein labelling mix (Perkin Elmer) at 6 h post-infection for 2 h.

At 8 h post-infection, MDCK cells that were infected in parallel, without the addition of radioisotope, were fixed, permeabilised, and immunostained for viral NP for all samples to assess infection rate. Fig 3.8A shows NP immunostaining for PR8-, O175A-, and O265B-infected cells, of which the majority were infected. Mock-infected cells did not contain detectable NP at the imaging parameters used. Cell lysates were generated at 8 h post-infection and levels of labelled proteins synthesised in the 6-8 h window were detected by autoradiography following SDS-PAGE on equal volumes of cell lysate (Fig 3.8B). Mock-infected cells did not synthesise detectable levels of viral proteins. In all virus-infected samples, the polymerase proteins, NP, HA, NS1, M1 and NEP were readily detected (see annotations on Fig 3.8B). Mock-infected cell lysates generally contained a higher level of labelled cellular proteins than infected cells, indicating greater synthesis rates. This was apparent by darker regions of the gel in comparison to virus-infected samples at molecular weights where no viral proteins were detected, particularly at higher molecular weight. In virus-infected cells, there was a clear bias for viral protein synthesis over host-cell proteins. To quantify cellular protein synthesis rates, actin was used as a marker as it is generally expressed at relatively high levels in uninfected cells and is therefore easily identified (see 42 kDa protein annotated in Fig 3.8B). The actin band was quantified by densitometry using ImageJ software (Fig 3.8C). All infected cells displayed a clear reduction in actin synthesis rates (at least two-fold on average) relative to mock-infected cells, and the ability to reduce actin synthesis rates was similar across both A- and B-allele reassortant viruses with no clear differences noted (Fig 3.8C).

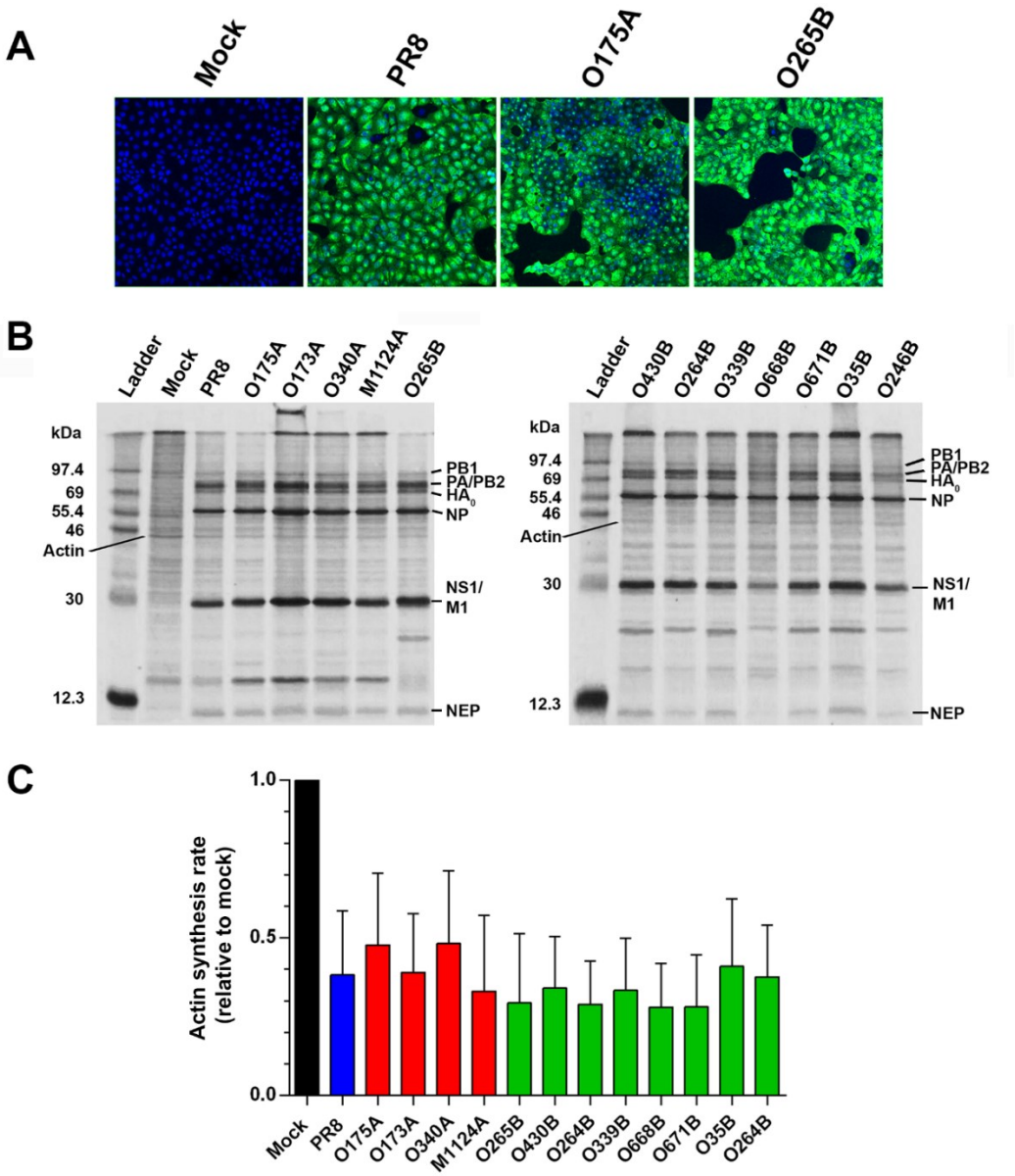

Fig 3.8. Host cell shut-off during infection with NS reassortant viruses. MDCK cells were infected at an MOI of 10. (A) Immunofluorescence of intracellular viral NP (green) at 8 h post-infection was used to estimate successful infection rates in all samples. Shown are PR8, O175A and O265B infections (images for other infections are not shown). DAPI staining (blue) shows cell nuclei. (B) Metabolic labelling was performed using a ^{35}S protein labelling mix between 6-8 h p.i.. Cell lysates were generated at 8 h p.i. using an SDS lysis buffer. Lysates were subjected to SDS-PAGE and proteins with ^{35}S were detected using autoradiography. (C) Actin synthesis rates were quantified by densitometry using ImageJ software. Data represent mean and range of two independent experiments.

These data do not support the hypothesis that there is not a major deficiency for B-allele NS reassortant viruses in inducing host-cell shut-off in the context of virus infection. However, while there is evidence that NS1 is involved in preventing cellular gene expression by preventing processing of host pre-mRNAs (described more thoroughly below), it is not clear from this experiment whether the shut-off observed was due to the NS1 protein alone or in combination with other shut-off mechanisms that have been described for IAV. Other mechanisms of shut-off include host mRNA 'cap-snatching' (Robertson et al., 1980, Dias et al., 2009), the degradation of host mRNA transcripts by PA-X (Jagger et al., 2012, Khaperskyy et al., 2016), the degradation of cellular RNA polymerase II (pol II) (Rodriguez et al., 2007, Vreede et al., 2010), and an inhibition of pol II elongation by the viral polymerase (Chan et al., 2006). Indeed, it has been reported previously that the NS1 protein may not be required for host shut-off (Salvatore et al., 2002). Therefore, the influence on NS1 proteins to inhibit a pol II promoter in isolation were studied next, as described below.

3.2.7 NS1 and suppression of RNA polymerase II promoter activity

NS1 has been implicated in suppressing host gene expression by inhibiting host pre-mRNA maturation, splicing and nuclear export by various mechanisms including binding to and inhibiting host CPSF30 and PABII (Nemeroff et al., 1998, Chen et al., 1999), U6 snRNA (Qiu et al., 1995), as well as inhibiting the mRNA nuclear export complex (Satterly et al., 2007), and this contributes to a dampening of the IFN response in infected cells (Noah et al., 2003, Kochs et al., 2007). All of the above studies were conducted using A-allele NS1 proteins, and to date there are no available reports assessing B-allele NS1 inhibition of cellular gene expression. To complement the metabolic labelling data, and to investigate the ability of A- and B-allele NS1 proteins

in isolation to inhibit cellular gene expression, a pol II reporter assay was employed. A plasmid vector containing a constitutively active pol II promoter (simian virus 40 (SV40)) upstream of the *Renilla reniformis (Renilla)* luciferase gene (pRL, kind gift from Dr. Finn Grey, the Roslin Institute, The University of Edinburgh) was co-transfected with various NS1-GFP constructs in 293T cells, and luciferase activity after 48 h was used as a readout for cellular pol II-driven gene expression. NP-GFP was used as a control, as NP is not known to influence host gene expression. A PR8 NS1-GFP mutant, which has the consensus CPSF30-binding site reinstated (S103F and I106M; 'PR8 S103F/I106M', made by Dr. Helen Wise of the Digard laboratory), was used as a positive control as this NS1 mutant was predicted to induce a greater level of shut-off than the WT PR8 NS1 (Kochs et al., 2007). A pDUAL plasmid expressing the A/chicken/Rostock/8/1934 (H7N1) (fowl plague virus, or FPV) PA gene, and also a PA-X gene known to have host-cell shut-off ability (unpublished data from Digard lab), was used as another positive control. Empty pDUAL plasmid was used as the appropriate negative control for this effector.

293T cells were seeded in 24-well plates, and were co-transfected with 100 ng of pRL reporter plasmid along with 400 ng of effector plasmid. At 24 h post-transfection, successful transfection was confirmed using epi-fluorescent microscopy for GFP fluorescence and all cells were transfected at similar levels (data not shown). After 48 h, cells were lysed and *Renilla* luciferase activity was quantified using Promega's *Renilla* Luciferase Assay System. *Renilla* luciferase activity was plotted as fold-change with respect to the appropriate control (NP-GFP for NS1-GFP effector plasmids, and empty pDUAL for pDUAL-PA). Background luminescence was determined by including a 'PR8-NS1-GFP only' and a 'lysis buffer only' negative

control – both of which gave relative luminescence values several orders of magnitude lower than samples expected to contain active luciferase (data not shown).

Luciferase activity was high in the NP-GFP (mean activity 6.3 x 10^7 RLU +/- 1.9 x 10^7 SD, n =4) and empty pDUAL plasmid (mean activity 2.5 x 10^8 RLU +/- 7.0 x 10^7 SD, n = 4) negative controls. The dashed line on the graph shows the luciferase activity of the NP-GFP and empty pDUAL plasmid controls (Fig 3.9). The pDUAL-FPV-PA effector suppressed mean luciferase activity to 0.17-fold compared to the empty pDUAL plasmid control sample. PR8 NS1-GFP actually increased luciferase activity by a mean of 2.84-fold compared to the NP-GFP control, while the PR8 S103F/I106M mutant reduced luciferase activity to 0.76-fold of the NP-GFP sample. The consensus North American LPAI NS1s, O175A and O265B, both supressed mean luciferase activity to 0.16-fold and 0.12-fold relative to the NP-GFP control, respectively. Transfection of NY6750A and Sw412A NS1-GFP plasmids both also reduced mean luciferase activity to 0.14-fold and 0.12-fold relative to NP-GFP. The NS1s of Alb88B, Sw418B and J89B likewise all suppressed the pRL pol II activity, with mean luciferase activities of 0.13-, 0.09- and 0.21-fold respectively relative to the NP-GFP negative control. The NS1-GFP plasmid for NY107B, however, increased luciferase activity to 6.51-fold relative to the NP-GFP control. The Sw418B NS1 protein induced a statistically significant reduction in luciferase activity in comparison to O175A NS1, while mean luciferase activity in the J89B sample was significantly higher than both the NY6750A and Sw412A samples (unpaired t-test, n = 4). A similar pattern of results was observed in experiments in which the pRL reporter plasmid was replaced with a plasmid constitutively expressing mCherry (pmCherry-N1, Clontech)

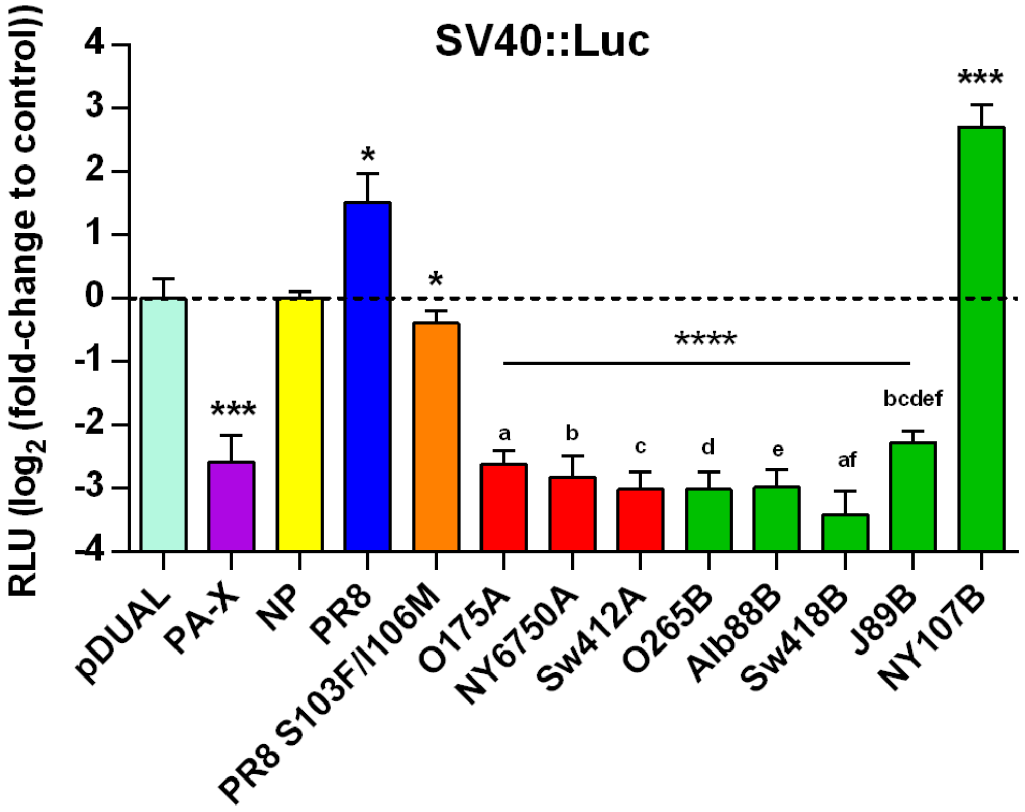

Fig 3.9. NS1 suppression of pol. II-mediated reporter gene expression. 293T cells were co-transfected with a plasmid constitutively expressing the *Renilla* luciferase gene under control of the SV40 promoter and NS1-GFP expression plasmids. Luciferase activity was measured at 48 h post-transfection. Data are plotted as fold-change with respect to appropriate negative control. NP-GFP was employed as negative control effector for all NS1-GFP effectors. A pDUAL segment 3 plasmid expressing high activity PA-X from A/chicken/Rostock/1934 (H7N1) was included as a positive control effector, with empty pDUAL plasmid as the negative control for this effector. Data represents mean +/- SD (n = 4). Statistically significant differences from respective negative control effectors (NP-GFP or empty pDUAL) in unpaired t-tests are marked with asterisk(s). * $p \leq 0.05$, ** $p \leq 0.01$, *** $p \leq 0.005$, **** $p \leq 0.001$. Samples labelled with the same letter are significantly different from each other in an unpaired t-test ($p \leq 0.05$).

and mCherry expression was quantified either by a fluorescence plate reader or western blotting of cell lysates (data not shown), validating the pattern of results seen in this system.

These data demonstrate a strain-dependent ability of NS1 proteins tested to reduce pol II-mediated gene expression. WT PR8 does not have either of F103 or M106, which are both reported to be important for CPSF30 inhibition (Kochs et al., 2007, Das et al., 2008). Mutating the NS1 protein to include these residues improved pol II promoter inhibition in comparison to WT, but did not reach the same levels as various other A- and B-allele NS1s tested. Interestingly, all B-allele NS1 proteins used in this experiment lack the F103 residue which has been suggested to be essential for CPSF30 binding and inhibition (Kochs et al., 2007, Das et al., 2008), and O668B additionally lacks M106 which is also apparently important (see Fig 2.1). All NS1 proteins investigated do, however, contain E186 which has been reported as being important for CPSF30-binding (Nemeroff et al., 1998, Li et al., 2001, Noah et al., 2003). Overall, although there is strain-dependent variability in shut-off ability, the data demonstrate that B-allele NS1 proteins are capable of inhibiting cellular pol II derived gene expression, despite the lack of the consensus CPSF30-binding site.

3.3 Discussion

In this section, the ability of segment 8 reassortant viruses to circumvent and suppress the host innate immune response was investigated. The primary reason for this being that previous studies have reported that B-allele NS1 proteins are deficient in their ability to suppress the mammalian IFN response. The Berg group published several studies investigating the ability of selected A- and B-allele NS1 proteins from closely related strains to prevent the up-regulation of type I IFN, NF-κβ, and AP-1 promoters using transfection-based reporter assays and IFN ELISAs during transfection and infection experiments. They proposed that B-allele NS1 proteins are deficient in supressing the activity of the aforementioned promoters and do not efficiently block the IFN response in mammalian cells (Zohari et al., 2010a, Munir et al., 2011a, Munir et al., 2011b, Munir et al., 2012). IFN-antagonism by the NS1 protein is essential for efficient virus replication (García-Sastre et al., 1998), and so if it was true that B-allele NS1 proteins are not capable of suppressing the mammalian IFN response, this could explain why B-allele viruses are rarely found in the mammalian host. However, the data presented in Chapter 2 points to full replicative ability of B-allele IAVs in mammalian cells, and so it was hypothesised that B-allele NS reassortant viruses would be able to control the IFN response in mammalian cells.

WT PR8 and consensus NS reassortant viruses O175A and O265B all coped similarly with the induction of the IFN response in A549 cells treated with IFN-β, displaying very similar IC_{90} values during multi-cycle infection experiments (Fig 3.1A). When type I IFN secretion was quantified following infection of human lung A549 cells with a panel of PR8- and Udorn72-based NS reassortant viruses, it was found that all viruses were able to suppress type I secretion during infection to below

inhibitory levels, except a PR8 NS1-mutant virus (Figs 3.2C, 3.3A and 3.3B). A panel of A- and B-allele NS1 proteins were also able to efficiently suppress the activation the human IFN-β promoter in cells stimulated with poly(I:C) (Fig 3.4A). Additionally, most of the NS1s tested were able to efficiently suppress the activation of the ISRE promoter element in a similar setup, barring PR8 and NY107B which either increased or failed to suppress ISRE activation, respectively (Fig 3.4B). An increase in ISRE activity in human cells stimulated with type I IFN has been noted in a previous study following transfection of a PR8 NS1 expression plasmid or infection with WT PR8 (Hayman et al., 2006). The mechanism behind this elevation in ISRE promoter activity, however, is not clear. These data, taken together, suggest that B-allele segment 8 viruses are able to supress type I IFN release during infection below inhibitory levels, and the NS1 proteins are acting to block IFN promoter activation. This is complemented by the findings of other studies that found B-allele avian NS1 proteins to be equally efficient at blocking IFN-β promoter activity in human cells as A-allele counterparts in transfection-based reporter studies (Hayman et al., 2007, Ma et al., 2010). Importantly, Sw418B displayed no evidence of a deficiency in blocking the mammalian IFN response, in both the context of viral infection and also in transfection-based reporter assays. Sw418B was a representative strain from the Berg group's reporter assay experiments in which it was concluded that B-allele NS1 proteins are deficient in IFN-antagonism in the mammalian host (Munir et al., 2011a, Munir et al., 2011b, Munir et al., 2012). Therefore, the data presented here directly contradict the findings and conclusions of the studies by the Berg group, even when using the same NS1 protein in a similar system. Although NS1-GFP was used as an effector here, rather than untagged NS1 as used by Munir and colleagues, it is not clear

how the GFP-tag would provide gain-of-function particularly when an appropriate control (NP-GFP) failed to efficiently block IFN-β and ISRE promoter activity. To be critical of the studies by the Berg group, they did not show that differences observed in reporter assays affected virus replication.

When human $CD14^+$ monocyte-derived macrophages were infected with consensus viruses, PR8, O175A and O265B all induced a pro-inflammatory response (Fig 3.5B and Table 3.1), with strong up-regulation of pro-inflammatory cytokines such as TNF-α, CCl5, and CXCL10, which have all been reported to be up-regulated during PR8 infection of human alveolar macrophages (Wang et al., 2012a). Interestingly, WT PR8 induced a higher level of pro-inflammatory cytokine release than O175A and O265B. A particularly striking up-regulation of TNF-α was noted in comparison to O175A- and O265B-infected macrophages. The pro-inflammatory response recruits inflammatory cells and contributes to inflammation-induced lung damage. Pro-inflammatory cytokines, particularly TNF-α and type I IFNs, have been proposed to be responsible for the increased lung pathology noted in human infection with HPAI H5N1 and the 2013 H7N9 virus (Cheung et al., 2002, Lee et al., 2009b, To et al., 2016). IL-1β has also been implicated in contributing to lung inflammation during infection with influenza A virus (Kim et al., 2015b), but this was only modestly up-regulated in all samples tested here (Fig 3.5B). Whether the increased cytokine release from PR8-infected macrophages was due the inability of its NS1 protein to block ISRE activation (Fig 3.4B), or another aspect of viral replication, is not clear. Importantly, an exaggerated immune response in macrophages infected with a B-allele virus was not noted. Therefore there was no evidence to suggest that B-allele viruses might elicit an overly-strong immune response when infecting mammalian hosts,

which may act to limit infection in these hosts. A more ideal experiment would have used alveolar macrophages rather than monocyte-derived macrophages from the blood, as these are the major macrophage population to encounter IAV in the lung. However, obtaining human alveolar macrophages is more challenging. In the next section, cytokine/chemokine profiling of infected mouse lung is described, which will reflect alveolar macrophage responses.

It has been reported elsewhere that the expression profiles of select ISGs, such as Mx1 and OAS, were similar during infection of avian cells with A- and B-allele viruses (Adams et al., 2013). However, a relevant study had not been reported using mammalian cells. Here, mass-spectrometry was employed to investigate proteome-wide changes in A549 cells that had been infected with A- and B-allele NS reassortant viruses at different time-points. Interestingly, WT PR8 up-regulated a host of antiviral factors to a greater extent than both O175A and O265B, and the ISG expression profiles of O175A and O265B were similar (Figs 3.7B and 3.7C). The antiviral roles of Mx1, OASL, IFIH1, IFIT1, IFIT2, and IFIT3 are discussed in more detail Chapter 1. All of these proteins are IFN-inducible. These findings complement the ISRE-promoter reporter data described above (Fig 3.4B), as well as previous studies reporting either a failure to supress ISRE activity or an increase in reporter assays by the PR8 NS1 protein or PR8 infection (Hayman et al., 2006, Hayman et al., 2007, Munir et al., 2011b). The quantitative temporal proteomics data did not support the hypothesis that a B-allele virus induces an exaggerated antiviral response in mammalian cells in comparison to A-allele counterparts.

Host cell shut-off was investigated, as it was observed that B-allele NS1 proteins do not contain the proposed CPSF30-binding motif (F103 & M106) (see Fig

2.1), and therefore it was plausible that B-allele viruses perhaps do not inhibit host cell gene expression efficiently, which could be detrimental to virus replication. Shut-off was assessed in virus infection by metabolic-labelling of infected MDCK cells and also by NS1 expression in transfected cells using a pol II reporter. All viruses tested were able to reduce actin synthesis rates to similar levels during infection (Figs 3.8B and 3.8C). The majority of NS1 proteins tested also reduced expression of a pol II reporter in transfection studies, except PR8 and NY107B NS1 which both increased expression (Fig 3.9). Therefore conversely, PR8 was able to reduce host actin synthesis during infection despite its NS1 protein seemingly increasing pol II promoter-driven gene expression. However, whole-virus infections and plasmid-based reporter assays are rather different systems and the functions of NS1 are likely to differ between the two. Additionally, the virus will be inducing shut-off through additional mechanisms including host mRNA 'cap-snatching' by the polymerase to prime viral mRNA transcription (Robertson et al., 1980, Dias et al., 2009), PA-X endonuclease activity targeting host mRNAs (Jagger et al., 2012, Khaperskyy et al., 2016), inhibition of cellular RNA pol II elongation (Chan et al., 2006) and inducing RNA pol II degradation (Rodriguez et al., 2007, Vreede et al., 2010), all of which will reduce actin synthesis rates. Indeed, Salvatore and colleagues proposed that the NS1 protein may not be required for host shut-off (Salvatore et al., 2002).

The mechanisms behind the increase in pol II driven gene expression in transfection-based studies with PR8 and NY107B NS1 proteins are not clear, and whether this is linked to the failure to inhibit ISRE activity (Fig 3.4B) and the strong ISG up-regulation in PR8-infected A549 cells (Figs 3.7B and 3.7C) is yet to be elucidated. ISG profiling of NY107B-infected cells would be a useful experiment to

help clarify this. Interestingly, both PR8 and NY107 have an R224G change in a region (223-230) that is thought to be important for PABPII binding and inhibition (Fig 2.1) (Chen et al., 1999, Li et al., 2001). An interesting experiment would be to mutate this reside to R224 (and also reciprocally mutate other NS1 proteins to harbour G224) and compare shut-off capabilities and PABPII-binding properties across the NS1 mutants.

It did not appear that the consensus F103 and M106 binding site for CPSF30 was essential for efficient shut-off, given several B-allele proteins contained Y103 and induced shut-off efficiently. An interesting question to address is whether or not B-allele NS1 proteins can bind CPSF30 without the consensus binding site (F103/M106). CPSF30 pull-downs were attempted but due to technical issues and time constraints, this question has currently not been answered. Perhaps F103 and M106 are not essential to inhibit CPSF30, or conceivably binding to PABPII is most important for efficient inhibition of 3' processing of cellular pre-mRNAs. A PR8 NS1 mutant with the F103 and M106 binding-site instated was not particularly efficient at inducing pol II shut-off in a reporter assay, but there was an improvement over WT PR8 NS1 (Fig 3.9), suggesting that CPSF30-binding is a contributor to shut-off but is not sufficient for a full-effect.

In summary, the data in this section of the study suggest that there is no obvious penalty for a mammalian-adapted virus harbouring a B-allele NS segment in terms of circumventing the mammalian innate immune response. Contrary to previous reports (Zohari et al., 2010a, Munir et al., 2011a, Munir et al., 2011b, Munir et al., 2012), these data provide evidence that any apparent restriction of B-allele viruses to avian hosts is unlikely to be a result of global deficiencies in mammalian IFN-antagonism within the B-allele lineage.

Chapter 4: *In vivo* studies with segment 8 reassortant viruses

4.1 Introduction

4.1.1 Aims

In the previous sections, A- and B- allele NS reassortant viruses were characterised *in vitro*, and it was concluded that mammalian viruses harbouring a B-allele segment 8 did not have a major replicative fitness penalty in mammalian cells, and were able to effectively circumvent and supress the innate immune response to allow efficient virus replication. In this section, the aim was to assess fitness of A- and B- allele NS reassortant viruses in the context of *in vivo* infections. It was asked whether i) a B-allele reassortant virus could replicate and cause disease *in vivo*, ii) a B-allele reassortant virus could suppress the innate immune response *in vivo,* and iii) whether there is a selection advantage for an A-allele NS segment into a mammalian-adapted virus background over a B-allele equivalent *in vivo*.

4.1.2 Hypothesis

As discussed in previous sections, there have been reports published with conflicting conclusions regarding the contribution of A- and B- allele NS genes to mammalian-virus fitness. Treanor et al concluded that introduction of a B-allele NS segment into a human H3N2 virus attenuated the virus in the squirrel monkey host (Treanor et al., 1989). However, Kim and colleagues tested PR8-based reassortant viruses with NS segments from avian H9N2 and H5N1 strains, assessed pathogenicity *in vivo* and reported different findings (Kim et al., 2015a). The B-allele PR8-based reassortant tested induced severe pathology and high mortality in BALB/c mice,

comparable to WT PR8, providing evidence against the hypothesis that B-allele NS segments attenuate IAV *in vivo*.

Given these observations, and the evidence presented in Chapters 2 and 3 that the *in vitro* fitness of an NS reassortant virus is independent of A- or B-allele lineage, it was hypothesised that a B-allele NS reassortant virus would be able to cause disease and replicate *in vivo*. Similarly, it was hypothesised that the B-allele reassortant virus would be able to supress innate immune responses as efficiently as an A-allele counterpart, and that there would not be a selection disadvantage for the B-allele NS segment *in vivo*.

4.1.3 Approach

BALB/c mice were used as a model of *in vivo* infection. To assess the ability of viruses to replicate and cause disease *in vivo*, mice were infected with WT PR8 or PR8-based reassortant viruses O175A and O265B and weighed daily while virus replication in the lung was assessed by plaque assay of lung homogenate. Lungs were fixed in formalin to allow assessment of histopathology and also virus tropism by immunohistofluorescence analysis of viral NP. The induction of the innate immune response was assessed by quantifying ISG expression by RT-qPCR from RNA extracted from lung tissue, as well as cytokine and chemokine profiling of mouse lung homogenate. Finally, *in vivo* competition assays were used to ask if there is a selection advantage for an A-allele NS segment over a B-allele equivalent during co-infections.

4.2 Results

4.2.1 Weight-loss of infected BALB/c mice

To assess the ability of NS reassortant viruses to cause disease *in vivo*, weight-loss and clinical symptoms were recorded during infection of BALB/c mice. Initially, a small-scale pilot study was performed in which groups of 4 mice were infected with either 100 PFU or 500 PFU of WT or consensus PR8-based reassortant viruses (O175A, or O265B) or mock-infected with media. Infections were administered via the intranasal route in anaesthetised mice in a 40 µl droplet. The inoculum of each virus was subsequently titrated by plaque assay to ensure equal input (data not shown). The mice were weighed at the same time each day, and any clinical symptoms were recorded. The 100 PFU study was conducted over 8 days, while the 500 PFU study was halted at day 7 post-infection for ethical reasons based on weight-loss and clinical symptoms.

Mock-infected mice did not lose weight at any time-point (Figs 4.1A & 4.1B). In both the 100 PFU and 500 PFU groups, the largest weight-loss was observed at day 7 post-infection for all viruses. PR8-infected mice lost the most weight, and O265B induced more weight-loss than O175A. WT PR8 induced significantly more weight-loss compared to mock-infected mice from day 6 onwards in the 100 PFU infection, and from day 3 onwards in the 500 PFU infection. By day 7 post-infection, mean weight-loss was 18.0% for the 100 PFU cohort, and 25.3% for the 500 PFU cohort. At day 8 post-infection, mice infected with 100 PFU showed recovery, with a mean weight-loss of 14.7%. With a 100 PFU infection, O175A-infected mice did not lose weight at any time-point, with a mean bodyweight of 101.7% starting weight at day 7

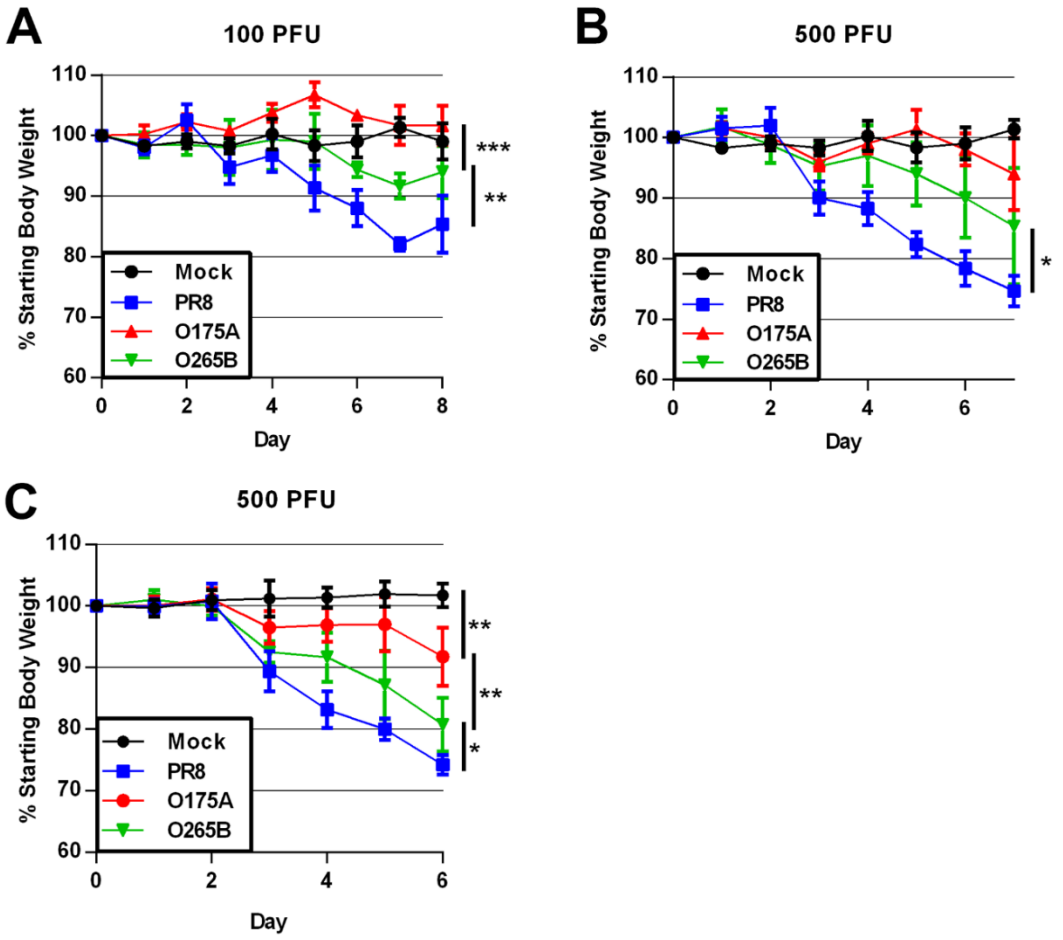

Fig 4.1. Weight-loss of infected BALB/c mice. (A + B) Pilot study. Four mice were infected with stated PFU of virus and mice were weighed at the same time each day. One mouse per cohort was euthanised at day 4 p.i. to harvest tissue. (C) As in (B) but cohort sizes at day 0 were larger (n = 15) and 5 mice were culled at each time-point of days 2, 4, and 6 p.i. * $p \leq 0.05$, ** $p \leq 0.01$, *** $p \leq 0.005$. Data are mean +/- SD.

post-infection. In the 500 PFU cohort, O175A-infected mice lost 6.0% starting weight by day 7, but this was not statistically different to the mock-infected group (unpaired *t*-test). Mice infected with 100 PFU of O265B lost a mean of 8.3% starting weight by day 7, but this was not significantly different to the mock-infected cohort (unpaired *t*-test). Mice infected with 100 PFU O265B displayed recovery at day 8 post-infection, with mean weight-loss reduced to 6.0%. Mice infected with 500 PFU of O265B lost 14.7% bodyweight by day 7 post-infection, and this was significantly more than mock-infected mice (unpaired *t*-test).

The clinical symptoms of the mice correlated with the severity of weight-loss. Mock-infected mice appeared healthy throughout the study. All infected mice in the 500 PFU cohort displayed clinical symptoms (ruffled coat, trembling, lethargy, huddling), from day 3 post-infection onwards. The severity of clinical symptoms was correlated with weight-loss, with PR8-infected mice displaying the most pronounced clinical symptoms and O175A-infected mice the least so. The 100 PFU groups had less severe clinical symptoms. The PR8- and O265B-infected mice showed only mild clinical symptoms (ruffled coat, mild lethargy), whereas O175A-infected mice did not show any clinical signs of infection (data not shown).

Using the pilot studies as a reference, it was decided to repeat the study on a larger scale using a 500 PFU dose, as this amount of inoculum resulted in the most significant weight-loss differences between the cohorts. Groups of 15 BALB/c mice were infected with 500 PFU of PR8, O175A or O265B, or mock-infected with media, in the same manner as in the pilot study described above. At days 2, 4 and 6 post-infection, 5 mice were culled per cohort and lung tissue collected for downstream analyses. All experiments described from this point onwards are from this study.

Mock-infected mice did not lose weight at any point during the study (Fig 4.1C), and did not show any clinical symptoms at any stage (data not shown). All virus-infected mice lost weight from day 3 post-infection onwards. At day 4 post-infection, mean weight-loss was 16.9%, 3.1% and 8.4% starting weight for PR8-, O175A and O265B-infected mice respectively (n = 10). By day 6 post-infection, PR8 induced a mean weight-loss of 25.8%, O175A induced 8.2% weight-loss and O265B-infected mice lost 19.3% initial starting weight (n = 5). All differences in weight-loss between groups were statistically significant from day 3 post-infection onwards, except in the O175A group which was not significantly different to mock-infected mice at day 5 post-infection (unpaired *t*-test). As in the pilot study, the severity of clinical symptoms correlated with weight-loss, with the WT PR8-infected mice displaying the most severe clinical symptoms (ruffled coat, shivering, lethargy, huddling) from day 4 post-infection onwards (data not shown).

Thus the introduction of an avian segment 8, from either the A- and B- allele lineages, into the PR8 backbone reduced pathogenicity in mice relative to the WT. Interestingly, O265B induced greater weight-loss than O175A in all studies performed. These data suggest that a mammalian-adapted virus harbouring an avian B-allele NS segment can cause disease in a mammalian host, and to a greater extent than an avian virus-derived A-allele counterpart.

4.2.2 Virus replication in the lungs of infected BALB/c mice

Next, replicative fitness of the NS reassortant viruses was analysed by titrating infectious virus in the lung by plaque assay. The left lung was removed from 5 euthanised mice at days 2 and 6 post-infection. The tissue was homogenised, clarified by centrifugation, and infectious virus titrated by plaque assay on MDCK cells.

At both day 2 and 6 post-infection, mock-infected mouse lung homogenate contained undetectable levels of infectious virus (limit of detection 2.5 PFU/ml). At day 2 post-infection, the three viruses replicated to high titres, and there were no statistically significant differences between the groups (n = 5, unpaired *t*-test) (Fig 4.2). WT PR8 replicated to a mean titre of 1.85 x 10^6 PFU/ml, which was approximately 2-fold higher than mean titres achieved by O175A (6.25 x 10^5 PFU/ml) and O265B (6.40 x 10^5 PFU/ml). At day 6 post-infection, all groups displayed a reduction in virus titre. WT PR8 had the most infectious virus in the lung, with a mean titre of 2.95 x 10^5 PFU/ml, and this was statistically significantly different from both O175A and O265B titres (n = 5, unpaired *t*-test). O265B had a statistically significant higher virus titre than O175A at day 6 post-infection, with a mean titre of 7.45 x 10^4 PFU/ml in comparison to O175A's mean titre of 2.26 x 10^4 PFU/ml (n = 5, student's *t*-test).

Therefore, WT PR8 was the most fit in the BALB/c mouse host, followed by O265B, with O175A the least fit. These data suggest that a mammalian-adapted virus harbouring an avian B-allele NS segment can replicate to high virus titre *in vivo*, and can persist longer than an A-allele counterpart.

4.2.3 Histopathology in infected mouse lung

To compare and contrast the severity of tissue damage and inflammation induced by infection of NS reassortant viruses, histopathology in the lungs of infected mice was assessed at day 6 post-infection. The right lungs of infected BALB/c mice were fixed with a neutral buffered formalin solution, and sections were processed and stained with haematoxylin and eosin (by the Easter Bush Pathology Laboratory) to allow assessment of induced histopathology using light microscopy. Samples from the day 6 post-infection cohort were imaged and assessed blind by a clinical pathologist

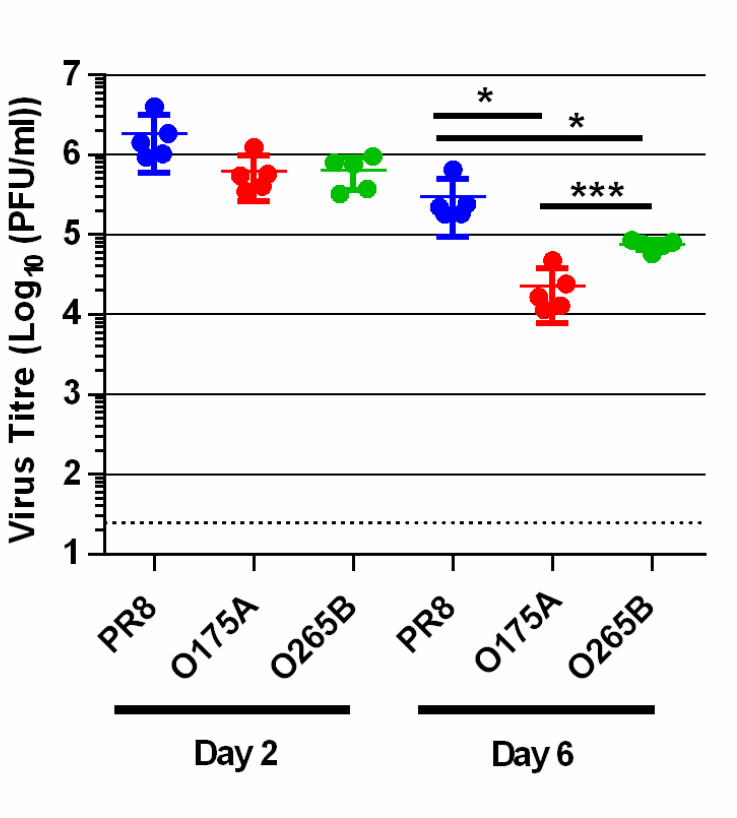

Fig 4.2. Virus titre in infected mouse lung. Groups of 5 BALB/c mice were infected with 500 PFU of virus, or mock-infected with media. The left lung of each euthanised mouse was removed and frozen at indicated time-points. Lung homogenates were generated in serum-free media and virus titre was calculated using plaque assay. Data are mean +/- SD. * $p \leq 0.05$ and *** $p \leq 0.001$.

(Dr. Philippa Beard, The Roslin Institute, The University of Edinburgh, UK). The following description was written by Dr. Philippa Beard:

'All three viruses caused lesions consistent with IAV infection, characterised by mild to marked, subacute, multifocal, nonsuppurative, bronchointerstitial pneumonia with necrosis and fibrin accumulation. Degeneration and necrosis of epithelial cells lining the airways, accompanied by peribronchiolar, peribronchial, and perivascular inflammation, was a consistent feature (Fig 4.3A). The inflammatory infiltrate was predominantly lymphocytic and histiocytic with variable numbers of neutrophils'.

An 'overall' score was assigned to blinded samples (0 representing lack of evidence of infection, and 1-3 increasing severity levels in ascending order). All mock-infected samples were assigned 0 during the blind scoring process, and no obvious difference in scoring was noted between virus-infected samples (Fig 4.3B). PR8 was assigned a mean score of 2.0, and O175A and O265B were both assigned a mean score of 2.1 (Fig 4.3B).

Therefore the introduction of an avian NS segment, from both A- and B-allele lineages, into the PR8 backbone did not notably affect lung pathology *in vivo,* despite differences noted in weight-loss and clinical symptoms across the different viruses.

4.2.4 Virus tropism in the lungs of infected mice

To assess virus tropism within the lungs of infected BALB/c mice, lung sections obtained from days 2, 4 and 6 post-infection were immunostained for intracellular NP. Unstained sections (processed by the Easter Bush Pathology Laboratory) were deparaffinised, permeabilised, and immunofluorescent staining of

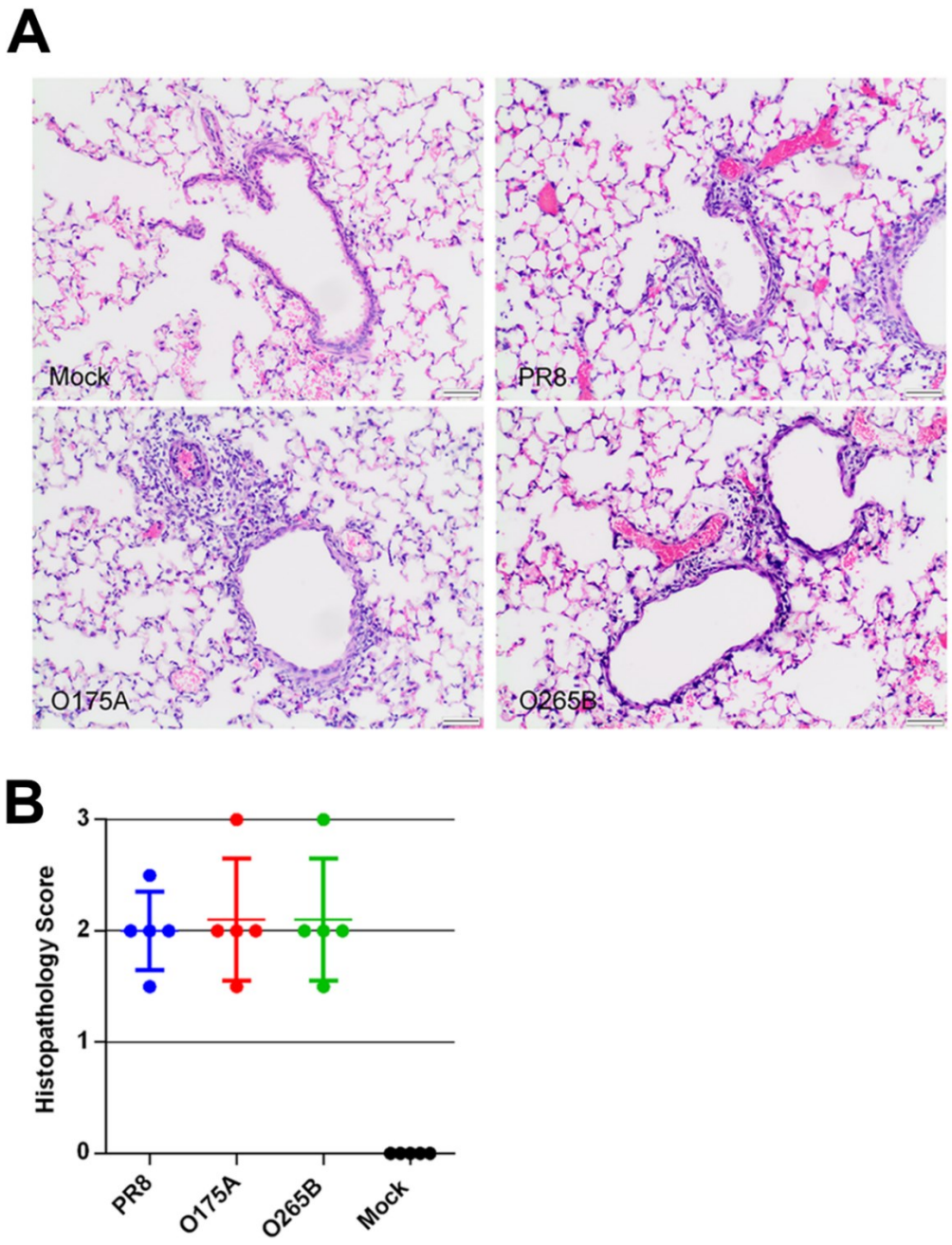

Fig 4.3. Histopathology in infected mouse lung. (A) At day 6 p.i., the right lung lobes of inoculated mice were collected, fixed, processed, and stained with haematoxylin and eosin. Mock-infected mice showed no significant changes, whereas infected mice showed degeneration and necrosis of epithelial cells lining airways with peribronchiolar and perivascular inflammation, and interstitial inflammation sometimes accompanied by necrosis and fibrin accumulation. The inflammatory infiltrate was predominately lymphocytes and macrophages with variable numbers of neutrophils. Scale bars are 50 µm. (B). Severity of pathology in the lung was assessed blind and an overall pathology score out of 3 was assigned. Data are mean +/- SD (n = 5). (Images shown in (A) were taken by Dr. Philippa Beard and the accompanying figure legend was also written by Dr. Beard).

intracellular viral NP and DAPI staining of cell nuclei was performed. Sections were imaged using confocal microscopy. Background levels of fluorescence were determined by including 'primary antibody only' and 'secondary antibody only' stained samples of PR8-infected lung sections (data not shown).

Mock-infected samples did not display viral NP staining above background levels at any time-point (Fig 4.4). In general, and at all time-points tested, intracellular viral NP from PR8, O175A and O265B was mostly localised to the epithelium of mouse lung airways, although there was also interstitial tissue staining observed in all virus-infected samples (Fig 4.4). The number of infected epithelia per section appeared to correlate with the virus titre data. PR8 appeared to infect more epithelia per section than the avian segment 8 reassortant viruses at each time-point tested when sections were manually inspected by epi-fluorescent microscopy (data not shown). Mean PR8 titres were approximately 2-fold greater at day 2 post-infection than O265B and O175A, and 3-fold greater by day 6 post-infection (Fig 4.2). The number of epithelia per section infected with O175A and O265B were similar at each time-point (data not shown). Similarly, the level of interstitial staining across whole sections appeared to be greater in PR8-infected mice, but more comparable between O175A- and O265B-infected mice (data not shown).

Overall, the cell tropism of the consensus viruses appeared similar in the lungs of infected BALB/c mice at all time-points tested, although the amount of viral staining looked to be greatest in PR8-infected mice. These data suggest that the source of segment 8 does not notably alter the cell type and location of infection, although the number of infected cells unsurprisingly correlated with lung titres.

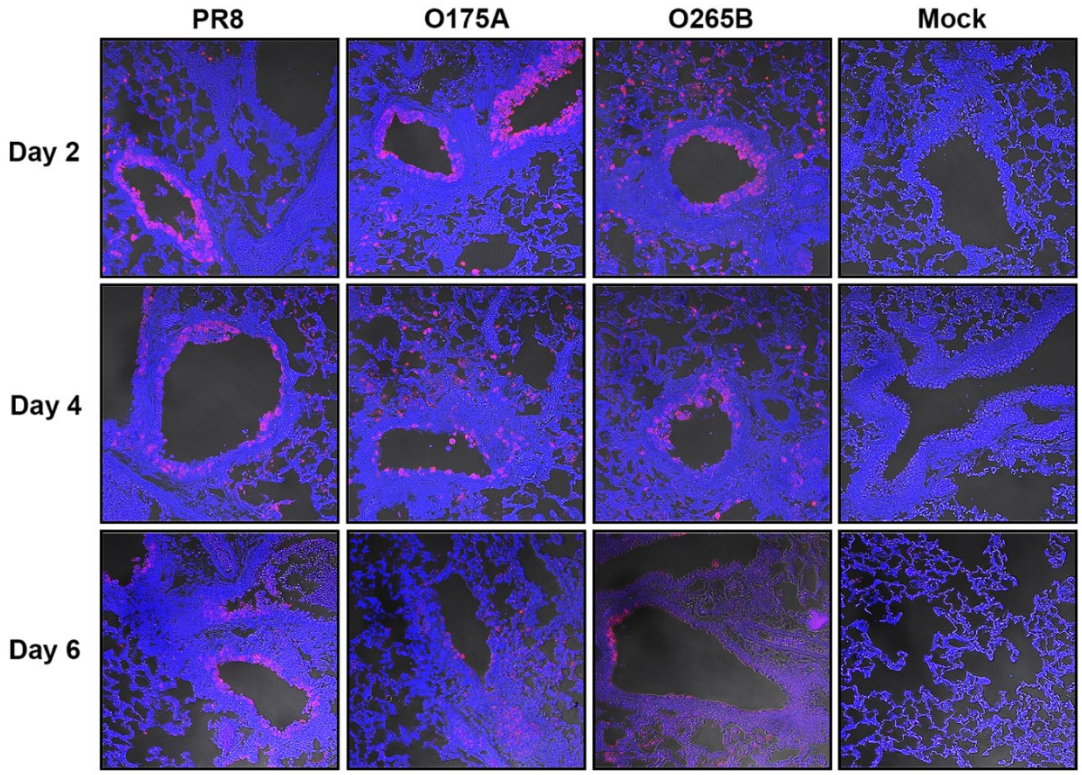

Fig 4.4. Virus tropism in infected mouse lung. The lungs of infected mice were fixed, sectioned, and immunostained for intracellular viral NP (red) and DNA (blue) at days 2, 4 and 6 post-infection. Images were taken by laser scanning confocal microscopy and differential interference contrast microscopy at 63x magnification using a tiling function on Ziess LSM710 software. Day 6 images were imaged and processed separately to days 2 and 4.

4.2.5 Antiviral gene expression in infected mouse-lung

In Chapter 3, the ability of NS reassortant viruses to circumvent and block the mammalian innate immune response *in vitro* was assessed. Here, similar assessments were performed for *in vivo* infections. An array of transcripts for cellular genes including cytokines and antiviral restriction factors (see Table 4.1) were quantified by RT-qPCR of RNA extracted from the lung at day 4 post-infection, to analyse the induction of the innate immune response. RNA from the tip of the right-lung of infected mice was extracted from 3 mice per cohort at day 4 post-infection. RNA was extracted from 50-80 mg of tissue and 25ng of RNA was used in a reverse transcription reaction using random hexamer primers. cDNA was loaded onto Taqman custom-designed qPCR array plates (designed by Dr. Brett Jagger, National Institute of Allergy and Infectious Diseases, Bethesda, Maryland, USA. See Table 4.1 for individual assays) and cycling threshold (CT) values were obtained. Each gene transcript was tested in triplicate per mouse, and the mean CT of this was normalised to the mean CT value of the GAPDH control (dCT). The mean dCT value for the three mice was plotted as 20 – dCT. Under PCR conditions of 100% efficiency, twice the amount of product results in an increase in the 20 – dCT value by 1.

The house-keeping control gene transcripts (18S, Gapdh, Hprt1, Gusb) were all detected at similar quantities in the 3 mice assessed per cohort, with no statistically significant differences noted by unpaired *t*-test (n = 3) (Fig 4.5). Overall, the majority of ISG transcripts quantified were up-regulated in all virus-infected samples relative to mock-infected mice. The transcript profiles were generally quite similar across the viruses tested, although there was a tendency for ISG transcripts to be detected at highest levels in PR8-infected mice, with higher levels in O265B than O175A-infected

Table 4.1. Individual cellular transcript assays for mouse RT-qPCR array. Individual RT-qPCR assays are available online (www.lifetechnologies.com).

Cellular Transcript	Taqman® Assay ID
18S	Hs99999901_s1
Gapdh	Mm99999915_g1
Hprt1	Mm00446968_m1
Gusb	Mm00446953_m1
Ifna2	Mm00833961_s1
Ifna4	Mm00833969_s1
Ifnb1	Mm00439546_s1
Igng	Mm00801778_m1
Il28b	Mm00663660_g1
Tnf	Mm00443259_g1
Tnfsf10	Mm00437174_m1
Il1b	Mm01336189_m1
Il6	Mm00446190_m1
Il10	Mm00439615_g1
Il17b	Mm00444686_m1
Cxcl1	Mm00433859_m1
Cxcl10	Mm00445235_m1
Ccl2	Mm00441242_m1
Ccl3	Mm00441259_g1
Ccl4	Mm00443111_m1
Csf1	Mm00432686_m1
Csf3	Mm00438335_g1
Ifit1	Mm00515153_m1
Ifit3	Mm01704846_s1
Ifih1	Mm00459183_m1
Irf7	Mm00516788_m1
Isg15	Mm01705338_s1
Oas1b	Mm00449297_m1
Mx1	Mm01217998_m1
Ddx58	Mm00554529_m1
Fasl	Mm00438864_m1
Stat1	Mm00439531_m1

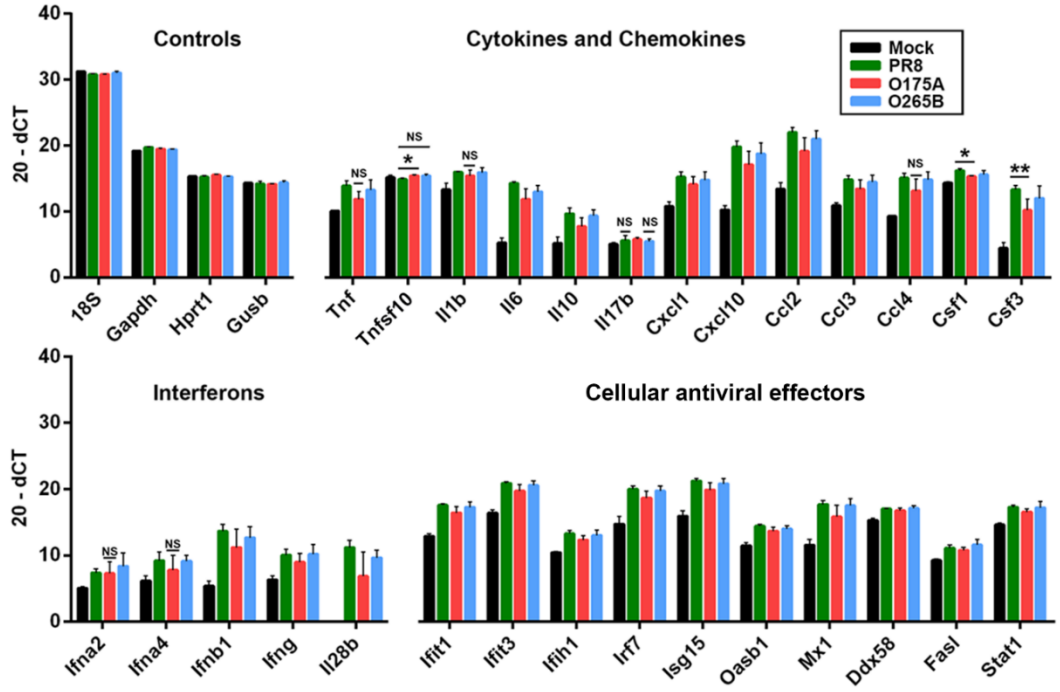

Fig 4.5. Antiviral gene expression in infected mouse lung. RNA was extracted from lungs of infected mice at day 4 p.i. and levels of various cytokines, chemokines, and antiviral gene expression were quantified using RT-qPCR. Assays were run on RNA from three separate mice per cohort and each assay was performed in triplicate. Data are plotted as mean (20- dCT) +/- SD. All infected samples were significantly different from the mock-infected sample, unless labelled with 'NS' which indicates no significant difference. * $p \leq 0.05$; ** $p \leq 0.01$.

mice. This pattern correlated with severity of weight-loss (Fig 4.1C). The majority of ISG transcripts quantified were statistically significantly up-regulated in virus-infected samples relative to mock-infected, except tumour necrosis factor (ligand) superfamily member 10 (Tnfsf10), an inducer of apoptosis, which was not significantly different to mock-infected in any of the virus-infected samples. TNF-α (Tnf), IL-1β (Il1b), chemokine (C-C motif) ligand 4 (Ccl4), IFN-α-2 (Ifna2) and IFN-α-4 (Ifna4), all pro-inflammatory mediators, were not significantly up- or down-regulated in O175A-infected samples in comparison to mock-infected mice. IL-17b (Il17b), a pro-inflammatory cytokine, was not significantly up- or down-regulated in PR8- or O265B-infected samples, but was significantly upregulated, albeit very modestly, in O175A-infected samples. All other gene transcripts were significantly up-regulated in all virus-infected samples relative to mock-infected. There were no transcripts significantly differentially regulated between O175A and O265B, nor between PR8 and O265B. The only statistically significant differences in transcript levels between virus-infected samples were Tnfsf10, colony stimulating factor 1 (Csf1) and colony stimulating factor 3 (Csf3)/granulocyte stimulating factor (G-CSF), which were all significantly different between PR8 and O175A samples. Tnfsf10 transcripts were detected at higher levels in O175A-samples whilst Csf1 and Csf3 transcripts, both predominantly pro-inflammatory cytokines, were both higher in PR8-infected mice (Fig 4.5).

While there were not many statistically significant differences in transcript levels between the virus-infected samples, the general pattern, barring certain exceptions, was for ISG transcripts to be detected at highest abundance in PR8-infected mice, and at higher abundance in O265B samples in comparison to O175A.

These included pro-inflammatory cytokines such as TNF-α (Tnf), IL-1β (Il1b) and CXCL10 (cxcl10), interferons IFN-β (ifnb1) and IFN-λ (Il28b), and antiviral restriction factors such as IFIT1 (Ifit1) and Mda5 (Ifih1). Notably, despite the fact PR8 induced the largest expression of antiviral transcripts during infection, PR8 actually replicated to the highest viral titres in the lungs of mice (Fig 4.2).

Overall, there was not an obvious up-regulation of host antiviral gene transcripts during a B-allele virus infection of a mammalian host *in vivo*. Thus, these results do not support the hypothesis that B-allele viruses elicit an exaggerated antiviral response in mammals which may lead to restriction in these hosts.

4.2.6 Cytokine and chemokine profiling of infected mouse lung

To follow on from the above experiment quantifying ISG transcripts in the lungs of mice, a cytokine and chemokine array was to ask whether a B-allele NS reassortant virus would elicit and exaggerated inflammatory response *in vivo*, at the protein level, in comparison to an A-allele counterpart. In Chapter 3, cytokine and chemokine profiling of infected human $CD14^+$ monocyte-derived macrophages was performed, and it was concluded that PR8 induced a larger pro-inflammatory response than either O175A or O265B, which both had comparable profiles (Fig 3.4B). Alveolar macrophages (AMs) are among the first immune cells to respond to viral infection and have been shown to be essential for efficient virus control (Tumpey et al., 2005, Kim et al., 2008, Tate et al., 2010). AMs are the primary producers of type I IFN and pro-inflammatory cytokines in response to virus infection in the lung (Kumagai et al., 2007), and so cytokine profiling of the lung will provide an idea of the extent of AM activation during infection with NS reassortant viruses.

The lung homogenates of five mice from day 4 post-infection were pooled and were used in a cytokine and chemokine immunoblot array as described in the previous chapter (see *3.2.4 Cytokine and chemokine secretion following infection of primary human macrophages with segment 8 reassortant viruses*). The mean intensity of duplicate spots was normalised to the mock-infected sample, and mean fold-induction values were ranked in descending order of relative abundance in the PR8 sample and plotted as a heat-map (Fig 4.6). Table 4.2 provides information on the roles of each cytokine and chemokine quantified, the mean fold-change values, and defines abbreviations.

The majority of the cytokines assayed were up-regulated in mice infected with all three viruses, and of these, most have pro-inflammatory functions (Fig 4.6 and Table 4.2). Cxcl10, Ccl3 and Ccl2, all chemotactic for inflammatory cells, were strongly up-regulated in all virus-infected samples. However, TIMP-1 and IL-1ra, both with anti-inflammatory roles, were also highly up-regulated in all cases. Certain cytokines were not strongly up- or down-regulated, such as chemokine Ccl17, a chemotactic for T-cells, IL-7, required for B- and T-lymphocyte development, and IL-13, an anti-inflammatory chemokine, which were all within a 2-fold range relative to mock-infected samples. In no cases was a cytokine detected as being down-regulated more than 2-fold relative to the mock-infected control.

A clear trend in the data was that PR8-infected mice produced a larger amount of cytokines, the majority pro-inflammatory, than either O175A or O265B. Indeed, all

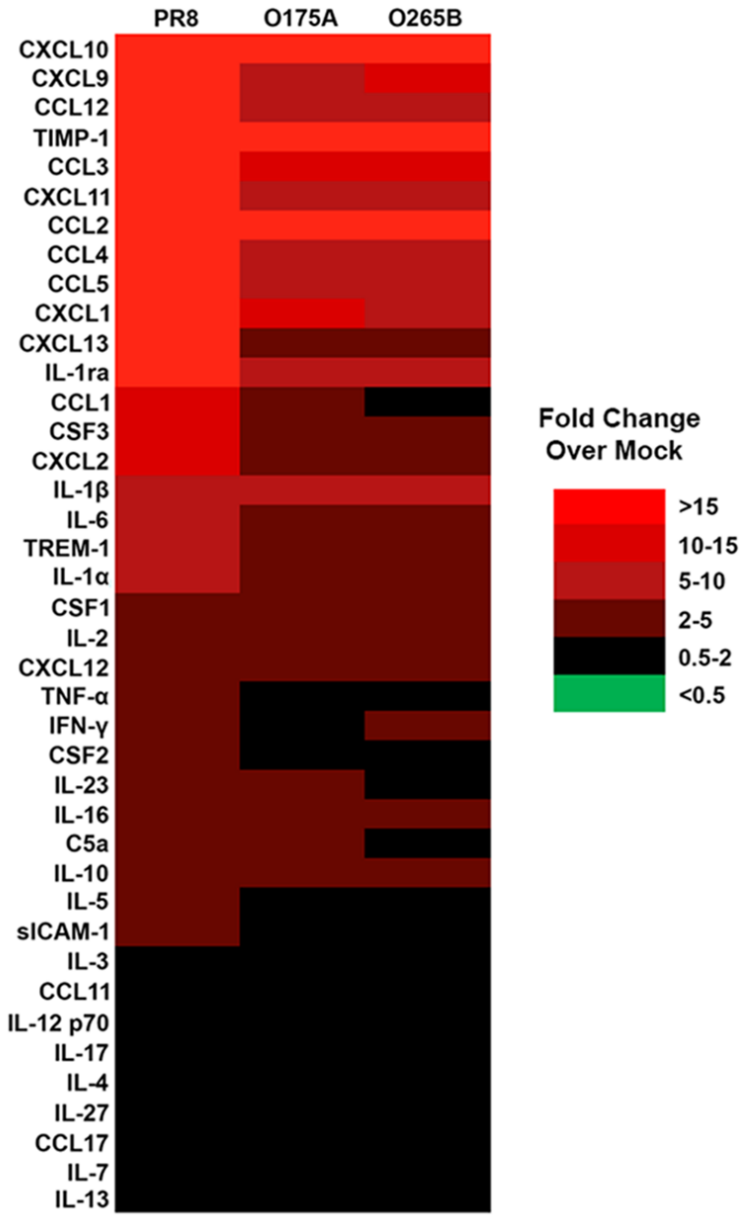

Fig 4.6. Cytokine and chemokine profiling of infected mouse lung. The levels of various cytokines and chemokines in pooled lung homogenates from groups of 5 mice culled at day 4 p.i. were determined using an immunoblot spot array. Values are represent mean fold-induction relative to mock-infected (n = 2) and are plotted as a heat map. Values were ranked in descending order of relative abundance from the PR8 sample.

Table 4.2. Cytokine and chemokine profiling of infected mouse lung. Cytokines and chemokines were quantified from pooled lung homogenate of five BALB/c mice. The fold-change values represent the abundance of protein relative to the mock-infected sample. A brief description of the main role(s) of each cytokine and chemokine is provided.

Cytokine/ chemokine	Alternative name	Function	Fold-change PR8	Fold-change O175A	Fold-change O265B	Reference
Cxcl10 (chemokine (C-X-C motif) ligand 10)	IFN-γ-induced protein 10,IP-10)	Chemotactic for monocytes, macrophages, NK cells, T-cells, and dendritic cells. Secretion is stimulated by IFN-γ and also pro-inflammatory cytokines. Important for RSV clearance in mice.	170.1	74.6	63.9	(Lindell et al., 2008)
Cxcl9	MIG (monokine induced by gamma interferon).	Strongly induced during infection and inflammatory responses by pro-inflammatory cytokines, principally IFN-γ. Chemoattractant for activated T-cells and NK cells.	52.4	9.9	14.1	(Muller et al., 2010)
Ccl12 (chemokine (C-C motif) ligand 12)	MCP-5 (monocyte chemotactic protein 5)	Chemotactic for peripheral blood monocytes to sites of inflammation.	48.7	8.7	9.3	(Sarafi et al., 1997)
TIMP-1 (Tissue inhibitors of metalloproteinases-1)	-	Anti-inflammatory roles by inhibiting matrix metalloproteases, which contribute to the inflammatory response.	41.8	38.7	25.0	(Lee et al., 2005)
Ccl3	MIP-1α (macrophage inflammatory protein)	Pro-inflammatory roles. Chemotactic for and activator of macrophages and $CD8^+$ T-cells.	39.8	10.7	13.0	(Trifilo et al., 2003)

Cytokine/ chemokine	Alternative name	Function	Fold-change PR8	Fold-change O175A	Fold-change O265B	Reference
Cxcl11	I-TAC; IP-9	Chemotactic for activated T-cells.	33.8	5.6	6.3	(Widney et al., 2000)
Ccl2	Monocyte chemoattractant protein 1 (MCP-1); JE	Chemotactic for monocytes, memory T-cells NK cells to sites of inflammation.	32.1	24.2	19.3	(Deshmane et al., 2009)
Ccl4	MIP-1β (macrophage inflammatory protein 1β)	Chemotactic for a variety of immune cells. Pro-inflammatory.	27.0	6.2	7.6	(Menten et al., 2002)
Ccl5	RANTES (Regulated on Activation Normal T Cell Expressed and Secreted)	Chemotactic for several immune cell populations at inflammatory sites. Activator of NK cells. Important for anti-apoptotic signalling of alveolar macrophages during clearance of influenza-infected apoptotic cells.	25.9	6.9	8.3	(Tyner et al., 2005)
Cxcl1	KC	Pro-inflammatory chemokine. Neutrophil chemotactic activity.	21.8	10.4	7.5	(Rubio and Sanz-Rodriguez, 2007)
Cxcl13	BLC (B lymphocyte chemoattractant)	Important for B cell development by recruiting naïve B-cells and follicular T-cells to lymphoid follicles.	19.6	3.5	2.8	(Luther et al., 2000)

Cytokine/ chemokine	Alternative name	Function	Fold-change PR8	Fold-change O175A	Fold-change O265B	Reference
IL-1ra (interleukin-1 receptor antagonist)	-	Anti-inflammatory cytokine. Antagonistic functions with the IL-1 receptor. Therefore inhibits of IL-1α and of IL-1β. Loss of IL-1ra leads to uncontrolled systemic inflammation and polyarthropathy.	15.2	6.1	6.9	(Horai et al., 2000)
Ccl1	I-309	Pro-inflammatory chemokine. Chemotactic for monocytes and T-cells.	13.9	2.1	1.9	(Miller and Krangel, 1992)
CSF3 (colony stimulating factor 3)	G-CSF (Granulocyte colony-stimulating factor).	Stimulates bone marrow stem cells to differentiate into granulocytes. Stimulates growth, proliferation and differentiation of neutrophils.	11.9	4.3	3.4	(Bendall and Bradstock, 2014)
Cxcl2	MIP-2α (macrophage inflammatory protein 2α) and GRO-β (growth related oncogene-β.	Pro-inflammatory chemokine. Chemoattractant of neutrophils.	10.5	4.7	4.9	(Wolpe et al., 1989)

Cytokine/ chemokine	Alternative name	Function	Fold-change PR8	Fold-change O175A	Fold-change O265B	Reference
IL-1β (interleukin-1β)	IL-1F2; catabolin	Pro-inflammatory interleukin produced following activation of the nucleotide-binding oligomerization domain (NOD)-like receptor family pyrin domain-containing 3 (NLRP3) inflammasome, which is activated by IAV M2 protein. Contributes to lung tissue damage during IAV infection.	9.6	7.1	6.3	(Ichinohe et al., 2010, Kim et al., 2015b)
IL-6	-	Pro-inflammatory cytokine secreted by T-cells and macrophages. Important mediator of fever and acute phase response. Essential for effective clearance of H1N1 IAV in mice.	9.5	2.3	2.7	(Dienz et al., 2012)
TREM-1 (triggering receptor expressed on myeloid cells)		Immunoglobulin receptor. Activates activation of neutrophils, monocytes and macrophages. Initiates secretion of pro-inflammatory cytokines during infection.	9.3	3.7	3.5	(Colonna and Facchetti, 2003)
IL-1α	-	Pro-inflammatory interleukin. Acts as an 'alarmin' to initiate the release of various pro-inflammatory cytokines and chemokines in acute inflammation.	5.8	3.3	2.9	(Garlanda et al., 2013)
CSF1 (macrophage colony stimulating factor 1)		Regulates the differentiation, chemotaxis and survival of monocytes and macrophages.	4.9	2.6	2.7	(Hamilton, 2008)

Cytokine/ chemokine	Alternative name	Function	Fold-change PR8	Fold-change O175A	Fold-change O265B	Reference
IL-2	-	Important for growth, proliferation and differentiation of T-cells and required for T-cell immunological memory. Also promotes proliferation of B cells and NK cells.	4.7	3.2	2.3	(Gaffen and Liu, 2004)
Cxcl12	SDF-1 (stromal cell-derived factor 1)	Chemotactic for leukocytes and up-regulated in inflammatory response. Required for $CD8^+$ T-cell recruitment during IAV infection.	4.4	2.2	2.2	(Lim et al., 2015)
TNF-α (Tumour Necrosis Factor α)	-	Pro-inflammatory roles. Mediator of fever and acute phase response. Antiviral properties by activating NF-κB pathway and inducing apoptosis. Correlated with lung tissue damage in HPAI infections.	3.7	1.5	1.5	(To et al., 2016, Lee et al., 2009b, Cheung et al., 2002)
IFN-γ (interferon gamma)	-	Type II IFN. Major macrophage activation roles. Chemoattractant of leukocytes, enhances NK cell activity, regulates B-cell functions.	3.3	1.3	2.2	(Schroder et al., 2004)
CSF2	GM-CSF (Granulocyte-macrophage colony stimulating factor).	Stimulates bone marrow stem cells to differentiate into granulocytes and monocytes.	3.3	1.6	1.2	(Shi et al., 2006)
IL-23	-	Pro-inflammatory cytokine. Stimulates type 17 helper T-cell response.	3.1	2.3	1.7	(Teng et al., 2015)
IL-16 (interleukin-16)	-	Pro-inflammatory cytokine. Chemoattractant for $CD4^+$ T-cells, monocytes, eosinophils and dendritic cells. Regulates $CD4^+$ T-cell development.	2.9	2.1	2.1	(Amiel et al., 1999)

Cytokine/ chemokine	Alternative name	Function	Fold-change PR8	Fold-change O175A	Fold-change O265B	Reference
C5a (complement component 5a)	-	Part of the complement system with multiple roles. Inflammatory peptide upregulating NF-κB and IL-1 in alveolar macrophages in lung injury.	2.9	2.1	1.4	(Guo and Ward, 2005)
IL-10	Human cytokine synthesis inhibitory factor.	Anti-inflammatory cytokine. Helps protect epithelial cell layers. Regulates production of pro-inflammatory cytokines such as TNF-α.	2.8	2.2	2.0	(Ouyang et al., 2011)
IL-5	-	Essential for eosinophil maturation and recruitment to infected airway during IAV infection and recovery phase.	2.4	1.6	1.3	(Gorski et al., 2013)
sICAM-1 (soluble intercellular adhesion molecule 1)	CD54; Cluster of Differentiation 54.	Adhesion molecule and activator of T-cells.	2.2	1.7	1.4	(Kuhlman et al., 1991)
IL-3		Produced by T cells. Works in conjunction with GM-CSF and IL-5 to activate a wide range of myeloid cells. Involved in mast cell and basophil production and activation.	1.9	1.2	1.0	(Broughton et al., 2012)
Ccl11	Eosinophil chemotactic protein/Eotaxin		1.9	1.4	1.1	(Rothenberg, 1999)

Cytokine/ chemokine	Alternative name	Function	Fold-change PR8	Fold-change O175A	Fold-change O265B	Reference
IL-12	p70	Pro-inflammatory cytokine. Stimulates differentiation of T-cells into IFN-γ producing class 1 helper T-cells.	1.8	1.2	1.6	(Teng et al., 2015)
IL-17	-	Pro-inflammatory cytokine produced by type 17 helper T-cells. Stimulates pro-inflammatory cytokine release and therefore recruits macrophages and neutrophils to sites of inflammation.	1.7	1.5	1.5	(Jin and Dong, 2013)
IL-4	-	Induces differentiation of naïve helper T-cells into type 2 helper T cells. Multifunctional roles in regulating macrophages and lymphocytes.	1.6	1.2	1.4	(Luzina et al., 2012)
IL-27	-	Anti-inflammatory cytokine. Suppressor of helper T cell responses and limits inflammation.	1.6	1.6	1.3	(Kastelein et al., 2007)
Ccl17	TARC (thymus and activation regulated chemokine)	Pro-inflammatory chemokine. Chemotactic for type II helper T-cells.	1.4	1.2	1.0	(Vestergaard et al., 2004)
IL-7		Essential for both B- and T-lymphocyte development.	1.0	0.6	0.7	(Hong et al., 2012)
IL-13	-	Anti-inflammatory cytokine. Inhibits pro-inflammatory cytokine production in airway disease and allergic inflammation.	0.9	0.9	1.2	(Wynn, 2003)

cytokines quantified, except IL-13 and Il-27 which are both anti-inflammatory cytokines, were found to be more up-regulated in PR8-infected mice than O175A- or O265B-infected mice. For example, Cxcl10 was up-regulated by a mean of 170.1-fold in PR8-infected mice relative to mock-infected mice, compared to 74.6- and 63.9-fold in O175A and O265B samples respectively. The profiles of O175A and O265B were much more comparable, and all cytokines were quantified within a 2-fold range between these two samples. While the RT-qPCR data described above showed that PR8-infected mice had the largest up-regulation of pro-inflammatory cytokine transcripts, the trend that transcripts were more abundant in O265B-infected mice compared to O175A-infected mice was not necessarily translated to increased cytokine profiling in this experiment (Figs 4.5 and 4.6). For example, the RT-qPCR data suggested there was more Cxcl10 transcripts in O265B-infected mice, but there was more Cxcl10 protein detected in O175A-infected lung homogenates.

Overall, these data show that WT PR8 infection stimulated a more pronounced inflammatory response in the lung than either O175A or O265B, which both had similar cytokine profiles. This demonstrates that the source of segment 8 influences the inflammatory response *in vivo*, but the lineage of avian NS segment is not crucial.

4.2.7 *In vivo* competition assays

In this experiment, mice were co-infected with O175A and O265B and a competition assay was employed to ask if an A-allele NS segment had a selection advantage in a mammalian-adapted virus backbone over a B-allele counterpart *in vivo*. Five BALB/c mice were infected with 250 PFU each of O175A and O265B. At day 6 post-infection, the left lung of each mouse was harvested. The lung was homogenised in 1.5 ml serum-free D-MEM, and subjected to plaque assay under an agarose overlay.

12 plaques per homogenate were purified and assayed by RT-PCR as described in Chapter 2 (see *2.2.9 Competition assays*)

When competition assays were performed across 5 individual mice, four of the five mice displayed a favourable score for O265B over O175A (Fig 4.7). In one mouse lung, all 12 plaques were O265B positive only. In the mouse lung in which O175A was most prevalent, O175A was present in 83% of plaques. The mean score, over all the mice tested, was 34% O175A compared with 66% O265B. Therefore, there was no evidence to suggest there was even a subtle replication advantage for O175A over O265B *in vivo*. This data complements the *in vitro* competition data, described in Chapter 2, which showed a similar trend.

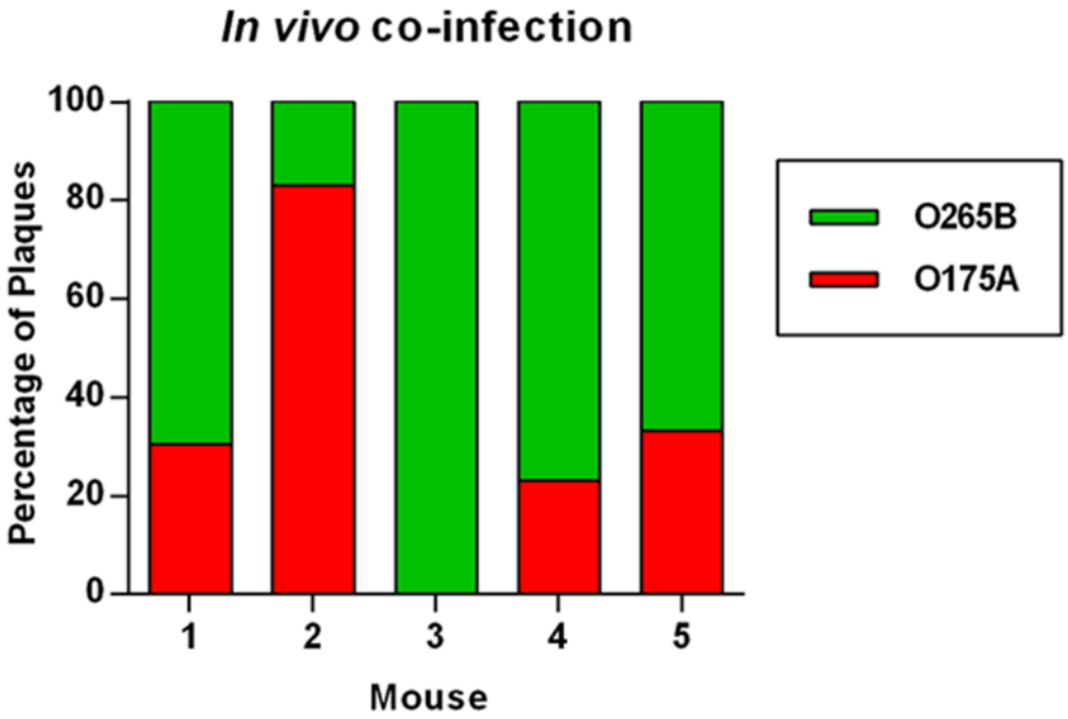

Fig 4.7. *In vivo* co-infections. 5 BALB/c mice were co-infected with 250 PFU each of O175A and O265B. At day 6 p.i., the left lung of each mouse was harvested and the proportion of each virus in the lung homogenate was determined by plaque purification of 12 plaques and RT-PCR.

4.3 Discussion

In this section, PR8-based NS reassortant viruses were characterised in the BALB/c mouse host to ask whether incorporation of an avian B-allele NS segment into a mammalian IAV strain would incur a fitness penalty in a mammalian host *in vivo*, which might explain an apparent avian-restriction of these genes in nature. In Chapters 2 and 3, it was concluded that B-allele reassortant viruses were replication competent in mammalian cells *in vitro*, and were able to circumvent and suppress the innate immune response as efficiently as A-allele counterpart viruses. *In vivo* infections, however, present a much more varied cellular environment, and are therefore important to validate conclusions drawn from *in vitro* work. WT PR8, as well as consensus PR8-based reassortant viruses, O175A and O265B, were used in infections of BALB/c mice to ask whether a B-allele virus could cause disease and replicate *in vivo*, as well as suppress innate immune responses, in comparison to an A-allele equivalent. Co-infection studies were also performed to ask if there was a selection advantage for an A-allele NS segment over a B-allele NS segment into a mammalian-adapted virus *in vivo*.

Notably, the consensus North American B-allele NS reassortant virus, O265B, was more pathogenic *in vivo*, inducing more weight-loss than the A-allele counterpart, O175A, whilst the WT PR8 was undoubtedly the most pathogenic (Figs 4.1A, 4.1B and 4.1C). These findings are important as they suggest that, in the rare case of an avian B-allele virus spill-over event into a mammalian host, significant pathology could ensue. Indeed, B-allele viruses persist and cause high pathogenic infections of poultry populations (Garcia et al., 1997, Suarez et al., 1999), and it is well documented that HPAI can cause high mortality in humans, usually following direct contact with

infected poultry (Chan, 2002). Furthermore, a highly pathogenic avian-like B-allele virus (A/equine/Jilin/1/1989 (H3N8)) caused widespread, high-mortality outbreaks in equine populations, providing direct evidence of a B-allele avian-like virus causing serious disease in a mammalian host (Guo et al., 1992). In a separate laboratory study assessing PR8-based NS reassortants, Kim and colleagues found that PR8 harbouring a B-allele NS gene from a LPAI H5N1 virus (A/wild duck/Korea/SNU50-5/2011 (H5N1)) induced significant pathology in BALB/c mice (Kim et al., 2015a). This was to similar levels as one counterpart A-allele reassortant (NS from A/chicken/Korea/01310/2001 (H9N2)), and significantly greater than a separate A-allele reassortant (NS from A/chicken/Korea/KBNP-0028/2000 (H9N2)) which did not induce any pathology (Kim et al., 2015a). These observations, all taken together, suggest that viruses harbouring a B-allele NS segment are capable of causing significant disease in mammals.

All viruses replicated well in the lung by day 2 post-infection, and appeared to display similar cell tropism (Figs 4.2 and 4.4). However, O175A was cleared the most rapidly, followed by O265B, with PR8 persisting at higher titres at day 6 post-infection (Fig 4.2). Therefore, the WT PR8 NS segment provided a fitness advantage over the avian NS segments tested *in vivo*, but interestingly O265B segment 8 provided a fitness advantage over O175A. PR8 has been passaged many times in the mouse host (Taylor, 1941), therefore it is not surprising to see that the PR8 NS segment is better suited for mouse infection, as adaptive mutations will likely have been incurred over time. Indeed, adaptive mutations in the NS segment, in both the NS1 and NEP genes, have been noted when forcibly adapting a human virus in mice (Forbes et al., 2012). Interestingly, the B-allele H3N2 reassortant virus used in the Treanor et al study

(Udorn72/Alb88B) was cleared more rapidly than an A-allele counterpart (Udorn72/NY6750A) from the nasopharynx of infected squirrel monkeys (Treanor et al., 1989). However tracheal virus titres were not significantly different between these viruses, demonstrating that the B-allele virus could still replicate well in the squirrel monkey host. Nonetheless the authors concluded that B-allele NS genes attenuate mammalian viruses in the mammalian host. The NS genes used in the Treanor et al study, NY6750A and Alb88B, were incorporated into PR8 in this study, but due to time constraints an *in vivo* study was not possible. It would be interesting to test these viruses in mice to see if similar trends would be observed as were seen for the O175A and O265B NS genes. Additionally, it would be useful to assess Udorn72 reassortant viruses, the same backbone strain used in the Treanor et al study, although the use of squirrel monkeys would be unrealistic. Nonetheless, the data described here provide clear evidence that an avian B-allele NS segment can support efficient replication of a mammalian IAV strain *in vivo*, and can contribute to significant disease.

When lung histopathology was assessed by haematoxylin and eosin staining of tissue sections, it was concluded that the source of segment 8 did not significantly alter the degree of tissue damage incurred during infection (Figs 4.3A and 4.3B). This was somewhat surprising given that WT PR8 induced more weight-loss, greater ISG expression and a stronger pro-inflammatory cytokine response than O175A and O265B during infection (Figs 4.1C, 4.5 and 4.6). Despite a strong pro-inflammatory response being linked to greater lung tissue damage, morbidity and mortality during infection with a highly pathogenic IAV strain (Cheung et al., 2002, Lee et al., 2009b, To et al., 2016), blind scoring of tissue sections did not reveal notable differences between the viruses assessed.

WT PR8-infection elicited a global increase in abundance of both ISG transcripts and pro-inflammatory cytokine levels in the lung, and to greater extents than O175A and O265B (Figs 4.5 and 4.6). While RT-qPCR analysis showed a trend of a greater abundance of ISG transcripts in the lung of O265B-infected mice than O175A-infected mice, this did not necessarily translate to a greater level of pro-inflammatory cytokines quantified by immunoblot in a cytokine array. Therefore, it is difficult to say with certainty that O265B elicited a greater inflammatory response *in vivo* than O175A, however O265B did induce greater weight-loss. The most likely cause of weight-loss induction is the strength of the inflammatory response, based on observations that susceptible mice have much stronger pro-inflammatory gene expression profiles than non-susceptible mice when infected with the same virus strain (Boon et al., 2009, Alberts et al., 2010). WT PR8 induced the greatest weight-loss and also unequivocally induced the largest pro-inflammatory response in the lung. Whether the increased inflammatory response in PR8-infection was caused by i) a more widespread infection in the lung, ii) greater viral load in the lung or iii) an inability of the virus to dampen the cytokine & ISG response, or a synergism of all three, is not clear. However, the observations that a 500 PFU input induced more weight-loss than a 100 PFU dose for all viruses tested (Figs 4.1A and 4.1B), and that a PR8-NS1-R38AK41A mutant virus that cannot control the IFN response induced less weight-loss in mice than WT (Donelan et al., 2003), suggests that the degree of virus replication, and probably spread, are the major determinants. Also, these data demonstrate that an increased antiviral response in the lung does not correlate with reduced virus replication, in fact the opposite was found. Therefore, assessing ISG and cytokine suppression may not be an appropriate marker for viral fitness *in vivo*.

Finally, co-infections were performed to ask if an A-allele NS segment would have a selection advantage over a B-allele NS segment into mammalian-adapted viruses *in vivo*, when both are present in the same host. Genetic reassortment between avian and mammalian viruses poses a real possibility for an avian-derived genomic segment(s) to enter mammalian-viruses in nature, and is often a prerequisite to pandemics in man (Steel and Lowen, 2014). Previous work in the Digard lab has highlighted differences in the RNA-packaging signal regions between A- and B-allele NS gene sequences, and this may lead to preferential packaging of A-allele sequences over B-allele sequences in mammalian viruses (Gog et al., 2007). In Chapter 2, *in vitro* competition assays were described, and it was concluded that O265B NS vRNP was packaged into the PR8 background as efficiently as O175A vRNP *in vitro* (Figs 2.14A and 2.14B). Here, a low multiplicity co-infection was performed *in vivo*, as this will resemble the most likely scenario for genetic reassortment in nature. Results provided no evidence of the O175A segment out-competing O265B, and in the majority of mice tested, the O265B NS segment was detected more frequently by plaque purification (Fig 4.7). This trend was consistent with *in vitro* analyses (Figs 2.14A and 2.14B), and so the data suggests that B-allele NS segment RNA-packaging signals are equally compatible for packaging into a mammalian-adapted virus background as A-allele NS segment packaging signals. Therefore, it appears unlikely that B-allele NS segments are restricted to avian viruses at the level of reassortment.

Overall, *in vivo* studies of NS reassortant viruses led to the conclusion that a mammalian-adapted virus harbouring an avian B-allele NS segment was able to cause disease and replicate *in vivo*, and in no scenario was an A-allele equivalent deemed to have superior fitness. In fact, there was more evidence to support the notion that the

B-allele reassortant was more fit in the BALB/c host - causing greater weight-loss and persisting in the lung for longer. Additionally, data suggested that an avian B-allele NS segment is able to reassort into a mammalian virus during co-infection. These findings, therefore, provide evidence that avian B-allele segment 8 genes that circulate in the avian population are able to complement the other 7 segments of mammalian viruses in a mammalian host, supporting serious pathology and disease. These genes, therefore, should not be discounted when risk-assessing avian influenza viruses and their ability infect and cause serious outbreaks, including pandemics, in mammalian hosts.

Chapter 5: Phylogenetic analyses of segment 8 genes of IAV – *Aves* to *Mammalia* transmission rates

5.1 Introduction

5.1.1 Aim

In the previous sections, B-allele NS reassortant viruses were characterised in the mammalian host *in vitro* and *in vivo*. There was no evidence that a mammalian virus harbouring an avian B-allele NS segment was less fit *in vitro* or *in vivo* than an avian A-allele reassortant equivalent. B-allele NS segments supported efficient virus replication, were packaged efficiently during co-infection studies when both A- and B-allele NS segments were available *in vitro,* and caused severe pathology in the BALB/c host. Therefore, it appeared unlikely that any potential avian-restriction of B-allele NS segments is at the level of virus replication.

It was therefore asked whether there is truly a bias against B-allele NS segments being introduced into mammalian hosts in nature. Using sequencing and surveillance information available for IAV, it is possible to estimate the apparent relative rates of introduction from birds to mammals for both the A- and B-allele lineage, and it was tested whether the relative rates are significantly reduced for avian B-allele genes.

5.1.2 Hypothesis

The hypothesis that B-allele NS segments are avian-restricted is founded on the observation that B-allele sequences are rarely isolated from mammalian hosts. However this view dates back over 25 years ago, when the number of IAV sequences

were only fractional in comparison to the number available now (Treanor et al., 1989). The number of available A-allele NS sequences, nevertheless, still heavily outnumbers the number of B-allele NS sequences in both the mammalian and avian host (Sevilla-Reyes et al., 2013). However one cannot use the total number of mammalian sequences per lineage as an accurate measure of ability of bird to mammal transmission. For example, there are thousands of NS A-allele sequences from human seasonal (H1N1, H2N2 or H3N2) infections, but all these sequences are derived from the pdm1918 H1N1 outbreak (Taubenberger and Morens, 2006) which stemmed from one *Aves* to *Mammalia* transmission event. Thus, one introduction of an avian A-allele NS segment into a mammalian host has led to thousands of mammalian virus NS sequences, which may be inaccurately interpreted as a bias for *Aves* to *Mammalia* transmission for A-allele NS segments over B-allele segments. Conversely, there is only one described sequence for the largest described B-allele outbreak in a mammalian host (A/equine/Jilin/1/89 (H3N8)) which was reported to have infected thousands of horses with a high morbidity and mortality rate (over 13 000 horses were estimated to have been infected (Guo et al., 1992)). Therefore, it is more appropriate to assess relative rates of introduction – i.e. normalising the number of estimated avian to mammalian introduction events by the total number of avian sequences available. This value more closely reflects the ability of an avian NS segment to transmit to mammals rather than the total number of mammalian sequences available, which can be distorted by large-scale epidemics or endemics resulting in many mammalian sequences recorded all stemming from one bird to mammal transmission event.

It was hypothesised that the relative rates of *Aves* to *Mammalia* transmission events would be similar across the two lineages of NS segments, given the data

reported in previous chapters suggesting B-allele NS segments are equally compatible in a mammalian virus background both *in vitro* and *in vivo*. It was speculated that the paucity of mammalian B-allele sequences could stem from a smaller pool of B-allele viruses circulating in the avian host.

5.1.3 Approach

This section reports a collaboration with Dr. Samantha Lycett (The Roslin Institute, The University of Edinburgh, Midlothian, UK). Due to the scale of task, programming expertise was required to manipulate the IAV segment 8 sequences available on GenBank for phylogenetic analyses. Dr. Lycett performed the download of all NS sequences from GenBank, alignments, phylogenetic clustering, phylogenetic tree annotation, sequence distribution calculations, estimates of wild or domestic bird source, and statistical analyses to compare introduction rates and sources across A- and B-allele sequences. Following Dr Lycett's input, 'sanity checks' of downloaded sequences (discussed below), literature research, and the analysis of the virological implications were performed. Interpretation of the phylogenetic data was a collaborative effort between Dr. Lycett, Prof. Paul Digard, and myself.

To estimate the number of independent segment 8 introduction events from avian hosts into mammals, all available NS sequences were downloaded from GenBank, phylogenetic trees were constructed, and mammalian-derived isolates were marked. Large clades of mammalian isolates were identified that likely acquired their NS from an avian source and these were scored as one introduction event per lineage (discussed below). For all other mammalian sequences identified in otherwise avian branches, manual inspection of the H and N subtype, year and location of isolation, host species, and sequence of the NS segment was conducted for each isolate, along

with researching any available literature, to estimate the likelihood of each mammalian NS sequence being an independent introduction from an avian host. In some cases, these apparently represented a single transmission event from an avian host to a mammal (accepting sampling bias). In other cases, an avian NS segment appeared to have been successfully introduced into the mammalian population long-term, such as the pdm1918 H1N1 NS segment which has persisted in humans and pigs since the 1918 'Spanish Flu' pandemic (Taubenberger and Morens, 2006). In both instances, this was considered one independent introduction event. An 'introduction rate' was calculated by normalising the number of expected introductions by the total number of available avian sequences for A- and B-alleles. These were subsequently compared using Fisher's Exact Test to ask if the relative rates of bird to mammal transmission events was different between avian A- and B-allele NS genes.

For each independent *Aves* to *Mammalia* introduction event identified, evidence was assessed to determine whether the likely source of segment 8 was from wild or domestic birds, to ask if the source of avian host differed between A- and B-allele lineages. The contact rate of domestic mammals with domestic birds can be rather different than with wild birds. This is an area of importance as HPAI infections of domestic mammals, with high morbidity and mortality rates, are thought to be predominantly mediated by direct contact with domestic birds (Chan, 2002, Schrauwen and Fouchier, 2014, Herfst et al., 2014). Therefore, it was of interest to compare wild and domestic bird-to-mammal transmission rates between A- and B-allele NS segments. Using a combination of BLAST analysis of closest relatives, manual inspection of Neighbour Joining Trees, and a discrete trait model for host

species, the avian ancestor was assigned as either wild or domestic bird and the relative rates compared across A- and B-alleles using Fisher's Exact Test.

5.2 Results

5.2.1 Phylogenetic clustering of available NS segments

All NS sequences available on GenBank were downloaded by Dr. Lycett on the 17th October 2014 via the Influenza Virus Resource (Bao et al., 2008). The sequences represented isolates from avian (43%), swine (10%), human (44%) and other (3%) hosts (Table 5.1). After removal of duplicated or erroneous sequences (see later), 28822 sequences remained, of which 2725 belonged to the B-allele lineage (Table 5.1). 8 of the 2725 (0.3%) B-allele sequences were mammalian isolates, while 16484 of the 26097 (63.2%) A-allele isolates were mammalian.

The following description of the protocol was provided by Dr. Lycett and adapted: 'Due to the large number of sequences, the sequences were aligned in groups, by nucleotides using ClustalW in BioEdit, manually adjusted for NS1 coding frame with the remaining nucleotides in the NEP coding frame, then aligned by amino acid using MUSCLE in MEGA6.0. The major lineages of influenza A segment 8 (Avian A, Human Seasonal, Classical Swine, H1N1-pdm09, Avian B) were identified in neighbour joining trees - the data was split into 10 random subsamples of approximately 3100 sequences each to make 10 trees, and all the sequences belonging to the Avian lineages were extracted from the random subsamples, combined and alignments re-checked. Sequences with identical isolate names, mixed subtypes, unknown location or year were excluded to make the Avian A (10914 sequences in

Table 5.1. Distribution of NS sequences. Shown is a breakdown of all segment 8 sequences downloaded from GenBank according to the host, subtype, location and clade. The major clades are described in the main text and represented diagrammatically in Fig 5.1. In this table, the Classical Swine group also includes triple reassortant swine viruses. The grouping is based on sequence homology of NS segment and it is expected that genetic reassortment accounts for certain examples of unexpected subtypes or hosts present in certain groups (e.g. H7, N3, and N8 subtypes in the Classical Swine group, H5 in the human seasonal group, and H3 and N2 subtypes in the pandemic 2009 group). For example, the internal gene segments of the pdm2009 H1N1 virus have been isolated from H1N2 and H3N2 swine viruses following genetic reassortment between swine viruses (Kirisawa et al., 2014). Values were calculated and the table constructed by Dr. Sam Lycett.

Lineage	AvianA	AvianB	ClassicalSwine	HumanSeasonal	Pandemic2009	All
Total	10914	2725	1872	7213	6098	28822

Host	AvianA	AvianB	ClassicalSwine	HumanSeasonal	Pandemic2009	All
Avian	9613	2717	22	2	5	12359
Swine	519	4	1807	72	561	2963
Human	325	1	38	7136	5518	13018
Equine	178	1	1	0	0	180
Canine	232	0	0	2	6	240
OtherMammal	47	2	4	1	8	62

Continent	AvianA	AvianB	ClassicalSwine	HumanSeasonal	Pandemic2009	All
Asia	5263	351	431	1700	1762	9507
Europe	1038	378	7	523	1241	3187
Africa	372	11	0	67	62	512
NorthAmerica	4092	1945	1434	3277	2408	13156
SouthAmerica	36	25	0	757	438	1256
Oceania	109	15	0	889	187	1200
Antarctica	4	0	0	0	0	4

H-subtype	AvianA	AvianB	ClassicalSwine	HumanSeasonal	Pandemic2009	All
H1	769	172	1176	1616	5924	9657
H2	321	87	3	98	0	509
H3	1294	648	692	5498	174	8306
H4	876	494	0	0	0	1370
H5	2981	337	0	1	0	3319
H6	1131	275	0	0	0	1406
H7	845	374	1	0	0	1220
H8	113	25	0	0	0	138
H9	1359	64	0	0	0	1423
H10	580	63	0	0	0	643
H11	387	141	0	0	0	528
H12	116	37	0	0	0	153
H13	92	1	0	0	0	93
H14	8	6	0	0	0	14
H15	8	1	0	0	0	9
H16	34	0	0	0	0	34

N-subtype	AvianA	AvianB	ClassicalSwine	HumanSeasonal	Pandemic2009	All
N1	3492	453	767	1575	5811	12098
N2	2763	681	1101	5638	287	10470
N3	751	135	3	0	0	889
N4	206	43	0	0	0	249
N5	228	93	0	0	0	321
N6	1111	467	0	0	0	1578
N7	677	66	0	0	0	743
N8	1113	652	1	0	0	1766
N9	573	135	0	0	0	708

total of which 9617 were avian) and Avian B (2725 sequences in total of which 2717 were avian) data sets'. Table 5.1 gives the distribution of sequences by all major lineages, hosts, geographic locations and subtypes.

'Sanity checks' involved examining the sequences of all prototypic strains that were identified for each estimate of *Aves* to *Mammalia* transmission in the 'Avian A' and 'Avian B' group to ensure the sequences i) were not uploaded to GenBank in error or ii) were not incorrectly classed as a unique introduction event based on the criteria given above. Uploading sequences to GenBank is at the authors' discretion. Errors can occur such as duplicating a previously reported isolate, reporting inaccurate sequences that are of unexpected length or composition, or incorrectly uploading the sequence of a commonly used laboratory strain of IAV as a new isolate following contamination issues (Li et al., 2010). Indeed, BLAST analysis of segments 1-7 of all prototypic strains identified revealed that an Avian A isolate, A/swine/Korea/S190/2004 (H9N2) (GenBank accession number AY790301), was likely misclassified as several segments were derived from the common laboratory strain A/WSN/33/1934 (H1N1). Thus, this isolate was removed from the study.

5.2.2 A-allele NS segment introductions into mammals

The A-allele NS sequences could be divided into four 'giant' clades following phylogenetic clustering. Fig 5.1 shows these clades highlighted in colour within the phylogenetic tree (colours on figure are included in parentheses in main text): i) human seasonal (H1N1, H3N2, H2N2) (orange), ii) classical and triple reassortant swine (magenta), iii) pdm2009 H1N1 (cyan), and iv) an 'avian A' clade composed of avian and 'avian-like' viruses (light blue). The 'avian A' clade contained several major

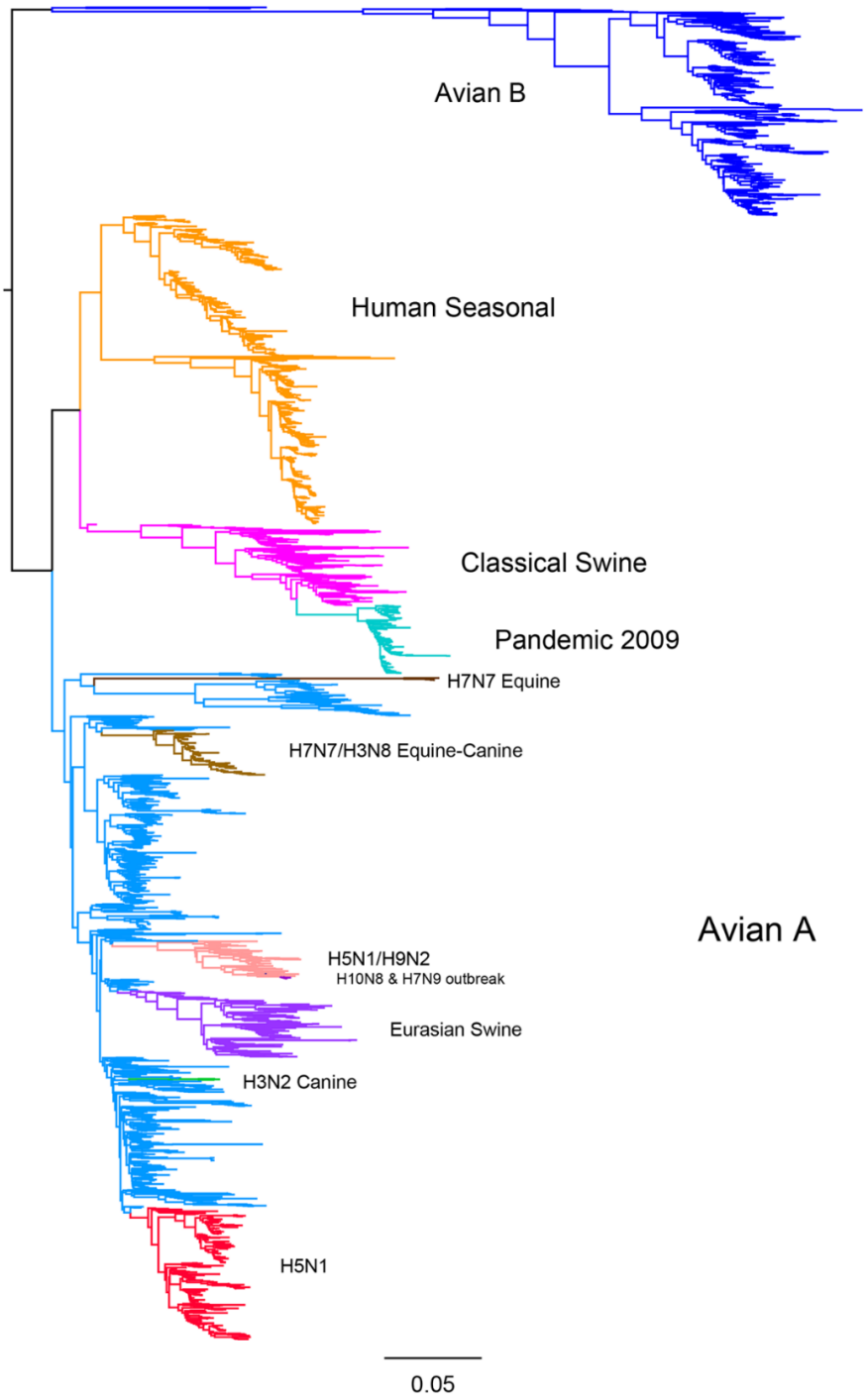

Fig 5.1. Major lineages of influenza A virus segment 8. Phylogenetic tree shown is of a sub-sample of all influenza A virus segment 8 sequences, with major lineages highlighted in colour. Dark blue shows all B-allele NS sequences. The A-allele sequences contain human seasonal (orange), classical swine (magenta) and pandemic 2009 (cyan). The rest belong to the 'Avian A' clade of avian and avian-like viruses (light blue). Within the Avian A group are specific lineages that are highlighted in colour and superimposed. Figure was made by Dr. Samantha Lycett.

lineages within: i) H7N7 Equine (dark brown), ii) H7N7/H3N8 Equine-Canine (Equine H3N8 viruses underwent reassortment with existing H7N7 viruses, resulting in a population of H7N7 and H3N8 viruses with the same NS (Murcia et al., 2011)) (light brown), iii) H5N1/H9N2 representing the 1997 Hong Kong H5N1 human infections and related H9N2 human and swine isolates in China 1997-2010 (pink), iv) the 2013 H7N9 outbreak in China (purple on pink), v) the 'precursor' to the H7N9 infections which includes closely related H10N8 and H7N9 human viruses and H3N2 and H9N2 swine viruses (purple on pink), vi) Eurasian swine (purple), vii) H3N2 canine (green), and viii) H5N1 representing the 2003 and onwards HPAI H5N1 infections in humans (red) (See Fig 5.1 for all major clades highlighted on a phylogenetic tree). Fig S5.1, included on CD, is an xls file showing a more detailed phylogenetic tree of the 'Avian A' group shown in Fig 5.1. Fig S5.1 can be viewed in FigTree (downloadable in Mac and PC versions from http://tree.bio.ed.ac.uk/software/figtree/) which allows large phylogenetic trees to be viewed on screen at a magnification that permits virus strain names to be read, which is otherwise not legible in text. Fig S5.1 was made by Dr. Samantha Lycett.

Each of the following were considered one independent introduction of an NS segment from an avian virus into a mammalian host; i) human seasonal (H1N1, H2N2 and H3N2) epidemics, the classical and triple-reassortant swine lineages, and the pdm2009 H1N1 viruses (the NS segment persisted from the pdm1918 H1N1 outbreak (Taubenberger and Morens, 2006)), ii) the 1997 H5N1/H9N2 lineage in the 'Avian A' clade, iii) the 2003 and onwards H5N1 lineage in 'Avian A', iv) Eurasian swine subtypes, v) the 2013 H7N9 cases, vi) the 2013 H7N9 'precursor' viruses of H10N8, H9N2, H7N9, and H3N2 subtypes isolated from humans and pigs, vii) the H7N7

equine influenza lineage, viii) the H7N7/H3N8 equine and canine lineage, and ix) the H3N2 canine viruses (Fig 5.1 and Table 5.2). The 'general' avian clade ('Avian A') was manually inspected and other independent introductions were estimated based on subtype, year and location of isolation, and sequence homology of NS segment. An additional 23 introductions were determined, giving 32 in total (Table 5.2).

Of the 32 A-allele introductions, 19 strains were estimated to have transmitted from mammal to mammal (Table 5.2), and 5 cases led to long-term establishment in a mammalian host: i) the pdm1918 H1N1/human seasonal and classic/triple reassortant swine lineage, ii) Eurasian swine, iii) H7N7 equine, iv) H7N7/H3N8 equine and canine, and v) H3N2 canine.

5.2.3 B-allele NS segment introductions into mammals

A phylogenetic tree of all B-allele NS sequences was constructed by Dr. Lycett using the neighbour joining method in MEGA6 (with the Tamura-Nei model, gamma distributed rates among sites and heterogeneous patterns among lineages) and the mammalian isolates were highlighted (Fig 5.2). The B-allele lineage split into North American and Eurasian clades. Initially, 9 mammalian isolates were highlighted. Upon manual inspection of these 9 isolates, it was apparent that one isolate was likely an erroneous entry into GenBank and two isolates were submitted in duplicate. The sequencing data of the former was reported to contain mixed virus strains in the sample (A/Auckland/4382/1982(mixed), accession CY112376), and so this was removed as the B-allele sequence may have arisen from a laboratory contamination event. A/muskrat/Buryatiya/1944/2000 (H4N6) (GenBank accession number GU052363) and A/musk rat/Buryatiya/1944/2000 (H4N6) (accession number EU580582)

Table 5.2. Independent introductions of avian A-allele NS segments into mammalian hosts. Shown are representative strains from each of the independent *Aves* to *Mammalia* transmission events for A-allele NS segments. The 'Transmission' column gives an estimate of whether the lineage of virus transmitted within mammalian hosts based on research of available literature. Accession column provides the GenBank identification number of the sequence.

Prototypic Strain	Host	Transmission	Notes	Accession (NS)	Avian Source
A/Brevig Mission/1/1918 (H1N1)	Human	Pandemic	Persists through classical swine, human H2N2, H3N2 and pdm2009 lineages	AF333238.1	Undetermined
A/equine/Prague/2/1956(H7N7)	Equine	Transmissible	Likely to be extinct.	CY087820	Undetermined
A/equine/Miami/1/1963 (H3N8)	Equine	Transmissible	Major circulating equine influenza A virus. Also endemic in US domestic dogs (canine H3N8).	CY028840	Wild
A/swine/China/8/1978 (H3N2)	Swine	Circulating in pigs	Kawaoka et al suggest this belongs in Eurasian-avian lineage that is circulating in European pigs (Kawaoka et al., 1998).	M80968	Domestic
A/swine/Belgium/WVL1/1979(H1N1)	Swine	Transmissible	Representative isolate for 'Eurasian swine flu'	CY037902	Domestic
A/seal/Massachusetts/1/1980(H7N7)	Seal	Epidemic in seals	Epidemic in seals with approximately 600 fatalities. (Webster et al., 1981)	AB284067	Wild
A/seal/Massachussetts/133/1982(H4N5)	Seal	Epidemic in seals	1983 outbreak in which 60 seals were reported dead. 39 were positive for an H4N5 indistinguishable from the prototype virus (Hinshaw et al., 1984)	M80947	Wild
A/mink/Sweden/3900/ 1984(H10N4)	Mink	Outbreak in Mink	One of the first identified cases of avian influenza able to transmit readily in mammalian host (Zohari et al., 2008)	GQ176140	Domestic
A/whale/Maine/328B/1984(H13N2)	Whale	Single isolate	Isolated from one sick pilot whale, no evidence of a transmission chain. (Groth et al., 2014).	KJ372724	Wild
A/seal/Massachusetts/3911/1992 (H3N3)	Seal	Likely transmissible	Two closely related H3N3 viruses were detected in three seals following an increase in the number of stranded seals in Cape Cod in 1992 (Callan et al., 1995).	GU052287	Wild
A/swine/Hong Kong/644/1993(H1N1)	Swine	Possible transmission.	3 independent H1N1 isolates from pigs with closely related NS segments, transmission information not disclosed in publication (Vijaykrishna et al., 2011).	CY085013	Domestic

Prototypic Strain	Host	Transmission	Notes	Accession (NS)	Avian Source
A/England/AV877/1996 (H7N7)	Human	Likely single isolate	Isolated from 43-year-old duck farmer with mild one-sided conjunctivitis (Kurtz et al., 1996)	GU053113	Domestic
A/swine/Eire/89/1996(H1N1)	Swine	Single isolate	No other closely related isolates of same subtype, host and year. (Lycett et al., 2012)	CY115892	Domestic
A/Hong Kong/482/97(H5N1)	Human	Individuals only.	Includes related H9N2 human and swine isolates in China 1997-2010.	AF084285	Domestic
A/Swine/Ontario/01911-1/99 (H4N6)	Swine	Likely transmission	Outbreak in pigs with pneumonia in Canada (Karasin et al., 2000)	AF285889	Wild
A/swine/KU/2/2001(H11N6)	Swine	Possible transmission	No published information available. 4 independent H11N6 pig isolates from same year and location suggests ability to transmit within pigs.	CY073456	Domestic
A/swine/Ontario/K01477/01(H3N3)	Swine	Likely transmission	Same H3N3 virus was isolated from more than one pig in a sick group (exact numbers not disclosed) (Karasin et al., 2004)	AY619965	Wild
A/Caspian seal/Russia/1884/2002 (H4N6)	Seal	Possible transmission?	Two H4N6 isolates from Caspian Seals in Russia 10 years apart with very closely related NS segments. Nothing published for these strains.	KJ847690	Wild
A/Netherlands/033/03 (H7N7)	Human	Poorly transmissible between humans	Mostly independent transmission events from birds to humans. H7N7 virus was epidemic in poultry in Netherlands in 2003 (Stegeman et al., 2004). H7N7 IAV was detected in 85 subjects, with 3 people from within a household (Fouchier et al., 2004, Koopmans et al., 2004).	AY342423	Domestic
A/Beijing/01/2003 (H5N1)	Human	Not transmissible in humans?	H5N1 'Bird Flu'. Human to human transmission is rare or non-existent.	EF587281.1	Domestic
A/Canada/rv504/2004 (H7N3)	Human	Likely single isolates.	Infection of two poultry workers on different farms during H7N3 poultry outbreak in British Columbia, Canada (Hirst et al., 2004)	CY015010	Domestic
A/swine/Korea/S452/2004(H9N2)	Swine	Likely single isolates	Two independent isolates of H9N2 swine viruses with very similar NS genes in 2004. Nature of infections not specified in literature (Dong et al., 2011).	AY790309	Domestic
A/canine/Guangdong/1/2006(H3N2)	Canine	Transmissible	Avian H3N2 adapted to canine host and transmits well in population.	GU433352	Wild

Prototypic Strain	Host	Transmission	Notes	Accession (NS)	Avian Source
A/swine/Hubei/10/2008 (H10N5)	Swine	Transmissible in pigs	Wholly avian virus, closely related to Eurasian swine IAV. (Wang et al., 2012b)	JX500447	Domestic
A/swine/Jilin/37/2008 (H3N2)	Swine	Likely single isolate	Authors sampled 279 sick pigs and this was isolated from one pig only. Has M and NS genes from H10 avian influenza (Cong et al., 2010)	GU215038	Wild
A/swine/Yangzhou/080/2009(H6N6)	Swine	Likely transmissible in pigs	Detected from clinical samples, co-infection with porcine circovirus type 2 in six pigs (Zhao et al., 2013). Closely related to A/swine/Guangdong/K6/2010(H6N6). 3.6% of 475 sick pigs sampled were seropositive against H6 IAV (Zhang et al., 2011).	JQ815882	Domestic
A/swine/HuBei/06/2009 (H4N1)	Swine	Single isolate	Apparent direct avian-to-pig infection without chain of transmission. First H4 avian virus detected in pigs (Hu et al., 2012).	JX878679	Wild
A/swine/Guangdong/K4/2011(H4N8)	Swine	Possibly transmissible in pigs	Isolated from a pig in a group displaying respiratory symptoms (H4N8 and H3N2). (Su et al., 2012)	JX151011	Domestic
A/harbor seal/Massachusetts/1/2011(H3N8)	Seal	Probable transmission	126 seals died from this outbreak of virus (Anthony et al., 2012)	JQ433883	Wild
A/Mexico/InDRE7218/2012 (H7N3)	Human	Likely single isolates	High-pathogenicity H7N3 virus isolated from Mexican poultry workers with conjunctivitis in 2012 (Lopez-Martinez et al., 2013). Likely direct infection from infected poultry. Similar NS segment to A/Canada/rv504/2004(H7N3) (CY015010) (Obenauer et al., 2006)	CY125732	Domestic
A/Jiangxi/IPB13/2013 (H10N8)	Human	Likely single isolates	Human H10N8 cases likely from live poultry markets in China (Zhang et al., 2014b). Closely related to the H7N9 'precursor' H9N2 strains.	KJ406559	Domestic
A/Nanjing/1/2013 (H7N9)	Human	Poorly transmissible in humans	2013 and onwards H7N9 zoonotic episodes in China.	KC896778	Domestic

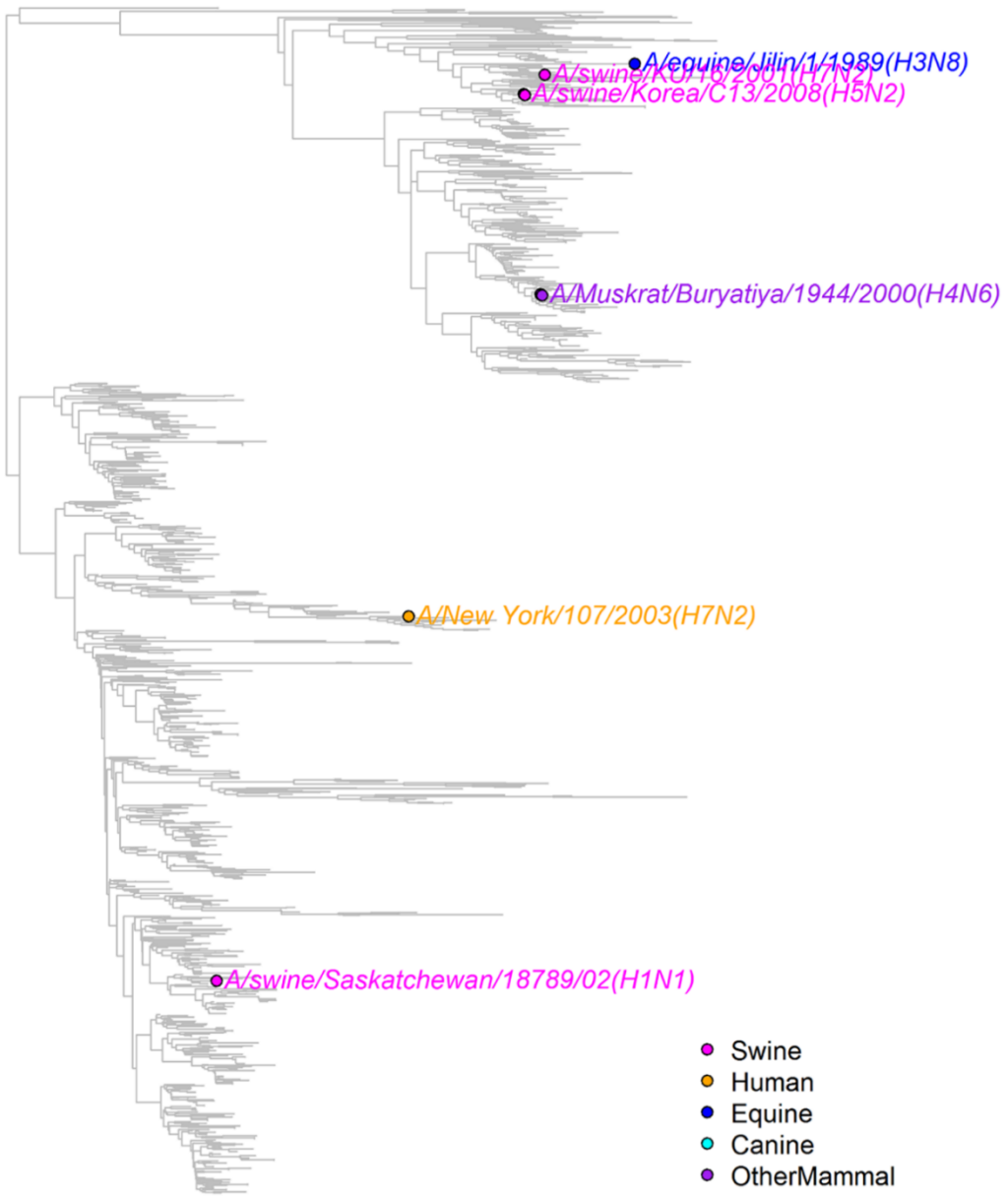

Fig 5.2. Mammalian B-allele segment 8 sequences. Phylogenetic tree of all avian B-allele lineage segment 8 sequences with the non-avian sequences highlighted. Figure was made by Dr. Sam Lycett.

represent two GenBank uploads from one virus isolation, therefore the latter was removed from the analysis. Additionally, it was apparent that two mammalian sequences in the B-allele lineage were likely from the same *Aves* to *Mammalia* transmission event. A/swine/Korea/C13/2008 (H5N2) (accession number FJ461601) and A/swine/Korea/C12/2008 (H5N2) (accession number FJ461600) both had very high segment 8 sequence homology, had the same H and N subtyping, and were isolated in the same year, at the same location, and from the same host. Therefore, these two mammalian isolates were scored as one mammalian introduction event. Following the removal of the aforementioned sequences, a total of 6 independent introduction events were estimated. 2 were from the North American clade and 4 from the Eurasian clade (Table 5.3 and Fig 5.2).

Of the six independent introduction events, three were estimated to have been transmissible within the mammalian population, of which A/equine/Jilin/1/1989 (H3N8) caused an epidemic of high mortality infections in the equine host (Guo et al., 1992). A/swine/Saskatchewan/18789/02 (H1N1) and A/swine/Korea/C13/2008 (H5N2) were thought to have transmitted within a population of pigs, given positive sampling from numerous other swine individuals within their respective farms (Karasin et al., 2004, Lee et al., 2009a). A/muskrat/Buryatiya/1944/2000 (H4N6), A/swine/KU/16/2001(H7N2), and A/New York/107/2003 (H7N2) were all predicted to be individual infection events, as there were no reports of additional mammalian infections from any of these strains (Lvov et al., 2015, Kwon et al., 2011, Ostrowsky et al., 2012).

Table 5.3. Independent introductions of avian B-allele NS segments into mammalian hosts. As described in Table 5.2 legend but for B-allele NS sequences.

Strain	Host	Transmission	Notes	Accession (NS)	Avian Source
A/equine/Jilin/1/1989 (H3N8)	Equine	Epidemic	Major equine influenza epidemic (Guo et al., 1992)	M65020	Domestic
A/muskrat/Buryatiya/1944/2000 (H4N6)	Muskrat	Single isolate	Closely related to H4N6 avian influenza circulating in Russia at similar time point (Lvov et al., 2015).	GU052363.1	Wild
A/swine/KU/16/2001(H7N2)	Swine	Likely single isolate	Isolated from 1 pig (532 tested) from a slaughterhouse. Apparent reassortment between avian H7N2 and H5N3 viruses (Kwon et al., 2011).	CY067690	Domestic
A/swine/Saskatchewan/18789/02 (H1N1)	Swine	Likely transmissible in pigs	Isolated from a 1200 sow pig farm where influenza-like symptoms affected pigs of all ages. Fully avian virus. (Karasin et al., 2004)	AY619957	Wild
A/New York/107/2003 (H7N2)	Human	Single isolate	Apparent individual infection of a 48-year-old immunocompromised man from the Caribbean with fever and flu-like symptoms. No apparent transmission to family. (Ostrowsky et al., 2012)	EU587374.2	Domestic
A/swine/Korea/C13/2008 (H5N2)	Swine	Apparent transmission	Serological evidence of transmission within pigs (maybe asymptomatic?) (Lee et al., 2009a)	FJ461601.1	Wild

5.2.4 Relative rates of *Aves* to *Mammalia* transmission events

The total number of A-allele (32) and B-allele (6) NS mammalian introduction events were in favour of A-allele by approximately five to one (Tables 5.2 and 5.3). However, the total number of avian NS sequences is unequal between the two clades, with 9613 avian A-allele sequences versus 2717 B-allele avian sequences (Table 5.1). Therefore, the rates of independent introductions into mammals relative to the total avian sequences available are 32/9613 = 0.0033 and 6/2717 = 0.0022 respectively (Table 5.4). Dr. Lycett performed Fisher's Exact Test, using the A-allele data and assuming a binomial distribution to calculate a range of expected B-allele introductions, and it was deemed that the number of mammalian introduction events per avian isolate were not significantly different between A- and B-allele lineages (p-value = 0.436) (Table 5.4). Additionally, similar analyses of the data revealed that the transmissibility of A- and B-allele IAV within mammals was not significantly different between the two lineages (p-value = 0.446, Table 5.4).

Therefore the available sequencing and surveillance data do not support the hypothesis that A-allele NS segments reassort into mammalian viruses at a higher rate than B-allele NS segments.

5.2.5 Comparisons of the avian source of mammalian introduction events

Next, it was considered whether the relative rates of A- and B-allele NS segment introduction into mammalian hosts differed between the sources of avian host (wild or domestic birds), given the contact rate between frequently sampled domestic mammals (e.g. human, swine) and domestic birds could be different than with wild

Table 5.4. Expected number of avian B-allele introductions. Values were calculated using data from A-alleles, assuming a binomial distribution. Figures in brackets represent the range of episodes that would still be statistically non-significant (p-values ≥ 0.1). Values were calculated and table was constructed by Dr. Samantha Lycett.

Data	A-allele			B-allele			Fisher test	
	Number of avian strains	Number of independent introductions	Introduction rate	Number of avian strains	Number of independent introductions	Introduction rate	p-value	Expected number of B-allele introductions
All avian	9617	32	0.0033	2717	6	0.0022	0.436	9.04 (4-15)
Transmissible	Undetermined	19	0.0020	Undetermined	3	0.0011	0.446	5.37 (0-10)
Single isolates or poor transmission	Undetermined	13	0.0014	Undetermined	3	0.0011	1.000	3.67 (0-8)
Domestic only	4391	18	0.0041	648	3	0.0046	0.756	2.66 (0-6)
Wild only	5168	12	0.0023	2053	3	0.0015	0.578	4.77 (1-9)

birds. Dr. Lycett used BLAST analysis and a discrete trait model (data not shown), as well as manual inspection of phylogenetic trees, to analyse the closest relatives of exemplar mammalian isolates for each introduction event to estimate the source of NS as being from wild or domestic birds (Tables 5.2, 5.3 and 5.4). In 2 of the 32 A-allele introduction events, it was not possible to determine whether the source was wild or domestic bird - A/Brevig Mission/1/1918 (H1N1) and A/equine/Prague/2/1956 (H7N7). Of the remaining 30 introductions, 18 were determined to be from domestic birds, and 12 from wild birds (Tables 5.2 and 5.4). Of the 6 B-allele introductions, there was evidence of 3 wild bird and 3 domestic bird introductions (Tables 5.3 and 5.4). Using the A-allele data and assuming a binomial distribution, a range for expected B-allele introduction events was determined for both wild and domestic birds. Using Fisher's exact test, there was no significant difference between A- and B-alleles when the domestic bird to mammalian host (p-value = 0.756) or wild bird to mammalian host (p-value = 0.578) introduction rates were compared (Table 5.4).

The distribution of all avian A- and B- NS sequences are depicted in Fig 5.3, showing the source of avian host and also the location of isolation by continent. Most notably, wild Anseriformes made up the largest proportion of the avian B-allele sequences, and there were proportionally more domestic bird (both Anseriformes and Galliformes) isolates in the A-allele group than the B-allele group (Fig 5.3). Additionally, the majority of B-allele sequences were isolated from North America, while the largest proportion of A-allele sequences were isolated in Asia.

Therefore, there was no apparent difference in the rates of mammalian introduction events from wild or domestic birds across the A- and B- allele linages, although the geography of the avian isolates suggests that the A-allele lineage is more

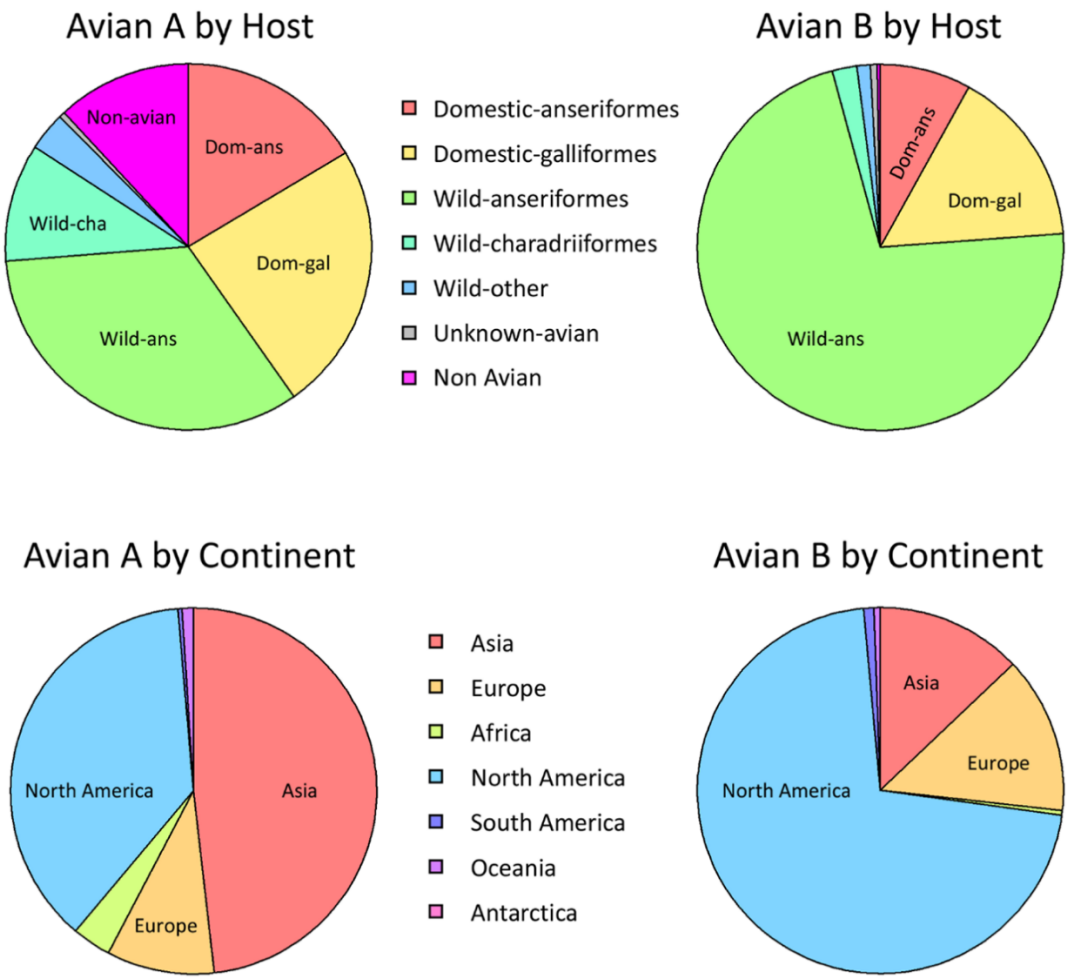

Fig 5.3. Distribution of avian segment 8 sequences. The host distribution and location of isolation is represented for all avian A- and B-allele segment 8 sequences. Figure was made by Dr. Samantha Lycett.

prevalent in Asia, a region where there is significant contact between poultry and domestic mammals.

5.3 Discussion

In Chapters 2, 3 and 4, it was concluded that mammalian-adapted IAVs forcibly reassorted with an avian B-allele NS segment were able to replicate efficiently in mammalian cells *in vitro* and *in vivo*. These reassortant viruses were also competent in antagonising the innate immune response in mammalian cells, and the NS segment was able to reassort into a mammalian adapted virus efficiently when both A- and B-allele NS segments were present during co-infection. These data contradicted conclusions drawn from other laboratories suggesting B-allele NS genes cannot efficiently support IAV replication in mammalian hosts (Treanor et al., 1989, Zohari et al., 2010a, Munir et al., 2011a, Munir et al., 2011b, Munir et al., 2012). The original hypothesis of the B-allele lineage of NS genes being restricted to avian hosts was partially based on a lack of sequences isolated from mammalian hosts at the time (Treanor et al., 1989). Since then, surveillance and sequencing efforts have increased dramatically, and the number of IAV genome sequences documented has risen exponentially. Since the first publication describing a mammalian B-allele virus in the equine host (Guo et al., 1992), there have been several more reports of B-allele viruses isolated from man, swine and muskrat (Table 5.3). Therefore, it was important to readdress the question of whether the introduction of an avian NS into mammals is biased towards the A-allele lineage over the B-allele lineage, using the comparatively larger bank of sequences available today.

Manual inspection of phylogenetic trees generated from all available NS sequences on GenBank, as well as consideration of the history of IAV evolution,

revealed 32 apparent independent incursions of an A-allele NS segment from birds to mammals, and 6 for B-alleles (Tables 5.2 and 5.3). The total number of avian NS sequences is heavily stacked in favour of A-alleles (9613 to 2317, Table 5.1), and when the relative rates of introduction per avian sequence was compared, these were not significantly different between A- and B-allele lineages (p value = 0.436, Table 5.4). Therefore, it is reasonable to speculate that the paucity of B-allele mammalian isolates can be explained by a smaller pool of B-allele viruses circulating in birds, rather than a selection disadvantage in mammals. In support of this suggestion, Worobey and colleagues performed an analysis on the evolutionary history of the IAV genome and proposed that there was an event (estimated to have occurred around the 1870s) in which the internal genes of an avian IAV (probably an H7N7 virus) 'swept' across the globe and selectively replaced all circulating avian IAV internal gene segments, but incompletely replaced the NS segments (Worobey et al., 2014a). This left a small ancestry pool in the avian host which are the ancestors of the B-allele NS genes (Worobey et al., 2014a). Thus, B-allele NS segments presumably provide sufficient fitness for avian IAVs to not be totally replaced by circulating A-allele NS segments. Further work examining A- and B-allele NS fitness in the avian host is required to understand this hypothesis further.

It is acknowledged that the interpretation of an independent introduction event is not definite and is open to debate. In some cases, a single infection of a mammalian host with an avian virus containing a phylogenetically distinct NS segment was relatively straightforward to score as one introduction event. In other cases such as the H7N7/H3N8 equine-canine lineage, there has been an avian to mammalian introduction event when an avian virus emerged in horses, followed by a subsequent

adaptation from an equine to canine host. This was counted as one introduction event, as this represents bird to mammal to mammal transmission, and therefore only one *Aves* to *Mammalia* transmission event occurred. In a similar fashion, all pdm2009 H1N1, human seasonal H1N1/H2N2/H3N2, and classical/triple reassortant swine isolates, accounting for thousands of mammalian A-allele sequences (Table 5.1), were classed as one introduction event as the NS segment has persisted from the pdm1918 H1N1 introduction from birds into humans. The recurring H5N1 infections of man from contact with poultry in China was not so obvious to define, as this reflects multiple individual infections of man with an avian virus, albeit the same virus circulating in poultry. These were treated as two independent introductions – the original 1997 infections in Hong Kong and the re-emergence from 2003 onwards, as the multiple NS sequences are monophyletic in both cases.

It is also accepted that these estimates are subject to influence from sampling bias. The observation that most avian NS sequences are A-allele may truly reflect that there are less B-allele viruses circulating in the avian population. Alternatively, B-allele viruses may predominantly infect avian species that are not sampled as frequently as others. For example, there is surveillance evidence that IAV can infect bird orders that are infrequently sampled such as Apodiformes, Passeriformes, and Columbiformes (Keawcharoen et al., 2011, Williams et al., 2012). Adams et al proposed that an H9N2 avian reassortant virus harbouring a B-allele segment 8 was less competent at replicating in chicken and turkey cells, but more fit in duck cells relative to an A-allele segment 8 reassortant counterpart (Adams et al., 2013). Additionally, Post and colleagues observed a reduction in pathogenicity and systemic virus load in chickens when two B-allele NS segments were introduced into an HPAI

H7N7 virus compared to the A-allele parent (Post et al., 2013). However, there is surveillance evidence suggesting avian B-allele viruses can infect poultry (Fig 5.3), persist and spread in poultry populations (Garcia et al., 1997, Suarez et al., 1999), and can cause highly pathogenic infections in domestic birds (Garcia et al., 1997). While the proportion of avian B-allele viruses isolated from domestic galliform birds was not as high as for A-allele viruses (Fig 5.3), there was still a sizeable number from this host. These observations, taken together, suggest it is unlikely that B-allele viruses are solely restricted to avian species that are not sampled frequently. The sampling of mammalian species is clearly biased towards domestic species such as swine and man. Although perhaps unlikely, it is not inconceivable that B-allele viruses are circulating in mammalian species that are not sampled for IAV.

Additionally, it was determined that the relative rates of introduction from wild and domestic birds into mammals were not significantly different between A- and B-alleles (Table 5.4), therefore it is unlikely that avian B-allele viruses are at a disadvantage for poultry-to-mammal transmissibility. Interestingly, B-allele sequences appeared to be found proportionally less frequently in Asia than A-allele sequences (Fig 5.3), a continent where live poultry markets are popular and present an increased opportunity for transmission of avian IAV into man (Chan, 2002). Therefore, while there does not appear to be a disadvantage for B-allele viruses in poultry to transmit to a mammalian host, there will undoubtedly be more domestic birds infected with A-allele viruses in Asia at any one time, in a region where contact between domestic mammals and poultry can be comparatively high due to farming methods and the popularity of poultry markets (Chan, 2002).

A successful cross-species transmission event does not always lead to long-term establishment within the new host. Further assessment of the *Aves* to *Mammalia* transmission events revealed occasions on which there was no documented evidence of further transmission within mammals, and examples where the NS genes seemingly persisted in a mammalian population(s) for a period of time. Of the 32 A-allele introductions, 19 of these were estimated to have transmitted within a mammalian population, compared to 3 of 6 B-allele introductions, and there was not a significant difference between these ratios (p-value = 0.446, Table 5.4). However, it is accepted that the sample size is small in this instance, and further work needs to be done to ask whether transmissibility between mammals is influenced by the lineage of NS segment. It is apparent that certain A-allele NS lineages have become established in the mammalian host (pdm1918 H1N1, Eurasian swine, H7N7/H3N8 equine and canine, H3N2 canine), whereas B-allele viruses have not persisted in mammals beyond epidemic levels to date, therefore it would be interesting to test the hypothesis that B-allele viruses are less well suited to mammal to mammal transmission than A-allele equivalents. Establishment of a mouse model for transmission was attempted, based on a report by Edenborough and colleagues, in which successful transmission of Udorn72 was observed between BALB/c mice (Edenborough et al., 2012). However, when this experimental set-up was attempted as part of this study, transmission was not detected between infected mice and naïve mice using plaque assay of lung homogenate and RT-PCR for segment 8 vRNA in the lung (data not shown).

Overall, thorough bioinformatic and phylogenetic analyses of all available NS sequences revealed that avian B-allele NS segments are introduced into the mammalian host at similar rates to avian A-allele segments in nature. It is proposed

that the observed paucity of B-allele NS sequences isolated from mammalian hosts is due to a smaller number of B-allele viruses circulating in avian hosts. Therefore, B-allele viruses should not be discounted during pandemic and zoonotic risk assessment of avian influenza viruses, as data collected here and in other reports suggest that B-allele viruses can cause significant disease in mammals.

Chapter 6: Concluding remarks

6.1 Conclusions

The aim of this study was to improve our understanding of IAV host adaptation. In particular, the contribution of the NS segment to mammalian host range and pathogenicity was studied. By elucidating the mechanisms restricting the B-allele lineage of NS segments to avian hosts, a hypothesis based primarily on the paucity of B-allele isolates in mammals, it was hypothesised that new insights into IAV host range could be developed. The data presented in this thesis provide evidence that avian B-allele NS segments are actually able to facilitate successful IAV infection of mammalian hosts and cause significant disease, and are estimated to enter the mammalian population at similar rates to avian A-allele NS segments. The findings challenge a dogma held in the field for over 20 years, and have important implications in the assessment of avian IAVs when considering zoonotic potential and pandemic risk. While the NS segment of IAV is important for host adaptation, this seems to be independent of A- or B-allele lineage.

6.2 Future work and directions

An important question to address is whether or not the lineage of NS segment impacts the transmissibility of IAV within mammalian hosts. Work presented in Chapter 5 showed that there is no strong evidence for bias in A- or B-allele avian NS segments transmitting from birds to mammals in nature. While available sequencing and surveillance information did not point to an obvious difference in transmissibility of A- and B-allele viruses within mammalian hosts (Table 5.4), the sample size was small and further work should be conducted to clarify this. Laboratory mice generally

do not reliably transmit IAV (Schulman and Kilbourne, 1963), even when infected with mouse-adapted strains of IAV or those that are highly transmissible in humans and readily cause disease in mice (Lowen et al., 2006). Despite this, Edenborough and colleagues demonstrated contact transmission of Udorn72 between BALB/c mice with relatively high efficiency (Edenborough et al., 2012). Therefore, a similar experimental setup was tested here in an attempt to establish a transmission model with an animal model readily available at the Roslin Institute. Two index mice were infected with $10^{4.5}$ PFU of Udorn72 via the intranasal route, and after 6 h were introduced to a cage containing three naïve contact mice. The mice were weighed daily but no weight-loss was seen, as expected with this dose of Udorn72 (data not shown). At day 4 post-infection, virus in the lung was titrated by plaque assay, and while the lungs of index mice had viral titres of 10^4 PFU/ml, there was no detectable virus in the lungs of contact mice by plaque assay or by RT-PCR of segment 8 vRNA (data not shown). Thus, no transmission was detected in this attempt. The most ideal transmission model of IAV is ferret infection, as the manifestation of infection is similar to that seen in humans and transmission between ferrets occurs with high efficiency (Reuman et al., 1989, Herlocher et al., 2001). However, ferrets are relatively very expensive and it is challenging to acquire cohort sizes large enough for meaningful experiments without the prior commitment of specific funding. Therefore, it was not realistic to perform an experiment using ferrets in this study. An alternative experiment could be to try the guinea pig model of transmission. Guinea pigs are highly susceptible to human IAV strains without prior adaptation and permit the airborne transmission of IAV with high efficiency (Lowen et al., 2006). Guinea pigs

are much cheaper and more readily available than ferrets, thus represent a realistic option for future studies.

Both NS1 and NEP amino acid sequences differ substantially between A- and B- allele lineages (Figs 2.1 and 2.2). Sequence alignments and a review of the literature revealed that the proposed CPSF30-binding site of NS1 is missing in B-allele NS1 proteins (Fig 2.1). However, transfection-based reporter assays described in Chapter 3 suggested that these NS1 proteins are still able to inhibit cellular gene expression efficiently despite the lack of the consensus CPSF30-binding site (Fig 3.7). Thus, an obvious question to ask is whether or not B-allele NS1 proteins can bind to CPSF30 in mammalian cells. It was planned to assess this by GFP-TRAP pulldown following co-transfection of NS1-GFP and CPSF30-FLAG expressing plasmids, but technical difficulties prevented the completion of this study within time constraints. Similar studies were also planned for other host factors reported to interact with NS1. In addition to the CPSF30-FLAG construct, expression plasmids for tagged human TRIM25, PKR, PI3K p85β, Riplet, and RIG-I were also kindly provided by Prof. Ben Hale (University of Zurich, Switzerland), but have yet to be tested. It was also planned to perform GFP-TRAP pulldown following NS1-GFP transfection on whole cell lysates to compare all cellular NS1 interactors between the two lineages. NEP-GFP constructs should also be made and tested in a similar fashion. Nevertheless, even if the interactors of A- and B-allele NS1 or NEP proteins differed, this would not detract from the overall conclusions of this study. By one means or another, B-allele NS1 and NEP proteins are able to perform essential functions efficiently in mammalian cells.

According to available sequence and surveillance data, there are less B-allele sequences in the natural host of IAV (Table 5.1). This was proposed in Chapter 5 to

explain the paucity of B-allele sequences in mammalian hosts, as there would be less opportunity for avian-to-mammalian transmission events in comparison to the more prevalent A-allele. It would be useful to generate avian IAV-based NS reassortant viruses and to ask if A-allele NS segments confer a fitness advantage in avian hosts. Adams and colleagues assessed an A- and a B-allele NS segment from isolated from waterfowl on the background of an H9N2 guinea fowl virus in duck, chicken and turkey cells (Adams et al., 2013). The authors suggested that the A-allele reassortant virus had a fitness advantage over the B-allele in chicken and turkey cells, but the B-allele was more suited to duck cells. In addition, Worobey and colleagues proposed that the B-allele NS genes represent a small pool of ancestry genes that survived a global 'sweep' of avian IAV internal genes that incompletely replaced all circulating NS segments (Worobey et al., 2014b). This suggests that the B-allele NS segments confer sufficient fitness for avian IAVs, otherwise one would expect them to have been fully succeeded by A-allele segments (as was predicted to have occurred for all other internal gene segments by Worobey and colleagues). However, further work is necessary to dissect this question.

Another question to address is whether there are particular genetic traits of segments 1-7 of IAV that are required for A- or B-allele NS segments to reassort into a mammalian-adapted viruses in nature. This would require another large-scale phylogenetic analysis and it may be necessary to look at sequence motifs within the other 7 segments, which would represent a challenging task. It could be hypothesised that avian A- and B-allele NS segments require specific complementation with one or more other segments of the IAV genome to successfully infect mammalian hosts. Given that there did not appear to be a difference in the relative rates of *Aves* to

Mammalia transmission across A- and B-allele lineages, perhaps the question should ask which genetic traits in the other 7 segments are required for any avian NS segment, independent of lineage, to successfully incorporate into a mammalian virus.

Chapter 7: Materials and methods

7.1 Materials

7.1.1 Suppliers of general reagents

General purpose reagents were supplied by Fisher Scientific, Scientific Laboratory Supplies Ltd, and Sigma. The Roslin Institute Central Services Unit (CSU) made and provided phosphate buffered saline (PBS). Other specific reagents are listed below alongside their respective suppliers.

Acrylamide:bisacrylamide (37.5:1) solution	Bio-Rad.
Agarose for electrophoresis	Invitrogen.
Amplify Fluorographic Reagent	GE Healthcare.
CAS-Block blocking agent	Invitrogen.
DNA molecular weight markers	Promega.
DNA plasmid miniprep kit	Promega.
DNA plasmid midiprep kit	Qiagen.
Guanidine HCl	Thermo Fisher.
HEPES	Sigma.
Lipofectamine 2000	Invitrogen.
Luciferase systems	Promega.
Neutral Buffered Formalin	Leica.
Nitrocellulose membrane	Bio-Rad.

PCR purification kit	Qiagen.
Polyinosinic:polycytidylic acid (poly(IC)).	InVivoGen.
Protein molecular weight markers	Promega.
Protein A-agarose beads	Roche.
Quantitative RT-PCR system	Bioline.
Resolving buffer for acrylamide gels	Protogel.
Stacking buffer for acrylaminde gels	Protogel.
Tetramethylethylenediamine (TEMED)	Protogel.
Trizol reagent	Invitrogen.
TrueBlue Peroxidase Substrate	Kirkegaard & Perry Laboratories, Inc.
X-ray film	Thermo Fisher.
Xylene	Genta Medical.

7.1.2 Enzymes

The following enzymes were supplied by the stated suppliers, and were used according to manufacturer's instructions unless otherwise stated:

DNA restriction endonucleases	New England Biolabs.
AMV Reverse Transcriptase	Promega.
Taq DNA polymerase	Invitrogen.
PFU DNA polymerase	Agilent.

DNase	Life Technologies.
T4 DNA ligase	New England Biolabs.
L-1-Tosylamide-2-phenylethyl chloromethyl ketone- -(TPCK)-treated bovine pancreatic trypsin	Sigma.
Trypsin acetylated from bovine pancreas (NAT)	Sigma.

7.1.3 Antibodies and dyes

Table 7.1. Primary antibodies and antisera raised against IAV proteins

Antibody	Application	Source/Reference
Rabbit polyclonal anti-PR8 NS1 (V29)	WB (1:500), IF (1:500), IP (1:100)	(Carrasco et al., 2004)
Rabbit polyclonal anti-O265B NS1 (A2)	WB (1:500), IP (1:100)	Custom made (Genosphere)
Rabbit polyclonal anti-PR8 NS1 (NS1-RBD)	WB (1:500), IF (1:250)	Custom made (Genosphere)
Rabbit polyclonal anti-PR8 NEP (V13)	WB (1:500), IP (1:100)	(Elton et al., 2001)
Rabbit polyclonal anti-PR8 M1 (2917)	WB (1:500)	(Amorim et al., 2007)
Rabbit polyclonal anti-PB1 (V19)	WB (1:500)	(Digard et al., 1989)
Rabbit polyclonal anti-MBP-PB2 (2N580)	WB (1:500)	(Carrasco et al., 2004)
Rabbit polyclonal anti-MBP-NP (2915)	WB (1:500), Plaque immunostaining (1:1000)	(Noton et al., 2007)
Mouse monoclonal anti-PR8 NP (AA5H)	IF (1:1000)	Abcam (abAA5H)
Rabbit polyclonal anti-PR8	IF (1:1000)	(Amorim et al., 2007)
Mouse monoclonal anti-M2 (ab5416)	WB (1:1000)	Abcam (ab5416)

Polyclonal rabbit antiserum raised against O265B NS1 (A2) and PR8 NS1-RBD (NS1-RBD) were custom made by Genosphere. A2 and NS1-RBD were raised by inoculating rabbits with a keyhole limpet hemocyanin (KHL)-peptide conjugate of sequence CGPPLPPKQKRYMARRV and CDRLRRDQKSLRGRGST respectively. Pre-immune serum/antiserum was provided in lyophilised form and reconstituted in sterile water as instructed by manufacturer.

To validate antisera A2 and NS1-RBD, infected cell lysates were analysed by western blot and probed with either antiserum or the corresponding pre-immune serum (Fig 7.1). The A2 antiserum detected avian A- and B-allele polypeptides (see lanes 3-13 in Fig 7.1A), but not WT PR8 NS1 (see lane 2). The A2 pre-immune serum did not detect NS1 in any sample above background levels. Successful infection was confirmed by detection of viral NP in all samples except the mock-infected. The NS1-RBD antiserum detected WT PR8 as well as consensus A- and B-allele avian NS1 (O175A and O265B) polypeptides (see lanes 2-4 of Fig 7.1B). As above, the pre-immune antiserum did not detect NS1 in any sample, and NP was only detected in viral-infected cell lysates and was not detected in mock-infected cells.

Table 7.2. Primary antibodies raised against cellular proteins.

Antibody	Application	Source
Rat monoclonal anti-alpha-tubulin	WB (1:1000)	Serotec (MCA77G), clone YL1/2
Rabbit polyclonal anti-Mx1 (N2C2)	WB (1:1000)	GeneTex GTX111153

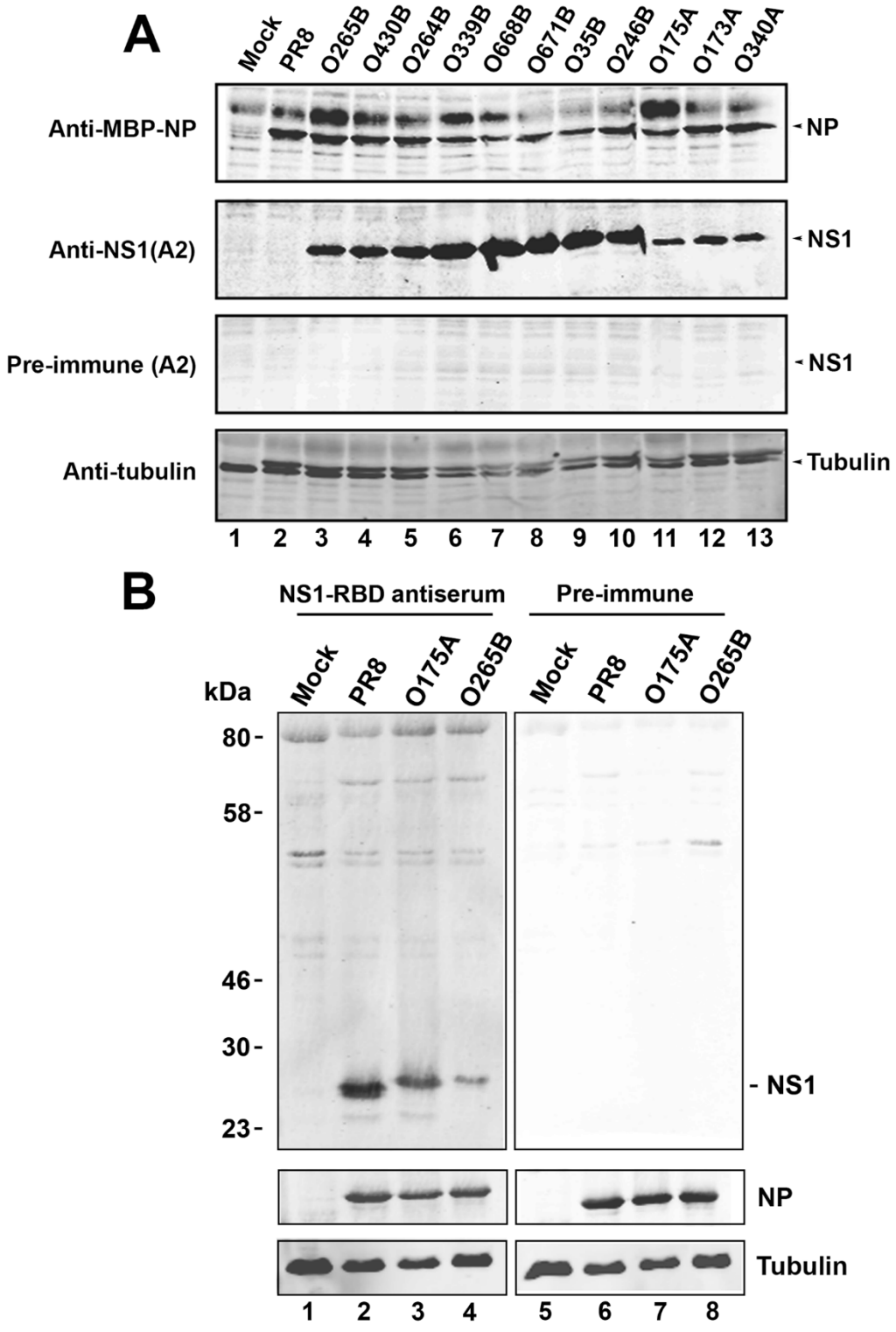

Fig 7.1. Validation of custom made anti-NS1 antisera. Western blot analysis of infected cell lysate ((A) MDCK cells and (B) A549 cells, MOI = 3, 8 h) was performed using antiserum and pre-immune serum in parallel at 1:500 dilution overnight at 4°C. Anti-MBP-NP was used to confirm successful infection. Anti-tubulin was used as a loading control.

Table 7.3. Primary antibody raised against GFP.

Antibody	Application	Source
Mouse monoclonal anti-GFP (JL8)	WB (1:5000)	Clontech 632380

Table 7.4. Secondary antibodies.

Antibody	Application	Source
Donkey anti-Mouse IgG (H+L) Secondary Antibody, Alexa Fluor® 488 conjugate	IF (1:1000)	Thermo Fisher (A-21202).
Donkey anti-Rabbit IgG (H+L) Secondary Antibody, Alexa Fluor® 488 conjugate	IF (1:1000)	Thermo Fisher (A-21206).
IRDye® 680LT Goat anti-Rat IgG (H + L)	WB (1:10000)	Li-Cor 925-68076
IRDye® 800CW Donkey anti-Mouse IgG (H + L)	WB (1:10000)	Li-Cor 925-32212
IRDye® 800CW Donkey anti-Rabbit IgG (H + L), 0.5 mg	WB (1:10000)	Li-Cor 926-32213
IRDye® 680LT Donkey anti-Mouse IgG (H + L)	WB (1:10000)	Li-Cor 925-68022
IRDye® 800CW Streptavidin	WB (1:2000)	Li-Cor 925-32230
Goat Anti-Rabbit IgG (H+L)-HRP Conjugate	Plaque assay (1:1000)	Bio-Rad 1721019.

Table 7.5. Fluorescent dyes.

Dye	Application	Source
ProLong Gold Antifade Mountant with DAPI	IF (neat)	Invitrogen
Hoechst 33342	IF (1:2000)	Thermo Fisher

7.1.4 Eukaryotic cell & bacterial culture medium

7.1.4.1 Eukaryotic cell culture

Media and additives used for culturing eukaryotic cells were purchased from the following suppliers:

Dulbecco's Modified Eagle Medium (D-MEM)	Sigma.
Fetal Bovine Serum (FBS)	Life Technologies.
L-Glutamine	Life Technologies.
Penicillin/Streptomycin	Life Technologies.
Geneticin	Life Technologies.
Blasticidin	InvivoGen.
Zeocin	InvivoGen.
0.25% Trypsin-EDTA	Life Technologies.
Calcium/Magnesium-free Phosphate Buffered Saline	Invitrogen.
Opti-MEM	Life Technologies.
RPMI-1640	Sigma.
Minimum Essential Medium	Gibco.
Methionine- and Cysteine-free D-MEM	Gibco.
Dialysed FBS	Life Technologies.

7.1.4.2 Bacterial Culture

Luria Broth (LB) and LB agar were made and provided by the Roslin Institute CSU.

Luria Broth	10 g/L tryptone, 5 g/L yeast extract, 5 g/L sodium chloride (pH 7.0).
LB agar	15 g/L agar, 10 g/L tryptone, 5 g/L yeast extract, 10 g/L sodium chloride (pH 7.0).

7.1.5 Eukaryotic cells

Madin-Darby Canine Kidney Cells (MDCK)	Sigma.
Human Embryonic Kidney 293T Cells (293T)	Sigma.
Human Adenocarcinomic Alveolar Basal Epithelial Cells (A549)	Sigma.
MDCK-Sialyltransferase 1 Cells (MDCK-SIAT)	Prof. John McCauley (The Francis Crick Institute, Mill Hill, London, UK).
Human Colorectal Adenocarcinomic Cells (CaCo-2)	Sigma.
HEK293-Blue IFN-α/β Cells (HEK-Blue)	InvivoGen.

7.1.6 Protein buffers and solutions

7.1.6.1 Lysis buffers

Laemmli's sample buffer	20% (v/v) glycerol, 2% (w/v) SDS, 100 mM DTT, 24 mM Tris, 0.016 % (v/v) bromophenol blue, 0.016% (v/v) xylene cyanol solution.

Tris-lysis buffer	50 mM Tris HCl (pH 8.0), 10% (v/v) glycerol, 0.5% (v/v) Nonidet P40, 200 mM sodium chloride, 1 mM DTT, 1 mM PMSF, 1 x protease inhibitor tablet (Fisher Scientific).
Guanidine HCl lysis buffer	6M Guanidine HCl, 50 mM HEPES.

7.1.6.2 Acrylamide gel electrophoresis

SDS-PAGE running buffer.	25 mM Tris, 192 mM glycine, 0.1% (w/v) SDS.
4 x resolving buffer (Protogel)	1.5 M Tris-HCl, 0.4 % (w/v) SDS, pH 8.8.
4 x stacking buffer (Protogel)	0.5 M Tris-HCl, 0.4 % (w/v) SDS, pH 6.8.
10% resolving polyacrylamide gel	3.33 ml 30% acrylamide:bisacrylamide (37.5:1), 2.5 ml 4 x resolving buffer, 4.06 ml water, 100 µl 10% (w/v) APS, 10 µl TEMED.
4% stacking polyacrylamide gel	1.3 ml 30 % acrylamide:bisacrylamide (37.5:1), 2.5 ml 4 x stacking buffer, 6.1 ml water, 50 µl 10% (w/v) APS, 10 µl TEMED.
Polyacrylamide gel fix solution	50% (v/v) methanol, 10% (v/v) acetic acid.

7.1.6.3 Western blotting

Protein transfer buffer.	25 mM Tris, 192 mM glycine, 0.1% (w/v) SDS, 20% (v/v) methanol.
Blocking solution	PBS/0.1% (v/v) Tween20, 5% (w/v) skimmed milk.

Wash buffer	PBS/0.1% (v/v) Tween20.

7.1.6.4 Pulldown buffers

Medium stringency IP buffer	100 mM KCl, 50 mM Tris-Cl pH 7.6, 5 mM $MgCl_2$, 1mM DTT, 1% (v/v) Triton X-100, 0.1% (w/v) SDS, 1% (w/v) sodium deoxycholate.
Low stringency IP buffer	100 mM KCl, 50 mM Tris-Cl pH 7.6, 5 mM $MgCl_2$, 0.1% (v/v) Nonidet P40.

7.1.7 Solutions and buffers for molecular cloning

7.1.7.1 Agarose gel electrophoresis

TAE running buffer was made and supplied by the Roslin Institute CSU.

TAE running buffer	40 mM Tris, 20 mM acetic acid, 1 mM EDTA.
6x DNA loading buffer	10 mM Tris-HCl (pH 7.6) 0.15% (w/v) Orange G dye, 0.03% (w/v) xylene cyanol FF, 60% (v/v) glycerol, 60 mM EDTA.

7.1.8 Other solutions and buffers

7.1.8.1 IHF buffers

Tris buffered saline (TBS)	15 mM Tris (pH 7.6), 137 mM sodium chloride.

Antigen retrieval buffer	10 mM sodium citrate (pH 6.0)/0.05% (v/v) Tween20.
Permeabilisation buffer	TBS/0.25% (v/v) Tween20.
Wash buffer	TBS/0.025% (v/v) Tween20.

7.1.9 Plasmids

Table 7.6. Plasmids.

Name	Description	Source
pDUAL	Reverse genetics plasmid. Bidirectional pol I and pol II promoters either side of insert lead to mRNA and vRNA-like RNA synthesis.	Gift from Prof. Ron Fouchier[a]
pHH21	Reverse genetics plasmid. Pol I promoter leads to vRNA-like RNA synthesis.	Gift from Prof. Robert Lamb[b]
pcDNA3.1	CMV pol II promoter upstream of insert leads to constitutively high protein expression	Gift from Prof. Robert Lamb[b]
pEGFP-N1	Constitutively expresses eGFP under control of CMV promoter. MCS upstream allows opportunity to clone C-terminally tagged proteins.	Clontech.
pRL	Constitutively expresses *Renilla* luciferase under control of SV40 promoter.	Gift from Dr. Finn Grey[c]
pPol I Luc	Reporter for RNP reconstitution assays. Contains firefly luciferase reporter gene in the reverse orientation and flanked by the UTRs of PR8 segment 8, under the control of a pol I promoter.	Gift from Prof. Laurence Tiley[d]
pIFN-β::Luc	Firefly luciferase under control of human IFN-β promoter.	Gift from Prof. Rick Randall[e]

Name	Description	Source
pISRE::Luc	Firefly luciferase under control of ISRE element.	Gift from Prof. Rick Randall[e]

[a] Erasmus University Medical Center, Rotterdam, Netherlands.

[b] Department of Molecular Biosciences, Northwestern University, Illinois, USA.

[c] The Roslin Institute, The University of Edinburgh, Edinburgh, UK.

[d] Department of Veterinary Medicine, The University of Cambridge, Cambridge, UK.

[e] Biomolecular Sciences Building, University of St. Andrews, St. Andrews, UK.

7.1.10 Viruses and reverse genetics systems

7.1.10.1 Reverse genetics systems

i) A/Puerto Rico/8/1934 (H1N1)

The eight-plasmid PR8 reverse genetics system was a kind gift from Prof. Ron Fouchier (Erasmus University Medical Center, Rotterdam, Netherlands) (de Wit et al., 2004).

Table 7.7. Reverse genetics system for A/Puerto Rico/8/1934 (H1N1).

Plasmid backbone	Segment	Accession number	Reference
pDUAL	PB2	EF467818	(de Wit et al., 2004)
	PB1	EF467819	
	PA	EF467820	
	HA	EF467821	
	NP	EF467822	
	NA	EF467823	
	M	EF467824	
	NS	EF467817	

ii) A/Udorn/1972 (H3N2)

The twelve-plasmid Udorn72 reverse genetics system was a kind gift from Prof. Robert Lamb (Department of Molecular Biosciences, Northwestern University, Illinois, USA).

Table 7.8. Reverse genetics plasmids for A/Udorn/1972 (H3N2).

Plasmid backbone	Segment	Accession number	Reference
pcDNA3.1	PB2	CY009643	(Chen et al., 2007)
	PB1	CY009642	
	PA	CY009641	
	NP	CY009639	
pHH21	PB2	CY009643	
	PB1	CY009642	
	PA	CY009641	
	HA	CY009636	
	NP	CY009639	
	NA	CY009638	
	M	CY009637	
	NS	CY009640	

iii) A/California/7/2009 (H1N1)

The Cal7 reverse genetics plasmids (pHW2000) were a kind gift from Prof. John McCauley (The Francis Crick Institute, Mill Hill, London, UK). Accession numbers of gene segments were not publically available at the time of writing this chapter.

7.1.10.2 A- and B- allele NS segment reverse genetics plasmids

NS reverse genetics plasmids are detailed in Table 7.9. pHH21 plasmids containing cDNA for LPAI NS segments were a kind gift of Prof. Jeffery Taubenberger (National Institute of Allergy and Infectious Diseases, Bethesda, Maryland, USA). cDNA corresponding to the NS segments of Alb88B, NY6750A, Sw412A, Sw418B, and NY107B was synthesised by Biomatik and cloned into the pDUAL vector (see below in *7.2.5.8 Cloning NS segments into pDUAL*). A/equine/Jilin/1/1989 (H3N8) (J89B) NS reverse genetics plasmid was a gift of Dr. Pablo Murcia (The Centre for Virus Research, The University of Glasgow, Glasgow, UK).

Table 7.9. Reverse genetics plasmids for A- and B- allele NS genes.

Short Name	Strain	Allele	Plasmid backbone	Accession number	Reference
O175A*	A/green-winged teal/Ohio/175/1986 (H2N1)	A	pHH21	CY018881.1	
O173A	A/mallard/Ohio/173/1990 (H11N9)	A	pHH21	CY021665.1	
O340A	A/green-winged teal/Ohio/340/1987 (H11N9)	A	pHH21	CY021873.1	
M1124A	A/mallard/Maryland/1124/2005 (H11N9)	A	pHH21	CY021473.1	
O265B*	A/Mallard/Ohio/265/1987 (H1N9)	B	pHH21	CY017279.1	
O430B	A/green-winged teal/Ohio/430/1987 (H1N1)	B	pHH21	CY011044.1	

Short Name	Strain	Allele	Plasmid backbone	Accession number	Reference
O264B	A/mallard/Ohio/264/1986 (H3N8)	B	pHH21	CY016399.1	
O339B	A/pintail/Ohio/339/1987 (H3N8)	B	pHH21	CY019201.1	
O668B	A/mallard/Ohio/668/2002 (H4N6)	B	pHH21	CY020793.1	
O671B	A/mallard/Ohio/671/2002 (H4N6)	B	pHH21	CY020801.1	
O35B	A/northern shoveler/Ohio/35/1986 (H3N8)	B	pHH21	CY020937.1	
O246B	A/bufflehead/Ohio/246/1986 (H11N2)	B	pHH21	CY017079.1	
Alb88	A/mallard/Alberta/88/1976	B	pDUAL	M25373.1	(Treanor et al., 1989)
NY6750	A/mallard/new york/6750/1978 (H2N2)	A	pDUAL	M25376.1	(Treanor et al., 1989)
Sw412	A/mallard/Sweden/S90412/2005(H6N8)	A	pDUAL	EU518721.1	(Munir et al., 2011b)
Sw418	A/mallard/Sweden/S90418/2005(H6N8)	B	pDUAL	EU518722	(Munir et al., 2011b)
NY107	A/New York/107/2003(H7N2)	B	pDUAL	EU587374.2	
J89B	A/Equine/Jilin/89/1/1989 (H3N8)	B	pDUAL	M65020.1	(Guo et al., 1992)

* O175A and O265B represent consensus A- and B-allele segments respectively.

7.1.11 Oligonucleotides

DNA oligonucleotides were synthesised by and purchased from Sigma.

Table 7.10. Sequencing primers.

Primer name	Sequence (5' to 3')	Description
pDUAL FP	ATGTCGTAACAACTCCGCCC	For sequencing from the 5' end of insert in pDUAL plasmid
pDUAL RP	TTTTTGGGGACAGGTGTCCG	For sequencing from the 3' end of insert in pDUAL plasmid
Uni 12	AGCAAAAGCAGG	Complementary to the 3' end of all IAV vRNA segments.
PD637	AGCAAAAGCAGGGTGAC	Complementary to 3' end of PR8 NS vRNA.
PD638	AGTAGAAACAAGGGTGTT TTTTAGTAC	Complementary to the 3' end of PR8 NS cRNA
A1643 FP	GCAACCGGTACCATGGACTCC AACACGATAACC	Complementary to 3' end of B-allele LPAI NS.
A1644 FP	GCAACCGGTACCATGGATTCC AACACTGTGTC	Complementary to 3' end of A-allele LPAI NS.
Alb88 NS FP	GCTATACGTCTCTGGGGAGCA AAAGCAGGGTGAC	For sequencing segment 8 cDNA of Alb88B, NY6750A, Sw412A, Sw418B, NY107B and J89B.
eGFPN1 FP	GGCGGTAGGCGTGTA	For sequencing insert from 5' end in pEGFPN1.

Table 7.11. Primers for NS1-GFP cloning.

Primer	Sequence (5' to 3')	Description
PR8 NS1-GFP Forward	GCAACCGGTACCATGGATCCAAACACTGTGTC	For cloning PR8 NS1 ORF with KpnI and AgeI restriction sites
PR8 NS1-GFP Reverse	GGTTGCACCGGTGTAACTTCTGACCTAATTGTTCC	
O265B NS1-GFP Forward	GCAACCGGTACCATGGACTCCAACACGATAACC	For cloning O265B NS1 ORF with KpnI and AgeI restriction sites
O265B NS1-GFP Reverse	GGTTGCACCGGTGTAACTTCTGACTCAACTCTTC	
O175A NS1-GFP Forward	GCAACCGGTACCATGGATTCCAACACTGTGTC	For cloning O175A NS1 ORF with KpnI and AgeI restriction sites
O175A NS1-GFP Reverse	GGTTGCACCGGTGTAACTTCTGACTCAATTGTTC	
O668B NS1-GFP Forward	GCAACCGGTACCATGGACTCCAACACGATAACC	For cloning O668B NS1 ORF with KpnI and AgeI restriction sites
O668B NS1-GFP Reverse	GGTTGCACCGGTGTAACTTCTGACTCAACTCTTC	
Alb88B NS1-GFP Forward	GCAACCGGTACCATGGATTCCAACACTGTAACC	For cloning Alb88B NS1 ORF with KpnI and AgeI restriction sites
Alb88B NS1-GFP Reverse	GGTTGCACCGGTGTAACTTCTGACTCAACTCTTCTCG	
NY6750A NS1-GFP Forward	GCAACCGGTACCATGGATTCCAACACTGTGTC	For cloning NY6750A NS1 ORF with KpnI and AgeI restriction sites
NY6750A NS1- Reverse	GGTTGCACCGGTGTAACTTCTGACTCAATTGTTCTCG	

Primer	Sequence (5' to 3')	Description
Sw412A NS1-GFP Forward	GCAACCGGTACCATGGATTCCAACACTGTGTC	For cloning Sw412A NS1 ORF with KpnI and AgeI restriction sites
Sw412A NS1-GFP Reverse	GGTTGCACCGGTGTAACTTCTGACTCAATTGTTCTCG	
Sw418B NS1-GFP Forward	GCAACCGGTACCATGGACTCCAACACGATAACC	For cloning Sw418B NS1 ORF with KpnI and AgeI restriction sites
Sw418B NS1-GFP Forward	GGTTGCACCGGTGTAACTTCTGACTCAACTCGTCTCG	
NY107B NS1-GFP Reverse	GCAACCGGTACCATGGACTCCAACACGATAACC	For cloning NY107B NS1 ORF with KpnI and AgeI restriction sites
NY107B NS1-GFP Forward	GGTTGCACCGGTGTAATTTCTGACTCAACTCTTCCCTC	
J89B NS1-GFP Forward	GCAACCGGTACCATGGATTCTAACACGACAACC	For cloning J89B NS1 ORF with KpnI and AgeI restriction sites
J89B NS1-GFP Reverse	GGTTGCACCGGTGTAACTTTTGGCTCAACTCGTC	

Table 7.12. Primers for cloning avian NS cDNA into pDUAL.

Primer name	Sequence (5' to 3')	Description
Alb88 NS Forward	GCTATACGTCTCTGGGGAGCAAAAGCAGGGTGAC	For cloning Alb88 segment 8 with BsmBI sites.
Alb88 NS Reverse	GGCGGCCGTCTCTTATTAGTAGAAACAAGGGTGTTTTTTAG	

NY6750 NS forward	GCTATACGTCTCTGGGGAGCAAAAGCAGGGTGAC	For cloning NY6750 segment 8 with BsmBI sites.
NY6750 NS reverse	GGCGGCCGTCTCTTATTAGTAGAAACAAGGGTGTTTTTTATC	
Sw412 NS forward	GCTATACGTCTCTGGGGAGCAAAAGCAGGGTGAC	For cloning Sw412 segment 8 with BsmBI sites.
Sw412 NS reverse	GGCGGCCGTCTCTTATTAGTAGAAACAAGGGGGTTTTTTATC	
Sw418 NS forward	GCTATACGTCTCTGGGGAGCAAAAGCAGGGTGAC	For cloning Sw418 segment 8 with BsmBI sites.
Sw418 NS reverse	GGCGGCCGTCTCTTATTAGTAGAAACAAGGGTGTTTTTTAG	
NY107 NS forward	GCTATACGTCTCTGGGGAGCAAAAGCAGGGTGAC	For cloning NY107 segment 8 with BsmBI sites.
NY107 NS reverse	GGCGGCCGTCTCTTATTAGTAGAAACAAGGGTGTTTTTTAG	

Table 7.13. Primers for reverse transcription.

Primer name	**Sequence (5' to 3')**	**Description**
Uni 12	AGCAAAAGCAGG	Complementary to the 5' end of vRNA of all IAV segments.
PD637	AGCAAAAGCAGGGTGAC	Complementary to the 5' end of PR8 segment 8 vRNA and also efficient for LPAI NS segments despite mismatches.

Table 7.14. Primers for RT-PCR based competition assay.

Primer name	Sequence (5' to 3')	Description
O175A NS1 FP	GCAACCGGTACCATGGACT CCAACACGATAACC	Designed to specifically amplify the NS1 ORF of O265B.
O175A NS1 RP	GGTTGCACCGGTGTAACTT CTGACTCAACTCTTC	
O265B NS1 FP	GCAACCGGTACCATGGATT CCAACACTGTGTC	Designed to specifically amplify the NS1 ORF of O175A.
O265B NS1 RP	GGTTGCACCGGTGTAACTT CTGACTCAATTGTTC	

Table 7.15. Primers for RT-qPCR of O175A and O265B vRNA levels in infected cells.

Primer name	Sequence (5' to 3')	Description
qO175A-FP	CTCCAAAGCAGAAACGGAAA	Designed to specifically amplify cDNA from O175A vRNA in RT-qPCR.
qO175A-RP	TCTTGCTCCACTTCAAGCAG	
qO265B-FP	AATCCTCATCGGTGGACTTG	Designed to specifically amplify cDNA from O265B vRNA in RT-qPCR.
qO265B-RP	TCTGCTCGAAGCTGTTCTCA	

7.1.12 Drugs

Excludes antibiotics used in eukaryotic cell culture as detailed above in *7.1.4.1 Eukaryotic cell culture*.

Ampicillin sodium salt used at 100 µg/µl Sigma.

Kanamycin sulfate salt used at 50 µg/µl Gibco.

Human recombinant IFN-β Abcam.

Human recombinant IFN-α 2a Abcam.

7.1.13 Radiochemicals

[^{35}S]-L-methionine and [^{35}S]-L-cysteine protein labelling mix Perkin-Elmer.

[^{14}C] Protein Molecular Weight Marker Perkin-Elmer.

7.2 Methods

7.2.1 Ethics statement

The following ethics statement was provided by Prof. Bernadette Dutia (The Roslin Institute, The University of Edinburgh, Edinburgh, UK): All animal experiments were carried out under the authority of a UK Home Office Project Licence (held by Prof. Bernadette Dutia at the Roslin Institute, The University of Edinburgh, Edinburgh, UK (60/4479)) within the terms and conditions of the strict regulations of the UK Home Office 'Animals (scientific procedures) Act 1986' and the Code of Practice for the housing and care of animals bred, supplied or used for scientific purposes. Ethical approval for experiments using human macrophages was obtained from the Lothian Research Ethics Committee (11/AL/0168). All subjects provided written informed consent at each donation.

7.2.2 Cell culture

7.2.2.1 Eukaryotic cell culture medium

i) **Complete D-MEM**: D-MEM supplemented with 10% (v/v) FBS, 2mM glutamine, 100 U/ml penicillin, and 100 μg/ml streptomycin.

ii) **Serum-free D-MEM**: Complete D-MEM with no added FBS.

7.2.2.2 Cell culture and manipulation

MDCK cells, 293T cells, A549 cells, and CaCo-2 cells were all grown in complete D-MEM at 37°C in 5% CO_2. MDCK-SIAT cells were cultured in complete D-MEM with 1mg/ml Geneticin. HEK-Blue cells were cultured in complete D-MEM supplemented with 30 μg/ml blasticidin and 100 μg/ml Zeocin. Cells were typically passaged twice weekly: cells were washed twice (once for 293T and HEK-blue) with PBS and dissociated using a 0.25% trypsin-EDTA solution (or Mg and Ca ion-free PBS for HEK-Blue). Cells were resuspended in complete D-MEM and typically split 1 in 10.

Primary CD14+ human monocytes were isolated from whole blood by Dr. Alasdair Jubb, Dr. Malcolm Fisher (both of the Prof. David Hume laboratory, the Roslin Institute, the University of Edinburgh, Edinburgh, UK) and Dr. Sara Clohisey (of the Dr. Ken Baillie laboratory, The Roslin Institute, The University of Edinburgh, Edinburgh, UK) as described below in *7.2.2.4 Isolation of human CD14+ monocytes*. Monocytes were plated in 24-well plates in RPMI supplemented with 10% (v/v) FBS, 2 mM glutamine, 100 U/ml penicillin, 100 μg/ml streptomycin and 104 U/ml (100 ng/ml) recombinant human (rh)CSF-1 (a gift from Chiron, Emeryville, California, USA) for 7 days for differentiation into macrophages. Infections were performed on day 8.

7.2.2.3 Cell counting

Cells were counted using a Neubauer cell counting chamber. Typically, 9 μl of cell suspension was added to each side of the chamber under a glass cover slip. Using a light microscope, the number of cells was counted in the designated 4 x 4 grid and

cell concentration was estimated (cell concentration (cells/ml) = number of counted cells x 10^4).

7.2.2.4 Isolation of human CD14$^+$ monocytes

All subjects provided written consent before donating blood, and samples were kept anonymous during research and labelled with a unique ID number that could be traced back to the subject.

Human CD14$^+$ monocytes were kindly isolated and provided by members of the Prof. David Hume and Dr. Ken Baillie laboratories as described above, which were isolated as described in (Irvine et al., 2009). Fresh blood was centrifuged (1200 x *g*, 5 min) without a brake to prevent disruption of cells. The plasma was removed by pipette, and the buffy coat was aspirated. Typically, 20 ml of buffy coat was obtained per sample. The 20 ml buffy coat was diluted to a total volume of 50 ml with RPMI media, gently laid over two 15 ml preparations of Ficoll (GE Healthcare), and centrifuged at room temperature with no brake (200 x *g*, 45 min). The uppermost layer (RPMI) was removed. The mononuclear cell layer was aspirated and washed with RPMI media (added to a total volume of 50 ml) by centrifugation (300 x *g*, 10 min). The cell pellet was resuspended in 10 ml of PBS, counted, and centrifuged (400 x *g*, 10 min, 10°C). The supernatant was removed and the cells were resuspended in 40 µl MACS buffer (PBS/2 mM EDTA and 0.5% (v/v) FBS) per 10^7 total cells. 10 µl of CD14 microbeads (Miltenyi Biotec) per 10^7 total cells were added and incubated at 4°C on an orbital shaker. 50 ml of chilled MACS buffer was added and this was centrifuged (400 x *g*, 5 min, 4°C). Supernatant was removed and cells were resuspended in 500 µl MACS buffer per 10^8 total cells. Magnetic separation columns (Miltenyi Biotec) were prepared by running through 3 ml of MACS buffer. 3 ml of

cell suspension was run through the magnetic separation column. The column was washed three times with 3 ml MACS buffer. Cells were eluted by running through 5 ml MACS buffer and applying plunger force. Cells were counted, centrifuged (400 x *g*, 5 min, 4°C), washed with 10 ml PBS and centrifuged (400 x *g*, 5 min, 4°C). Supernatant was removed and cells were resuspended and plated in culture medium as described above in *7.2.2.2 Cell culture and manipulation*.

7.2.3 Virus work

7.2.3.1 Virus culture medium and solutions

i) **Virus growth medium**: D-MEM supplemented with 2 mM glutamine, 100 U/ml penicillin, 100 µg/ml streptomycin, 0.14% (w/v) BSA, and 1 µg/ml TPCK-treated trypsin.

ii) **Reverse genetics medium**: Virus growth medium with 5 µg/ml TPCK-treated trypsin.

iii) **Acid wash buffer**: 10 mM HCl, 150 mM NaCl (pH 3.0).

7.2.3.2 Generation of P_0 stocks

Reverse genetics plasmid sets were transfected into 293T cells in 6-well plates using Lipofectamine2000 reagent (Invitrogen). Reverse genetics plasmids (250 ng each for PR8 and Cal7 systems, 500 ng each for Udorn72) were diluted in 100 µl Opti-MEM. 4 µl Lipofectamine2000 was mixed with 100 µl Opti-MEM medium (or 6 µl in 100 µl for Udorn72) for 10 min then incubated with diluted DNA for 30 min. 293T cells were harvested (a T75 flask resuspended in 25 ml complete D-MEM) and 1 ml was added to each well of a 6-well plate. The transfection mix was added dropwise over 293T cells in suspension. 16 h post-transfection, the medium was changed to 1.6

ml reverse genetics medium. Following a 48 h incubation, supernatants were collected and stored at -80°C as P_0 stocks.

7.2.3.3 Generation of P_1 stocks

MDCK cells were seeded in T25 flasks. When fully confluent, cells were washed twice with 10 ml serum-free D-MEM. 100 µl of P_0 stock was diluted in 1 ml reverse genetics medium. The serum-free D-MEM wash was removed from the cells, and 1 ml of diluted P_0 stock was added. Cells were incubated for 1 h at 37°C and 5 ml of reverse genetics medium added. Cells were incubated at 37°C for 48 h. Supernatants were clarified by centrifugation (3000 rpm, 5 min) and stored at -80°C in 0.5 ml or 1 ml aliquots. Virus titration was always performed after one freeze-thaw cycle to account for loss of infectivity.

7.2.3.4 Egg grown virus stocks

Embryonated chicken eggs (Henry Stewart & Co.) were incubated at 37°C, 40-50% humidity, for 10 days and were candled to check viability of embryo prior to infection. Virus was diluted to 10^4 PFU/ml in serum-free D-MEM. A small hole was punctured in the egg shell just below the line of the air sac. The shell was sterilised with 70% (v/v) ethanol and, using a 1 ml syringe and 25 G needle, 100 µl of diluted virus stock was gently inoculated into the allantoic cavity. The puncture was then sealed with Scotch Magic Tape and eggs were incubated at 37° C, 40-50% humidity, for 48-72 h.

Eggs were culled by chilling overnight at 4° C. The top of the shell was removed using forceps, and the air sac membrane punctured using a P1000 Gilson tip.

Allantoic fluid was collected using a P1000 Gilson, clarified (4000 rpm, 10 min), and stored in 0.5-1 ml aliquots at -80°C.

7.2.3.5 Virus infections

Cells were typically plated the day prior to infection to achieve approximately 90% confluency (unless otherwise stated) on the day of infection. Cells were washed with serum-free D-MEM to remove FBS. Virus stocks were diluted in serum-free D-MEM and were applied to cells in a low volume (e.g. 200 µl for 24-well plate format) for 1 h at 37ºC. For multicycle infections, cells were overlaid with virus growth medium. For single-cycle infections, inoculum was aspirated, acid wash buffer was applied for 1 min to inactivate non-internalised particles, and cells were washed three with PBS prior to overlay with serum-free D-MEM. For infections to be analysed using immunofluorescence or proteomics, cells were overlaid with complete D-MEM. Supernatants were clarified (3000 rpm, 5 min) and stored at -80°C prior to downstream analyses.

7.2.3.6 Plaque assays – PR8 and Udorn72

MDCK cells were seeded in 6-well plates the day prior to plaque assay to achieve 100% confluency the next day. Typically, this was achieved by seeding 4 x 10^6 cells per well in a 2 ml volume of complete D-MEM. Cells were washed with 2 ml serum-free D-MEM. Virus samples were serially diluted ten-fold in serum-free D-MEM. 400 µl of virus dilution was applied to each well and incubated for 1 h at 37°C. After incubation, 2 ml of overlay was added to each well. For Avicel overlay, virus growth media was supplemented with 1.2% (w/v) Avicel. For 0.6% agarose plaque assays, 2% (w/v) agar was boiled and incubated at 55° C, and 7.5 ml was mixed with 17.5 ml of an MEM solution (0.3% (w/v) BSA fraction V, 0.2% (v/v) Sodium

Bicarbonate, 10 mM HEPES, 0.007% (w/v) Dextran, 3 mM L-Glutamine, 140 U/ml penicillin, 140 µg/ml streptomycin, and 1.4 µg/ml NAT) incubated at 37°C. Virus inoculum was aspirated and 2 ml of agarose overlay was added per well. After agarose had set, plates were incubated upside down at 37°C.

Unless otherwise stated, plaque assays were incubated at 37°C for 48 h. For fixing and staining, 2 ml of 10% neutral buffered formalin was added per well and incubated for 20 min – 24 h. The formalin and remaining overlay were removed and cells stained with 0.1% (w/v) toluidine blue for 20 min – 6 h. Toluidine blue stain was removed and cells were washed with water prior to plaque counting and titre calculations. For plaque purification, live cellular debris/agarose was taken up using a P1000 Gilson by scraping isolated plaques and aspirating agarose. This material was then ejected onto a monolayer of fresh MDCK cells in 24-well plates under 0.5 ml virus growth medium. Cells were incubated at 37°C for 24 h to allow virus amplification.

7.2.3.7 Plaque assays – Cal7

Plaque assays for Cal7 backbone viruses were performed essentially as described above in *7.2.3.6 Plaque assays – PR8 and Udorn72*, but using MDCK-SIAT cells and a modified overlay: serum-free D-MEM with 1 µg/ml TCPK-treated trypsin and 0.8% (w/v) Avicel. Cells were immunostained for intracellular NP:

Cells were fixed by adding 2 ml of 10% NBF per well and incubating for 30 min. Overlay was removed and cells were washed with 2 ml PBS per well. Cells were permeabilised with 1 ml PBS/0.2% (v/v) Triton X-100 per well for 10 min. Cells were washed twice with PBS and incubated with 0.5 ml per well A2915 rabbit polyclonal

anti-MBP-NP diluted 1:1000 in PBS/2% (w/v) BSA fraction V for 1 h at room temperature on a rocker. Cells were washed twice with PBS and then incubated with 0.5 ml per well with a goat anti-rabbit IgG-HRP conjugated secondary antibody diluted to 1:1000 in PBS/2% (w/v) BSA fraction V for 1 h at room temperature on a rocker. Cells were washed three times with PBS and 0.5 ml per well of TrueBlue peroxidase substrate was added. Cells were incubated at room-temperature until plaques were visible with blue staining. Cells were then washed with water, allowed to dry, and plaques counted.

7.2.3.8 Virus RNA extraction from supernatant of infected cells

Virus RNA was extracted using Trizol reagent (Invitrogen). Typically, 750 µl of Trizol reagent was added to 250 µl of infected cell supernatant and mixed thoroughly. Lysates were typically stored overnight at -80°C. 200 µl of chloroform was added, mixed extensively, and incubated at room temperature for 5 min. Samples were centrifuged at full speed in a standard microcentrifuge machine at 4°C for 20-30 min. The aqueous layer, containing RNA, was transferred to a clean microcentrifuge tube. RNA was precipitated by adding 500 µl isopropanol, mixing, and incubating at -20° C for 30 min. Samples were centrifuged at 13000 rpm for 20 min at 4°C. The isopropanol was removed and RNA was washed with 500 µl 70% (v/v) ethanol. Samples were centrifuged at 13000 rpm for 5 min at 4°C, and the ethanol wash removed. At this point, RNA was either resuspended in 44 µl water and stored at -80°C or, if sequencing of P_1 stocks was desired, treated with DNase to remove potential residual plasmid carryover from P_0 generation. DNase treatment was performed using TURBO DNase (Life Technologies) in a 50 µl reaction (as instructed by manufacturer) for 15 min at room temperature. To stop the reaction and purify the

RNA, 200 µl of water was added, and RNA was purified by performing another round of phenol:chloroform extraction: 250 µl of phenol:chloroform:isoamyl alcohol (25:24:1, Sigma), was added and mixed well, and samples were centrifuged (15000 rpm, 4°C, 5 min). 250 µl chloroform was added, mixed well, and samples were centrifuged again (15000 rpm, 4°C, 5 min). The aqueous layer was transferred to a clean microcentrifuge tube. 625 µl of ethanol and 25 µl of 3 M sodium acetate (pH 5.2) was added, mixed, and incubated at -20°C for 10 min. Samples were centrifuged (15000 rpm, 20 min, 4° C), the ethanol & sodium acetate removed, and a wash was performed by adding 500 µl 70% (v/v) ethanol and centrifuging the sample (15000 rpm, 5 min, 4°C). The ethanol wash was removed, the RNA was resuspended in 15 µl water, and samples stored at -80°C prior to downstream analysis.

7.2.3.9 Viral RNA extraction from infected cells

Typically, cells were washed with PBS and 200 µl Trizol reagent was added to a 24-well. RNA extraction was performed as described above in *7.2.3.8 Virus RNA extraction from supernatant of infected cells* using appropriately adjusted volumes of chloroform and isopropanol.

7.2.3.10 Virus sequencing

Viral RNA was extracted from P_1 stocks (infected cell supernatants or egg allantoic fluid) using Trizol reagent as described above. 4 µl of resuspended RNA was used in a reverse transcriptase reaction using AMV RTase (Promega). 4 µl of 10 µM RT primer was annealed to the RNA in a 10 µl volume by heating at 75°C for 5 min, and then immediately placing on ice for 2-5 min. A 25 µl reaction was set up with 1 x AMV RTase buffer (Promega), 1 mM (each) dNTPs, and 5 units AMV RTase. The

reaction was incubated at 42° C for 1 h. The AMV RTase was deactivated by heating at 75° C for 10 min. cDNA was stored at -20° C or used immediately.

3 µl of cDNA product was amplified using PCR prior to sequencing. Taq DNA polymerase was employed in a 25 µl reaction containing 1.5 mM magnesium chloride, 1 x Taq PCR buffer (Invitrogen), 200 nM forward primer, 200 nM reverse primer, 250 µM (each) dNTPs, and 2.5 units Taq DNA polymerase. Thermocycling conditions were adjusted depending on target amplicon. Typically, a primer annealing temperature of Tm – 5° C (for primer with lowest Tm) was employed, and a range of annealing temperatures were tested for new primer:template combinations. The following describes thermocycling conditions for amplification of WT PR8 NS segment cDNA with PD637 and PD638 primers: Initial denaturation of template DNA was performed by heating at 94° C for 2 min. Then, 30 cycles of a 1 min 94°C denaturation step, a 1 min 50°C primer annealing step, and a 3 min 72°C amplicon elongation step were performed. After 30 cycles of the above, a 10 min 72°C amplicon elongation step was performed and reaction cooled to 4°C. Product was stored at -20°C or purified immediately. PD637 and PD638 (Table 7.10) were efficient at amplifying B-allele NS segment cDNA, but not A-allele NS cDNA. A-allele segment 8 cDNA was successfully amplified using PD637 and A1644 RP (Table 7.10). Alb88B, NY6750A, Sw418B, and NY107B were amplified using terminal primers described in Table 7.12.

Before sequencing, PCR product was purified by column purification using QIAGEN's QIAquick PCR Purification kit (cat# 28104) as described in manufacturer's instructions. PCR product was eluted with 30 µl water. 5 µl of purified

PCR product was added to 5 µl of 5µM appropriate forward primer (see Table 7.10). Sanger sequencing of cDNA was performed by GATC.

7.2.3.11 Competition Assays

i) Validation of primers in RT-PCR

To test the specificity of primers designed to be specific for the NS1 ORF of O175A (O175A NS1 FP and O175A NS1 RP) and O265B (O265B NS1 FP and O265B NS1 RP) cDNA (Table 7.14), PCR was set-up with Taq DNA polymerase (as described above in *7.2.3.10 Virus sequencing*) using pHH21 plasmids for O175A and O265B with the O175A and O265B primer pairs. Initial PCR conditions tested were i) 94°C: 5min, ii) 94°C: 30 sec, iii) 50°C: 30 sec, iv) 72°C: 2 min, v) 72°C 10 min (40 cycles of ii, iii and iv) : Strong amplification was only detected in homologous primer-template pairings (Fig 7.2). To test the specificity of primers following plaque purification, the same primer-template pairings and PCR conditions were tested following plaque purification, RNA extraction, and RT of segment 8 vRNA (using PD637 primer) for both O175A and O265B. Primer specificity was only optimally achieved following modifications of the PCR cycling conditions to increase the primer annealing temperature and reduce the number of cycles due to undesirable background (Fig 7.2). Optimal cycling conditions were: i) 94°C: 2 min, ii) 94°C: 1 min, iii) 62°C: 1 min, iv) 72°C: 3 min, v) 72°C: 10 min (30 cycles of steps ii, iii and iv). Therefore, primer specificity was confirmed and competition assays could be performed.

ii) Competition assays.

MDCK cells were infected with equal PFU of two viruses in a multicycle setup (MOI 0.001 each, 48 h) or a single-cycle setup (MOI 3 each, 16 h). The progeny virus

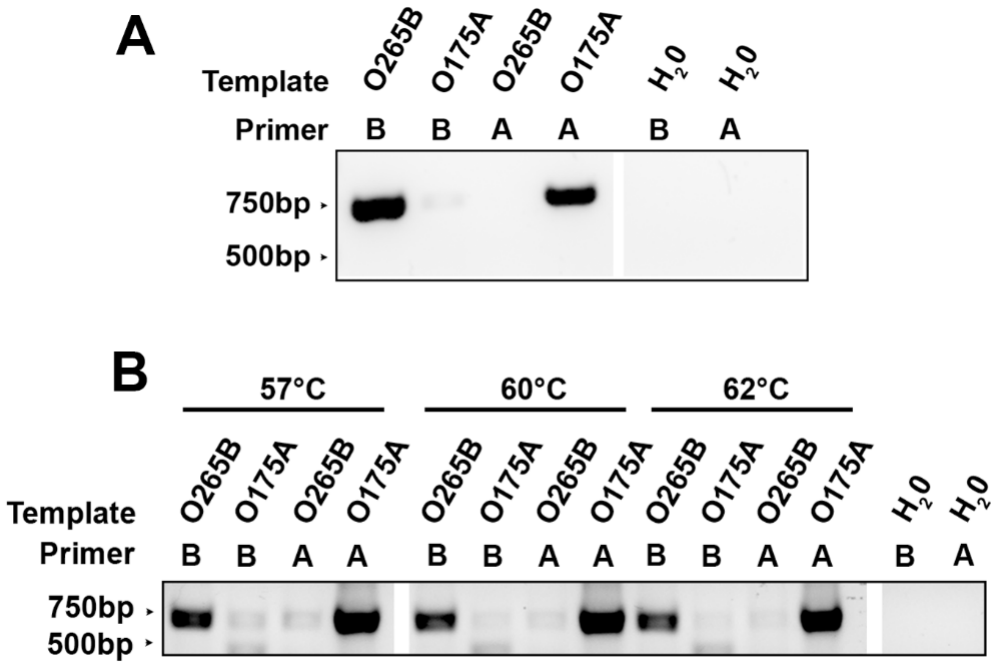

Fig 7.2. Validation of primers for competition assay. (A) Primers were tested in PCR on O175A and O265B NS1 ORFs in pHH21 plasmids. (B) Primers were tested in RT-PCR following plaque purification of O175A and O265B viruses, RNA extraction, and reverse transcription of NS vRNA using PD637 primer. Temperatures denote primer annealing temperatures tested in RT-PCR. 'A' and 'B' represent O175A and O265B NS1 ORF primers respectively.

was subjected to plaque assay under a 0.6% agarose overlay for 48 h**.** Individual plaque picks were amplified in MDCK cells by transferring cellular debris and agarose to fresh MDCK cells under 0.5 ml of virus growth medium in 24-well plates. After 24 h, viral RNA in the supernatant was extracted using Trizol Reagent (Life Technologies) as described above and the cells were lysed in Laemmli's sample buffer. To identify the source of segment 8, cDNA was synthesised as described above using PD637 primer and RT-PCR was performed using Taq DNA polymerase (Invitrogen) with primers specific for the NS1 ORF of O175A and O265B as described above. Alternatively, the NS1 content of cell lysates was analysed by SDS-PAGE and western blotting, using the differential reactivity of rabbit polyclonal antisera V29 (detects PR8 and O175A NS1) and A2 (detects O175A and O265B NS1) to score plaque picks. Typically, 25 plaques were scored for each assay. Where passaging of output was involved, the progeny virus mix was infected in MDCK cells at MOI 0.001 for 48 h.

7.2.3.12 RT-qPCR of O175A and O265B NS segment vRNA

RT-qPCR to quantify O175A and O265B vRNA levels in co-infected cells was performed using the SensiFAST SYBR Hi-ROX system (cat# BIO92005, Bioline). Primers specific for the cDNA derived from O175A and O265B NS segment vRNA (Table 7.15) were designed using Primer3 online software (http://bioinfo.ut.ee/primer3-0.4.0/primer3/) to achieve parameters recommended by manufacturer (amplicon length 80 - 200 bp, Tm ~ 60°C). Primers were validated by testing primer pairs in triplicate on a 10-fold dilution series of pHH21 plasmids (100 ng to 0.0001 ng) for both O175A and O265B NS sequences to assess specificity. RT-qPCR was set up as recommended by manufacturer and run on a Qiagen Rotor-Gene Q thermocycler machine with Rotor-Gene Q Series software (v2.1.0) using a three-

step cycling set-up (initial polymerase activation step of 3 min at 95°C, followed by 40 cycles of a 20 sec 95°C step to denature dsDNA, 20 sec at 60°C for primer annealing, and 20 sec at 72°C after which SYBR Green fluorescence was read. This was followed by a 50°C to 99°C melt analysis as programmed by software) based on recommendations by Bioline for the SensiFAST SYBR Hi-ROX system. Amplification was only detected within 30 cycles with homologous primer-template matches, therefore O175A and O265B primers were specific to their respective targets (data not shown). Additionally, amplicon quantification increased linearly with 10-fold increases in pHH21 template amount, suggesting accurate quantification of template with these primers (data not shown). Melt analysis results showed no obvious amplification of a second amplicon for both primer pairs on respective templates (data not shown).

To assess the relative values of O175A and O265B vRNA in co-infected cells, total RNA was extracted from co-infected (or infected with one strain only) MDCK cells (as described in *7.2.3.9 Viral RNA extraction from infected cells*) and quality of preparations were assessed by a NanoDrop ND-1000 spectrophotometer and contaminants removed using sodium acetate precipitation and ethanol wash as described below in *7.2.5.4 Spectrophotometer analysis of nucleic acid preparations*. cDNA synthesised from vRNA using the Uni12 primer using equal amounts of total RNA (1 µg) was performed using AMV RTase (Promega) as described above in *7.2.3.10 Virus sequencing*. RT-qPCR was set up as above including a set of pHH21 standards at three quantities in triplicate (100 ng, 10 ng, 1 ng) and the cDNA samples were run at 10^{-1} and 10^{-2} dilutions with both O175A- and O265B-specific primers in triplicate. Amplification of control infections (O175A or O265B only) was only

detected within 30 cycles in homologous primer-template samples, demonstrating adequate primer specificity (data not shown). Similarly, no RT and no template controls did not show amplicon amplification within 30 cycles of PCR (data not shown). Threshold levels and Ct values were calculated by the Rotor-Gene Q Series software (v2.1.0). The quantities of pHH21 standards were entered into the Rotor-Gene Q Series software (v2.1.0) and subsequent quantification of O175A and O265B vRNA levels per sample were calculated by the software based on these standards.

7.2.3.13 RNP reconstitution assays

2 x 10^5 293T cells were seeded in 1 ml complete D-MEM per well of a 24-well plate to achieve 70-80% confluency the following day for transfection. 50 ng of pDUAL plasmids for each of the IAV polymerase components (PB2, PB1, PA, NP) and the NS segment were added to 20 ng of firefly reporter construct (pPol I Luc). The plasmid DNA mix was diluted in 50 µl Opti-MEM. 1 µl lipofectamine2000 was mixed with 50 µl of Opti-MEM per transfection, and incubated at room temperature for 5-10 min at room temperature. 51 µl of lipofectamine2000/Opti-MEM mix was added to each sample, mixed, and incubated for 30 min. The media for the 293T cells was removed and replaced with 0.5 ml Opti-MEM per well. 100 µl of transfection mixture was added dropwise to each well. Cells were incubated at 37° C for 48 h.

The media was gently removed and cells were lysed with 100 µl 1 x Reporter Lysis Buffer (Promega). Cells were scraped and mixed with a P200 Gilson tip and cell lysates were centrifuged (12000 x *g*, 2 min, 4°C). 60 µl of cell lysate was added to a white-bottomed 96-well plate and kept on ice. A Promega GloMax Multi Detection unit was employed to inject 25 µl of 0.6 mM beetle luciferin (Promega) per well, and

to measure the luciferase activity (injection speed 200 µl/sec, 0.5 sec gap, 5 sec integration time) following manufacturer's instructions.

7.2.3.14 NS1 pol II shut-off assays

2 x 10^5 293T cells were seeded in 1 ml complete D-MEM in 24-well plates (with 13 mm glass coverslips for samples to be analysed by IF) to achieve 70-80% confluency the following day for transfection. 100 ng of pRL was mixed with 400 ng of effector plasmid (pEGFPN1 or pDUAL with relevant insert), and diluted with 50 µl Opti-MEM. 1 µl lipofectamine2000 reagent was mixed with 50 µl Opti-MEM and incubated for 5-10 min. 51 µl of the Lipofectamine2000/Opti-MEM mixture was mixed with the diluted plasmid DNA and incubated for 30 min. The media on the 293T cells was changed to 400 µl transfection medium (complete D-MEM minus antibiotics) per well, and 100 µl of transfection mixture was added dropwise. Cells were incubated for 48 h. Successful transfection, and efficiency, was gauged by fluorescent microscopy for NS1-GFP fluorescence. Cells were transfected in triplicate.

Renilla luciferase expression was quantified using Promega's Renilla Luciferase Assay kit (cat# E2810), using a Promega GloMax Multi Detection Unit as instructed by manufacturer. Briefly, the cells were washed gently with 1 ml PBS. The cells were subsequently lysed in 100 µl 1 x lysis buffer and rocked for 15 min. Cells were scraped, mixed, and collected on ice using a P200 Gilson. 20 µl of cell lysate was added to a white-bottomed 96-well plate. 100 µl of 1 x Renilla luciferase substrate was injected (200 µl/sec, 2 sec delay, 10 sec integration time) and luminescence measured.

7.2.4 Protein analyses

7.2.4.1 Protein Electrophoresis

Proteins were separated by molecular weight by sodium dodecyl sulphate polyacrylamide gel electrophoresis (SDS-PAGE) using a discontinuous polyacrylamide gel. All SDS-PAGE apparatus was supplied by Bio-Rad (Mini-PROTEAN tetra system). Polyacrylamide gels were cast using buffers and solutions supplied by Protogel according to manufacturer's instructions, altering the concentration of acrylamide:bisacrylamide (37.5:1) solution to achieve desired percentage for resolving gel – large proteins requiring a lower percentage resolving gel to be efficiently resolved and vice versa. Stacking gels were cast at 4%. See *7.1.6.2 Acrylamide gel electrophoresis* for example recipes for 10% resolving gels and 4% stacking gels. 0.75 mm spacer plates were used with appropriate short plates.

To generate cell lysates, typically 4 x 10^5 cells in a 24-well plate were lysed with 200 µl of Laemmli's solution. Samples were boiled at 95°C for 5 min, vortexed for 5 sec, centrifuged briefly, boiled for a second time and centrifuged at 13 000 rpm for 5 min. 4-20µl of sample was loaded per lane of each gel. Gels were run vertically at a constant voltage of 120V for desired length of time, using a pre-stained protein molecular weight marker (Promega) as a guide for protein migration.

7.2.4.2 Western Blotting

Proteins separated by SDS-PAGE were blotted onto nitrocellulose membrane (Bio-Rad) using a wet electroblotting setup (Bio-Rad). The nitrocellulose membrane was placed onto the polyacrylamide gel (on the positive cathode side) supported by 3 pieces of 3MM Whatman paper either side, and placed between two sponges inside a cassette. The cassette was loaded into a tank and submerged in transfer buffer. Protein

transfers were run at 100 V for 1 h. Nitrocellulose membranes were blocked in PBS/0.1% (v/v) Tween20 with 5% (w/v) skimmed milk (Marvel) for 30 min on a platform rocker. Blocked membranes were washed three times with PBS/0.1% (v/v) Tween20 before probing with primary antibody, diluted in PBS/0.1% (v/v) Tween20. Primary antibody incubation was typically performed overnight at 4°C or for 1 h at room temperature with rocking. Membranes were washed three times as above, and secondary antibody, diluted in PBS/0.1% (v/v) Tween20, was added for 45 min at room temperature on a platform rocker. Membranes were washed three times with PBS/0.1% (v/v) Tween20 before imaging on the LiCor Odyssey imaging platform.

7.2.4.3 ^{35}S-methionine/cysteine- labelled protein immunoprecipitation

For immunoprecipitation studies, MDCK cells were seeded in 24-well plates and infected at an MOI of 10 as described in *7.2.3.5 Virus infections* with ^{35}S metabolic labelling as described in *7.2.8.1 $^{35S\text{-}methionine}$/cysteine metabolic labelling of infected cells*. Cells were lysed in 500 µl medium stringency IP buffer. Cells were scraped, collected, and clarified (13000 rpm, 5 min, 4°C). 100 µl of clarified cell lysate was diluted in 100 µl medium stringency IP buffer and incubated on ice for 30 min. 2 µl of rabbit polyclonal antiserum (or pre-immune rabbit serum) was added and samples were mixed and incubated on ice for 1 h. Protein-A agarose beads (Roche) were washed 3 times in medium stringency IP buffer and resuspended to 50% (v/v) in medium stringency IP buffer. 50 µl of resuspended protein-A agarose beads was added to each lysate and incubated for 30 min on a rotator at room temperature. The beads were pelleted by pulsing in a microcentrifuge for 10 sec. The beads were washed twice with 750 µl medium stringency IP buffer by mixing, pulsing, and removing the supernatant. A third wash with 750 µl low stringency IP buffer was performed to

remove sodium deoxycholate which interferes with SDS-PAGE. Supernatant was removed and protein eluted from the beads by addition of 40 µl Laemmli's sample buffer and boiling at 95°C for 5 min. Protein-A agarose beads were pelleted by pulsing the samples before loading onto a polyacrylamide gel for protein separation by SDS-PAGE as described in *7.1.6.2 Acrylamide gel electrophoresis*. Autoradiography of dried polyacrylamide gels was performed as described below in *7.2.8.2 Autoradiography of dried polyacrylamide gels*.

7.2.4.4 Densitometry

Protein quantification following western blotting was determined by densitometry using the LiCor Odyssey software package. Protein quantification following SDS-PAGE and autoradiography was performed using the gel analyser tool on scans of exposed film in ImageJ.

7.2.4.5 Quantitative temporal proteomics of infected A549 cells

5 x 10^6 A549 cells were seeded in 100 mm x 20 mm dishes with two glass coverslips included in 10 ml complete D-MEM. The following day, cells were infected at MOI 5 using 2 ml of inoculum following standard infection protocols. After 1 h incubation at 37º C, inoculum was aspirated and cells overlaid with 10 ml complete D-MEM. Cells were infected for 8 h, 16 h and 24 h. After the desired length of time, the two coverslips per dish were retrieved and processed for IF and western blot analysis to validate infection. Cells were washed twice with 10 ml cold PBS before lysis in 420 µl 6 M guanidine lysis buffer. Cells were scraped, collected, and stored on ice. Cell lysates were sonicated in a water bath sonicator with ice added (full power, 30 sec on 30 sec off, 10 cycles). Lysates were clarified by centrifugation (21 000 x *g*, 10 min, 4º C). Samples were snap frozen in liquid nitrogen. Mass spectrometry was

conducted by Dr. Michael Weekes (Cambridge Institute for Medical Research, University of Cambridge, Cambridge, UK), Dr. Joao Paulo and Dr. Steven Gygi (Department of Cell Biology, Harvard Medical School, Boston, Massachusetts, USA) as described in a previous report (Weekes et al., 2014). Dr. Weekes interpreted the spectrometry data and provided fold-change values for all peptides quantified relative to highest abundance detected across the 10 samples.

7.2.5 Molecular cloning

7.2.5.1 Making agar plates for selection of transformed DH5α bacteria

LB agar was heated in a microwave until all agar had dissolved. When cool, appropriate selection antibiotic was added to molten agar and the solution mixed. Molten LB agar was poured into 100 mm x 20 mm dishes, working under the flame of a Bunsen burner to reduce contamination. Agar was allowed to set at room temperature.

7.2.5.2 Transformation of competent DH5α cells with plasmid DNA

250 ng of plasmid DNA (or equivalent volume of water) was added to 10 µl of competent DH5α cells kept on ice, gently mixed, and incubated for 5-15 min (20 µl of cells were used for subcloning work). Cells were transformed by a 45 sec heat shock at 42° C, and cells were immediately placed on ice for 2 min. 900 µl of LB broth was added and cells allowed to recover in a shaker (200rpm) for 1 h at 37°C. Cells were pelleted using centrifugation (13000 rpm, 1 min), and all but 100 µl of supernatant was removed. Cells were resuspended in remaining supernatant, and 10 µl of resuspension was spread on an agar plate containing appropriate antibiotic using a sterile spreader working under a Bunsen burner flame to reduce contamination. For subcloning work, all the cells were plated.

Agar plates were incubated for 12-18 h at 37° C. Antibiotic selection was confirmed by absence of colonies on the water-only control sample. Single colonies were grown in LB broth (2 ml for mini-prep, 100 ml for midi-prep) at 37° C in a shaker (200 rpm) with appropriate selection antibiotic added for 16 h. Bacterial cells were pelleted by centrifugation (4300 rpm, 20 min, 4°C) and supernatant removed. Cells were used immediately or stored at -20°C.

7.2.5.3 Plasmid DNA purification.

Plasmid DNA mini-preps were performed using Promega's Wizard SV mini-prep kit (cat# A1460) according to manufacturer's instructions. Plasmid DNA midi-preps were performed using QIAGEN's Plasmid DNA Midi Prep (cat# 12143) kit according to manufacturer's instructions. The concentration and quality of purified plasmid DNA was assessed using a NanoDrop ND-1000 spectrophotometer.

7.2.5.4 Spectrophotometer analysis of nucleic acid preparations

Typically, 1.5 µl of resuspended nucleic acid preparation was loaded onto a NanoDrop ND-1000 spectrophotometer for analysis. Nucleic acid absorbs maximally at 260 nm wavelength while other contaminants such as protein and phenol absorb maximally at 280 nm and EDTA, carbohydrates and phenol absorb maximally at 230 nm. Absorbance ratios at wavelengths 260/280 and 260/230 were calculated and used as an indicator of quality and presence of any contaminants. A 260/280 ratio of ~ 1.8 for DNA and ~2.0 for RNA, and a 260/230 ratio of 2.0 – 2.2 indicate pure preparations. If ratios were considerably lower, sodium acetate (pH 5.2) was added to achieve a final concentration of 0.3 M and mixed. 3 volumes of 100 % ethanol was added and kept on ice for 40 min. Samples were centrifuged at 15000 rpm for 20 min (4 °C) and supernatant was aspirated before resuspension of nucleic in desired volume of water.

7.2.5.5 Restriction enzyme digests

DNA endonuclease enzymes were obtained from New England Biolabs, and digests were performed as instructed by manufacturer. Typically, 1 µg of DNA was digested in a 50 µl reaction. The buffer used, amount of enzyme added, and incubation conditions were determined using NEB's NEB Cloner tool (http://nebcloner.neb.com/#!/redigest).

7.2.5.6 DNA gel electrophoresis

Agarose was boiled in 1 x TAE running buffer at desired concentration (typically 0.8 – 1.0% (w/v), higher percentage for smaller DNA products and vice versa) and 1 x SYBR Safe DNA gel stain (Thermo Fisher) was added to cooled molten agarose and mixed. DNA samples were mixed with 1x DNA loading dye (final concentration) and loaded into set agarose gel alongside Promega 1 kb DNA ladder marker. Gels were typically run at 100 V for desired length of time, using Orange G and xylene blue FF dyes as markers for DNA migration.

7.2.5.7 NS1-GFP cloning using eGFPN1 vector

The ORF of various NS1 proteins were cloned out of appropriate pDUAL or pHH21 plasmids using primers designed to incorporate a 5' KpnI site and a 3' AgeI site (Table 7.11). 10 ng of plasmid DNA template was amplified in a 50 µl PCR using Pfu Ultra II Fusion HS DNA Polymerase (Agilent) using a reaction setup as recommended by the manufacturer. Thermocycling conditions were as follows: i) a 2 min denaturation step at 95°C, ii) a 20 sec denaturation step at 95°C, iii) a 20 sec primer annealing step at 60°C, iv) a 15 sec elongation step at 72°C, with steps ii) – iv) performed for 30 cycles, and v) a final 3 min elongation step at 72°C.

PCR product was analysed by DNA gel electrophoresis and purified using Qiagen's QIAquick PCR purification kit as instructed by manufacturer, but eluting with 30 µl water. The whole purified PCR product and 5 µg of pEGFPN1 vector was digested with KpnI and AgeI-HF DNA endonucleases (New England Biolabs) using conditions recommended by the NEB Cloner tool (http://nebcloner.neb.com/#!/redigest), and purified as above. 50 ng of cut pEGFPN1 was used in a DNA ligation reaction at a molar ratio of 5:1 (insert:vector) using T4 DNA ligase (New England Biolabs), as recommended by manufacturer. 2 µl of ligase reaction product was transformed into competent DH5α cells as described in *7.2.5.2 Transformation of competent DH5α cells with plasmid DNA*. Individual colonies were grown overnight (37ºC, 200 rpm shaking) in 2 ml LB with kanamycin (50 µg/µl). Plasmid DNA was extracted from individual clonal bacterial suspensions by mini-prep plasmid purification and samples were screened for successful plasmid transformation by digesting mini-preps with KpnI and AgeI-HF, which cuts either side of the insert site, and using DNA gel electrophoresis to identify plasmid preparations with 690bp insert. Positive cultures were added 1:1000 to 100 ml LB with kanamycin (50 µg/µl) and grown overnight. Midi-prep plasmid purification was performed, validated with restriction digest and DNA gel electrophoresis as above, and plasmid DNA was sequence verified by GATC to confirm desired insert was present. To test that NS1-GFP was expressed in transfected cells, 500 ng of select NS1-GFP expressing plasmids was transfected into 293T cells in 24-wells (as described above in *7.2.3.14 NS1 pol II shut-off assays*). GFP fluorescence was confirmed by epi-fluorescence of live cells, and at 48 h post-transfection cell lysates were generated in 200 µl Laemmli's sample

buffer. NS1-GFP expression was confirmed by western blot analysis using the mouse monoclonal anti-GFP (JL8) antibody (Fig 7.3).

7.2.5.8 Cloning NS segments into pDUAL

Corresponding cDNA for the NS genes of Alb88B, NY6750A, Sw412A, Sw418B, and NY107B were synthesised and cloned into a backbone vector (pBSK(+)-Amp) by Biomatik. As the full 890bp gene sequence was not available in any case, the termini of the NS segment was taken from the closest relative using a web-based nucleotide BLAST tool (https://blast.ncbi.nlm.nih.gov/Blast.cgi?PAGE_TYPE=BlastSearch) – see Table 7.16. NS genes were checked for BsmBI sites using the web-based endonuclease site finder WebCutter 2.0 (http://rna.lundberg.gu.se/cutter2/). For the NS genes with BsmBI sites (Alb88 and Sw418), the nucleotide sequence was altered as to remove the site, but not affect NS1 or NEP protein sequence – for mutations see Table 7.16.

Primers were designed to allow amplification of the NS genes with ends compatible for ligation into pDUAL vector following BsmBI digestion (Table 7.12). 10 ng of plasmid DNA template was amplified in a 50 µl PCR using Pfu Ultra II Fusion HS DNA Polymerase (Agilent) using a reaction setup recommended by the manufacturer. Thermocycling conditions were as follows: i) a 2 min denaturation step at 95°C, ii) a 20 sec denaturation step at 95°C, iii) a 20 sec primer annealing step at 60°C, iv) a 15 sec elongation step at 72°C, with steps ii) – iv) performed for 30 cycles, and v) a final 3 min elongation step at 72°C.

PCR product was analysed by DNA gel electrophoresis and purified using Qiagen's QIAquick PCR purification kit as instructed by manufacturer, but eluting

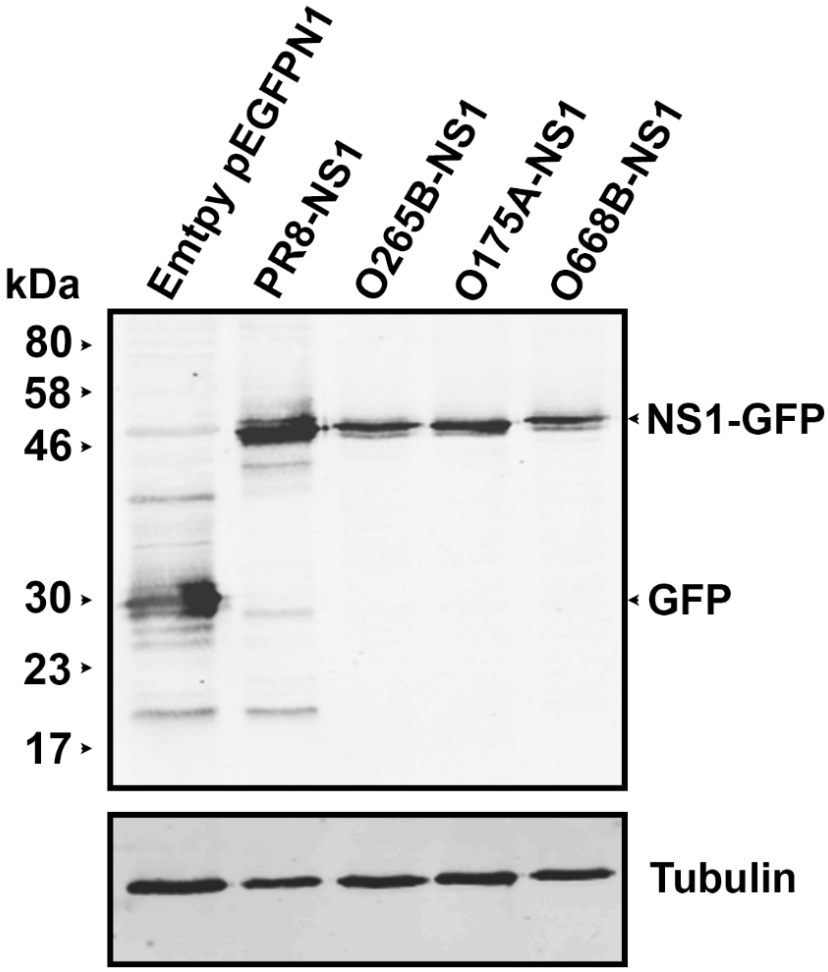

Fig 7.3. Western blot validation of NS1-GFP expression from pEGFPN1 plasmid. 293T cells were seeded in 24-wells and were transfected for 48 h with 500 ng of plasmid DNA. Cell lysates were generated in Laemmli's sample buffer and western blot analysis using a mouse monoclonal anti-GFP antibody (JL8) was performed. Top panel shows anti-GFP blot, bottom panel shows anti-tubulin loading control.

with 30 µl water. The whole purified PCR product and 5 µg of pDUAL vector was digested with BsmBI DNA endonuclease (New England Biolabs) as recommended by the NEB Cloner tool (http://nebcloner.neb.com/#!/redigest), and PRC-purified using Qiagen's PCR purification kit as above. 50 ng of cut pDUAL was used in a DNA ligation reaction at a molar ratio of 5:1 (insert:vector) using T4 DNA ligase (New England Biolabs), as recommended by manufacturer. 2 µl of ligase reaction product was transformed into competent DH5α cells as described in *7.2.5.2 Transformation of competent DH5α cells with plasmid DNA*. Individual colonies were then screened for successful plasmid transformation by digesting mini-preps with SacI (NEB), which cuts either side of the insert site of pDUAL, and using DNA gel electrophoresis to check for presence of insert. Midi-preps were performed on cultures showing positive results, and plasmid DNA was sequence verified by GATC.

Table 7.16 Avian IAV NS gene cloning into pDUAL.

Plasmid	NS gene source	Allele	Accession	Other info
pDUAL Alb88 NS	A/mallard/Alberta/ 88/1976 (H6N8)	B	M25373.1	BsmbI site removed by g242a mutation. Has termini of A/blue-winged teal/ALB/221/1978(H7N2) CY005035.1 to make 890bp full gene.
pDUAL Sw412 NS	A/mallard/Sweden /S90412/2005 (H6N8)	A	EU518721. 1	Has termini of A/duck/Italy/194659/2006(H3N2) (FJ432766.1) to make full 890bp gene.
pDUAL NY6750 NS	A/mallard/new york/6750/1978 (H2N2)	A	M25376.1	Has the termini of A/mallard/New York/6750/1978(H2N2) (M80945.1)
pDUAL Sw418 NS	A/mallard/Sweden /S90418/2005 (H6N8)	B	EU518722	BsmBI site removed by a696c mutation. Has termini of A/tufted duck/Mongolia/1409/2010(H1N1) (KC871435.1)
pDUAL NY107 NS	A/New York/107/2003 (H7N2)	B	EU587374. 2	Has termini of A/guinea fowl/New York/20221-11/1995(H2N2) (CY014833.1).

7.2.6 Immunofluorescent staining

Cells were seeded on 13 mm glass coverslips (SLS) in 24-well plates and infected using standard protocols. After infection, cells were washed with 1 x 1 ml PBS and fixed using 250 µl PBS/4% (v/v) formaldehyde for 20 min. Fixed cells were washed 3 x 1 ml PBS and permeabilised using 250 µl PBS/0.2% (v/v) Triton X-100 for 5 min. Permeabilised cells were washed 3 x 1 ml PBS/1% (v/v) FBS and stained with appropriate primary antibody diluted in PBS/1% (v/v) FBS (1 h at room temperature or overnight at 4°C on a platform rocker). Cells were washed as above and incubated with appropriate secondary antibody diluted in PBS/1% (v/v) FBS at room temperature for 45 min with rocking, protected from exposure to light by foil. Cells were washed as above and coverslips were mounted on glass microscopy slides (Thermo Scientific) using 2 µl ProLong Gold Antifade reagent. Slides were cured for at least 24 h before imaging using a confocal microscope (Zeiss LSM 710).

7.2.7 Interferon and cytokine assays

7.2.7.1 IFN-β dose-inhibition experiments

A549 cells were seeded in 24-well plates at 2 x 10^5 cells per well in 1 ml complete D-MEM. The following day, cells were treated with varying concentrations of exogenous human interferon-β (Abcam) diluted in 1 ml complete D-MEM. 24 h after treatment, a 48 h multicycle infection (MOI 0.01) was performed using standard infection protocols. At 48 h p.i., cell lysates were generated for western blot analysis of viral NP and cellular interferon-induced GTP-binding protein Mx1 to confirm IFN-β had activated the JAK/STAT signalling pathway. Cell supernatant was clarified (3000 rpm for 5 min), and stored at -80°C prior to titration of virus by plaque assay.

Titres were normalised to no-IFN control and IC_{90} values were calculated using GraphPad Prism 6 software.

7.2.7.2 HEK-Blue type I interferon assays

A549 cells were seeded in 24-well plates at 2 x 10^5 cells per well in 1 ml complete D-MEM, on 13 mm coverslips. The following day, cells were infected at varying multiplicities for 24 h, using a serum- and trypsin-free virus growth medium. Supernatant was collected and immediately placed on ice. Supernatants were clarified (3000 rpm for 5 min) and stored at -80°C prior to assaying. The cells were fixed and stained for virus NP, as described in *7.2.6 Immunofluorescent staining*, to determine the successful infection rate.

Samples were UV-treated to inactivate infectious virus particles by transferring 300 µl of sample to a 24-well plate, kept on ice with lid removed, and treating at 120000 µJ/cm^2 for 10 min in a CL-1000 Ultraviolet Crosslinker (UVP). To determine levels of type I IFN in the supernatant of infected cells, 180 µl of HEK-Blue cell suspension (at 2.8 x 10^5 cells/ml) was added to 20 µl of UV-treated sample in 96-well plates and incubated for 24 h at 37°C. 20 µl of HEK-Blue cell supernatant was transferred to 180 µl of Quanti-Blue substrate (InVivoGen) in a separate 96-well plate and incubated for 1 h at 37°C. Absorbance at 630 nm was recorded using a micro plate reader (BioTek) using Gen5 software and used as a read-out for active type I IFN levels in the initial samples. A standard curve was generated in parallel by incubating known quantities of UV-treated human IFN-β or IFN-α.

7.2.7.3 Plasmid-based IFN and ISRE reporter studies

1.5 x 10^5 293T cells were seeded per well of a 24-well plate in 1 ml of complete D-MEM the day prior to transfection. The following day, cells were co-transfected with 50 ng of reporter plasmid (IFN-β::Luc or ISRE::Luc) and 400 ng of pEGFPN1 with appropriate NS1 ORF upstream of eGFP gene (PR8 NP-GFP was used as a negative control) using Lipofectamine 2000 (Invitrogen) as described in *7.2.3.14 NS1 pol II shut-off assays*. 24 h after transfection, cells were stimulated (or mock stimulated) with 5 µg/well of poly(IC) (InvivoGen) by transfection using Lipofectamine 2000 – as above except the transfection mix involved a 2:50 Lipofectamine 2000: Opti-MEM mixture. Mock-stimulated cells were transfected with a transfection mix in which poly(IC) had been replaced with Opti-MEM medium. 24 h post-stimulation, luciferase activity in cell lysates were measured using Promega's Luciferase Assay System (cat# E1500) by following manufacturer's instructions using the Promega GloMax Multi Detection unit.

7.2.7.4 Primary human macrophage cytokine array

Primary human $CD14^+$ monocyte-derived macrophages were isolated and plated as described in *7.2.2.4 Isolation of human CD14+ monocytes*. On the day of infection, macrophages were washed with 1 ml serum-free RPMI. Virus stocks were diluted in serum-free RPMI medium so that a 200 µl inoculum would achieve an estimated MOI of 1. 200 µl of diluted virus was incubated on macrophages for 1 h at 37°C. The virus inoculum was removed, and macrophages were overlaid with 1 ml serum-free RPMI. After 24 h, the supernatant was clarified (3000 rpm, 5 min) and stored at -80°C. Macrophages were fixed and stained with AA5H anti-NP antibody as described in *7.2.6 Immunofluorescent staining* to confirm successful infection.

The supernatant was used in R & D System's human cytokine panel A proteome profiling kit (cat# ARY005), and quantified using the near infrared detection system using the Li-Cor Odyssey system. Briefly, supernatant was incubated with a cocktail of biotinylated detection antibodies for various human cytokines and chemokines. The antibody-cytokine mixture was then run over a nitrocellulose membrane with capture antibodies spotted, in duplicate, which capture the detection antibody/cytokine complex. A streptavidin-tagged secondary conjugate was run over the membrane, and the amount of dye present at each spot quantified using the Li-Cor Odyssey system. The amount of dye in a spot was proportional to the quantity of corresponding cytokine in the supernatant of infected macrophages. Mean fold-change over mock-infected sample was calculated and plotted as a heat map created in Microsoft Excel.

7.2.8 Radioactive isotope experiments

7.2.8.1 ^{35}S-methionine/cysteine metabolic labelling of infected cells

MDCK cells were seeded in 24-well plates and infected at an MOI of 10 using standard protocols. Cells were seeded in duplicate to allow generation of cell lysates and also assessment of successful infection rate by IF.

At 6 h post-infection, cells were washed twice with warm PBS and overlaid with 1 ml Methionine- and Cysteine-free D-MEM supplemented with 5% (v/v) dialysed PBS and 2 mM L-Glutamine to starve the cells of methionine and cysteine. At 8 h post-infection, cells were washed twice with warm PBS and overlaid with 0.5 ml of methionine- and cysteine-free D-MEM (with 2 mM L-Glutamine and 5% (v/v) dialysed FBS) supplemented with ^{35}S-methione/cysteine protein labelling mix (Perkin Elmer) at 0.8 MBq/ml. Cells were incubated at 37°C in a vented box containing

activated charcoal (Fisher). After a 1 h pulse, cells were washed once with ice-cold PBS. PBS wash was removed and cells were lysed/fixed for downstream processing.

7.2.8.2 Autoradiography of dried polyacrylamide gels

SDS-PAGE was run as described in *7.2.4.1 Protein Electrophoresis*. Gels were fixed by rocking in gel fix solution (50% methanol (v/v), 10% acetic acid (v/v)) for 5 min. The fix solution was replaced and gels were incubated twice further for 5 min. Gels were incubated in Amplify Fluorographic Reagent (GE Healthcare) for 15 min with rocking. Gels were laid onto 3MM Whatman filter paper and covered with film. The gels were dried in a gel dryer (Bio-Rad) by heating to 80°C for 2 h under vacuum pressure. Dried gels were placed in sealed cassette with X-ray film (Thermo Fisher) overnight at -80°C, or for longer periods of time according to desired signal strength. X-ray film was developed using a Konica SRX-101A X-ograph film processer using manufacturer's instructions.

7.2.9 Mouse experiments

7.2.9.1 Viral infections

BALB/c mice were purchased from Harlan UK Ltd (Oxon, UK) and housed in the Roslin Institute Biomedical Research Facility (BRF). All work was carried out under a UK Home Office licence according to the Animals (Scientific Procedures) Act 1986. Infection of BALB/c mice was conducted by Prof. Bernadette Dutia, Dr. Helen Wise, and Dr. Marlynne Nicol (The Roslin Institute, The University of Edinburgh, Edinburgh, UK). Five- to 6-week-old female mice were anaesthetized using isofluorane (Merial Animal Health Ltd) and infected intranasally with 100 or 500 PFU of virus in 40 µl serum-free D-MEM. Mice were weighed daily and assessed for visual signs of clinical disease, including inactivity, ruffled fur and laboured breathing. At

days 2, 4, and 6 p.i., mice were euthanized by CO_2 asphyxiation, performed by Prof. Dutia and Dr. Nicol. Tissue collection was performed with the help of Prof. Dutia, Dr. Nicol, Dr. Yvonne Ligertwood, and Dr. Gareth Hardisty (The Roslin Institute, The University of Edinburgh, Edinburgh, UK). The tip of the left lung was harvested into 200 µl preservative (RNA later, Life Technologies) prior to RNA extraction, while the remainder of the left lung was removed onto dry ice. Both were stored at -80°C prior to downstream processing. For titration of infectious virus in the left lung, and cytokine profiling, the left lung was diced with a sterile scalpel and added to 1.5 ml serum-free D-MEM with 0.1 mM Pefa-Bloc (Sigma). The lung tissue was homogenised using the Tissue Lyser II (Qiagen) system. Briefly, a 5 mm diameter metallic ball bearing (cat # 69989) was added and the sample shaken at 28000 Hz for 4 min. Homogenised tissue was clarified by centrifugation (3000 rpm, 5 min). Titres of infectious virus in the left lung were determined by plaque assay on MDCK cells as described above in *7.2.3.6 Plaque assays – PR8 and Udorn72.*

7.2.9.2 Histopathology

The lobes of the right lung were inflated with and fixed in 10% neutral buffered formalin. Fixed lung tissue was processed and embedded in paraffin*. 5 µm thick sections were cut and stained with haematoxylin and eosin* before being assessed (blinded) by a pathologist and lesions scored (Dr. Philippa Beard, the Roslin Institute, The University of Edinburgh, Edinburgh, UK). The scoring system was designed by Dr. Beard and provided as follows: 0, no lesions; 1, mild, focal inflammation and rare degeneration and necrosis; 2, moderate, multifocal inflammation with frequent necrotic cells; 3, marked, multifocal inflammation with common necrosis and occasional fibrin accumulation.

*Performed by the University of Edinburgh Easter Bush Histopathology Laboratory.

7.2.9.3 Immunohistofluorescence

For immunohistofluorescence imaging, lung tissue was deparaffinised by incubating sections for 3 min in xylene, and repeating with fresh xylene. Sections were then incubated in decreasing concentrations of ethanol (3 min each step: 100% (v/v) ethanol, 100% (v/v) ethanol, 100% (v/v) ethanol, 95% (v/v) ethanol, 70% (v/v) ethanol, 50% (v/v) ethanol) before being rinsed with water for 5 min.

An antigen retrieval step was performed by heating sections in sodium citrate buffer at 96°C for 30 min. After cooling, slides were rinsed with water for 5 min. Slides were washed three times for 5 min on a rocker with TBS/0.025% (v/v) Triton X-100 (TBST). Cells were permeabilised by incubating sections in TBS/0.25% (v/v) Triton X-100 on a rocker for 10 min. Cells were washed three times in TBST for 5 min. Samples were blocked by incubating in TBST/10% (v/v) FBS for 30 min on a rocker. Sections were washed three times with TBST, and 200 µl CAS-blocking agent was added and sections were incubated on a rocker for 1.5 h. Slides were washed with TBST three times as above. Immunological staining was performed essentially as described for staining fixed cells *in vitro* in *7.2.6 Immunofluorescent staining,* except antibodies were diluted in CAS-block blocking agent rather than PBS/1% (v/v) FBS. Sections were stained for intracellular viral NP using rabbit polyclonal antiserum anti-MBP-NP (2915). The lung tissue was subsequently stained with an anti-rabbit IgG antibody conjugated with a fluorescent dye (Alexa Fluor 594, Life Technologies) at 1:1000 in CAS-block blocking agent for 45 min at room temperature prior to immunofluorescent imaging using a confocal microscope (Zeiss LSM 710).

7.2.9.4 Mouse quantitative reverse-transcription PCR (RT-qPCR) array.

Custom Taqman® Array Plates (Applied Biosystems) were designed by Dr. Brett Jagger (National Institute of Allergy and Infectious Diseases, Bethesda, Maryland, USA) to analyse 3 RNA samples in triplicate per plate, with 32 unique assays per sample (see Table 4.1 in Chapter 4 for individual RT-qPCR assays for cellular transcripts). RNA extraction and RT-qPCR was performed with the aid of Dr. Nikki Smith (The Roslin Institute, The University of Edinburgh, Edinburgh, UK). Total RNA was extracted from the tip of the left lung (50 – 80 mg of tissue) of 3 mice per cohort at day 4 p.i. using Qiagen's QIAshredder RNA extraction kit (cat# 79654) as instructed by manufacturer. Reverse transcription of 25 ng total RNA was performed using random hexamer primers and the high-capacity RNA-to-DNA reverse transcription kit (Applied Biosystems) according to manufacturer's instructions. cDNA was mixed with Taqman Universal Mastermix (Life Technologies) and 20 µl loaded into each well of the array plate. Plates were sealed with film and centrifuged briefly. RT-qPCR was run in a 7500 Q-PCR thermocycler (Applied Biosystems) as recommended by the manufacturer. Cycling conditions were as follows: i) 2 min hold step at 50ºC, ii) a 10 min hold step at 95ºC, and 40 cycles of iii) 15 sec at 95 ºC and iv) 1 min annealing and extension at 60 ºC. Cycle threshold (CT) values were obtained using 7500 Software v2.0.6 (Applied Biosystems) and data was exported to Microsoft Excel for further analysis. Mean CT values were calculated from triplicate data and were normalised to mean Gapdh CT values (dCT). dCT values were plotted as 20 – dCT for each mouse, thus the higher the value the more transcript RNA in the lung.

7.2.9.5 Mouse cytokine array

Cytokines and chemokines in the left lung homogenate were quantified using a mouse cytokine array (Mouse Cytokine Antibody Array Panel A, R & D Systems). Lung homogenate of the five mice per cohort at day 4 post-infection were pooled and assayed as described in manufacturer's instructions using the near infrared detection protocol, essentially as described earlier for the human cytokine array in *7.2.7.4 Primary human macrophage cytokine array*. Imaging and quantification was performed using the LiCor Odyssey Imaging platform. Mean fold-change over mock-infected sample was calculated and plotted as a heat map created in Microsoft Excel.

7.2.10 Statistical analyses

All statistical tests described were conducting using GraphPad Prism 6 software.

References

.

ADAMS, S., XING, Z., LI, J., MENDOZA, K., PEREZ, D., REED, K. & CARDONA, C. 2013. The effect of avian influenza virus NS1 allele on virus replication and innate gene expression in avian cells. *Mol Immunol,* 56**,** 358-68.

AHMED, S., MARATHA, A., BUTT, A. Q., SHEVLIN, E. & MIGGIN, S. M. 2013. TRIF-mediated TLR3 and TLR4 signaling is negatively regulated by ADAM15. *J Immunol,* 190**,** 2217-28.

AKARSU, H., BURMEISTER, W. P., PETOSA, C., PETIT, I., MULLER, C. W., RUIGROK, R. W. & BAUDIN, F. 2003. Crystal structure of the M1 protein-binding domain of the influenza A virus nuclear export protein (NEP/NS2). *Embo j,* 22**,** 4646-55.

ALBERTS, R., SRIVASTAVA, B., WU, H., VIEGAS, N., GEFFERS, R., KLAWONN, F., NOVOSELOVA, N., DO VALLE, T. Z., PANTHIER, J. J. & SCHUGHART, K. 2010. Gene expression changes in the host response between resistant and susceptible inbred mouse strains after influenza A infection. *Microbes Infect,* 12**,** 309-18.

ALONSO-CAPLEN, F. V., NEMEROFF, M. E., QIU, Y. & KRUG, R. M. 1992. Nucleocytoplasmic transport: the influenza virus NS1 protein regulates the transport of spliced NS2 mRNA and its precursor NS1 mRNA. *Genes Dev,* 6**,** 255-67.

AMIEL, C., DARCISSAC, E., TRUONG, M. J., DEWULF, J., LOYENS, M., MOUTON, Y., CAPRON, A. & BAHR, G. M. 1999. Interleukin-16 (IL-16) inhibits human immunodeficiency virus replication in cells from infected subjects, and serum IL-16 levels drop with disease progression. *J Infect Dis,* 179**,** 83-91.

AMINI-BAVIL-OLYAEE, S., CHOI, Y. J., LEE, J. H., SHI, M., HUANG, I. C., FARZAN, M. & JUNG, J. U. 2013. The antiviral effector IFITM3 disrupts intracellular cholesterol homeostasis to block viral entry. *Cell Host Microbe,* 13**,** 452-64.

AMORIM, M. J., READ, E. K., DALTON, R. M., MEDCALF, L. & DIGARD, P. 2007. Nuclear export of influenza A virus mRNAs requires ongoing RNA polymerase II activity. *Traffic,* 8**,** 1-11.

AMORIM, M. J., BRUCE, E. A., READ, E. K., FOEGLEIN, A., MAHEN, R., STUART, A. D. & DIGARD, P. 2011. A Rab11- and microtubule-dependent mechanism for cytoplasmic transport of influenza A virus viral RNA. *J Virol,* 85**,** 4143-56.

ANTHONY, S. J., ST LEGER, J. A., PUGLIARES, K., IP, H. S., CHAN, J. M., CARPENTER, Z. W., NAVARRETE-MACIAS, I., SANCHEZ-LEON, M., SALIKI, J. T., PEDERSEN, J., KARESH, W., DASZAK, P., RABADAN, R., ROWLES, T. & LIPKIN, W. I. 2012. Emergence of fatal avian influenza in New England harbor seals. *MBio,* 3**,** e00166-12.

ARAGÓN, T., DE LA LUNA, S., NOVOA, I., CARRASCO, L., ORTÍN, J. & NIETO, A. 2000. Eukaryotic Translation Initiation Factor 4GI Is a Cellular Target for NS1 Protein, a Translational Activator of Influenza Virus. *Molecular and Cellular Biology,* 20**,** 6259-6268.

ARRANZ, R., COLOMA, R., CHICHÓN, F. J., CONESA, J. J., CARRASCOSA, J. L., VALPUESTA, J. M., ORTÍN, J. & MARTÍN-BENITO, J. 2012. The Structure of Native Influenza Virion Ribonucleoproteins. *Science,* 338**,** 1634-1637.

AYLLON, J., GARCIA-SASTRE, A. & HALE, B. G. 2012. Influenza A viruses and PI3K: are there time, place and manner restrictions? *Virulence,* 3**,** 411-4.

BAO, Y., BOLOTOV, P., DERNOVOY, D., KIRYUTIN, B., ZASLAVSKY, L., TATUSOVA, T., OSTELL, J. & LIPMAN, D. 2008. The influenza virus resource at the National Center for Biotechnology Information. *J Virol,* 82**,** 596-601.

BAUDIN, F., BACH, C., CUSACK, S. & RUIGROK, R. W. 1994. Structure of influenza virus RNP. I. Influenza virus nucleoprotein melts secondary structure in panhandle RNA and exposes the bases to the solvent. *Embo j,* 13**,** 3158-65.

BELSHE, R. B., SMITH, M. H., HALL, C. B., BETTS, R. & HAY, A. J. 1988. Genetic basis of resistance to rimantadine emerging during treatment of influenza virus infection. *J Virol,* 62**,** 1508-12.

BENDALL, L. J. & BRADSTOCK, K. F. 2014. G-CSF: From granulopoietic stimulant to bone marrow stem cell mobilizing agent. *Cytokine Growth Factor Rev,* 25**,** 355-67.

BENITEZ, A. A., PANIS, M., XUE, J., VARBLE, A., SHIM, J. V., FRICK, A. L., LOPEZ, C. B., SACHS, D. & TENOEVER, B. R. 2015. In Vivo RNAi Screening Identifies MDA5 as a Significant Contributor to the Cellular Defense against Influenza A Virus. *Cell Rep,* 11**,** 1714-26.

BERAN, J., PEETERS, M., DEWE, W., RAUPACHOVA, J., HOBZOVA, L. & DEVASTER, J. M. 2013. Immunogenicity and safety of quadrivalent versus trivalent inactivated influenza vaccine: a randomized, controlled trial in adults. *BMC Infect Dis,* 13**,** 224.

BERGMANN, M., GARCIA-SASTRE, A., CARNERO, E., PEHAMBERGER, H., WOLFF, K., PALESE, P. & MUSTER, T. 2000. Influenza virus NS1 protein counteracts PKR-mediated inhibition of replication. *J Virol,* 74**,** 6203-6.

BIER, K., YORK, A. & FODOR, E. 2011. Cellular cap-binding proteins associate with influenza virus mRNAs. *J Gen Virol,* 92**,** 1627-34.

BLAAS, D., PATZELT, E. & KUECHLER, E. 1982. Identification of the cap binding protein of influenza virus. *Nucleic Acids Res,* 10**,** 4803-12.

BLUMENKRANTZ, D., ROBERTS, K. L., SHELTON, H., LYCETT, S. & BARCLAY, W. S. 2013. The short stalk length of highly pathogenic avian influenza H5N1 virus neuraminidase limits transmission of pandemic H1N1 virus in ferrets. *J Virol,* 87**,** 10539-51.

BOON, A. C., DEBEAUCHAMP, J., HOLLMANN, A., LUKE, J., KOTB, M., ROWE, S., FINKELSTEIN, D., NEALE, G., LU, L., WILLIAMS, R. W. & WEBBY, R. J. 2009. Host genetic variation affects resistance to infection with a highly pathogenic H5N1 influenza A virus in mice. *J Virol,* 83**,** 10417-26.

BORNHOLDT, Z. A. & PRASAD, B. V. 2006. X-ray structure of influenza virus NS1 effector domain. *Nat Struct Mol Biol,* 13**,** 559-60.

BRAAM, J., ULMANEN, I. & KRUG, R. M. 1983. Molecular model of a eucaryotic transcription complex: functions and movements of influenza P proteins during capped RNA-primed transcription. *Cell,* 34**,** 609-18.

BRASS, A. L., HUANG, I. C., BENITA, Y., JOHN, S. P., KRISHNAN, M. N., FEELEY, E. M., RYAN, B. J., WEYER, J. L., VAN DER WEYDEN, L., FIKRIG, E., ADAMS, D. J., XAVIER, R. J., FARZAN, M. & ELLEDGE, S. J. 2009. The IFITM proteins mediate cellular resistance to influenza A H1N1 virus, West Nile virus, and dengue virus. *Cell,* 139**,** 1243-54.

BROUGHTON, S. E., DHAGAT, U., HERCUS, T. R., NERO, T. L., GRIMBALDESTON, M. A., BONDER, C. S., LOPEZ, A. F. & PARKER, M. W. 2012. The GM-CSF/IL-3/IL-5 cytokine receptor family: from ligand recognition to initiation of signaling. *Immunol Rev,* 250**,** 277-302.

BUI, M., WHITTAKER, G. & HELENIUS, A. 1996. Effect of M1 protein and low pH on nuclear transport of influenza virus ribonucleoproteins. *J Virol,* 70**,** 8391-401.

BULLIDO, R., GOMEZ-PUERTAS, P., ALBO, C. & PORTELA, A. 2000. Several protein regions contribute to determine the nuclear and cytoplasmic localization of the influenza A virus nucleoprotein. *J Gen Virol,* 81**,** 135-42.

BULLIDO, R., GOMEZ-PUERTAS, P., SAIZ, M. J. & PORTELA, A. 2001. Influenza A virus NEP (NS2 protein) downregulates RNA synthesis of model template RNAs. *J Virol,* 75**,** 4912-7.

BURGUI, I., ARAGÓN, T., ORTÍN, J. & NIETO, A. 2003. PABP1 and eIF4GI associate with influenza virus NS1 protein in viral mRNA translation initiation complexes. *Journal of General Virology,* 84**,** 3263-3274.

CADY, S. D., SCHMIDT-ROHR, K., WANG, J., SOTO, C. S., DEGRADO, W. F. & HONG, M. 2010. Structure of the amantadine binding site of influenza M2 proton channels in lipid bilayers. *Nature,* 463**,** 689-692.

CALANDRA, T. & ROGER, T. 2003. Macrophage migration inhibitory factor: a regulator of innate immunity. *Nat Rev Immunol,* 3**,** 791-800.

CALLAN, R. J., EARLY, G., KIDA, H. & HINSHAW, V. S. 1995. The appearance of H3 influenza viruses in seals. *J Gen Virol,* 76 (Pt 1)**,** 199-203.

CARRASCO, M., AMORIM, M. J. & DIGARD, P. 2004. Lipid raft-dependent targeting of the influenza A virus nucleoprotein to the apical plasma membrane. *Traffic,* 5**,** 979-92.

CARRILLO, B., CHOI, J. M., BORNHOLDT, Z. A., SANKARAN, B., RICE, A. P. & PRASAD, B. V. 2014. The influenza A virus protein NS1 displays structural polymorphism. *J Virol,* 88**,** 4113-22.

CAULDWELL, A. V., LONG, J. S., MONCORGE, O. & BARCLAY, W. S. 2014. Viral determinants of influenza A virus host range. *J Gen Virol,* 95**,** 1193-210.

CENTERS FOR DISEASE CONTROL AND PREVENTION. 2009. *Seasonal Influenza (Flu)* [Online]. Available: http://www.cdc.gov/flu/weekly/weeklyarchives2008-2009/weekly35.htm [Accessed 17/08/16.

CHAN, A. Y., VREEDE, F. T., SMITH, M., ENGELHARDT, O. G. & FODOR, E. 2006. Influenza virus inhibits RNA polymerase II elongation. *Virology,* 351**,** 210-217.

CHAN, P. K. 2002. Outbreak of avian influenza A(H5N1) virus infection in Hong Kong in 1997. *Clin Infect Dis,* 34 Suppl 2**,** S58-64.

CHASE, G. P., RAMEIX-WELTI, M. A., ZVIRBLIENE, A., ZVIRBLIS, G., GOTZ, V., WOLFF, T., NAFFAKH, N. & SCHWEMMLE, M. 2011. Influenza virus ribonucleoprotein complexes gain preferential access to cellular export machinery through chromatin targeting. *PLoS Pathog,* 7**,** e1002187.

CHEN, B. J., LESER, G. P., MORITA, E. & LAMB, R. A. 2007. Influenza virus hemagglutinin and neuraminidase, but not the matrix protein, are required for assembly and budding of plasmid-derived virus-like particles. *J Virol,* 81**,** 7111-23.

CHEN, B. J., LESER, G. P., JACKSON, D. & LAMB, R. A. 2008. The influenza virus M2 protein cytoplasmic tail interacts with the M1 protein and influences virus assembly at the site of virus budding. *J Virol,* 82**,** 10059-70.

CHEN, G. W., CHANG, S. C., MOK, C. K., LO, Y. L., KUNG, Y. N., HUANG, J. H., SHIH, Y. H., WANG, J. Y., CHIANG, C., CHEN, C. J. & SHIH, S. R. 2006a. Genomic signatures of human versus avian influenza A viruses. *Emerg Infect Dis,* 12**,** 1353-60.

CHEN, H., SMITH, G. J., LI, K. S., WANG, J., FAN, X. H., RAYNER, J. M., VIJAYKRISHNA, D., ZHANG, J. X., ZHANG, L. J., GUO, C. T., CHEUNG, C. L., XU, K. M., DUAN, L., HUANG, K., QIN, K., LEUNG, Y. H., WU, W. L., LU, H. R., CHEN, Y., XIA, N. S., NAIPOSPOS, T. S., YUEN, K. Y., HASSAN, S. S., BAHRI, S., NGUYEN, T. D., WEBSTER, R. G., PEIRIS, J. S. & GUAN, Y. 2006b. Establishment of multiple sublineages of H5N1 influenza virus in Asia: implications for pandemic control. *Proc Natl Acad Sci U S A,* 103**,** 2845-50.

CHEN, W., CALVO, P. A., MALIDE, D., GIBBS, J., SCHUBERT, U., BACIK, I., BASTA, S., O'NEILL, R., SCHICKLI, J., PALESE, P., HENKLEIN, P., BENNINK, J. R. & YEWDELL, J. W. 2001. A novel influenza A virus mitochondrial protein that induces cell death. *Nat Med,* 7**,** 1306-12.

CHEN, Z., LI, Y. & KRUG, R. M. 1999. Influenza A virus NS1 protein targets poly(A)-binding protein II of the cellular 3'-end processing machinery. *The EMBO Journal,* 18**,** 2273-2283.

CHEUNG, C. Y., POON, L. L., LAU, A. S., LUK, W., LAU, Y. L., SHORTRIDGE, K. F., GORDON, S., GUAN, Y. & PEIRIS, J. S. 2002. Induction of proinflammatory cytokines in human macrophages by influenza A (H5N1) viruses: a mechanism for the unusual severity of human disease? *Lancet,* 360**,** 1831-7.

CHOU, Y. Y., VAFABAKHSH, R., DOGANAY, S., GAO, Q., HA, T. & PALESE, P. 2012. One influenza virus particle packages eight unique viral RNAs as shown by FISH analysis. *Proc Natl Acad Sci U S A,* 109**,** 9101-6.

CHUA, M. A., SCHMID, S., PEREZ, J. T., LANGLOIS, R. A. & TENOEVER, B. R. 2013. Influenza A virus utilizes suboptimal splicing to coordinate the timing of infection. *Cell Rep,* 3**,** 23-9.

CHUTINIMITKUL, S., HERFST, S., STEEL, J., LOWEN, A. C., YE, J., VAN RIEL, D., SCHRAUWEN, E. J., BESTEBROER, T. M., KOEL, B., BURKE, D. F., SUTHERLAND-CASH, K. H., WHITTLESTON, C. S., RUSSELL, C. A., WALES, D. J., SMITH, D. J., JONGES, M., MEIJER, A., KOOPMANS, M., RIMMELZWAAN, G. F., KUIKEN, T., OSTERHAUS, A. D., GARCIA-SASTRE, A., PEREZ, D. R. & FOUCHIER, R. A. 2010. Virulence-associated substitution D222G in the hemagglutinin of 2009 pandemic influenza A(H1N1) virus affects receptor binding. *J Virol,* 84**,** 11802-13.

CINGOLANI, G., BEDNENKO, J., GILLESPIE, M. T. & GERACE, L. 2002. Molecular Basis for the Recognition of a Nonclassical Nuclear Localization Signal by Importin β. *Molecular Cell,* 10**,** 1345-1353.

CLIFFORD, M., TWIGG, J. & UPTON, C. 2009. Evidence for a novel gene associated with human influenza A viruses. *Virol J,* 6**,** 198.

COLE, K. E., STRICK, C. A., PARADIS, T. J., OGBORNE, K. T., LOETSCHER, M., GLADUE, R. P., LIN, W., BOYD, J. G., MOSER, B., WOOD, D. E., SAHAGAN, B. G. & NEOTE, K. 1998. Interferon-inducible T cell alpha chemoattractant (I-TAC): a novel non-ELR CXC chemokine with potent activity on activated T cells through selective high affinity binding to CXCR3. *J Exp Med,* 187**,** 2009-21.

COLONNA, M. & FACCHETTI, F. 2003. TREM-1 (triggering receptor expressed on myeloid cells): a new player in acute inflammatory responses. *J Infect Dis,* 187 Suppl 2**,** S397-401.

COMPANS, R. W., CONTENT, J. & DUESBERG, P. H. 1972. Structure of the ribonucleoprotein of influenza virus. *J Virol,* 10**,** 795-800.

CONENELLO, G. M., TISONCIK, J. R., ROSENZWEIG, E., VARGA, Z. T., PALESE, P. & KATZE, M. G. 2011. A single N66S mutation in the PB1-F2 protein of influenza A virus increases virulence by inhibiting the early interferon response in vivo. *J Virol,* 85**,** 652-62.

CONG, Y., WANG, G., GUAN, Z., CHANG, S., ZHANG, Q., YANG, G., WANG, W., MENG, Q., REN, W., WANG, C. & DING, Z. 2010. Reassortant between Human-Like H3N2 and Avian H5 Subtype Influenza A Viruses in Pigs: A Potential Public Health Risk. *PLoS One,* 5**,** e12591.

CONNOR, R. J., KAWAOKA, Y., WEBSTER, R. G. & PAULSON, J. C. 1994. Receptor specificity in human, avian, and equine H2 and H3 influenza virus isolates. *Virology,* 205**,** 17-23.

CORNELISSEN, J. B., VERVELDE, L., POST, J. & REBEL, J. M. 2013. Differences in highly pathogenic avian influenza viral pathogenesis and associated early inflammatory response in chickens and ducks. *Avian Pathol,* 42**,** 347-64.

CROS, J. F., GARCIA-SASTRE, A. & PALESE, P. 2005. An unconventional NLS is critical for the nuclear import of the influenza A virus nucleoprotein and ribonucleoprotein. *Traffic,* 6**,** 205-13.

CROTTA, S., DAVIDSON, S., MAHLAKOIV, T., DESMET, C. J., BUCKWALTER, M. R., ALBERT, M. L., STAEHELI, P. & WACK, A. 2013. Type I and Type III Interferons Drive Redundant Amplification Loops to Induce a Transcriptional Signature in Influenza-Infected Airway Epithelia. *PLoS Pathog,* 9**,** e1003773.

DAS, K., MA, L. C., XIAO, R., RADVANSKY, B., ARAMINI, J., ZHAO, L., MARKLUND, J., KUO, R. L., TWU, K. Y., ARNOLD, E., KRUG, R. M. & MONTELIONE, G. T.

2008. Structural basis for suppression of a host antiviral response by influenza A virus. *Proc Natl Acad Sci U S A,* 105**,** 13093-8.

DE HARO, C., MENDEZ, R. & SANTOYO, J. 1996. The eIF-2alpha kinases and the control of protein synthesis. *Faseb j,* 10**,** 1378-87.

DE JONG, M. D., SIMMONS, C. P., THANH, T. T., HIEN, V. M., SMITH, G. J., CHAU, T. N., HOANG, D. M., CHAU, N. V., KHANH, T. H., DONG, V. C., QUI, P. T., CAM, B. V., HA DO, Q., GUAN, Y., PEIRIS, J. S., CHINH, N. T., HIEN, T. T. & FARRAR, J. 2006. Fatal outcome of human influenza A (H5N1) is associated with high viral load and hypercytokinemia. *Nat Med,* 12**,** 1203-7.

DE LA LUNA, S., FORTES, P., BELOSO, A. & ORTIN, J. 1995. Influenza virus NS1 protein enhances the rate of translation initiation of viral mRNAs. *J Virol,* 69**,** 2427-33.

DE WIT, E., SPRONKEN, M. I., BESTEBROER, T. M., RIMMELZWAAN, G. F., OSTERHAUS, A. D. & FOUCHIER, R. A. 2004. Efficient generation and growth of influenza virus A/PR/8/34 from eight cDNA fragments. *Virus Res,* 103**,** 155-61.

DENG, T., VREEDE, F. T. & BROWNLEE, G. G. 2006a. Different de novo initiation strategies are used by influenza virus RNA polymerase on its cRNA and viral RNA promoters during viral RNA replication. *J Virol,* 80**,** 2337-48.

DENG, T., ENGELHARDT, O. G., THOMAS, B., AKOULITCHEV, A. V., BROWNLEE, G. G. & FODOR, E. 2006b. Role of ran binding protein 5 in nuclear import and assembly of the influenza virus RNA polymerase complex. *J Virol,* 80**,** 11911-9.

DESHMANE, S. L., KREMLEV, S., AMINI, S. & SAWAYA, B. E. 2009. Monocyte chemoattractant protein-1 (MCP-1): an overview. *J Interferon Cytokine Res,* 29**,** 313-26.

DIAS, A., BOUVIER, D., CREPIN, T., MCCARTHY, A. A., HART, D. J., BAUDIN, F., CUSACK, S. & RUIGROK, R. W. 2009. The cap-snatching endonuclease of influenza virus polymerase resides in the PA subunit. *Nature,* 458**,** 914-8.

DIDCOCK, L., YOUNG, D. F., GOODBOURN, S. & RANDALL, R. E. 1999. The V protein of simian virus 5 inhibits interferon signalling by targeting STAT1 for proteasome-mediated degradation. *J Virol,* 73**,** 9928-33.

DIENZ, O., RUD, J. G., EATON, S. M., LANTHIER, P. A., BURG, E., DREW, A., BUNN, J., SURATT, B. T., HAYNES, L. & RINCON, M. 2012. Essential role of IL-6 in protection against H1N1 influenza virus by promoting neutrophil survival in the lung. *Mucosal Immunol,* 5**,** 258-66.

DIGARD, P., BLOK, V. C. & INGLIS, S. C. 1989. Complex formation between influenza virus polymerase proteins expressed in Xenopus oocytes. *Virology,* 171**,** 162-9.

DITTMANN, J., STERTZ, S., GRIMM, D., STEEL, J., GARCIA-SASTRE, A., HALLER, O. & KOCHS, G. 2008. Influenza A virus strains differ in sensitivity to the antiviral action of Mx-GTPase. *J Virol,* 82**,** 3624-31.

DITTMANN, M., HOFFMANN, H. H., SCULL, M. A., GILMORE, R. H., BELL, K. L., CIANCANELLI, M., WILSON, S. J., CROTTA, S., YU, Y., FLATLEY, B., XIAO, J. W., CASANOVA, J. L., WACK, A., BIENIASZ, P. D. & RICE, C. M. 2015. A serpin shapes the extracellular environment to prevent influenza A virus maturation. *Cell,* 160**,** 631-43.

DONELAN, N. R., BASLER, C. F. & GARCIA-SASTRE, A. 2003. A Recombinant Influenza A Virus Expressing an RNA-Binding-Defective NS1 Protein Induces High Levels of Beta Interferon and Is Attenuated in Mice. *J Virol,* 77**,** 13257-13266.

DONG, G., LUO, J., ZHANG, H., WANG, C., DUAN, M., DELIBERTO, T. J., NOLTE, D. L., JI, G. & HE, H. 2011. Phylogenetic diversity and genotypical complexity of H9N2 influenza A viruses revealed by genomic sequence analysis. *PLoS One,* 6**,** e17212.

DONG, G., PENG, C., LUO, J., WANG, C., HAN, L., WU, B., JI, G. & HE, H. 2015. Adamantane-Resistant Influenza A Viruses in the World (1902?2013): Frequency and Distribution of M2 Gene Mutations. *PLoS ONE,* 10**,** e0119115.

DONNELLY, R. P. & KOTENKO, S. V. 2010. Interferon-lambda: a new addition to an old family. *J Interferon Cytokine Res,* 30**,** 555-64.
DRAKE, J. W. 1993. Rates of spontaneous mutation among RNA viruses. *Proc Natl Acad Sci U S A,* 90**,** 4171-5.
DRAPPIER, M. & MICHIELS, T. 2015. Inhibition of the OAS/RNase L pathway by viruses. *Curr Opin Virol,* 15**,** 19-26.
DUHAUT, S. D. & MCCAULEY, J. W. 1996. Defective RNAs Inhibit the Assembly of Influenza Virus Genome Segments in a Segment-Specific Manner. *Virology,* 216**,** 326-337.
EDENBOROUGH, K. M., GILBERTSON, B. P. & BROWN, L. E. 2012. A mouse model for the study of contact-dependent transmission of influenza A virus and the factors that govern transmissibility. *J Virol,* 86**,** 12544-51.
EIBAUER, M., PELLANDA, M., TURGAY, Y., DUBROVSKY, A., WILD, A. & MEDALIA, O. 2015. Structure and gating of the nuclear pore complex. *Nat Commun,* 6**,** 7532.
EIERHOFF, T., HRINCIUS, E. R., RESCHER, U., LUDWIG, S. & EHRHARDT, C. 2010. The epidermal growth factor receptor (EGFR) promotes uptake of influenza A viruses (IAV) into host cells. *PLoS Pathog,* 6**,** e1001099.
EISFELD, A. J., KAWAKAMI, E., WATANABE, T., NEUMANN, G. & KAWAOKA, Y. 2011. RAB11A is essential for transport of the influenza virus genome to the plasma membrane. *J Virol,* 85**,** 6117-26.
EISFELD, A. J., NEUMANN, G. & KAWAOKA, Y. 2015. At the centre: influenza A virus ribonucleoproteins. *Nat Rev Microbiol,* 13**,** 28-41.
ELTON, D., SIMPSON-HOLLEY, M., ARCHER, K., MEDCALF, L., HALLAM, R., MCCAULEY, J. & DIGARD, P. 2001. Interaction of the influenza virus nucleoprotein with the cellular CRM1-mediated nuclear export pathway. *J Virol,* 75**,** 408-19.
ENGELHARDT, O. G., SMITH, M. & FODOR, E. 2005. Association of the influenza A virus RNA-dependent RNA polymerase with cellular RNA polymerase II. *J Virol,* 79**,** 5812-8.
EVERITT, A. R., CLARE, S., PERTEL, T., JOHN, S. P., WASH, R. S., SMITH, S. E., CHIN, C. R., FEELEY, E. M., SIMS, J. S., ADAMS, D. J., WISE, H. M., KANE, L., GOULDING, D., DIGARD, P., ANTTILA, V., BAILLIE, J. K., WALSH, T. S., HUME, D. A., PALOTIE, A., XUE, Y., COLONNA, V., TYLER-SMITH, C., DUNNING, J., GORDON, S. B., SMYTH, R. L., OPENSHAW, P. J., DOUGAN, G., BRASS, A. L. & KELLAM, P. 2012. IFITM3 restricts the morbidity and mortality associated with influenza. *Nature,* 484**,** 519-523.
FEELEY, E. M., SIMS, J. S., JOHN, S. P., CHIN, C. R., PERTEL, T., CHEN, L.-M., GAIHA, G. D., RYAN, B. J., DONIS, R. O., ELLEDGE, S. J. & BRASS, A. L. 2011. IFITM3 Inhibits Influenza A Virus Infection by Preventing Cytosolic Entry. *PLoS Pathog,* 7**,** e1002337.
FENSTERL, V. & SEN, G. C. 2015. Interferon-induced Ifit proteins: their role in viral pathogenesis. *J Virol,* 89**,** 2462-8.
FIRTH, A. E., JAGGER, B. W., WISE, H. M., NELSON, C. C., PARSAWAR, K., WILLS, N. M., NAPTHINE, S., TAUBENBERGER, J. K., DIGARD, P. & ATKINS, J. F. 2012. Ribosomal frameshifting used in influenza A virus expression occurs within the sequence UCC_UUU_CGU and is in the +1 direction. *Open Biol,* 2**,** 120109.
FODOR, E. & SMITH, M. 2004. The PA subunit is required for efficient nuclear accumulation of the PB1 subunit of the influenza A virus RNA polymerase complex. *J Virol,* 78**,** 9144-53.
FODOR, E. 2013. The RNA polymerase of influenza a virus: mechanisms of viral transcription and replication. *Acta Virol,* 57**,** 113-22.

FOEGLEIN, A., LOUCAIDES, E. M., MURA, M., WISE, H. M., BARCLAY, W. S. & DIGARD, P. 2011. Influence of PB2 host-range determinants on the intranuclear mobility of the influenza A virus polymerase. *J Gen Virol,* 92**,** 1650-61.

FORBES, N. E., PING, J., DANKAR, S. K., JIA, J. J., SELMAN, M., KELETA, L., ZHOU, Y. & BROWN, E. G. 2012. Multifunctional adaptive NS1 mutations are selected upon human influenza virus evolution in the mouse. *PLoS One,* 7**,** e31839.

FORT, M. M., CHEUNG, J., YEN, D., LI, J., ZURAWSKI, S. M., LO, S., MENON, S., CLIFFORD, T., HUNTE, B., LESLEY, R., MUCHAMUEL, T., HURST, S. D., ZURAWSKI, G., LEACH, M. W., GORMAN, D. M. & RENNICK, D. M. 2001. IL-25 induces IL-4, IL-5, and IL-13 and Th2-associated pathologies in vivo. *Immunity,* 15**,** 985-95.

FORTES, P., BELOSO, A. & ORTÍN, J. 1994. Influenza virus NS1 protein inhibits pre-mRNA splicing and blocks mRNA nucleocytoplasmic transport. *The EMBO Journal,* 13**,** 704-712.

FOUCHIER, R. A., SCHNEEBERGER, P. M., ROZENDAAL, F. W., BROEKMAN, J. M., KEMINK, S. A., MUNSTER, V., KUIKEN, T., RIMMELZWAAN, G. F., SCHUTTEN, M., VAN DOORNUM, G. J., KOCH, G., BOSMAN, A., KOOPMANS, M. & OSTERHAUS, A. D. 2004. Avian influenza A virus (H7N7) associated with human conjunctivitis and a fatal case of acute respiratory distress syndrome. *Proc Natl Acad Sci U S A,* 101**,** 1356-61.

FRENSING, T., PFLUGMACHER, A., BACHMANN, M., PESCHEL, B. & REICHL, U. 2014. Impact of defective interfering particles on virus replication and antiviral host response in cell culture-based influenza vaccine production. *Appl Microbiol Biotechnol,* 98**,** 8999-9008.

FUJII, K., OZAWA, M., IWATSUKI-HORIMOTO, K., HORIMOTO, T. & KAWAOKA, Y. 2009. Incorporation of influenza A virus genome segments does not absolutely require wild-type sequences. *J Gen Virol,* 90**,** 1734-40.

FUJII, Y., GOTO, H., WATANABE, T., YOSHIDA, T. & KAWAOKA, Y. 2003. Selective incorporation of influenza virus RNA segments into virions. *Proc Natl Acad Sci U S A,* 100**,** 2002-7.

FULVINI, A. A., RAMANUNNINAIR, M., LE, J., POKORNY, B. A., ARROYO, J. M., SILVERMAN, J., DEVIS, R. & BUCHER, D. 2011. Gene constellation of influenza A virus reassortants with high growth phenotype prepared as seed candidates for vaccine production. *PLoS One,* 6**,** e20823.

FURUTA, Y., GOWEN, B. B., TAKAHASHI, K., SHIRAKI, K., SMEE, D. F. & BARNARD, D. L. 2013. Favipiravir (T-705), a novel viral RNA polymerase inhibitor. *Antiviral Res,* 100**,** 446-54.

GABRIEL, G., KLINGEL, K., OTTE, A., THIELE, S., HUDJETZ, B., ARMAN-KALCEK, G., SAUTER, M., SHMIDT, T., ROTHER, F., BAUMGARTE, S., KEINER, B., HARTMANN, E., BADER, M., BROWNLEE, G. G., FODOR, E. & KLENK, H. D. 2011. Differential use of importin-alpha isoforms governs cell tropism and host adaptation of influenza virus. *Nat Commun,* 2**,** 156.

GACK, M. U., SHIN, Y. C., JOO, C. H., URANO, T., LIANG, C., SUN, L., TAKEUCHI, O., AKIRA, S., CHEN, Z., INOUE, S. & JUNG, J. U. 2007. TRIM25 RING-finger E3 ubiquitin ligase is essential for RIG-I-mediated antiviral activity. *Nature,* 446**,** 916-920.

GACK, M. U., ALBRECHT, R. A., URANO, T., INN, K. S., HUANG, I. C., CARNERO, E., FARZAN, M., INOUE, S., JUNG, J. U. & GARCIA-SASTRE, A. 2009. Influenza A virus NS1 targets the ubiquitin ligase TRIM25 to evade recognition by the host viral RNA sensor RIG-I. *Cell Host Microbe,* 5**,** 439-49.

GAFFEN, S. L. & LIU, K. D. 2004. Overview of interleukin-2 function, production and clinical applications. *Cytokine,* 28**,** 109-23.

GALE, M., JR. & KATZE, M. G. 1998. Molecular mechanisms of interferon resistance mediated by viral-directed inhibition of PKR, the interferon-induced protein kinase. *Pharmacol Ther,* 78**,** 29-46.

GAO, H., XU, G., SUN, Y., QI, L., WANG, J., KONG, W., SUN, H., PU, J., CHANG, K. C. & LIU, J. 2015a. PA-X is a virulence factor in avian H9N2 influenza virus. *J Gen Virol,* 96**,** 2587-94.

GAO, H., SUN, Y., HU, J., QI, L., WANG, J., XIONG, X., WANG, Y., HE, Q., LIN, Y., KONG, W., SENG, L. G., SUN, H., PU, J., CHANG, K. C., LIU, X. & LIU, J. 2015b. The contribution of PA-X to the virulence of pandemic 2009 H1N1 and highly pathogenic H5N1 avian influenza viruses. *Sci Rep,* 5**,** 8262.

GAO, R., CAO, B., HU, Y., FENG, Z., WANG, D., HU, W., CHEN, J., JIE, Z., QIU, H., XU, K., XU, X., LU, H., ZHU, W., GAO, Z., XIANG, N., SHEN, Y., HE, Z., GU, Y., ZHANG, Z., YANG, Y., ZHAO, X., ZHOU, L., LI, X., ZOU, S., ZHANG, Y., LI, X., YANG, L., GUO, J., DONG, J., LI, Q., DONG, L., ZHU, Y., BAI, T., WANG, S., HAO, P., YANG, W., ZHANG, Y., HAN, J., YU, H., LI, D., GAO, G. F., WU, G., WANG, Y., YUAN, Z. & SHU, Y. 2013. Human infection with a novel avian-origin influenza A (H7N9) virus. *N Engl J Med,* 368**,** 1888-97.

GARAIGORTA, U. & ORTIN, J. 2007. Mutation analysis of a recombinant NS replicon shows that influenza virus NS1 protein blocks the splicing and nucleo-cytoplasmic transport of its own viral mRNA. *Nucleic Acids Res,* 35**,** 4573-82.

GARCÍA-SASTRE, A., EGOROV, A., MATASSOV, D., BRANDT, S., LEVY, D. E., DURBIN, J. E., PALESE, P. & MUSTER, T. 1998. Influenza A Virus Lacking the NS1 Gene Replicates in Interferon-Deficient Systems. *Virology,* 252**,** 324-330.

GARCIA, M., SUAREZ, D. L., CRAWFORD, J. M., LATIMER, J. W., SLEMONS, R. D., SWAYNE, D. E. & PERDUE, M. L. 1997. Evolution of H5 subtype avian influenza A viruses in North America. *Virus Res,* 51**,** 115-24.

GARLANDA, C., DINARELLO, C. A. & MANTOVANI, A. 2013. The interleukin-1 family: back to the future. *Immunity,* 39**,** 1003-18.

GARTEN, R. J., DAVIS, C. T., RUSSELL, C. A., SHU, B., LINDSTROM, S., BALISH, A., SESSIONS, W. M., XU, X., SKEPNER, E., DEYDE, V., OKOMO-ADHIAMBO, M., GUBAREVA, L., BARNES, J., SMITH, C. B., EMERY, S. L., HILLMAN, M. J., RIVAILLER, P., SMAGALA, J., DE GRAAF, M., BURKE, D. F., FOUCHIER, R. A., PAPPAS, C., ALPUCHE-ARANDA, C. M., LOPEZ-GATELL, H., OLIVERA, H., LOPEZ, I., MYERS, C. A., FAIX, D., BLAIR, P. J., YU, C., KEENE, K. M., DOTSON, P. D., JR., BOXRUD, D., SAMBOL, A. R., ABID, S. H., ST GEORGE, K., BANNERMAN, T., MOORE, A. L., STRINGER, D. J., BLEVINS, P., DEMMLER-HARRISON, G. J., GINSBERG, M., KRINER, P., WATERMAN, S., SMOLE, S., GUEVARA, H. F., BELONGIA, E. A., CLARK, P. A., BEATRICE, S. T., DONIS, R., KATZ, J., FINELLI, L., BRIDGES, C. B., SHAW, M., JERNIGAN, D. B., UYEKI, T. M., SMITH, D. J., KLIMOV, A. I. & COX, N. J. 2009. Antigenic and genetic characteristics of swine-origin 2009 A(H1N1) influenza viruses circulating in humans. *Science,* 325**,** 197-201.

GEISER, T., DEWALD, B., EHRENGRUBER, M. U., CLARK-LEWIS, I. & BAGGIOLINI, M. 1993. The interleukin-8-related chemotactic cytokines GRO alpha, GRO beta, and GRO gamma activate human neutrophil and basophil leukocytes. *J Biol Chem,* 268**,** 15419-24.

GERBER, M., ISEL, C., MOULES, V. & MARQUET, R. 2014. Selective packaging of the influenza A genome and consequences for genetic reassortment. *Trends in Microbiology,* 22**,** 446-455.

GIBOT, S., KOLOPP-SARDA, M. N., BENE, M. C., BOLLAERT, P. E., LOZNIEWSKI, A., MORY, F., LEVY, B. & FAURE, G. C. 2004. A soluble form of the triggering receptor expressed on myeloid cells-1 modulates the inflammatory response in murine sepsis. *J Exp Med,* 200**,** 1419-26.

GIRARD, M. P., TAM, J. S., ASSOSSOU, O. M. & KIENY, M. P. 2010. The 2009 A (H1N1) influenza virus pandemic: A review. *Vaccine,* 28**,** 4895-902.

GOG, J. R., AFONSO EDOS, S., DALTON, R. M., LECLERCQ, I., TILEY, L., ELTON, D., VON KIRCHBACH, J. C., NAFFAKH, N., ESCRIOU, N. & DIGARD, P. 2007. Codon conservation in the influenza A virus genome defines RNA packaging signals. *Nucleic Acids Res,* 35**,** 1897-907.

GORAI, T., GOTO, H., NODA, T., WATANABE, T., KOZUKA-HATA, H., OYAMA, M., TAKANO, R., NEUMANN, G., WATANABE, S. & KAWAOKA, Y. 2012. F1Fo-ATPase, F-type proton-translocating ATPase, at the plasma membrane is critical for efficient influenza virus budding. *Proc Natl Acad Sci U S A,* 109**,** 4615-20.

GORSKI, S. A., HAHN, Y. S. & BRACIALE, T. J. 2013. Group 2 innate lymphoid cell production of IL-5 is regulated by NKT cells during influenza virus infection. *PLoS Pathog,* 9**,** e1003615.

GRAEF, K. M., VREEDE, F. T., LAU, Y. F., MCCALL, A. W., CARR, S. M., SUBBARAO, K. & FODOR, E. 2010. The PB2 subunit of the influenza virus RNA polymerase affects virulence by interacting with the mitochondrial antiviral signaling protein and inhibiting expression of beta interferon. *J Virol,* 84**,** 8433-45.

GREENSPAN, D., PALESE, P. & KRYSTAL, M. 1988. Two nuclear location signals in the influenza virus NS1 nonstructural protein. *J Virol,* 62**,** 3020-6.

GROTH, M., LANGE, J., KANRAI, P., PLESCHKA, S., SCHOLTISSEK, C., KRUMBHOLZ, A., PLATZER, M., SAUERBREI, A. & ZELL, R. 2014. The genome of an influenza virus from a pilot whale: relation to influenza viruses of gulls and marine mammals. *Infect Genet Evol,* 24**,** 183-6.

GUO, R. F. & WARD, P. A. 2005. Role of C5a in inflammatory responses. *Annu Rev Immunol,* 23**,** 821-52.

GUO, Y., WANG, M., KAWAOKA, Y., GORMAN, O., ITO, T., SAITO, T. & WEBSTER, R. G. 1992. Characterization of a new avian-like influenza A virus from horses in China. *Virology,* 188**,** 245-55.

HAGMAIER, K., STOCK, N., GOODBOURN, S., WANG, L. F. & RANDALL, R. 2006. A single amino acid substitution in the V protein of Nipah virus alters its ability to block interferon signalling in cells from different species. *J Gen Virol,* 87**,** 3649-53.

HALE, B. G., JACKSON, D., CHEN, Y. H., LAMB, R. A. & RANDALL, R. E. 2006. Influenza A virus NS1 protein binds p85beta and activates phosphatidylinositol-3-kinase signaling. *Proc Natl Acad Sci U S A,* 103**,** 14194-9.

HALE, B. G., BARCLAY, W. S., RANDALL, R. E. & RUSSELL, R. J. 2008a. Structure of an avian influenza A virus NS1 protein effector domain. *Virology,* 378**,** 1-5.

HALE, B. G., RANDALL, R. E., ORTIN, J. & JACKSON, D. 2008b. The multifunctional NS1 protein of influenza A viruses. *J Gen Virol,* 89**,** 2359-76.

HALE, B. G., KNEBEL, A., BOTTING, C. H., GALLOWAY, C. S., PRECIOUS, B. L., JACKSON, D., ELLIOTT, R. M. & RANDALL, R. E. 2009. CDK/ERK-mediated phosphorylation of the human influenza A virus NS1 protein at threonine-215. *Virology,* 383**,** 6-11.

HALE, B. G., KERRY, P. S., JACKSON, D., PRECIOUS, B. L., GRAY, A., KILLIP, M. J., RANDALL, R. E. & RUSSELL, R. J. 2010a. Structural insights into phosphoinositide 3-kinase activation by the influenza A virus NS1 protein. *Proc Natl Acad Sci U S A,* 107**,** 1954-9.

HALE, B. G., STEEL, J., MEDINA, R. A., MANICASSAMY, B., YE, J., HICKMAN, D., HAI, R., SCHMOLKE, M., LOWEN, A. C., PEREZ, D. R. & GARCIA-SASTRE, A. 2010b. Inefficient control of host gene expression by the 2009 pandemic H1N1 influenza A virus NS1 protein. *J Virol,* 84**,** 6909-22.

HALE, B. G., STEEL, J., MANICASSAMY, B., MEDINA, R. A., YE, J., HICKMAN, D., LOWEN, A. C., PEREZ, D. R. & GARCIA-SASTRE, A. 2010c. Mutations in the

NS1 C-terminal tail do not enhance replication or virulence of the 2009 pandemic H1N1 influenza A virus. *J Gen Virol,* 91**,** 1737-42.
HAMILTON, J. A. 2008. Colony-stimulating factors in inflammation and autoimmunity. *Nat Rev Immunol,* 8**,** 533-44.
HAN, H., CUI, Z. Q., WANG, W., ZHANG, Z. P., WEI, H. P., ZHOU, Y. F. & ZHANG, X. E. 2010. New regulatory mechanisms for the intracellular localization and trafficking of influenza A virus NS1 protein revealed by comparative analysis of A/PR/8/34 and A/Sydney/5/97. *J Gen Virol,* 91**,** 2907-17.
HAO, L., SAKURAI, A., WATANABE, T., SORENSEN, E., NIDOM, C. A., NEWTON, M. A., AHLQUIST, P. & KAWAOKA, Y. 2008. Drosophila RNAi screen identifies host genes important for influenza virus replication. *Nature,* 454**,** 890-3.
HARA, K., SCHMIDT, F. I., CROW, M. & BROWNLEE, G. G. 2006. Amino acid residues in the N-terminal region of the PA subunit of influenza A virus RNA polymerase play a critical role in protein stability, endonuclease activity, cap binding, and virion RNA promoter binding. *J Virol,* 80**,** 7789-98.
HARRIS, A., CARDONE, G., WINKLER, D. C., HEYMANN, J. B., BRECHER, M., WHITE, J. M. & STEVEN, A. C. 2006. Influenza virus pleiomorphy characterized by cryoelectron tomography. *Proc Natl Acad Sci U S A,* 103**,** 19123-7.
HATADA, E. & FUKUDA, R. 1992. Binding of influenza A virus NS1 protein to dsRNA *in vitro*. *Journal of General Virology,* 73**,** 3325-3329.
HATADA, E., TAKIZAWA, T. & FUKUDA, R. 1992. Specific binding of influenza A virus NS1 protein to the virus minus-sense RNA *in vitro*. *Journal of General Virology,* 73**,** 17-25.
HATADA, E., SAITO, S., OKISHIO, N. & FUKUDA, R. 1997. Binding of the influenza virus NS1 protein to model genome RNAs. *J Gen Virol,* 78 (Pt 5)**,** 1059-63.
HATTA, M., GAO, P., HALFMANN, P. & KAWAOKA, Y. 2001. Molecular basis for high virulence of Hong Kong H5N1 influenza A viruses. *Science,* 293**,** 1840-2.
HAY, A. J., SKEHEL, J. J. & MCCAULEY, J. 1982. Characterization of influenza virus RNA complete transcripts. *Virology,* 116**,** 517-522.
HAY, A. J., ZAMBON, M. C., WOLSTENHOLME, A. J., SKEHEL, J. J. & SMITH, M. H. 1986. Molecular basis of resistance of influenza A viruses to amantadine. *J Antimicrob Chemother,* 18 Suppl B**,** 19-29.
HAYASHI, T., MACDONALD, L. A. & TAKIMOTO, T. 2015. Influenza A Virus Protein PA-X Contributes to Viral Growth and Suppression of the Host Antiviral and Immune Responses. *J Virol,* 89**,** 6442-52.
HAYMAN, A., COMELY, S., LACKENBY, A., MURPHY, S., MCCAULEY, J., GOODBOURN, S. & BARCLAY, W. 2006. Variation in the ability of human influenza A viruses to induce and inhibit the IFN-beta pathway. *Virology,* 347**,** 52-64.
HAYMAN, A., COMELY, S., LACKENBY, A., HARTGROVES, L. C., GOODBOURN, S., MCCAULEY, J. W. & BARCLAY, W. S. 2007. NS1 proteins of avian influenza A viruses can act as antagonists of the human alpha/beta interferon response. *J Virol,* 81**,** 2318-27.
HE, Y., XU, K., KEINER, B., ZHOU, J., CZUDAI, V., LI, T., CHEN, Z., LIU, J., KLENK, H. D., SHU, Y. L. & SUN, B. 2010. Influenza A virus replication induces cell cycle arrest in G0/G1 phase. *J Virol,* 84**,** 12832-40.
HEIKKINEN, L. S., KAZLAUSKAS, A., MELEN, K., WAGNER, R., ZIEGLER, T., JULKUNEN, I. & SAKSELA, K. 2008. Avian and 1918 Spanish influenza a virus NS1 proteins bind to Crk/CrkL Src homology 3 domains to activate host cell signaling. *J Biol Chem,* 283**,** 5719-27.
HERFST, S., IMAI, M., KAWAOKA, Y. & FOUCHIER, R. A. 2014. Avian influenza virus transmission to mammals. *Curr Top Microbiol Immunol,* 385**,** 137-55.

HERLOCHER, M. L., ELIAS, S., TRUSCON, R., HARRISON, S., MINDELL, D., SIMON, C. & MONTO, A. S. 2001. Ferrets as a transmission model for influenza: sequence changes in HA1 of type A (H3N2) virus. *J Infect Dis,* 184**,** 542-6.

HINSHAW, V. S., BEAN, W. J., WEBSTER, R. G., REHG, J. E., FIORELLI, P., EARLY, G., GERACI, J. R. & ST AUBIN, D. J. 1984. Are seals frequently infected with avian influenza viruses? *J Virol,* 51**,** 863-5.

HIRST, M., ASTELL, C. R., GRIFFITH, M., COUGHLIN, S. M., MOKSA, M., ZENG, T., SMAILUS, D. E., HOLT, R. A., JONES, S., MARRA, M. A., PETRIC, M., KRAJDEN, M., LAWRENCE, D., MAK, A., CHOW, R., SKOWRONSKI, D. M., TWEED, S. A., GOH, S., BRUNHAM, R. C., ROBINSON, J., BOWES, V., SOJONKY, K., BYRNE, S. K., LI, Y., KOBASA, D., BOOTH, T. & PAETZEL, M. 2004. Novel avian influenza H7N3 strain outbreak, British Columbia. *Emerg Infect Dis,* 10**,** 2192-5.

HOLM, C. K., RAHBEK, S. H., GAD, H. H., BAK, R. O., JAKOBSEN, M. R., JIANG, Z., HANSEN, A. L., JENSEN, S. K., SUN, C., THOMSEN, M. K., LAUSTSEN, A., NIELSEN, C. G., SEVERINSEN, K., XIONG, Y., BURDETTE, D. L., HORNUNG, V., LEBBINK, R. J., DUCH, M., FITZGERALD, K. A., BAHRAMI, S., MIKKELSEN, J. G., HARTMANN, R. & PALUDAN, S. R. 2016. Influenza A virus targets a cGAS-independent STING pathway that controls enveloped RNA viruses. *Nat Commun,* 7**,** 10680.

HONG, C., LUCKEY, M. A. & PARK, J. H. 2012. Intrathymic IL-7: the where, when, and why of IL-7 signaling during T cell development. *Semin Immunol,* 24**,** 151-8.

HORAI, R., SAIJO, S., TANIOKA, H., NAKAE, S., SUDO, K., OKAHARA, A., IKUSE, T., ASANO, M. & IWAKURA, Y. 2000. Development of chronic inflammatory arthropathy resembling rheumatoid arthritis in interleukin 1 receptor antagonist-deficient mice. *J Exp Med,* 191**,** 313-20.

HRINCIUS, E. R., WIXLER, V., WOLFF, T., WAGNER, R., LUDWIG, S. & EHRHARDT, C. 2010. CRK adaptor protein expression is required for efficient replication of avian influenza A viruses and controls JNK-mediated apoptotic responses. *Cell Microbiol,* 12**,** 831-43.

HRINCIUS, E. R., HENNECKE, A. K., GENSLER, L., NORDHOFF, C., ANHLAN, D., VOGEL, P., MCCULLERS, J. A., LUDWIG, S. & EHRHARDT, C. 2012. A single point mutation (Y89F) within the non-structural protein 1 of influenza A viruses limits epithelial cell tropism and virulence in mice. *Am J Pathol,* 180**,** 2361-74.

HSIANG, T. Y., ZHOU, L. & KRUG, R. M. 2012. Roles of the phosphorylation of specific serines and threonines in the NS1 protein of human influenza A viruses. *J Virol,* 86**,** 10370-6.

HSU, M. T., PARVIN, J. D., GUPTA, S., KRYSTAL, M. & PALESE, P. 1987. Genomic RNAs of influenza viruses are held in a circular conformation in virions and in infected cells by a terminal panhandle. *Proc Natl Acad Sci U S A,* 84**,** 8140-4.

HU, J., MO, Y., WANG, X., GU, M., HU, Z., ZHONG, L., WU, Q., HAO, X., HU, S., LIU, W., LIU, H., LIU, X. & LIU, X. 2015a. PA-X decreases the pathogenicity of highly pathogenic H5N1 influenza A virus in avian species by inhibiting virus replication and host response. *J Virol,* 89**,** 4126-42.

HU, Y., LIU, X., LI, S., GUO, X., YANG, Y. & JIN, M. 2012. Complete genome sequence of a novel H4N1 influenza virus isolated from a pig in central China. *J Virol,* 86**,** 13879.

HU, Y., LIU, X., ZHANG, A., ZHOU, H., LIU, Z., CHEN, H. & JIN, M. 2015b. CHD3 facilitates vRNP nuclear export by interacting with NES1 of influenza A virus NS2. *Cell Mol Life Sci,* 72**,** 971-82.

HUANG, S., CHEN, J., CHEN, Q., WANG, H., YAO, Y., CHEN, J. & CHEN, Z. 2013. A second CRM1-dependent nuclear export signal in the influenza A virus NS2 protein contributes to the nuclear export of viral ribonucleoproteins. *J Virol,* 87**,** 767-78.

HUANG, T. S., PALESE, P. & KRYSTAL, M. 1990. Determination of influenza virus proteins required for genome replication. *J Virol,* 64**,** 5669-73.

HURT, A. C., ERNEST, J., DENG, Y. M., IANNELLO, P., BESSELAAR, T. G., BIRCH, C., BUCHY, P., CHITTAGANPITCH, M., CHIU, S. C., DWYER, D., GUIGON, A., HARROWER, B., KEI, I. P., KOK, T., LIN, C., MCPHIE, K., MOHD, A., OLVEDA, R., PANAYOTOU, T., RAWLINSON, W., SCOTT, L., SMITH, D., D'SOUZA, H., KOMADINA, N., SHAW, R., KELSO, A. & BARR, I. G. 2009a. Emergence and spread of oseltamivir-resistant A(H1N1) influenza viruses in Oceania, South East Asia and South Africa. *Antiviral Res,* 83**,** 90-3.

HURT, A. C., HOLIEN, J. K., PARKER, M. W. & BARR, I. G. 2009b. Oseltamivir resistance and the H274Y neuraminidase mutation in seasonal, pandemic and highly pathogenic influenza viruses. *Drugs,* 69**,** 2523-31.

HUTCHINSON, E. C., CURRAN, M. D., READ, E. K., GOG, J. R. & DIGARD, P. 2008. Mutational analysis of cis-acting RNA signals in segment 7 of influenza A virus. *J Virol,* 82**,** 11869-79.

HUTCHINSON, E. C., WISE, H. M., KUDRYAVTSEVA, K., CURRAN, M. D. & DIGARD, P. 2009. Characterisation of influenza A viruses with mutations in segment 5 packaging signals. *Vaccine,* 27**,** 6270-5.

HUTCHINSON, E. C., VON KIRCHBACH, J. C., GOG, J. R. & DIGARD, P. 2010. Genome packaging in influenza A virus. *J Gen Virol,* 91**,** 313-28.

HUTCHINSON, E. C., DENHAM, E. M., THOMAS, B., TRUDGIAN, D. C., HESTER, S. S., RIDLOVA, G., YORK, A., TURRELL, L. & FODOR, E. 2012. Mapping the phosphoproteome of influenza A and B viruses by mass spectrometry. *PLoS Pathog,* 8**,** e1002993.

HUTCHINSON, E. C. & FODOR, E. 2012. Nuclear import of the influenza A virus transcriptional machinery. *Vaccine,* 30**,** 7353-8.

HUTCHINSON, E. C., CHARLES, P. D., HESTER, S. S., THOMAS, B., TRUDGIAN, D., MARTINEZ-ALONSO, M. & FODOR, E. 2014. Conserved and host-specific features of influenza virion architecture. *Nat Commun,* 5**,** 4816.

ICHINOHE, T., PANG, I. K. & IWASAKI, A. 2010. Influenza virus activates inflammasomes via its intracellular M2 ion channel. *Nat Immunol,* 11**,** 404-10.

IRVINE, K. M., ANDREWS, M. R., FERNANDEZ-ROJO, M. A., SCHRODER, K., BURNS, C. J., SU, S., WILKS, A. F., PARTON, R. G., HUME, D. A. & SWEET, M. J. 2009. Colony-stimulating factor-1 (CSF-1) delivers a proatherogenic signal to human macrophages. *J Leukoc Biol,* 85**,** 278-88.

ISHIKAWA, H., MA, Z. & BARBER, G. N. 2009. STING regulates intracellular DNA-mediated, type I interferon-dependent innate immunity. *Nature,* 461**,** 788-92.

IWAI, A., SHIOZAKI, T., KAWAI, T., AKIRA, S., KAWAOKA, Y., TAKADA, A., KIDA, H. & MIYAZAKI, T. 2010. Influenza A virus polymerase inhibits type I interferon induction by binding to interferon beta promoter stimulator 1. *J Biol Chem,* 285**,** 32064-74.

IWATSUKI-HORIMOTO, K., HORIMOTO, T., FUJII, Y. & KAWAOKA, Y. 2004. Generation of influenza A virus NS2 (NEP) mutants with an altered nuclear export signal sequence. *J Virol,* 78**,** 10149-55.

JACKSON, D., HOSSAIN, M. J., HICKMAN, D., PEREZ, D. R. & LAMB, R. A. 2008. A new influenza virus virulence determinant: the NS1 protein four C-terminal residues modulate pathogenicity. *Proc Natl Acad Sci U S A,* 105**,** 4381-6.

JACKSON, D., ELDERFIELD, R. A. & BARCLAY, W. S. 2011. Molecular studies of influenza B virus in the reverse genetics era. *J Gen Virol,* 92**,** 1-17.

JAGGER, B. W., WISE, H. M., KASH, J. C., WALTERS, K. A., WILLS, N. M., XIAO, Y. L., DUNFEE, R. L., SCHWARTZMAN, L. M., OZINSKY, A., BELL, G. L., DALTON, R. M., LO, A., EFSTATHIOU, S., ATKINS, J. F., FIRTH, A. E., TAUBENBERGER, J. K. & DIGARD, P. 2012. An overlapping protein-coding

region in influenza A virus segment 3 modulates the host response. *Science,* 337**,** 199-204.
JARDETZKY, T. S. & LAMB, R. A. 2004. Virology: a class act. *Nature,* 427**,** 307-8.
JIANG, W., WANG, Q., CHEN, S., GAO, S., SONG, L., LIU, P. & HUANG, W. 2013. Influenza A virus NS1 induces G0/G1 cell cycle arrest by inhibiting the expression and activity of RhoA protein. *J Virol,* 87**,** 3039-52.
JIN, W. & DONG, C. 2013. IL-17 cytokines in immunity and inflammation. *Emerg Microbes Infect,* 2**,** e60.
JOHNSON, C. A., PEKAS, D. J. & WINZLER, R. J. 1964. NEURAMINIDASES AND INFLUENZA VIRUS INFECTION IN EMBRYONATED EGGS. *Science,* 143**,** 1051-2.
KARASIN, A. I., BROWN, I. H., CARMAN, S. & OLSEN, C. W. 2000. Isolation and characterization of H4N6 avian influenza viruses from pigs with pneumonia in Canada. *J Virol,* 74**,** 9322-7.
KARASIN, A. I., WEST, K., CARMAN, S. & OLSEN, C. W. 2004. Characterization of avian H3N3 and H1N1 influenza A viruses isolated from pigs in Canada. *J Clin Microbiol,* 42**,** 4349-54.
KASTELEIN, R. A., HUNTER, C. A. & CUA, D. J. 2007. Discovery and biology of IL-23 and IL-27: related but functionally distinct regulators of inflammation. *Annu Rev Immunol,* 25**,** 221-42.
KATHUM, O. A., SCHRADER, T., ANHLAN, D., NORDHOFF, C., LIEDMANN, S., PANDE, A., MELLMANN, A., EHRHARDT, C., WIXLER, V. & LUDWIG, S. 2016. Phosphorylation of influenza A virus NS1 protein at threonine 49 suppresses its interferon antagonistic activity. *Cell Microbiol,* 18**,** 784-91.
KAWAGUCHI, A., MATSUMOTO, K. & NAGATA, K. 2012. YB-1 functions as a porter to lead influenza virus ribonucleoprotein complexes to microtubules. *J Virol,* 86**,** 11086-95.
KAWAI, N., IKEMATSU, H., IWAKI, N., KONDOU, K., HIROTSU, N., KAWASHIMA, T., MAEDA, T., TANAKA, O., DONIWA, K. & KASHIWAGI, S. 2009. Clinical effectiveness of oseltamivir for influenza A(H1N1) virus with H274Y neuraminidase mutation. *J Infect,* 59**,** 207-12.
KAWAOKA, Y., GORMAN, O. T., ITO, T., WELLS, K., DONIS, R. O., CASTRUCCI, M. R., DONATELLI, I. & WEBSTER, R. G. 1998. Influence of host species on the evolution of the nonstructural (NS) gene of influenza A viruses. *Virus Res,* 55**,** 143-56.
KEAWCHAROEN, J., VAN DEN BROEK, J., BOUMA, A., TIENSIN, T., OSTERHAUS, A. D. & HEESTERBEEK, H. 2011. Wild birds and increased transmission of highly pathogenic avian influenza (H5N1) among poultry, Thailand. *Emerg Infect Dis,* 17**,** 1016-22.
KERRY, P. S., AYLLON, J., TAYLOR, M. A., HASS, C., LEWIS, A., GARCIA-SASTRE, A., RANDALL, R. E., HALE, B. G. & RUSSELL, R. J. 2011a. A transient homotypic interaction model for the influenza A virus NS1 protein effector domain. *PLoS One,* 6**,** e17946.
KERRY, P. S., LONG, E., TAYLOR, M. A. & RUSSELL, R. J. 2011b. Conservation of a crystallographic interface suggests a role for beta-sheet augmentation in influenza virus NS1 multifunctionality. *Acta Crystallogr Sect F Struct Biol Cryst Commun,* 67**,** 858-61.
KHAPERSKYY, D. A., SCHMALING, S., LARKINS-FORD, J., MCCORMICK, C. & GAGLIA, M. M. 2016. Selective Degradation of Host RNA Polymerase II Transcripts by Influenza A Virus PA-X Host Shutoff Protein. *PLoS Pathog,* 12**,** e1005427.
KILLINGLEY, B. & NGUYEN-VAN-TAM, J. 2013. Routes of influenza transmission. *Influenza Other Respir Viruses,* 7 Suppl 2**,** 42-51.

KILLIP, M. J., FODOR, E. & RANDALL, R. E. 2015. Influenza virus activation of the interferon system. *Virus Res,* 209**,** 11-22.
KIM, H. M., LEE, Y. W., LEE, K. J., KIM, H. S., CHO, S. W., VAN ROOIJEN, N., GUAN, Y. & SEO, S. H. 2008. Alveolar macrophages are indispensable for controlling influenza viruses in lungs of pigs. *J Virol,* 82**,** 4265-74.
KIM, I. H., KWON, H. J., LEE, S. H., KIM, D. Y. & KIM, J. H. 2015a. Effects of different NS genes of avian influenza viruses and amino acid changes on pathogenicity of recombinant A/Puerto Rico/8/34 viruses. *Vet Microbiol,* 175**,** 17-25.
KIM, J. I., HWANG, M. W., LEE, I., PARK, S., LEE, S., BAE, J. Y., HEO, J., KIM, D., JANG, S. I., PARK, M. S., KWON, H. J., SONG, J. W. & PARK, M. S. 2014. The PDZ-binding motif of the avian NS1 protein affects transmission of the 2009 influenza A(H1N1) virus. *Biochem Biophys Res Commun,* 449**,** 19-25.
KIM, K. S., JUNG, H., SHIN, I. K., CHOI, B. R. & KIM, D. H. 2015b. Induction of interleukin-1 beta (IL-1beta) is a critical component of lung inflammation during influenza A (H1N1) virus infection. *J Med Virol,* 87**,** 1104-12.
KING, P. & GOODBOURN, S. 1994. The beta-interferon promoter responds to priming through multiple independent regulatory elements. *J Biol Chem,* 269**,** 30609-15.
KING, P. & GOODBOURN, S. 1998. STAT1 is inactivated by a caspase. *J Biol Chem,* 273**,** 8699-704.
KIRISAWA, R., OGASAWARA, Y., YOSHITAKE, H., KODA, A. & FURUYA, T. 2014. Genomic reassortants of pandemic A (H1N1) 2009 virus and endemic porcine H1 and H3 viruses in swine in Japan. *J Vet Med Sci,* 76**,** 1457-70.
KLENK, H. D., ROTT, R., ORLICH, M. & BLODORN, J. 1975. Activation of influenza A viruses by trypsin treatment. *Virology,* 68**,** 426-39.
KLENK, H. D. & GARTEN, W. 1994. Host cell proteases controlling virus pathogenicity. *Trends Microbiol,* 2**,** 39-43.
KLUMPP, K., RUIGROK, R. W. & BAUDIN, F. 1997. Roles of the influenza virus polymerase and nucleoprotein in forming a functional RNP structure. *Embo j,* 16**,** 1248-57.
KNEPPER, J., SCHIERHORN, K. L., BECHER, A., BUDT, M., TÖNNIES, M., BAUER, T. T., SCHNEIDER, P., NEUDECKER, J., RÜCKERT, J. C., GRUBER, A. D., SUTTORP, N., SCHWEIGER, B., HIPPENSTIEL, S., HOCKE, A. C. & WOLFF, T. 2013. The Novel Human Influenza A(H7N9) Virus Is Naturally Adapted to Efficient Growth in Human Lung Tissue. *mBio,* 4**,** e00601-13.
KOCHS, G., GARCIA-SASTRE, A. & MARTINEZ-SOBRIDO, L. 2007. Multiple anti-interferon actions of the influenza A virus NS1 protein. *J Virol,* 81**,** 7011-21.
KOK, K. H., LUI, P. Y., NG, M. H., SIU, K. L., AU, S. W. & JIN, D. Y. 2011. The double-stranded RNA-binding protein PACT functions as a cellular activator of RIG-I to facilitate innate antiviral response. *Cell Host Microbe,* 9**,** 299-309.
KONIG, R., STERTZ, S., ZHOU, Y., INOUE, A., HOFFMANN, H. H., BHATTACHARYYA, S., ALAMARES, J. G., TSCHERNE, D. M., ORTIGOZA, M. B., LIANG, Y., GAO, Q., ANDREWS, S. E., BANDYOPADHYAY, S., DE JESUS, P., TU, B. P., PACHE, L., SHIH, C., ORTH, A., BONAMY, G., MIRAGLIA, L., IDEKER, T., GARCIA-SASTRE, A., YOUNG, J. A., PALESE, P., SHAW, M. L. & CHANDA, S. K. 2010. Human host factors required for influenza virus replication. *Nature,* 463**,** 813-7.
KOOPMANS, M., WILBRINK, B., CONYN, M., NATROP, G., VAN DER NAT, H., VENNEMA, H., MEIJER, A., VAN STEENBERGEN, J., FOUCHIER, R., OSTERHAUS, A. & BOSMAN, A. 2004. Transmission of H7N7 avian influenza A virus to human beings during a large outbreak in commercial poultry farms in the Netherlands. *Lancet,* 363**,** 587-93.
KORNILUK, A., KEMONA, H. & DYMICKA-PIEKARSKA, V. 2014. Multifunctional CD40L: pro- and anti-neoplastic activity. *Tumour Biol,* 35**,** 9447-57.

KOSHIBA, T., YASUKAWA, K., YANAGI, Y. & KAWABATA, S.-I. 2011. Mitochondrial Membrane Potential Is Required for MAVS-Mediated Antiviral Signaling. *Science Signaling,* 4**,** ra7-ra7.

KOTENKO, S. V., GALLAGHER, G., BAURIN, V. V., LEWIS-ANTES, A., SHEN, M., SHAH, N. K., LANGER, J. A., SHEIKH, F., DICKENSHEETS, H. & DONNELLY, R. P. 2003. IFN-lambdas mediate antiviral protection through a distinct class II cytokine receptor complex. *Nat Immunol,* 4**,** 69-77.

KRUG, R. M. 2015. Functions of the influenza A virus NS1 protein in antiviral defense. *Curr Opin Virol,* 12**,** 1-6.

KUCHIPUDI, S. V., TELLABATI, M., SEBASTIAN, S., LONDT, B. Z., JANSEN, C., VERVELDE, L., BROOKES, S. M., BROWN, I. H., DUNHAM, S. P. & CHANG, K. C. 2014. Highly pathogenic avian influenza virus infection in chickens but not ducks is associated with elevated host immune and pro-inflammatory responses. *Vet Res,* 45**,** 118.

KUHLMAN, P., MOY, V. T., LOLLO, B. A. & BRIAN, A. A. 1991. The accessory function of murine intercellular adhesion molecule-1 in T lymphocyte activation. Contributions of adhesion and co-activation. *J Immunol,* 146**,** 1773-82.

KUMAGAI, Y., TAKEUCHI, O., KATO, H., KUMAR, H., MATSUI, K., MORII, E., AOZASA, K., KAWAI, T. & AKIRA, S. 2007. Alveolar macrophages are the primary interferon-alpha producer in pulmonary infection with RNA viruses. *Immunity,* 27**,** 240-52.

KUMAR, A., HAQUE, J., LACOSTE, J., HISCOTT, J. & WILLIAMS, B. R. 1994. Double-stranded RNA-dependent protein kinase activates transcription factor NF-kappa B by phosphorylating I kappa B. *Proceedings of the National Academy of Sciences of the United States of America,* 91**,** 6288-6292.

KUNIYOSHI, K., TAKEUCHI, O., PANDEY, S., SATOH, T., IWASAKI, H., AKIRA, S. & KAWAI, T. 2014. Pivotal role of RNA-binding E3 ubiquitin ligase MEX3C in RIG-I-mediated antiviral innate immunity. *Proc Natl Acad Sci U S A,* 111**,** 5646-51.

KUO, R. L., ZHAO, C., MALUR, M. & KRUG, R. M. 2010. Influenza A virus strains that circulate in humans differ in the ability of their NS1 proteins to block the activation of IRF3 and interferon-beta transcription. *Virology,* 408**,** 146-58.

KUO, R. L., LI, L. H., LIN, S. J., LI, Z. H., CHEN, G. W., CHANG, C. K., WANG, Y. R., TAM, E. H., GONG, Y. N., KRUG, R. M. & SHIH, S. R. 2016. Role of N Terminus-Truncated NS1 Proteins of Influenza A Virus in Inhibiting IRF3 Activation. *J Virol,* 90**,** 4696-705.

KURTZ, J., MANVELL, R. J. & BANKS, J. 1996. Avian influenza virus isolated from a woman with conjunctivitis. *Lancet,* 348**,** 901-2.

KWON, T. Y., LEE, S. S., KIM, C. Y., SHIN, J. Y., SUNWOO, S. Y. & LYOO, Y. S. 2011. Genetic characterization of H7N2 influenza virus isolated from pigs. *Vet Microbiol,* 153**,** 393-7.

LAMB, R. A. & LAI, C.-J. 1980. Sequence of Interrupted and Uninterrupted mRNAs and Cloned DNA Coding for the Two Overlapping Nonstructural Proteins of Influenza Virus. *Cell,* 21**,** 475-485.

LAMB, R. A. & CHOPPIN, P. W. 1981. Identification of a second protein (M2) encoded by RNA segment 7 of influenza virus. *Virology,* 112**,** 729-37.

LARSEN, S., BUI, S., PEREZ, V., MOHAMMAD, A., MEDINA-RAMIREZ, H. & NEWCOMB, L. L. 2014. Influenza polymerase encoding mRNAs utilize atypical mRNA nuclear export. *Virol J,* 11**,** 154.

LAURING, A. S. & ANDINO, R. 2010. Quasispecies Theory and the Behavior of RNA Viruses. *PLoS Pathog,* 6**,** e1001005.

LAVER, W. G. & VALENTINE, R. C. 1969. Morphology of the isolated hemagglutinin and neuraminidase subunits of influenza virus. *Virology,* 38**,** 105-19.

LEE, J. H., PASCUA, P. N. Q., SONG, M. S., BAEK, Y. H., KIM, C. J., CHOI, H. W., SUNG, M. H., WEBBY, R. J., WEBSTER, R. G., POO, H. & CHOI, Y. K. 2009a. Isolation and Genetic Characterization of H5N2 Influenza Viruses from Pigs in Korea. *J Virol,* 83**,** 4205-4215.

LEE, M. M., YOON, B. J., OSIEWICZ, K., PRESTON, M., BUNDY, B., VAN HEECKEREN, A. M., WERB, Z. & SOLOWAY, P. D. 2005. Tissue inhibitor of metalloproteinase 1 regulates resistance to infection. *Infect Immun,* 73**,** 661-5.

LEE, S. M., GARDY, J. L., CHEUNG, C. Y., CHEUNG, T. K., HUI, K. P., IP, N. Y., GUAN, Y., HANCOCK, R. E. & PEIRIS, J. S. 2009b. Systems-level comparison of host-responses elicited by avian H5N1 and seasonal H1N1 influenza viruses in primary human macrophages. *PLoS One,* 4**,** e8072.

LESER, G. P. & LAMB, R. A. 2005. Influenza virus assembly and budding in raft-derived microdomains: a quantitative analysis of the surface distribution of HA, NA and M2 proteins. *Virology,* 342**,** 215-27.

LI, J., ZU DOHNA, H., MILLER, J., CARDONA, C. J. & CARPENTER, T. E. 2010. Identifying errors in avian influenza virus gene sequences and implications for data usage of public databases. *Genomics,* 95**,** 29-36.

LI, Y., YAMAKITA, Y. & KRUG, R. M. 1998. Regulation of a nuclear export signal by an adjacent inhibitory sequence: the effector domain of the influenza virus NS1 protein. *Proc Natl Acad Sci U S A,* 95**,** 4864-9.

LI, Y., CHEN, Z. Y., WANG, W., BAKER, C. C. & KRUG, R. M. 2001. The 3'-end-processing factor CPSF is required for the splicing of single-intron pre-mRNAs in vivo. *Rna,* 7**,** 920-31.

LI, Y., BANERJEE, S., WANG, Y., GOLDSTEIN, S. A., DONG, B., GAUGHAN, C., SILVERMAN, R. H. & WEISS, S. R. 2016. Activation of RNase L is dependent on OAS3 expression during infection with diverse human viruses. *Proc Natl Acad Sci U S A,* 113**,** 2241-6.

LI, Z., CHEN, H., JIAO, P., DENG, G., TIAN, G., LI, Y., HOFFMANN, E., WEBSTER, R. G., MATSUOKA, Y. & YU, K. 2005. Molecular Basis of Replication of Duck H5N1 Influenza Viruses in a Mammalian Mouse Model. *Journal of Virology,* 79**,** 12058-12064.

LIANG, Y., HONG, Y. & PARSLOW, T. G. 2005. cis-Acting packaging signals in the influenza virus PB1, PB2, and PA genomic RNA segments. *J Virol,* 79**,** 10348-55.

LIM, K., HYUN, Y. M., LAMBERT-EMO, K., CAPECE, T., BAE, S., MILLER, R., TOPHAM, D. J. & KIM, M. 2015. Neutrophil trails guide influenza-specific CD8(+) T cells in the airways. *Science,* 349**,** aaa4352.

LINDELL, D. M., LANE, T. E. & LUKACS, N. W. 2008. CXCL10/CXCR3-mediated responses promote immunity to respiratory syncytial virus infection by augmenting dendritic cell and CD8(+) T cell efficacy. *Eur J Immunol,* 38**,** 2168-79.

LIU, G., PARK, H. S., PYO, H. M., LIU, Q. & ZHOU, Y. 2015a. Influenza A Virus Panhandle Structure Is Directly Involved in RIG-I Activation and Interferon Induction. *J Virol,* 89**,** 6067-79.

LIU, J., LYNCH, P. A., CHIEN, C. Y., MONTELIONE, G. T., KRUG, R. M. & BERMAN, H. M. 1997. Crystal structure of the unique RNA-binding domain of the influenza virus NS1 protein. *Nat Struct Biol,* 4**,** 896-9.

LIU, X., LAI, C., WANG, K., XING, L., YANG, P., DUAN, Q. & WANG, X. 2015b. A Functional Role of Fibroblast Growth Factor Receptor 1 (FGFR1) in the Suppression of Influenza A Virus Replication. *PLoS One,* 10**,** e0124651.

LONG, J. S., GIOTIS, E. S., MONCORGE, O., FRISE, R., MISTRY, B., JAMES, J., MORISSON, M., IQBAL, M., VIGNAL, A., SKINNER, M. A. & BARCLAY, W. S. 2016. Species difference in ANP32A underlies influenza A virus polymerase host restriction. *Nature,* 529**,** 101-4.

LOO, Y. M. & GALE, M., JR. 2011. Immune signaling by RIG-I-like receptors. *Immunity,* 34**,** 680-92.

LOPEZ-MARTINEZ, I., BALISH, A., BARRERA-BADILLO, G., JONES, J., NUNEZ-GARCIA, T. E., JANG, Y., APARICIO-ANTONIO, R., AZZIZ-BAUMGARTNER, E., BELSER, J. A., RAMIREZ-GONZALEZ, J. E., PEDERSEN, J. C., ORTIZ-ALCANTARA, J., GONZALEZ-DURAN, E., SHU, B., EMERY, S. L., POH, M. K., REYES-TERAN, G., VAZQUEZ-PEREZ, J. A., AVILA-RIOS, S., UYEKI, T., LINDSTROM, S., VILLANUEVA, J., TOKARS, J., RUIZ-MATUS, C., GONZALEZ-ROLDAN, J. F., SCHMITT, B., KLIMOV, A., COX, N., KURI-MORALES, P., DAVIS, C. T. & DIAZ-QUINONEZ, J. A. 2013. Highly pathogenic avian influenza A(H7N3) virus in poultry workers, Mexico, 2012. *Emerg Infect Dis,* 19**,** 1531-4.

LOWEN, A. C., MUBAREKA, S., TUMPEY, T. M., GARCIA-SASTRE, A. & PALESE, P. 2006. The guinea pig as a transmission model for human influenza viruses. *Proc Natl Acad Sci U S A,* 103**,** 9988-92.

LU, Y., QIAN, X. Y. & KRUG, R. M. 1994. The influenza virus NS1 protein: a novel inhibitor of pre-mRNA splicing. *Genes Dev,* 8**,** 1817-28.

LUDWIG, S., SCHULTZ, U., MANDLER, J., FITCH, W. M. & SCHOLTISSEK, C. 1991. Phylogenetic relationship of the nonstructural (NS) genes of influenza A viruses. *Virology,* 183**,** 566-77.

LUDWIG, S., WANG, X., EHRHARDT, C., ZHENG, H., DONELAN, N., PLANZ, O., PLESCHKA, S., GARCIA-SASTRE, A., HEINS, G. & WOLFF, T. 2002. The influenza A virus NS1 protein inhibits activation of Jun N-terminal kinase and AP-1 transcription factors. *J Virol,* 76**,** 11166-71.

LUTHER, S. A., LOPEZ, T., BAI, W., HANAHAN, D. & CYSTER, J. G. 2000. BLC expression in pancreatic islets causes B cell recruitment and lymphotoxin-dependent lymphoid neogenesis. *Immunity,* 12**,** 471-81.

LUTZ, A., DYALL, J., OLIVO, P. D. & PEKOSZ, A. 2005. Virus-inducible reporter genes as a tool for detecting and quantifying influenza A virus replication. *Journal of Virological Methods,* 126**,** 13-20.

LUYTJES, W., KRYSTAL, M., ENAMI, M., PARVIN, J. D. & PALESE, P. 1989. Amplification, expression, and packaging of foreign gene by influenza virus. *Cell,* 59**,** 1107-13.

LUZINA, I. G., KEEGAN, A. D., HELLER, N. M., ROOK, G. A., SHEA-DONOHUE, T. & ATAMAS, S. P. 2012. Regulation of inflammation by interleukin-4: a review of "alternatives". *J Leukoc Biol,* 92**,** 753-64.

LVOV, D. K., SHCHELKANOV, M. Y., ALKHOVSKY, S. V. & DERYABIN, P. G. 2015. Zoonotic Viruses of Northern Eurasia: Taxonomy and Ecology. *Chapter 8: Single-Stranded RNA Viruses.*

.

LYCETT, S. J., BAILLIE, G., COULTER, E., BHATT, S., KELLAM, P., MCCAULEY, J. W., WOOD, J. L., BROWN, I. H., PYBUS, O. G., LEIGH BROWN, A. J. & COMBATING SWINE INFLUENZA INITIATIVE, C. C. 2012. Estimating reassortment rates in co-circulating Eurasian swine influenza viruses. *J Gen Virol,* 93**,** 2326-36.

MA, W., BRENNER, D., WANG, Z., DAUBER, B., EHRHARDT, C., HOGNER, K., HEROLD, S., LUDWIG, S., WOLFF, T., YU, K., RICHT, J. A., PLANZ, O. & PLESCHKA, S. 2010. The NS segment of an H5N1 highly pathogenic avian influenza virus (HPAIV) is sufficient to alter replication efficiency, cell tropism, and host range of an H7N1 HPAIV. *J Virol,* 84**,** 2122-33.

MACDONALD, D. C., SINGH, H., WHELAN, M. A., ESCORS, D., ARCE, F., BOTTOMS, S. E., BARCLAY, W. S., MAINI, M., COLLINS, M. K. & ROSENBERG, W. M.

2014. Harnessing alveolar macrophages for sustained mucosal T-cell recall confers long-term protection to mice against lethal influenza challenge without clinical disease. *Mucosal Immunol,* 7**,** 89-100.
MAGOR, K. E., MIRANZO NAVARRO, D., BARBER, M. R., PETKAU, K., FLEMING-CANEPA, X., BLYTH, G. A. & BLAINE, A. H. 2013. Defense genes missing from the flight division. *Dev Comp Immunol,* 41**,** 377-88.
MALUR, M., GALE, M. & KRUG, R. M. 2012. LGP2 Downregulates Interferon Production during Infection with Seasonal Human Influenza A Viruses That Activate Interferon Regulatory Factor 3. *Journal of Virology,* 86**,** 10733-10738.
MÄNZ, B., BRUNOTTE, L., REUTHER, P. & SCHWEMMLE, M. 2012. Adaptive mutations in NEP compensate for defective H5N1 RNA replication in cultured human cells. *Nat Commun,* 3**,** 802.
MARC, D., BARBACHOU, S. & SOUBIEUX, D. 2013. The RNA-binding domain of influenzavirus non-structural protein-1 cooperatively binds to virus-specific RNA sequences in a structure-dependent manner. *Nucleic Acids Res,* 41**,** 434-49.
MARTIN, K. & HELENIUS, A. 1991. Nuclear transport of influenza virus ribonucleoproteins: the viral matrix protein (M1) promotes export and inhibits import. *Cell,* 67**,** 117-30.
MASSIN, P., VAN DER WERF, S. & NAFFAKH, N. 2001. Residue 627 of PB2 is a determinant of cold sensitivity in RNA replication of avian influenza viruses. *J Virol,* 75**,** 5398-404.
MATROSOVICH, M., TUZIKOV, A., BOVIN, N., GAMBARYAN, A., KLIMOV, A., CASTRUCCI, M. R., DONATELLI, I. & KAWAOKA, Y. 2000. Early alterations of the receptor-binding properties of H1, H2, and H3 avian influenza virus hemagglutinins after their introduction into mammals. *J Virol,* 74**,** 8502-12.
MATROSOVICH, M., MATROSOVICH, T., CARR, J., ROBERTS, N. A. & KLENK, H. D. 2003. Overexpression of the alpha-2,6-sialyltransferase in MDCK cells increases influenza virus sensitivity to neuraminidase inhibitors. *J Virol,* 77**,** 8418-25.
MATROSOVICH, M. N., MATROSOVICH, T. Y., GRAY, T., ROBERTS, N. A. & KLENK, H. D. 2004. Human and avian influenza viruses target different cell types in cultures of human airway epithelium. *Proc Natl Acad Sci U S A,* 101**,** 4620-4.
MATSUOKA, Y., SWAYNE, D. E., THOMAS, C., RAMEIX-WELTI, M. A., NAFFAKH, N., WARNES, C., ALTHOLTZ, M., DONIS, R. & SUBBARAO, K. 2009. Neuraminidase stalk length and additional glycosylation of the hemagglutinin influence the virulence of influenza H5N1 viruses for mice. *J Virol,* 83**,** 4704-8.
MCGEOGH, D., FELLNER, P. & NEWTON, C. 1976. Influenza virus genome consists of eight distinct RNA species. *PNAS,* 73**,** 3045-3049.
MEHLE, A. & DOUDNA, J. A. 2009. Adaptive strategies of the influenza virus polymerase for replication in humans. *Proc Natl Acad Sci U S A,* 106**,** 21312-6.
MELEN, K., KINNUNEN, L., FAGERLUND, R., IKONEN, N., TWU, K. Y., KRUG, R. M. & JULKUNEN, I. 2007. Nuclear and nucleolar targeting of influenza A virus NS1 protein: striking differences between different virus subtypes. *J Virol,* 81**,** 5995-6006.
MENTEN, P., WUYTS, A. & VAN DAMME, J. 2002. Macrophage inflammatory protein-1. *Cytokine Growth Factor Rev,* 13**,** 455-81.
MIBAYASHI, M., MARTINEZ-SOBRIDO, L., LOO, Y. M., CARDENAS, W. B., GALE, M., JR. & GARCIA-SASTRE, A. 2007. Inhibition of retinoic acid-inducible gene I-mediated induction of beta interferon by the NS1 protein of influenza A virus. *J Virol,* 81**,** 514-24.
MILLER, M. D. & KRANGEL, M. S. 1992. The human cytokine I-309 is a monocyte chemoattractant. *Proc Natl Acad Sci U S A,* 89**,** 2950-4.
MIN, J. Y. & KRUG, R. M. 2006. The primary function of RNA binding by the influenza A virus NS1 protein in infected cells: Inhibiting the 2'-5' oligo (A) synthetase/RNase L pathway. *Proc Natl Acad Sci U S A,* 103**,** 7100-5.

MIN, J. Y., LI, S., SEN, G. C. & KRUG, R. M. 2007. A site on the influenza A virus NS1 protein mediates both inhibition of PKR activation and temporal regulation of viral RNA synthesis. *Virology,* 363**,** 236-43.

MOELLER, A., KIRCHDOERFER, R. N., POTTER, C. S., CARRAGHER, B. & WILSON, I. A. 2012. Organization of the influenza virus replication machinery. *Science,* 338**,** 1631-4.

MOMOSE, F., SEKIMOTO, T., OHKURA, T., JO, S., KAWAGUCHI, A., NAGATA, K. & MORIKAWA, Y. 2011. Apical transport of influenza A virus ribonucleoprotein requires Rab11-positive recycling endosome. *PLoS One,* 6**,** e21123.

MONCORGE, O., MURA, M. & BARCLAY, W. S. 2010. Evidence for avian and human host cell factors that affect the activity of influenza virus polymerase. *J Virol,* 84**,** 9978-86.

MORENS, D. M., TAUBENBERGER, J. K. & FAUCI, A. S. 2008. Predominant Role of Bacterial Pneumonia as a Cause of Death in Pandemic Influenza: Implications for Pandemic Influenza Preparedness. *Journal of Infectious Diseases,* 198**,** 962-970.

MOSLEY, V. M. & WYCKOFF, R. W. 1946. Electron micrography of the virus of influenza. *Nature,* 157**,** 263.

MUDHASANI, R., TRAN, J. P., RETTERER, C., RADOSHITZKY, S. R., KOTA, K. P., ALTAMURA, L. A., SMITH, J. M., PACKARD, B. Z., KUHN, J. H., COSTANTINO, J., GARRISON, A. R., SCHMALJOHN, C. S., HUANG, I. C., FARZAN, M. & BAVARI, S. 2013. IFITM-2 and IFITM-3 but not IFITM-1 restrict Rift Valley fever virus. *J Virol,* 87**,** 8451-64.

MULLER, M., CARTER, S., HOFER, M. J. & CAMPBELL, I. L. 2010. Review: The chemokine receptor CXCR3 and its ligands CXCL9, CXCL10 and CXCL11 in neuroimmunity--a tale of conflict and conundrum. *Neuropathol Appl Neurobiol,* 36**,** 368-87.

MUNIR, M., ZOHARI, S. & BERG, M. 2011a. Non-structural protein 1 of avian influenza A viruses differentially inhibit NF-kappaB promoter activation. *Virol J,* 8**,** 383.

MUNIR, M., ZOHARI, S., METREVELI, G., BAULE, C., BELAK, S. & BERG, M. 2011b. Alleles A and B of non-structural protein 1 of avian influenza A viruses differentially inhibit beta interferon production in human and mink lung cells. *J Gen Virol,* 92**,** 2111-21.

MUNIR, M., ZOHARI, S., BELAK, S. & BERG, M. 2012. Double-stranded RNA-induced activation of activating protein-1 promoter is differentially regulated by the non-structural protein 1 of avian influenza A viruses. *Viral Immunol,* 25**,** 79-85.

MURAMOTO, Y., NODA, T., KAWAKAMI, E., AKKINA, R. & KAWAOKA, Y. 2013. Identification of novel influenza A virus proteins translated from PA mRNA. *J Virol,* 87**,** 2455-62.

MURCIA, P. R., WOOD, J. L. & HOLMES, E. C. 2011. Genome-scale evolution and phylodynamics of equine H3N8 influenza A virus. *J Virol,* 85**,** 5312-22.

NAFFAKH, N., MASSIN, P., ESCRIOU, N., CRESCENZO-CHAIGNE, B. & VAN DER WERF, S. 2000. Genetic analysis of the compatibility between polymerase proteins from human and avian strains of influenza A viruses. *J Gen Virol,* 81**,** 1283-91.

NAKAJIMA, K., DESSELBERGER, U. & PALESE, P. 1978. Recent human influenza A (H1N1) viruses are closely related genetically to strains isolated in 1950. *Nature,* 274**,** 334-339.

NAYAK, D. P. 1980. Defective interfering influenza viruses. *Annu Rev Microbiol,* 34**,** 619-44.

NEMEROFF, M. E., BARABINO, S. M. L., LI, Y., KELLER, W. & KRUG, R. M. 1998. Influenza Virus NS1 Protein Interacts with the Cellular 30kDa Subunit of CPSF and Inhibits 3' End Formation of Cellular Pre-mRNAs. *Molecular Cell,* 1**,** 991-1000.

NEUMANN, G., HUGHES, M. T. & KAWAOKA, Y. 2000. Influenza A virus NS2 protein mediates vRNP nuclear export through NES-independent interaction with hCRM1. *Embo j,* 19**,** 6751-8.

NEWBY, C. M., SABIN, L. & PEKOSZ, A. 2007. The RNA binding domain of influenza A virus NS1 protein affects secretion of tumor necrosis factor alpha, interleukin-6, and interferon in primary murine tracheal epithelial cells. *J Virol,* 81**,** 9469-80.

NICOL, M. Q. & DUTIA, B. M. 2014. The role of macrophages in influenza A virus infection. *Future Virology,* 9**,** 847-862.

NOAH, D. L., TWU, K. Y. & KRUG, R. M. 2003. Cellular antiviral responses against influenza A virus are countered at the posttranscriptional level by the viral NS1A protein via its binding to a cellular protein required for the 3' end processing of cellular pre-mRNAS. *Virology,* 307**,** 386-95.

NODA, T., SAGARA, H., YEN, A., TAKADA, A., KIDA, H., CHENG, R. H. & KAWAOKA, Y. 2006. Architecture of ribonucleoprotein complexes in influenza A virus particles. *Nature,* 439**,** 490-2.

NODA, T., SUGITA, Y., AOYAMA, K., HIRASE, A., KAWAKAMI, E., MIYAZAWA, A., SAGARA, H. & KAWAOKA, Y. 2012. Three-dimensional analysis of ribonucleoprotein complexes in influenza A virus. *Nat Commun,* 3**,** 639.

NOTON, S. L., MEDCALF, E., FISHER, D., MULLIN, A. E., ELTON, D. & DIGARD, P. 2007. Identification of the domains of the influenza A virus M1 matrix protein required for NP binding, oligomerization and incorporation into virions. *J Gen Virol,* 88**,** 2280-90.

NOTON, S. L., SIMPSON-HOLLEY, M., MEDCALF, E., WISE, H. M., HUTCHINSON, E. C., MCCAULEY, J. W. & DIGARD, P. 2009. Studies of an influenza A virus temperature-sensitive mutant identify a late role for NP in the formation of infectious virions. *J Virol,* 83**,** 562-71.

O'NEILL, R. E., JASKUNAS, R., BLOBEL, G., PALESE, P. & MOROIANU, J. 1995. Nuclear import of influenza virus RNA can be mediated by viral nucleoprotein and transport factors required for protein import. *J Biol Chem,* 270**,** 22701-4.

O'NEILL, R. E., TALON, J. & PALESE, P. 1998. The influenza virus NEP (NS2 protein) mediates the nuclear export of viral ribonucleoproteins. *EMBO J,* 17**,** 288-96.

OBENAUER, J. C., DENSON, J., MEHTA, P. K., SU, X., MUKATIRA, S., FINKELSTEIN, D. B., XU, X., WANG, J., MA, J., FAN, Y., RAKESTRAW, K. M., WEBSTER, R. G., HOFFMANN, E., KRAUSS, S., ZHENG, J., ZHANG, Z. & NAEVE, C. W. 2006. Large-scale sequence analysis of avian influenza isolates. *Science,* 311**,** 1576-80.

ODAGIRI, T., TOMINAGA, K., TOBITA, K. & OHTA, S. 1994. An amino acid change in the non-structural NS2 protein of an influenza A virus mutant is responsible for the generation of defective interfering (DI) particles by amplifying DI RNAs and suppressing complementary RNA synthesis. *J Gen Virol,* 75 (Pt 1)**,** 43-53.

OHUCHI, R., OHUCHI, M., GARTEN, W. & KLENK, H. D. 1997. Oligosaccharides in the stem region maintain the influenza virus hemagglutinin in the metastable form required for fusion activity. *J Virol,* 71**,** 3719-25.

OLSEN, B., MUNSTER, V. J., WALLENSTEN, A., WALDENSTRÖM, J., OSTERHAUS, A. D. M. E. & FOUCHIER, R. A. M. 2006. Global Patterns of Influenza A Virus in Wild Birds. *Science,* 312**,** 384-388.

ORTEGA, J., MARTIN-BENITO, J., ZURCHER, T., VALPUESTA, J. M., CARRASCOSA, J. L. & ORTIN, J. 2000. Ultrastructural and Functional Analyses of Recombinant Influenza Virus Ribonucleoproteins Suggest Dimerization of Nucleoprotein during Virus Amplification. *J Virol,* 74**,** 156-163.

OSHIUMI, H., MATSUMOTO, M., HATAKEYAMA, S. & SEYA, T. 2009. Riplet/RNF135, a RING finger protein, ubiquitinates RIG-I to promote interferon-beta induction during the early phase of viral infection. *J Biol Chem,* 284**,** 807-17.

OSTROWSKY, B., HUANG, A., TERRY, W., ANTON, D., BRUNAGEL, B., TRAYNOR, L., ABID, S., JOHNSON, G., KACICA, M., KATZ, J., EDWARDS, L., LINDSTROM, S., KLIMOV, A. & UYEKI, T. M. 2012. Low pathogenic avian

influenza A (H7N2) virus infection in immunocompromised adult, New York, USA, 2003. *Emerg Infect Dis,* 18**,** 1128-31.
OUYANG, W., RUTZ, S., CRELLIN, N. K., VALDEZ, P. A. & HYMOWITZ, S. G. 2011. Regulation and functions of the IL-10 family of cytokines in inflammation and disease. *Annu Rev Immunol,* 29**,** 71-109.
PAL, S., SANTOS, A., ROSAS, J. M., ORTIZ-GUZMAN, J. & ROSAS-ACOSTA, G. 2011. Influenza A virus interacts extensively with the cellular SUMOylation system during infection. *Virus Res,* 158**,** 12-27.
PALESE, P., TOBITA, K., UEDA, M. & COMPANS, R. W. 1974. Characterization of temperature sensitive influenza virus mutants defective in neuraminidase. *Virology,* 61**,** 397-410.
PEREZ, J. T., VARBLE, A., SACHIDANANDAM, R., ZLATEV, I., MANOHARAN, M., GARCIA-SASTRE, A. & TENOEVER, B. R. 2010. Influenza A virus-generated small RNAs regulate the switch from transcription to replication. *Proc Natl Acad Sci U S A,* 107**,** 11525-30.
PERREIRA, J. M., CHIN, C. R., FEELEY, E. M. & BRASS, A. L. 2013. IFITMs restrict the replication of multiple pathogenic viruses. *J Mol Biol,* 425**,** 4937-55.
PICA, N. & PALESE, P. 2013. Toward a universal influenza virus vaccine: prospects and challenges. *Annu Rev Med,* 64**,** 189-202.
PICHLMAIR, A., LASSNIG, C., EBERLE, C. A., GORNA, M. W., BAUMANN, C. L., BURKARD, T. R., BURCKSTUMMER, T., STEFANOVIC, A., KRIEGER, S., BENNETT, K. L., RULICKE, T., WEBER, F., COLINGE, J., MULLER, M. & SUPERTI-FURGA, G. 2011. IFIT1 is an antiviral protein that recognizes 5'-triphosphate RNA. *Nat Immunol,* 12**,** 624-30.
PLATANIAS, L. C. 2005. Mechanisms of type-I- and type-II-interferon-mediated signalling. *Nat Rev Immunol,* 5**,** 375-86.
PLOTCH, S. J., BOULOY, M., ULMANEN, I. & KRUG, R. M. 1981. A unique cap(m7GpppXm)-dependent influenza virion endonuclease cleaves capped RNAs to generate the primers that initiate viral RNA transcription. *Cell,* 23**,** 847-58.
POON, L. L., PRITLOVE, D. C., FODOR, E. & BROWNLEE, G. G. 1999. Direct evidence that the poly(A) tail of influenza A virus mRNA is synthesized by reiterative copying of a U track in the virion RNA template. *J Virol,* 73**,** 3473-6.
POST, J., PEETERS, B., CORNELISSEN, J. B., VERVELDE, L. & REBEL, J. M. 2013. Contribution of the NS1 gene of H7 avian influenza virus strains to pathogenicity in chickens. *Viral Immunol,* 26**,** 396-403.
QIU, Y. & KRUG, R. M. 1994. The influenza virus NS1 protein is a poly(A)-binding protein that inhibits nuclear export of mRNAs containing poly(A). *J Virol,* 68**,** 2425-32.
QIU, Y., NEMEROFF, M. & KRUG, R. M. 1995. The influenza virus NS1 protein binds to a specific region in human U6 snRNA and inhibits U6-U2 and U6-U4 snRNA interactions during splicing. *RNA,* 1**,** 304-16.
RAJSBAUM, R., ALBRECHT, R. A., WANG, M. K., MAHARAJ, N. P., VERSTEEG, G. A., NISTAL-VILLAN, E., GARCIA-SASTRE, A. & GACK, M. U. 2012. Species-specific inhibition of RIG-I ubiquitination and IFN induction by the influenza A virus NS1 protein. *PLoS Pathog,* 8**,** e1003059.
RANDALL, R. E. & GOODBOURN, S. 2008. Interferons and viruses: an interplay between induction, signalling, antiviral responses and virus countermeasures. *J Gen Virol,* 89**,** 1-47.
READ, E. K. & DIGARD, P. 2010. Individual influenza A virus mRNAs show differential dependence on cellular NXF1/TAP for their nuclear export. *J Gen Virol,* 91**,** 1290-301.
REUMAN, P. D., KEELY, S. & SCHIFF, G. M. 1989. Assessment of signs of influenza illness in the ferret model. *Journal of Virological Methods,* 24**,** 27-34.

REUTHER, P., GIESE, S., GOTZ, V., RIEGGER, D. & SCHWEMMLE, M. 2014a. Phosphorylation of highly conserved serine residues in the influenza A virus nuclear export protein NEP plays a minor role in viral growth in human cells and mice. *J Virol,* 88**,** 7668-73.

REUTHER, P., GIESE, S., GOTZ, V., KILB, N., MANZ, B., BRUNOTTE, L. & SCHWEMMLE, M. 2014b. Adaptive mutations in the nuclear export protein of human-derived H5N1 strains facilitate a polymerase activity-enhancing conformation. *J Virol,* 88**,** 263-71.

RICHARDSON, J. C. & AKKINA, R. K. 1991. NS2 protein of influenza virus is found in purified virus and phosphorylated in infected cells. *Arch Virol,* 116**,** 69-80.

ROBB, N. C., SMITH, M., VREEDE, F. T. & FODOR, E. 2009. NS2/NEP protein regulates transcription and replication of the influenza virus RNA genome. *J Gen Virol,* 90**,** 1398-407.

ROBB, N. C., JACKSON, D., VREEDE, F. T. & FODOR, E. 2010. Splicing of influenza A virus NS1 mRNA is independent of the viral NS1 protein. *J Gen Virol,* 91**,** 2331-40.

ROBB, N. C., CHASE, G., BIER, K., VREEDE, F. T., SHAW, P. C., NAFFAKH, N., SCHWEMMLE, M. & FODOR, E. 2011. The influenza A virus NS1 protein interacts with the nucleoprotein of viral ribonucleoprotein complexes. *J Virol,* 85**,** 5228-31.

ROBB, N. C. & FODOR, E. 2012. The accumulation of influenza A virus segment 7 spliced mRNAs is regulated by the NS1 protein. *J Gen Virol,* 93**,** 113-8.

ROBERTSON, H. D., DICKSON, E., PLOTCH, S. J. & KRUG, R. M. 1980. Identification of the RNA region transferred from a representative primer, beta-globin mRNA, to influenza mRNA during in vitro transcription. *Nucleic Acids Res,* 8**,** 925-42.

ROBERTSON, J. S. 1979. 5' and 3' terminal nucleotide sequences of the RNA genome segments of influenza virus. *Nucleic Acids Res,* 6**,** 3745-57.

ROBERTSON, J. S., SCHUBERT, M. & LAZZARINI, R. A. 1981. Polyadenylation sites for influenza virus mRNA. *J Virol,* 38**,** 157-63.

RODRIGUEZ, A., PEREZ-GONZALEZ, A. & NIETO, A. 2007. Influenza virus infection causes specific degradation of the largest subunit of cellular RNA polymerase II. *J Virol,* 81**,** 5315-24.

ROSSMAN, J. S., JING, X., LESER, G. P. & LAMB, R. A. 2010. Influenza virus M2 protein mediates ESCRT-independent membrane scission. *Cell,* 142**,** 902-13.

ROSSMAN, J. S., LESER, G. P. & LAMB, R. A. 2012. Filamentous Influenza Virus Enters Cells via Macropinocytosis. *Journal of Virology,* 86**,** 10950-10960.

ROTHENBERG, M. E. 1999. Eotaxin. An essential mediator of eosinophil trafficking into mucosal tissues. *Am J Respir Cell Mol Biol,* 21**,** 291-5.

ROZO, M. & GRONVALL, G. K. 2015. The Reemergent 1977 H1N1 Strain and the Gain-of-Function Debate. *MBio,* 6.

RUBIO, N. & SANZ-RODRIGUEZ, F. 2007. Induction of the CXCL1 (KC) chemokine in mouse astrocytes by infection with the murine encephalomyelitis virus of Theiler. *Virology,* 358**,** 98-108.

RUIGROK, R., BAUDIN, F., PETIT, I. & WEISSENHORN, W. 2001. Role of influenza virus M1 protein in the viral budding process. *International Congress Series,* 1219**,** 397-404.

RUIGROK, R. W., BARGE, A., DURRER, P., BRUNNER, J., MA, K. & WHITTAKER, G. R. 2000. Membrane interaction of influenza virus M1 protein. *Virology,* 267**,** 289-98.

SALVATORE, M., BASLER, C. F., PARISIEN, J. P., HORVATH, C. M., BOURMAKINA, S., ZHENG, H., MUSTER, T., PALESE, P. & GARCIA-SASTRE, A. 2002. Effects of influenza A virus NS1 protein on protein expression: the NS1 protein enhances translation and is not required for shutoff of host protein synthesis. *J Virol,* 76**,** 1206-12.

SANTOS, A., PAL, S., CHACON, J., MERAZ, K., GONZALEZ, J., PRIETO, K. & ROSAS-ACOSTA, G. 2013. SUMOylation affects the interferon blocking activity of the

influenza A nonstructural protein NS1 without affecting its stability or cellular localization. *J Virol,* 87**,** 5602-20.

SARAFI, M. N., GARCIA-ZEPEDA, E. A., MACLEAN, J. A., CHARO, I. F. & LUSTER, A. D. 1997. Murine monocyte chemoattractant protein (MCP)-5: a novel CC chemokine that is a structural and functional homologue of human MCP-1. *J Exp Med,* 185**,** 99-109.

SATTERLY, N., TSAI, P. L., VAN DEURSEN, J., NUSSENZVEIG, D. R., WANG, Y., FARIA, P. A., LEVAY, A., LEVY, D. E. & FONTOURA, B. M. 2007. Influenza virus targets the mRNA export machinery and the nuclear pore complex. *Proc Natl Acad Sci U S A,* 104**,** 1853-8.

SCHEIFFELE, P., RIETVELD, A., WILK, T. & SIMONS, K. 1999. Influenza viruses select ordered lipid domains during budding from the plasma membrane. *J Biol Chem,* 274**,** 2038-44.

SCHLEE, M., ROTH, A., HORNUNG, V., HAGMANN, C. A., WIMMENAUER, V., BARCHET, W., COCH, C., JANKE, M., MIHAILOVIC, A., WARDLE, G., JURANEK, S., KATO, H., KAWAI, T., POECK, H., FITZGERALD, K. A., TAKEUCHI, O., AKIRA, S., TUSCHL, T., LATZ, E., LUDWIG, J. & HARTMANN, G. 2009. Recognition of 5' triphosphate by RIG-I helicase requires short blunt double-stranded RNA as contained in panhandle of negative-strand virus. *Immunity,* 31**,** 25-34.

SCHOLTISSEK, C., ROHDE, W., VON HOYNINGEN, V. & ROTT, R. 1978. On the origin of the human influenza virus subtypes H2N2 and H3N2. *Virology,* 87**,** 13-20.

SCHOLTISSEK, C., BURGER, H., BACHMANN, P. A. & HANNOUN, C. 1983. Genetic relatedness of hemagglutinins of the H1 subtype of influenza A viruses isolated from swine and birds. *Virology,* 129**,** 521-3.

SCHOLTISSEK, C. 1985. Stability of infectious influenza A viruses at low pH and at elevated temperature. *Vaccine,* 3**,** 215-8.

SCHRAUWEN, E. J., BESTEBROER, T. M., MUNSTER, V. J., DE WIT, E., HERFST, S., RIMMELZWAAN, G. F., OSTERHAUS, A. D. & FOUCHIER, R. A. 2011. Insertion of a multibasic cleavage site in the haemagglutinin of human influenza H3N2 virus does not increase pathogenicity in ferrets. *J Gen Virol,* 92**,** 1410-5.

SCHRAUWEN, E. J., HERFST, S., LEIJTEN, L. M., VAN RUN, P., BESTEBROER, T. M., LINSTER, M., BODEWES, R., KREIJTZ, J. H., RIMMELZWAAN, G. F., OSTERHAUS, A. D., FOUCHIER, R. A., KUIKEN, T. & VAN RIEL, D. 2012. The multibasic cleavage site in H5N1 virus is critical for systemic spread along the olfactory and hematogenous routes in ferrets. *J Virol,* 86**,** 3975-84.

SCHRAUWEN, E. J. & FOUCHIER, R. A. 2014. Host adaptation and transmission of influenza A viruses in mammals. *Emerg Microbes Infect,* 3**,** e9.

SCHRODER, K., HERTZOG, P. J., RAVASI, T. & HUME, D. A. 2004. Interferon-gamma: an overview of signals, mechanisms and functions. *J Leukoc Biol,* 75**,** 163-89.

SCHULMAN, J. L. & KILBOURNE, E. D. 1963. EXPERIMENTAL TRANSMISSION OF INFLUENZA VIRUS INFECTION IN MICE. II. SOME FACTORS AFFECTING THE INCIDENCE OF TRANSMITTED INFECTION. *J Exp Med,* 118**,** 267-75.

SELMAN, M., DANKAR, S. K., FORBES, N. E., JIA, J.-J. & BROWN, E. G. 2012. Adaptive mutation in influenza A virus non-structural gene is linked to host switching and induces a novel protein by alternative splicing. *Emerging Microbes & Infections,* 1**,** e42.

SEVILLA-REYES, E. E., CHAVARO-PEREZ, D. A., PITEN-ISIDRO, E., GUTIERREZ-GONZALEZ, L. H. & SANTOS-MENDOZA, T. 2013. Protein Clustering and RNA Phylogenetic Reconstruction of the Influenza a Virus NS1 Protein Allow an Update in Classification and Identification of Motif Conservation. *PLoS One,* 8**,** e63098.

SHAPIRO, G. I., GURNEY, T., JR. & KRUG, R. M. 1987. Influenza virus gene expression: control mechanisms at early and late times of infection and nuclear-cytoplasmic transport of virus-specific RNAs. *J Virol,* 61**,** 764-73.

SHEPPARD, P., KINDSVOGEL, W., XU, W., HENDERSON, K., SCHLUTSMEYER, S., WHITMORE, T. E., KUESTNER, R., GARRIGUES, U., BIRKS, C., RORABACK, J., OSTRANDER, C., DONG, D., SHIN, J., PRESNELL, S., FOX, B., HALDEMAN, B., COOPER, E., TAFT, D., GILBERT, T., GRANT, F. J., TACKETT, M., KRIVAN, W., MCKNIGHT, G., CLEGG, C., FOSTER, D. & KLUCHER, K. M. 2003. IL-28, IL-29 and their class II cytokine receptor IL-28R. *Nat Immunol,* 4**,** 63-8.

SHI, Y., LIU, C. H., ROBERTS, A. I., DAS, J., XU, G., REN, G., ZHANG, Y., ZHANG, L., YUAN, Z. R., TAN, H. S., DAS, G. & DEVADAS, S. 2006. Granulocyte-macrophage colony-stimulating factor (GM-CSF) and T-cell responses: what we do and don't know. *Cell Res,* 16**,** 126-33.

SHIH, S. R., NEMEROFF, M. E. & KRUG, R. M. 1995. The choice of alternative 5' splice sites in influenza virus M1 mRNA is regulated by the viral polymerase complex. *Proc Natl Acad Sci U S A,* 92**,** 6324-8.

SHIH, S. R., SUEN, P. C., CHEN, Y. S. & CHANG, S. C. 1998. A novel spliced transcript of influenza A/WSN/33 virus. *Virus Genes,* 17**,** 179-83.

SHIN, Y. K., LI, Y., LIU, Q., ANDERSON, D. H., BABIUK, L. A. & ZHOU, Y. 2007. SH3 binding motif 1 in influenza A virus NS1 protein is essential for PI3K/Akt signaling pathway activation. *J Virol,* 81**,** 12730-9.

SHODA, H., FUJIO, K., YAMAGUCHI, Y., OKAMOTO, A., SAWADA, T., KOCHI, Y. & YAMAMOTO, K. 2006. Interactions between IL-32 and tumor necrosis factor alpha contribute to the exacerbation of immune-inflammatory diseases. *Arthritis Res Ther,* 8**,** R166.

SKEHEL, J. J., STEVENS, D. J., DANIELS, R. S., DOUGLAS, A. R., KNOSSOW, M., WILSON, I. A. & WILEY, D. C. 1984. A carbohydrate side chain on hemagglutinins of Hong Kong influenza viruses inhibits recognition by a monoclonal antibody. *Proc Natl Acad Sci U S A,* 81**,** 1779-83.

SKEHEL, J. J. & WILEY, D. C. 2000. Receptor binding and membrane fusion in virus entry: the influenza hemagglutinin. *Annu Rev Biochem,* 69**,** 531-69.

SMITH, G. J., BAHL, J., VIJAYKRISHNA, D., ZHANG, J., POON, L. L., CHEN, H., WEBSTER, R. G., PEIRIS, J. S. & GUAN, Y. 2009. Dating the emergence of pandemic influenza viruses. *Proc Natl Acad Sci U S A,* 106**,** 11709-12.

SMITH, J., SMITH, N., YU, L., PATON, I. R., GUTOWSKA, M. W., FORREST, H. L., DANNER, A. F., SEILER, J. P., DIGARD, P., WEBSTER, R. G. & BURT, D. W. 2015. A comparative analysis of host responses to avian influenza infection in ducks and chickens highlights a role for the interferon-induced transmembrane proteins in viral resistance. *BMC Genomics,* 16**,** 574.

STAEHELI, P., HALLER, O., BOLL, W., LINDENMANN, J. & WEISSMANN, C. 1986. Mx protein: constitutive expression in 3T3 cells transformed with cloned Mx cDNA confers selective resistance to influenza virus. *Cell,* 44**,** 147-58.

STEEL, J., LOWEN, A. C., MUBAREKA, S. & PALESE, P. 2009. Transmission of Influenza Virus in a Mammalian Host Is Increased by PB2 Amino Acids 627K or 627E/701N. *PLoS Pathog,* 5**,** e1000252.

STEEL, J. & LOWEN, A. C. 2014. Influenza A virus reassortment. *Curr Top Microbiol Immunol,* 385**,** 377-401.

STEGEMAN, A., BOUMA, A., ELBERS, A. R., DE JONG, M. C., NODELIJK, G., DE KLERK, F., KOCH, G. & VAN BOVEN, M. 2004. Avian influenza A virus (H7N7) epidemic in The Netherlands in 2003: course of the epidemic and effectiveness of control measures. *J Infect Dis,* 190**,** 2088-95.

STEGMANN, T., BOOY, F. P. & WILSCHUT, J. 1987. Effects of low pH on influenza virus. Activation and inactivation of the membrane fusion capacity of the hemagglutinin. *J Biol Chem,* 262**,** 17744-9.

STEWART, M. 2007. Molecular mechanism of the nuclear protein import cycle. *Nat Rev Mol Cell Biol,* 8**,** 195-208.

STIENEKE-GRÖßER, A., VEY, M., ANGLIKER, H., SHAW, E., THOMAS, G., ROBERTS, C., KLENK, H. D. & GARTEN, W. 1992. Influenza virus hemagglutinin with multibasic cleavage site is activated by furin, a subtilisin-like endoprotease. *Embo j,* 11**,** 2407-14.

STUBBS, T. M. & TE VELTHUIS, A. J. W. 2014. The RNA-dependent RNA polymerase of the influenza A virus. *Future virology,* 9**,** 863-876.

SU, S., QI, W. B., CHEN, J. D., CAO, N., ZHU, W. J., YUAN, L. G., WANG, H. & ZHANG, G. H. 2012. Complete genome sequence of an avian-like H4N8 swine influenza virus discovered in southern China. *J Virol,* 86**,** 9542.

SUAREZ, D. L. & PERDUE, M. L. 1998. Multiple alignment comparison of the non-structural genes of influenza A viruses. *Virus Research,* 54**,** 59-69.

SUAREZ, D. L., GARCIA, M., LATIMER, J., SENNE, D. & PERDUE, M. 1999. Phylogenetic analysis of H7 avian influenza viruses isolated from the live bird markets of the Northeast United States. *J Virol,* 73**,** 3567-73.

SUBBARAO, E. K., LONDON, W. & MURPHY, B. R. 1993. A single amino acid in the PB2 gene of influenza A virus is a determinant of host range. *J Virol,* 67**,** 1761-4.

TAFT, A. S., OZAWA, M., FITCH, A., DEPASSE, J. V., HALFMANN, P. J., HILL-BATORSKI, L., HATTA, M., FRIEDRICH, T. C., LOPES, T. J. S., MAHER, E. A., GHEDIN, E., MACKEN, C. A., NEUMANN, G. & KAWAOKA, Y. 2015. Identification of mammalian-adapting mutations in the polymerase complex of an avian H5N1 influenza virus. *Nat Commun,* 6.

TAKEDA, M., LESER, G. P., RUSSELL, C. J. & LAMB, R. A. 2003. Influenza virus hemagglutinin concentrates in lipid raft microdomains for efficient viral fusion. *Proc Natl Acad Sci U S A,* 100**,** 14610-7.

TALON, J., HORVATH, C. M., POLLEY, R., BASLER, C. F., MUSTER, T., PALESE, P. & GARCIA-SASTRE, A. 2000. Activation of interferon regulatory factor 3 is inhibited by the influenza A virus NS1 protein. *J Virol,* 74**,** 7989-96.

TAPIA, K., KIM, W.-K., SUN, Y., MERCADO-LÓPEZ, X., DUNAY, E., WISE, M., ADU, M. & LÓPEZ, C. B. 2013. Defective Viral Genomes Arising <italic>In Vivo</italic> Provide Critical Danger Signals for the Triggering of Lung Antiviral Immunity. *PLoS Pathog,* 9**,** e1003703.

TARENDEAU, F., BOUDET, J., GUILLIGAY, D., MAS, P. J., BOUGAULT, C. M., BOULO, S., BAUDIN, F., RUIGROK, R. W., DAIGLE, N., ELLENBERG, J., CUSACK, S., SIMORRE, J. P. & HART, D. J. 2007. Structure and nuclear import function of the C-terminal domain of influenza virus polymerase PB2 subunit. *Nat Struct Mol Biol,* 14**,** 229-33.

TATE, M. D., PICKETT, D. L., VAN ROOIJEN, N., BROOKS, A. G. & READING, P. C. 2010. Critical role of airway macrophages in modulating disease severity during influenza virus infection of mice. *J Virol,* 84**,** 7569-80.

TAUBENBERGER, J. K., REID, A. H., LOURENS, R. M., WANG, R., JIN, G. & FANNING, T. G. 2005. Characterization of the 1918 influenza virus polymerase genes. *Nature,* 437**,** 889-893.

TAUBENBERGER, J. K. & MORENS, D. M. 2006. 1918 Influenza: the mother of all pandemics. *Emerg Infect Dis,* 12**,** 15-22.

TAWARATSUMIDA, K., PHAN, V., HRINCIUS, E. R., HIGH, A. A., WEBBY, R., REDECKE, V. & HACKER, H. 2014. Quantitative proteomic analysis of the influenza A virus nonstructural proteins NS1 and NS2 during natural cell infection

identifies PACT as an NS1 target protein and antiviral host factor. *J Virol,* 88**,** 9038-48.

TAYLOR, R. M. 1941. EXPERIMENTAL INFECTION WITH INFLUENZA A VIRUS IN MICE : THE INCREASE IN INTRAPULMONARY VIRUS AFTER INOCULATION AND THE INFLUENCE OF VARIOUS FACTORS THEREON. *J Exp Med,* 73**,** 43-55.

TCHATALBACHEV, S., FLICK, R. & HOBOM, G. 2001. The packaging signal of influenza viral RNA molecules. *RNA,* 7**,** 979-989.

TENG, M. W., BOWMAN, E. P., MCELWEE, J. J., SMYTH, M. J., CASANOVA, J. L., COOPER, A. M. & CUA, D. J. 2015. IL-12 and IL-23 cytokines: from discovery to targeted therapies for immune-mediated inflammatory diseases. *Nat Med,* 21**,** 719-29.

TESKE, S., BOHN, A. A., REGAL, J. F., NEUMILLER, J. J. & LAWRENCE, B. P. 2005. Activation of the aryl hydrocarbon receptor increases pulmonary neutrophilia and diminishes host resistance to influenza A virus. *Am J Physiol Lung Cell Mol Physiol,* 289**,** L111-24.

TO, K. F., CHAN, P. K., CHAN, K. F., LEE, W. K., LAM, W. Y., WONG, K. F., TANG, N. L., TSANG, D. N., SUNG, R. Y., BUCKLEY, T. A., TAM, J. S. & CHENG, A. F. 2001. Pathology of fatal human infection associated with avian influenza A H5N1 virus. *J Med Virol,* 63**,** 242-6.

TO, K. K., LAU, C. C., WOO, P. C., LAU, S. K., CHAN, J. F., CHAN, K. H., ZHANG, A. J., CHEN, H. & YUEN, K. Y. 2016. Human H7N9 virus induces a more pronounced pro-inflammatory cytokine but an attenuated interferon response in human bronchial epithelial cells when compared with an epidemiologically-linked chicken H7N9 virus. *Virol J,* 13**,** 42.

TONG, S., LI, Y., RIVAILLER, P., CONRARDY, C., CASTILLO, D. A., CHEN, L. M., RECUENCO, S., ELLISON, J. A., DAVIS, C. T., YORK, I. A., TURMELLE, A. S., MORAN, D., ROGERS, S., SHI, M., TAO, Y., WEIL, M. R., TANG, K., ROWE, L. A., SAMMONS, S., XU, X., FRACE, M., LINDBLADE, K. A., COX, N. J., ANDERSON, L. J., RUPPRECHT, C. E. & DONIS, R. O. 2012. A distinct lineage of influenza A virus from bats. *Proc Natl Acad Sci U S A,* 109**,** 4269-74.

TONG, S., ZHU, X., LI, Y., SHI, M., ZHANG, J., BOURGEOIS, M., YANG, H., CHEN, X., RECUENCO, S., GOMEZ, J., CHEN, L. M., JOHNSON, A., TAO, Y., DREYFUS, C., YU, W., MCBRIDE, R., CARNEY, P. J., GILBERT, A. T., CHANG, J., GUO, Z., DAVIS, C. T., PAULSON, J. C., STEVENS, J., RUPPRECHT, C. E., HOLMES, E. C., WILSON, I. A. & DONIS, R. O. 2013. New world bats harbor diverse influenza A viruses. *PLoS Pathog,* 9**,** e1003657.

TREANOR, J. J., SNYDER, M. H., LONDON, W. T. & MURPHY, B. R. 1989. The B allele of the NS gene of avian influenza viruses, but not the A allele, attenuates a human influenza A virus for squirrel monkeys. *Virology,* 171**,** 1-9.

TRIFILO, M. J., BERGMANN, C. C., KUZIEL, W. A. & LANE, T. E. 2003. CC chemokine ligand 3 (CCL3) regulates CD8(+)-T-cell effector function and migration following viral infection. *J Virol,* 77**,** 4004-14.

TUMPEY, T. M., GARCIA-SASTRE, A., TAUBENBERGER, J. K., PALESE, P., SWAYNE, D. E., PANTIN-JACKWOOD, M. J., SCHULTZ-CHERRY, S., SOLORZANO, A., VAN ROOIJEN, N., KATZ, J. M. & BASLER, C. F. 2005. Pathogenicity of influenza viruses with genes from the 1918 pandemic virus: functional roles of alveolar macrophages and neutrophils in limiting virus replication and mortality in mice. *J Virol,* 79**,** 14933-44.

TWU, K. Y., KUO, R. L., MARKLUND, J. & KRUG, R. M. 2007. The H5N1 influenza virus NS genes selected after 1998 enhance virus replication in mammalian cells. *J Virol,* 81**,** 8112-21.

TYNER, J. W., UCHIDA, O., KAJIWARA, N., KIM, E. Y., PATEL, A. C., O'SULLIVAN, M. P., WALTER, M. J., SCHWENDENER, R. A., COOK, D. N., DANOFF, T. M. &

HOLTZMAN, M. J. 2005. CCL5-CCR5 interaction provides antiapoptotic signals for macrophage survival during viral infection. *Nat Med,* 11**,** 1180-7.

VARGA, Z. T., RAMOS, I., HAI, R., SCHMOLKE, M., GARCIA-SASTRE, A., FERNANDEZ-SESMA, A. & PALESE, P. 2011. The influenza virus protein PB1-F2 inhibits the induction of type I interferon at the level of the MAVS adaptor protein. *PLoS Pathog,* 7**,** e1002067.

VARGA, Z. T., GRANT, A., MANICASSAMY, B. & PALESE, P. 2012. Influenza virus protein PB1-F2 inhibits the induction of type I interferon by binding to MAVS and decreasing mitochondrial membrane potential. *J Virol,* 86**,** 8359-66.

VARKI, A., CUMMINGS, R. D., ESKO, J. D., FREEZE, H. H., STANLEY, P., BERTOZZI, C. R., HART, G. W. & ETZLER, M. E. 2009. *In:* VARKI, A., CUMMINGS, R. D., ESKO, J. D., FREEZE, H. H., STANLEY, P., BERTOZZI, C. R., HART, G. W. & ETZLER, M. E. (eds.) *Essentials of Glycobiology.* Cold Spring Harbor (NY): Cold Spring Harbor Laboratory Press.

VERHELST, J., PARTHOENS, E., SCHEPENS, B., FIERS, W. & SAELENS, X. 2012. Interferon-inducible protein Mx1 inhibits influenza virus by interfering with functional viral ribonucleoprotein complex assembly. *J Virol,* 86**,** 13445-55.

VESTERGAARD, C., DELEURAN, M., GESSER, B. & LARSEN, C. G. 2004. Thymus- and activation-regulated chemokine (TARC/CCL17) induces a Th2-dominated inflammatory reaction on intradermal injection in mice. *Exp Dermatol,* 13**,** 265-71.

VIJAYKRISHNA, D., SMITH, G. J., PYBUS, O. G., ZHU, H., BHATT, S., POON, L. L., RILEY, S., BAHL, J., MA, S. K., CHEUNG, C. L., PERERA, R. A., CHEN, H., SHORTRIDGE, K. F., WEBBY, R. J., WEBSTER, R. G., GUAN, Y. & PEIRIS, J. S. 2011. Long-term evolution and transmission dynamics of swine influenza A virus. *Nature,* 473**,** 519-22.

VOLMER, R., MAZEL-SANCHEZ, B., VOLMER, C., SOUBIES, S. M. & GUERIN, J. L. 2010. Nucleolar localization of influenza A NS1: striking differences between mammalian and avian cells. *Virol J,* 7**,** 63.

VON ITZSTEIN, M., WU, W. Y., KOK, G. B., PEGG, M. S., DYASON, J. C., JIN, B., VAN PHAN, T., SMYTHE, M. L., WHITE, H. F., OLIVER, S. W. & ET AL. 1993. Rational design of potent sialidase-based inhibitors of influenza virus replication. *Nature,* 363**,** 418-23.

VREEDE, F. T., CHAN, A. Y., SHARPS, J. & FODOR, E. 2010. Mechanisms and functional implications of the degradation of host RNA polymerase II in influenza virus infected cells. *Virology,* 396**,** 125-34.

WACK, A., TERCZYNSKA-DYLA, E. & HARTMANN, R. 2015. Guarding the frontiers: the biology of type III interferons. *Nat Immunol,* 16**,** 802-809.

WAGNER, R., MATROSOVICH, M. & KLENK, H. D. 2002. Functional balance between haemagglutinin and neuraminidase in influenza virus infections. *Rev Med Virol,* 12**,** 159-66.

WANG, H., FENG, Z., SHU, Y., YU, H., ZHOU, L., ZU, R., HUAI, Y., DONG, J., BAO, C., WEN, L., WANG, H., YANG, P., ZHAO, W., DONG, L., ZHOU, M., LIAO, Q., YANG, H., WANG, M., LU, X., SHI, Z., WANG, W., GU, L., ZHU, F., LI, Q., YIN, W., YANG, W., LI, D., UYEKI, T. M. & WANG, Y. 2008a. Probable limited person-to-person transmission of highly pathogenic avian influenza A (H5N1) virus in China. *Lancet,* 371**,** 1427-34.

WANG, J., NIKRAD, M. P., TRAVANTY, E. A., ZHOU, B., PHANG, T., GAO, B., ALFORD, T., ITO, Y., NAHREINI, P., HARTSHORN, K., WENTWORTH, D., DINARELLO, C. A. & MASON, R. J. 2012a. Innate immune response of human alveolar macrophages during influenza A infection. *PLoS One,* 7**,** e29879.

WANG, N., ZOU, W., YANG, Y., GUO, X., HUA, Y., ZHANG, Q., ZHAO, Z. & JIN, M. 2012b. Complete genome sequence of an H10N5 avian influenza virus isolated from pigs in central China. *J Virol,* 86**,** 13865-6.

WANG, W., RIEDEL, K., LYNCH, P., CHIEN, C. Y., MONTELIONE, G. T. & KRUG, R. M. 1999. RNA binding by the novel helical domain of the influenza virus NS1 protein requires its dimer structure and a small number of specific basic amino acids. *Rna,* 5**,** 195-205.

WANG, W., CUI, Z. Q., HAN, H., ZHANG, Z. P., WEI, H. P., ZHOU, Y. F., CHEN, Z. & ZHANG, X. E. 2008b. Imaging and characterizing influenza A virus mRNA transport in living cells. *Nucleic Acids Res,* 36**,** 4913-28.

WANG, X., LI, M., ZHENG, H., MUSTER, T., PALESE, P., BEG, A. A. & GARCIA-SASTRE, A. 2000. Influenza A virus NS1 protein prevents activation of NF-kappaB and induction of alpha/beta interferon. *J Virol,* 74**,** 11566-73.

WANG, Z., ROBB, N. C., LENZ, E., WOLFF, T., FODOR, E. & PLESCHKA, S. 2010. NS reassortment of an H7-type highly pathogenic avian influenza virus affects its propagation by altering the regulation of viral RNA production and antiviral host response. *J Virol,* 84**,** 11323-35.

WASHINGTON, N., STEELE, R. J., JACKSON, S. J., BUSH, D., MASON, J., GILL, D. A., PITT, K. & RAWLINS, D. A. 2000. Determination of baseline human nasal pH and the effect of intranasally administered buffers. *Int J Pharm,* 198**,** 139-46.

WATANABE, K., TAKIZAWA, N., KATOH, M., HOSHIDA, K., KOBAYASHI, N. & NAGATA, K. 2001. Inhibition of nuclear export of ribonucleoprotein complexes of influenza virus by leptomycin B. *Virus Research,* 77**,** 31-42.

WEBSTER, R. G., LAVER, W. G. & KILBOURNE, E. D. 1968. Reactions of antibodies with surface antigens of influenza virus. *J Gen Virol,* 3**,** 315-26.

WEBSTER, R. G., YAKHNO, M., HINSHAW, V. S., BEAN, W. J. & MURTI, K. G. 1978. Intestinal influenza: replication and characterization of influenza viruses in ducks. *Virology,* 84**,** 268-78.

WEBSTER, R. G., HINSHAW, V. S., BEAN, W. J., VAN WYKE, K. L., GERACI, J. R., ST AUBIN, D. J. & PETURSSON, G. 1981. Characterization of an influenza A virus from seals. *Virology,* 113**,** 712-24.

WEBSTER, R. G. & ROTT, R. 1987. Influenza virus A pathogenicity: the pivotal role of hemagglutinin. *Cell,* 50**,** 665-6.

WEBSTER, R. G., BEAN, W. J., GORMAN, O. T., CHAMBERS, T. M. & KAWAOKA, Y. 1992. Evolution and ecology of influenza A viruses. *Microbiol Rev,* 56**,** 152-79.

WEEKES, M. P., TOMASEC, P., HUTTLIN, E. L., FIELDING, C. A., NUSINOW, D., STANTON, R. J., WANG, E. C., AICHELER, R., MURRELL, I., WILKINSON, G. W., LEHNER, P. J. & GYGI, S. P. 2014. Quantitative temporal viromics: an approach to investigate host-pathogen interaction. *Cell,* 157**,** 1460-72.

WEIS, W., BROWN, J. H., CUSACK, S., PAULSON, J. C., SKEHEL, J. J. & WILEY, D. C. 1988. Structure of the influenza virus haemagglutinin complexed with its receptor, sialic acid. *Nature,* 333**,** 426-31.

WIDNEY, D. P., XIA, Y. R., LUSIS, A. J. & SMITH, J. B. 2000. The murine chemokine CXCL11 (IFN-inducible T cell alpha chemoattractant) is an IFN-gamma- and lipopolysaccharide-inducible glucocorticoid-attenuated response gene expressed in lung and other tissues during endotoxemia. *J Immunol,* 164**,** 6322-31.

WILEY, D. C. & SKEHEL, J. J. 1987. The structure and function of the hemagglutinin membrane glycoprotein of influenza virus. *Annu Rev Biochem,* 56**,** 365-94.

WILLIAMS, R. A., SEGOVIA-HINOSTROZA, K., GHERSI, B. M., GONZAGA, V., PETERSON, A. T. & MONTGOMERY, J. M. 2012. Avian Influenza infections in nonmigrant land birds in Andean Peru. *J Wildl Dis,* 48**,** 910-7.

WISE, H. M., FOEGLEIN, A., SUN, J., DALTON, R. M., PATEL, S., HOWARD, W., ANDERSON, E. C., BARCLAY, W. S. & DIGARD, P. 2009. A complicated message: Identification of a novel PB1-related protein translated from influenza A virus segment 2 mRNA. *J Virol,* 83**,** 8021-31.

WISE, H. M., BARBEZANGE, C., JAGGER, B. W., DALTON, R. M., GOG, J. R., CURRAN, M. D., TAUBENBERGER, J. K., ANDERSON, E. C. & DIGARD, P. 2011. Overlapping signals for translational regulation and packaging of influenza A virus segment 2. *Nucleic Acids Res,* 39**,** 7775-90.

WISE, H. M., HUTCHINSON, E. C., JAGGER, B. W., STUART, A. D., KANG, Z. H., ROBB, N., SCHWARTZMAN, L. M., KASH, J. C., FODOR, E., FIRTH, A. E., GOG, J. R., TAUBENBERGER, J. K. & DIGARD, P. 2012. Identification of a novel splice variant form of the influenza A virus M2 ion channel with an antigenically distinct ectodomain. *PLoS Pathog,* 8**,** e1002998.

WOLPE, S. D., SHERRY, B., JUERS, D., DAVATELIS, G., YURT, R. W. & CERAMI, A. 1989. Identification and characterization of macrophage inflammatory protein 2. *Proc Natl Acad Sci U S A,* 86**,** 612-6.

WORLD HEALTH ORGANISATION. 2013. *Human Infection with Avian Influenza A(H7N9) Virus – July 2013 Update* [Online]. Available: http://www.who.int/csr/don/2013_07_04/en/ [Accessed 16/08/16.

WORLD HEALTH ORGANISATION. 2014. *Influenza (Seasonal) Fact sheet* [Online]. Available: http://www.who.int/mediacentre/factsheets/fs211/en/ [Accessed 16/08/16.

WORLD HEALTH ORGANISATION. 2016a. *Situation Updates - Avian Influenza* [Online]. Available: http://www.who.int/influenza/human_animal_interface/avian_influenza/archive/en/ [Accessed 16/08/16.

WORLD HEALTH ORGANISATION. 2016b. *May 2016 Update* [Online]. Available: http://www.who.int/influenza/human_animal_interface/EN_GIP_20160509cumulativenumberH5N1cases.pdf?ua=1 [Accessed 15/08/16.

WORLD HEALTH ORGANISATION. 2016c. *Past pandemics* [Online]. Available: http://www.euro.who.int/en/health-topics/communicable-diseases/influenza/pandemic-influenza/past-pandemics [Accessed 15/08/16.

WOROBEY, M., HAN, G. Z. & RAMBAUT, A. 2014a. A synchronized global sweep of the internal genes of modern avian influenza virus. *Nature,* 508**,** 254-7.

WOROBEY, M., HAN, G.-Z. & RAMBAUT, A. 2014b. A synchronized global sweep of the internal genes of modern avian influenza virus. *Nature,* 508**,** 254-257.

WOROBEY, M., HAN, G. Z. & RAMBAUT, A. 2014c. Genesis and pathogenesis of the 1918 pandemic H1N1 influenza A virus. *Proc Natl Acad Sci U S A,* 111**,** 8107-12.

WYNN, T. A. 2003. IL-13 effector functions. *Annu Rev Immunol,* 21**,** 425-56.

XIA, C., VIJAYAN, M., PRITZL, C. J., FUCHS, S. Y., MCDERMOTT, A. B. & HAHM, B. 2015. Hemagglutinin of Influenza A Virus Antagonizes Type I Interferon (IFN) Responses by Inducing Degradation of Type I IFN Receptor 1. *J Virol,* 90**,** 2403-17.

XU, K., KLENK, C., LIU, B., KEINER, B., CHENG, J., ZHENG, B. J., LI, L., HAN, Q., WANG, C., LI, T., CHEN, Z., SHU, Y., LIU, J., KLENK, H. D. & SUN, B. 2011. Modification of nonstructural protein 1 of influenza A virus by SUMO1. *J Virol,* 85**,** 1086-98.

YAMADA, S., HATTA, M., STAKER, B. L., WATANABE, S., IMAI, M., SHINYA, K., SAKAI-TAGAWA, Y., ITO, M., OZAWA, M., WATANABE, T., SAKABE, S., LI, C., KIM, J. H., MYLER, P. J., PHAN, I., RAYMOND, A., SMITH, E., STACY, R., NIDOM, C. A., LANK, S. M., WISEMAN, R. W., BIMBER, B. N., O'CONNOR, D. H., NEUMANN, G., STEWART, L. J. & KAWAOKA, Y. 2010. Biological and Structural Characterization of a Host-Adapting Amino Acid in Influenza Virus. *PLoS Pathog,* 6**,** e1001034.

YAMAYOSHI, S., WATANABE, M., GOTO, H. & KAWAOKA, Y. 2016. Identification of a Novel Viral Protein Expressed from the PB2 Segment of Influenza A Virus. *J Virol,* 90**,** 444-56.

YASUDA, J., NAKADA, S., KATO, A., TOYODA, T. & ISHIHAMA, A. 1993. Molecular assembly of influenza virus: association of the NS2 protein with virion matrix. *Virology,* 196**,** 249-55.

YE, Q., KRUG, R. M. & TAO, Y. J. 2006. The mechanism by which influenza A virus nucleoprotein forms oligomers and binds RNA. *Nature,* 444**,** 1078-82.

YEN, H. L. 2016. Current and novel antiviral strategies for influenza infection. *Curr Opin Virol,* 18**,** 126-134.

YONEYAMA, M., KIKUCHI, M., NATSUKAWA, T., SHINOBU, N., IMAIZUMI, T., MIYAGISHI, M., TAIRA, K., AKIRA, S. & FUJITA, T. 2004. The RNA helicase RIG-I has an essential function in double-stranded RNA-induced innate antiviral responses. *Nat Immunol,* 5**,** 730-7.

YORK, A. & FODOR, E. 2013. Biogenesis, assembly, and export of viral messenger ribonucleoproteins in the influenza A virus infected cell. *RNA Biol,* 10**,** 1274-82.

YUAN, P., BARTLAM, M., LOU, Z., CHEN, S., ZHOU, J., HE, X., LV, Z., GE, R., LI, X., DENG, T., FODOR, E., RAO, Z. & LIU, Y. 2009. Crystal structure of an avian influenza polymerase PA(N) reveals an endonuclease active site. *Nature,* 458**,** 909-13.

ZEBEDEE, S. L. & LAMB, R. A. 1988. Influenza A virus M2 protein: monoclonal antibody restriction of virus growth and detection of M2 in virions. *J Virol,* 62**,** 2762-72.

ZHANG, G., KONG, W., QI, W., LONG, L. P., CAO, Z., HUANG, L., QI, H., CAO, N., WANG, W., ZHAO, F., NING, Z., LIAO, M. & WAN, X. F. 2011. Identification of an H6N6 swine influenza virus in southern China. *Infect Genet Evol,* 11**,** 1174-7.

ZHANG, H., LI, X., GUO, J., LI, L., CHANG, C., LI, Y., BIAN, C., XU, K., CHEN, H. & SUN, B. 2014a. The PB2 E627K mutation contributes to the high polymerase activity and enhanced replication of H7N9 influenza virus. *J Gen Virol,* 95**,** 779-86.

ZHANG, J., LESER, G. P., PEKOSZ, A. & LAMB, R. A. 2000. The cytoplasmic tails of the influenza virus spike glycoproteins are required for normal genome packaging. *Virology,* 269**,** 325-34.

ZHANG, S., WANG, J., WANG, Q. & TOYODA, T. 2010. Internal initiation of influenza virus replication of viral RNA and complementary RNA in vitro. *J Biol Chem,* 285**,** 41194-201.

ZHANG, T., BI, Y., TIAN, H., LI, X., LIU, D., WU, Y., JIN, T., WANG, Y., CHEN, Q., CHEN, Z., CHANG, J., GAO, G. F. & XU, B. 2014b. Human infection with influenza virus A(H10N8) from live poultry markets, China, 2014. *Emerg Infect Dis,* 20**,** 2076-9.

ZHAO, C., HSIANG, T. Y., KUO, R. L. & KRUG, R. M. 2010. ISG15 conjugation system targets the viral NS1 protein in influenza A virus-infected cells. *Proc Natl Acad Sci U S A,* 107**,** 2253-8.

ZHAO, G., CHEN, C., HUANG, J., WANG, Y., PENG, D. & LIU, X. 2013. Characterisation of one H6N6 influenza virus isolated from swine in China. *Res Vet Sci,* 95**,** 434-6.

ZHIRNOV, O. P., POYARKOV, S. V., VOROB'EVA, I. V., SAFONOVA, O. A., MALYSHEV, N. A. & KLENK, H. D. 2007. Segment NS of influenza A virus contains an additional gene NSP in positive-sense orientation. *Dokl Biochem Biophys,* 414**,** 127-33.

ZHOU, N. N., SENNE, D. A., LANDGRAF, J. S., SWENSON, S. L., ERICKSON, G., ROSSOW, K., LIU, L., YOON, K., KRAUSS, S. & WEBSTER, R. G. 1999. Genetic reassortment of avian, swine, and human influenza A viruses in American pigs. *J Virol,* 73**,** 8851-6.

ZHU, J., ZHANG, Y., GHOSH, A., CUEVAS, R. A., FORERO, A., DHAR, J., IBSEN, M. S., SCHMID-BURGK, J. L., SCHMIDT, T., GANAPATHIRAJU, M. K., FUJITA, T., HARTMANN, R., BARIK, S., HORNUNG, V., COYNE, C. B. & SARKAR, S. N. 2014. Antiviral activity of human OASL protein is mediated by enhancing signaling of the RIG-I RNA sensor. *Immunity,* 40**,** 936-48.

ZIMMERMANN, P., MANZ, B., HALLER, O., SCHWEMMLE, M. & KOCHS, G. 2011. The viral nucleoprotein determines Mx sensitivity of influenza A viruses. *J Virol,* 85**,** 8133-40.

ZOHARI, S., GYARMATI, P., THOREN, P., CZIFRA, G., BROJER, C., BELAK, S. & BERG, M. 2008. Genetic characterization of the NS gene indicates co-circulation of two sub-lineages of highly pathogenic avian influenza virus of H5N1 subtype in Northern Europe in 2006. *Virus Genes,* 36**,** 117-25.

ZOHARI, S., MUNIR, M., METREVELI, G., BELAK, S. & BERG, M. 2010a. Differences in the ability to suppress interferon beta production between allele A and allele B NS1 proteins from H10 influenza A viruses. *Virol J,* 7**,** 376.

ZOHARI, S., METREVELI, G., KISS, I., BELAK, S. & BERG, M. 2010b. Full genome comparison and characterization of avian H10 viruses with different pathogenicity in Mink (Mustela vison) reveals genetic and functional differences in the non-structural gene. *Virol J,* 7**,** 145.